The role of the secondary messenger NAADP in physiological and pathological calcium signalling in pancreatic acinar cells

Thesis submitted in accordance with the requirements of Cardiff University for the degree of Doctor of Philosophy

Martyn Richard Charlesworth

April, 2017

To my Mother

For the inspiration she provided and the endless support, encouragement and faith she has given me throughout.

Abstract

Acute Pancreatitis (AP) is inflammatory disease characterised by the pathological activation of the digestive enzymes and extensive necrosis of the pancreases and surrounding tissue, which currently has no effective treatment. Pathological agents like the bile acid taurolithocholic acid-3-sulfate (TLC-S) have been shown to induce necrosis of pancreatic acinar cells by causing intracellular calcium (Ca^{2+}) to reach cytotoxic concentrations. TLC-S acts on elements of the secondary Ca^{2+} messenger pathways normally used in physiological signalling to achieve these Ca^{2+} increases.

Nicotinic acid adenine dinucleotide phosphate (NAADP) is the most novel of these secondary Ca^{2+} messengers to be identified and several recent advancements have been made regarding its activity. This study has used these advancements to better characterise NAADP-induced Ca^{2+} release in PAC, and its role in both physiological and pathological Ca^{2+} signalling.

NAADP-induced Ca^{2+} release was found to involve the activity of both Two-pore channel (TPC) and Ryanodine receptor (RyR) Ca^{2+} channels; with a varying involvement of the 2 TPC and 3 RyR isoforms. The NAADP antagonist Ned-19 completely inhibited Ca^{2+} responses to a physiological concentration of the secretagogue cholecystokinin (CCK) and had a protective effect against a pathological concentration of CCK.

The size of the Ca^{2+} response to TLC-S was significantly inhibited in the presence of Ned-19, and the antagonist significantly reduced the amount of necrosis induced. Another related bile acid, cholate, was found to have a similar necrotic effect to PAC as a result of pathological increases in cytosolic Ca^{2+}. While neither Ned-19 or GSK-7975A (an inhibitor of store-

operated Ca^{2+} entry) alone had a significant effect on cholate-induced necrosis, a combination of the two did have a protective effect.

These findings suggest that Ned-19 may provide a potential therapeutic solution to AP, though it may need to be used in combination with inhibitors of other Ca^{2+} signalling to be effective.

Acknowledgments

First I would like to thank my supervisors' Dr Oleg Gerasimenko and Dr Julia Gerasimenko for their support and advice throughout my time under their supervision. Together their theoretical, practical and technical knowledge helped guide my project and develop my skills as a scientist.

I am also thankful to my other supervisor Professor Ole Petersen for his role in reviewing the data I produced and providing advice on the directions my project should take.

Thank you to my student advisor Professor David Lloyd for critiquing my annual reports and contributing a perspective from someone outside my specific area of research.

I received much help from the other members of my group: Dr Bill Williams, Dr Monika Jakubowska and especially Dr Pawel Ferdek for all the assistance they provided. I would also like to thank my fellow PhD students Eloise Stapleton and Shuang Peng for sharing the experience with me and acting as my sounding boards.

Thanks to Dr Parrington for providing the TPC2 knockout mice and Professor Barry Potter for providing the BZ194 compound used in this study. Also thank you to Dr Katsuhiko Mikoshiba for providing access to his colony of RyR3 knockout mice.

Many thanks to Cardiff University for providing me with the opportunity to perform this research project and all the assistance that was provide by the members of its postgraduate team, academic staff, animal unit and fellow PhD students.

Finally, thank you to the Medical Research Council for providing the funding that allowed this project to occur.

Table of Content

Table of Figures

Abbreviations

$[Ca^{2+}]$	calcium concentration
$[Ca^{2+}]_c$	cytoplasmic calcium concentration
$[Ca^{2+}]_e$	extracellular calcium concentration
$[Ca^{2+}]_i$	intracellular calcium concentration
$[Ca^{2+}]_l$	luminal calcium concentration
2-APB	2-Aminoethoxydiphenyl borate
8-Br-cADPR	8-bromo-cADPR
8-NH_2-cADPR	8-amino-cADPR
ACh	acetylcholine
ADH	alcohol dehydrogenase
AP	acute pancreatitis
ATP	adenosine triphosphate
*At*TPC1	*Arabidopsis thaliana* two-pore channel 1
ADP	adenosine diphosphate
AM	acetoxymethyl
BAPTA	1,2-bis(2-amino-phenoxy)ethane-N,N,N',N'-tetraacetic acid
BSEP	bile salt export pump
BZ194	3-carboxyl-1-octylcarbamoylmethyl-pyridinium
cADPR	cyclic adenosine diphosphate-Ribose
CA	cholic acid
CCE	capacitative calcium entry
CD	cluster of differentiation
CD38	cluster of differentiation 38
$CD38^{-/-}$	cluster of differentiation 38 knockout animal
CDCA	chenodeoxycholic acid
CCK	cholecystokinin
CCK_A	cholecystokinin receptor type 1

CCK_B	cholecystokinin receptor type 2
CICR	calcium-induced calcium release
CM_128	CalciMedica_128
CRAC	calcium release-activated channel
CYP7A1	7 α-hydroxylase
DAG	diglyceride
DCA	Deoxycholic acid
EDTA	ethylenediaminetetraacetic
ER	endoplasmic reticulum
FA	fatty acid
FAEE	fatty acid ethyl esters
FK-506	tacrolimus
FKBP12.6	FK-506 binding protein 12.6
FXR	farnesoid X receptor
GDP	guanosine diphosphate
GPN	glycyl-L-phenylalanine-naphthylamide
GTP	guanosine-5'-triphosphate
GSK-7975A	GlaxoSmithKline-7975A
HEK293	human embryonic kidney cells 293
IC_{50}	half maximal inhibitory concentration
ID_{STIM}	inactivation domain of STIM1
IP_3	inositol 1,4,5-trisphosphate
IP_3R	inositol 1,4,5-trisphosphate receptor
Kras	V-Ki-ras2 Kirsten rat sarcoma viral oncogene homolog
LAMP-1	lysosomal-associated membrane protein 1
LCA	lithocholic acid
M-ACh M3	muscarinic ACh receptor M3
MCU	mitochondrial calcium uniporter
MBP	myelin basic protein
mPTP	mitochondrial Permeability Transition Pore
mTOR	mechanistic target of rapamycin

NAADP	nicotinic acid adenine dinucleotide phosphate
NAD	nicotinamide adenine dinucleotide
NADP	nicotinamide adenine dinucleotide phosphate
NCLX	mitochondrial sodium-calcium exchanger
NCX	plasma membrane sodium-calcium exchanger
Ned	NAADP EON Discovered
Ned-19	NAADP EON Discovered-hit rank 19
NF-κB	nuclear factor kappa-light-chain-enhancer of activated B cells
NFAT	nuclear factor of activated T-cells
NR1H	nuclear receptor subfamily 1 Group H
Nrd	NAADP ROCS Discovered
P_o	open state probability
$P2Y_{11}$	P2Y purinoceptor 11
PAC	pancreatic acinar cell
PDAC	pancreatic ductal adenocarcinoma
PI	propidium iodide
PI(3,5)P2	phosphatidylinositol 3,5-bisphosphate
PIP_2	phosphatidylinositol 4,5-bisphosphate
PLC	phospholipase C
PM	plasma membrane
PMCA	plasma membrane calcium ATPase
POAEE	palmitoleic acid ethyl ester
PP	polypeptide
ROCS	Rapid Overlay of Chemical Structures
ROI	region of interest
ROS	reactive oxygen species
RR	ruthenium red
RyR	ryanodine receptor
$RyR3^{-/-}$	ryanodine receptor type 3 knockout
SAM	sterile alpha motif
SCID T cell	severe combined immunodeficiency T lymphocyte

SERCA	sarco/endoplasmic reticulum calcium ATPase
shRNA	short hairpin RNA
SOCE	store-operated calcium entry
Sp	*Strongylocentrotus purpuratus*
SR	sarcoplasmic reticulum
STIM	stromal interaction molecule
TMB-8	3,4,5-trimethoxybenzoic acid 8-(diethylamino)octyl ester
TC	taurocholate
TDC	taurodeoxycholate
Tg	thapsigargin
TLC-S	taurolithocholic acid 3-sulfate
TPC	two-pore channel
TPCN2$^{-/-}$	two-pore channel type 2 knockout
TPCN1/2$^{-/-}$	two-pore channel type 1 and type 2 double knockout
TPEN	N,N,N′,N′-Tetrakis(2-pyridylmethyl)ethylenediamine
Trien	triethylenetetramine
TRPC	transient receptor potential canonical
TRP-ML	transient receptor potential mucolipin
TRPM	transient receptor potential melastatin
U-73122	1-[6-[((17β)-3-Methoxyestra-1,3,5[10]-trien-17-yl)amino]hexyl]-1H-pyrrole-2,5-dione
V-ATPase	Vacuolar-type H+-ATPase
ZINC	Zinc Is Not Commercial

CHAPTER 1:
INTRODUCTION

Chapter 1: Introduction

1.1 Calcium signalling

1.1.1 Calcium as a signal

The importance of calcium ions (Ca^{2+}) on cellular processes was first identified in 1883 by Sydney Ringer during the development of his physiological saline solution (Ringer 1883). He observed that solutions made with tap water rather than distilled water allowed the continued beating of an isolated frog heart due to a contaminate he identified as lime (Ca^{2+}). Since this initial discovery, Ca^{2+} has been shown to act as an intracellular signal in most cell types studied and play a role in a wide range of cellular processes (Berridge et al. 2000).

Ca^{2+} can interact with many important biological molecules thanks to its physical properties (Jaiswal 2001) and proteins have evolved a specific structural domain, the EF hand, to do so (Schäfer and Heizmann 1996). Binding of Ca^{2+} to these domains can have a drastic effect on their activity (Ikura 1996); making Ca^{2+} a potent signal. Due to its ability to interact with biological molecules excessive Ca^{2+} is toxic to cells casing disruption of lipid membranes, aggregation of proteins and nucleic acids, and precipitation of phosphates. Because of this, all cellular life has evolved a system of pumps and exchangers to maintain Ca^{2+} homeostasis (Case et al. 2007). Eukaryotic cells maintain a resting cytosolic Ca^{2+} concentration ($[Ca^{2+}]_c$) around 100 nM compared to an extracellular concentration of 1 mM ($[Ca^{2+}]_e$). Eukaryotes make a greater use of Ca^{2+} signalling than prokaryotes, this is probably due to the presence of organelles in eukaryotic cells, which act as intracellular Ca^{2+} stores (Williams 1980). This creates three possible mechanisms for an increase in $[Ca^{2+}]_c$: entry of Ca^{2+} from the extracellular space, release from organelles or a coordination of the two (Chavis et al. 1996).

1.1.2 Calcium Homeostasis

Homeostasis is a process by which various elements of a biological system act to maintain a state of equilibrium; one such example is the $[Ca^{2+}]_c$ which is maintained by a series of ion channels, pumps and organelle stores, which together form the cell's 'Ca^{2+} signalling toolkit' (Berridge et al. 2003). As Ca^{2+} itself is a potent signal, involved in a wide and diverse range of cellular processes (Berridge et al. 2000), increases in $[Ca^{2+}]_c$ occur often in cells and must rapidly be returned to resting levels (*Fig. 1.1.2*).

The largest source of increases to $[Ca^{2+}]_c$ is entry of Ca^{2+} from the extracellular space, with Ca^{2+} freely moving down a concentration gradient through the opening of channels in the plasma membrane (PM) (Clapham 2007). Cells can be divided into two types, excitable and non-excitable, based on whether or not they express voltage-gated channels in their plasma membranes, though both express ligand gated channels (Mahaut-Smith et al. 2016). Voltage-gated channels are gated by the electrical potential across the plasma membrane, allowing rapid entry of Ca^{2+} in response to depolarisation of the membrane (Catterall 1995). As non-excitable cells lack these types of channel, there are resistant to changes in membrane potential.

While extracellular Ca^{2+} might be the largest pool from which $[Ca^{2+}]_c$ increases can occur, it is not the sole source. The ability of physiological stimuli to induce $[Ca^{2+}]_c$ increases in Ca^{2+} free extra cellular conditions (Chew 1986), shows the presence of a stored pool of Ca^{2+} within cells that can readily be mobilized.

The endoplasmic reticulum (ER), or the sarcoplasmic reticulum (SR) in myocytes, forms the largest Ca^{2+} store in most cells (Verkhratsky 2005), with a luminal free Ca^{2+} concentration ($[Ca^{2+}]_l$) in the 100 µM range (Lam and Galione 2013). $[Ca^{2+}]_l$ storage is facilitated by various Ca^{2+} binding proteins, e.g. calsequeastrin and calreticulin (Milner et al. 1992), which

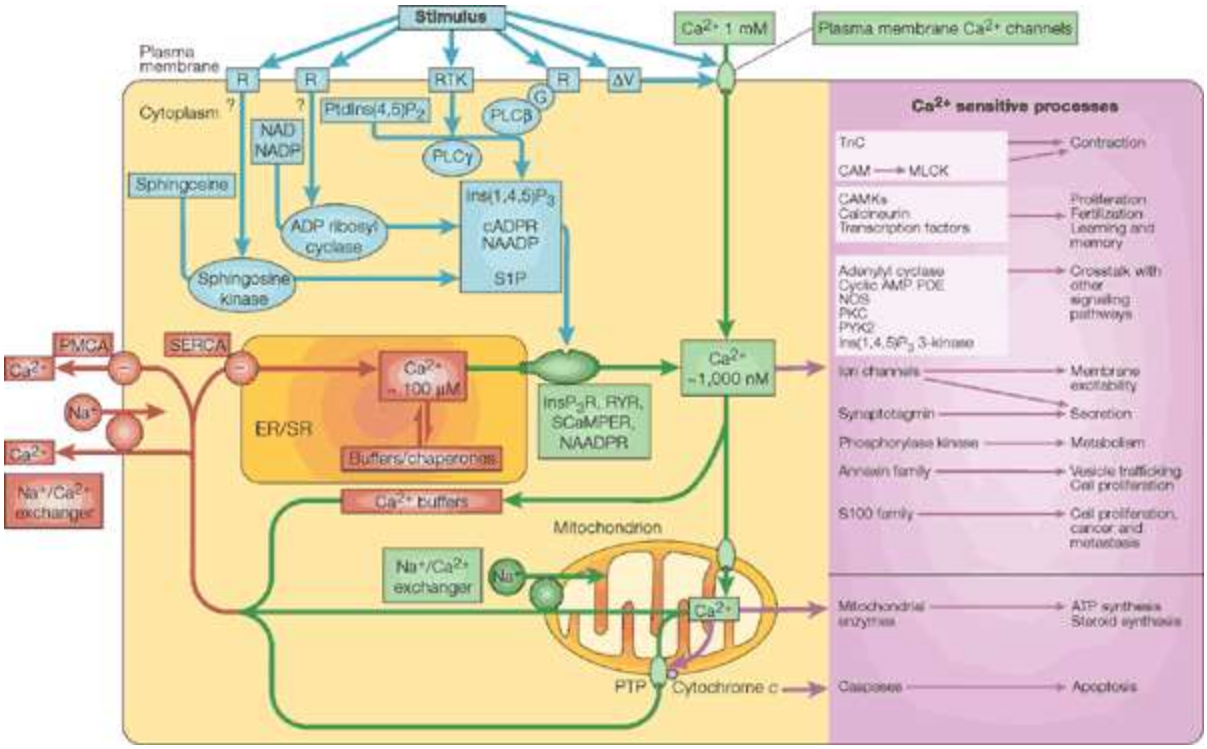

Fig. 1.1.2 The cell's 'Calcium Signalling Toolkit'

Stimuli at the cell's plasma membrane can induce elevations in cytoplasmic calcium either by the influx of extracellular calcium through the opening of plasma membrane channels, the release of calcium from organelle stores via the production of intracellular messengers or a combination of the two. Such elevations can drive a range of calcium sensitive cellular processes. Cytoplasmic calcium is restored to resting levels by extrusion from the cell, uptake into organelle stores or binding by buffer proteins.

prevent the toxic effects mentioned previously. Release of Ca^{2+} from the ER is tightly controlled by ligand gated ion channels, the activation of which results in a rapid increase in $[Ca^{2+}]_c$ (Streb et al. 1983). Maintenance of $[Ca^{2+}]_l$ is achieved by the sarco/endoplasmic reticulum Ca^{2+} ATPase (SERCA) (Periasamy and Kalyanasundaram 2007), which actively pumps Ca^{2+} from the cytoplasm into the ER lumen. This action reduces the $[Ca^{2+}]_c$ and increases the $[Ca^{2+}]_l$ after efflux of Ca^{2+} into the cytosol, aiding in cellular Ca^{2+} homeostasis. Myocytes show coupling of voltage gated channels in the plasma membrane to channels in their SR, allowing for a depolarization in the plasma membrane to trigger a release of Ca^{2+} from the SR (Dulhunty et al. 2017).

Mitochondria also play an important role in Ca^{2+} homeostasis, acting as buffers in response to elevations in $[Ca^{2+}]_c$ (Williams et al. 2013). Such an elevation results in a rapid influx of Ca^{2+} into mitochondria via the mitochondrial Ca^{2+} uniporter (MCU) (Kirichok et al. 2004) which uses the negative charge of the inner mitochondrial membrane to facilitate uptake. This is followed by a slower release of Ca^{2+} back into the cytosol by mitochondrial Sodium (Na^+) Ca^{2+} exchanger (NCLX). The rapid influx of Ca^{2+} into the mitochondria prevents a toxic level of $[Ca^{2+}]_c$ being reached, while the slow extrusion creates a smaller increase in $[Ca^{2+}]_c$ which is taken back up by the ER via SERCA pumps. Increases in mitochondrial Ca^{2+} also trigger the production of ATP (Tarasov et al. 2012), ensuring that there is a ready supply of the nucleotide for the Ca^{2+} ATPases that help restore resting $[Ca^{2+}]_c$ by pumping Ca^{2+} across membranes against its concentration gradient.

In recent years it has become apparent that the ER is not the only Ca^{2+} store in cells, with a range of acidic organelles combining to form a pool of mobilizable Ca^{2+} (Patel and Docampo 2010). Of these organelles lysosomes have received the largest amount of interest, due to the disruption of lysosomes by glycyl-L-phenylalanine-naphthylamide (GPN) blocking aspects of

Ca^{2+} release (Churchill et al. 2002). Other organelles have also been shown to release Ca^{2+}, e.g. the nucleus (Gerasimenko et al. 2003) or the Golgi body (Yang et al. 2015); though due to the amount of Ca^{2+} contained within these organelles there is only small localised elevation in $[Ca^{2+}]_{c,}$ which is probably linked to the organelle's function, e.g. gene transcription (Brailoiu et al. 2006).

In addition to buffering by mitochondria and uptake back into stores, elevations in $[Ca^{2+}]_c$ are returned to resting levels by extrusion of Ca^{2+} across the plasma membrane into the extracellular space. This is performed actively by the plasma membrane Ca^{2+} ATPase (PMCA) (Carafoli 1991) and in excitable cells by secondary active transport via Na^+ Ca^{2+} exchangers (NCX) (Dipolo and Beaugé 2006).

Together this community of stores, buffers and pumps create a dynamic system; where by a rapid elevation in $[Ca^{2+}]_c$ can occur in response to stimuli, allowing the activation of Ca^{2+} binding proteins and a physiological response. This elevation in $[Ca^{2+}]_c$ is then returned to basal levels before a cytotoxic level of $[Ca^{2+}]_c$ is reached and allows for repeat stimulation of cells to occur.

1.1.3 Secondary messengers

Various extracellular messengers (e.g. Thrombin (Sacks et al. 2008), insulin (Contreras-Ferrat et al. 2010) or ghrelin (Camiña et al. 2003)) have been found to be capable of inducing increases in the $[Ca^{2+}]_c$ by inducing the release of Ca^{2+} from intracellular organelle Ca^{2+} stores. As these extracellular messengers act on receptors located on the plasma membrane of cells there is a need for the creation of a second messenger within the cell to convey the extracellular messenger's signal to the organelle stores. Currently three such intracellular

secondary Ca^{2+} messengers have been identified: Inositol Trisphosphate (IP_3), cyclic ADP-Ribose (cADPR) and Nicotinic Acid Adenine Dinucleotide Phosphate (NAADP) (Berridge et al. 2003).

1.1.3.1 IP_3-induced calcium release

IP_3 was the first of these messengers identified by Berridge et al. in 1983. Using the salivary glands from blowfly he showed that there was an increase in IP_3 in response to 5-hydroxytryptamine (Berridge et al. 1983), which was known to induce fluid secretion via an increase in $[Ca^{2+}]_c$ (Prince et al. 1972). Its Ca^{2+} mobilizing activity was then confirmed in pancreatic acinar cells (PAC), where micromolar concentrations were shown to induce a rise in intracellular Ca^{2+} from a non-mitochondria store (Streb et al. 1983). Since this initial discovery IP_3 has been shown to have activity in a range of different cell types including leukocytes (Burgess, McKinney, et al. 1984), hepatocytes (Burgess, Godfrey, et al. 1984) and β cells (Biden et al. 1984).

Production of IP_3 occurs via the hydrolysis of plasma membrane associated phosphatidylinositol 4,5-bisphosphate by phospholipase C (PLC) into IP_3 and diacylglycerol (Berridge et al. 2000). There are multiple isoforms of PLC (Rhee 2001), which can be activated by various mechanisms in a stimuli specific manner (Berridge et al. 2003), allowing for an integration of stimuli or creating cell specificity for a signal.

IP_3 mobilizes Ca^{2+} from the ER (Delfert et al. 1986), as seen by its sensitivity to thapsigargin (Tg), which inhibits SERCA pump (Thastrup et al. 1990). IP_3 induces Ca^{2+} release though its own receptor (IP_3R) (Mourey et al. 1990), of which there are three isoforms that can form either homo or heterotetramers (Taylor et al. 1999). IP_3R's also show a sensitivity to

increases in $[Ca^{2+}]_c$, with uncaging of Ca^{2+} able to induce release of Ca^{2+} from the ER via IP_3R's (Wang et al. 2006). This phenomenon, named Ca^{2+}-induced Ca^{2+} release (CICR), creates a form of positive feedback that amplifies the amount of Ca^{2+} released in response to a stimulus. While IP_3 has been shown to bind directly to its receptor (Ferris et al. 1989; Mignery and Südhof 1990; Yoshikawa et al. 1999) it has been suggested that rather than directly gating the channel itself it promotes the binding of Ca^{2+} to the receptor, which in turn induces opening of the channel's pore (Taylor et al. 2004). This would suggest that IP_3's mechanism of action is to reduce the requirement for CICR to occur.

1.1.3.2 cADPR-induced calcium release

Despite IP_3's Ca^{2+} mobilizing activity being demonstrated it was thought unlikely to be the sole secondary messenger used by cells due to the spatiotemporal calcium release exhibited in response to distinct or integrated stimuli. Lee et al. had previously reported that IP_3 was able to mobilise Ca^{2+} from a non-mitochondrial store via a novel assay using sea urchin egg homogenate (Clapper and Lee 1985). Using this new assay they decided to test the effect of pyridine metabolite nucleotides, which were known to alter in concentration during fertilization (Schomer and Epel 1998) with NAD being rapidly phosphorylated, and the resulting NADP being reduced to NADPH.

Lee's group found that both NAD and NADP could mobilize Ca^{2+} from stores in the homogenate at physiological concentrations, after a short delay in the case of NAD but not NADP (Clapper et al. 1987). This delay in response to NAD could be abated by an alkaline pre-treatment prior to use on the homogenate. The same alkaline pre-treatment on NADP significantly reduced the concentration required to activate Ca^{2+} release; indicating that a modification to the nicotinamide of both dinucleotides is required for the activity observed

for both NAD and NADP. Not knowing what these modified forms of the dinucleotides were Lee named them *E*-NAD and *A*-NADP respectively, unknowingly having discovered both cADPR and NAADP.

As well as discovering what would later be identified as the two secondary messengers, Lee's paper also identified several of the characteristics of their signalling. First, both *E*-NAD and *A*-NADP acted on a store that was not the mitochondria, as previously suggested for the release of Ca^{2+} induced by pyridine nucletodies (Frei et al. 1985). The second characteristic observed was that repeat applications of a single activator (either of these new messengers or IP_3) showed desensitisation, with the Ca^{2+} response to subsequent applications being diminished compared to the initial release. However, application of a second different activator following treatment with one of the other two still produced a large response, implying that the three act independently of each other. Finally, separation of organelle stores by gradient centrifugation showed a partial separation of *A*-NADP's activity from that of *E*-NAD and IP_3, with all three acting on non-mitochondrial stores. These observations, over time, would be confirmed and lay the foundation for the mechanism and kinetics of these secondary Ca^{2+} messengers.

With the discovery that an active form of both NAD and NADP could induce release from Ca^{2+} stores Lee et al. then aimed to identify the molecular structure of these compounds. The first to be identified was *E*-NAD two years later through a combination of techniques, and found to be to be cADPR (Lee et al. 1989). The newly identified messenger was shown to mobilize Ca^{2+} in a receptor dependent manner; with its activity distinct from IP_3's, but from overlapping Ca^{2+} stores (Dargie et al. 1990). Pituitary cells were the first mammalian cell type shown to be sensitive to cADPR-induced Ca^{2+} release (Koshiyama et al. 1991); with a

diverse range since also found to be sensitive including T-lymphocytes (Bruzzone et al. 2003), smooth muscle (Bai et al. 2005) and mesenchymal stem cells (Tao et al. 2011).

cADPR acts on the same ER Tg-sensitive store as IP_3, and (due to its sensitivity to micromolar concentrations of ryanodine) cADPR induced Ca^{2+} release was identified as occurring through ryanodine receptors (RyR) (Mészáros et al. 1993). These channels are closely related to IP_3R in structure and activity (Taylor and Tovey 2010; Amador et al. 2013), indicating a shared evolutionary history between the activity of IP_3 and cADPR. They are activated by Ca^{2+} binding to its large cytoplasmic domain (Hadad et al. 1994), with RyR1 displaying a bell-shaped dependence towards Ca^{2+} (Meissner 1984). RyR form large multi-proteins complexes both in the cytoplasm and ER lumen (Lanner et al. 2010), with many of them affecting their activity (Bers 2004). This includes calmodulin in the cytoplasm (Fruen et al. 2000) and calsequestrin in the lumen (Beard et al. 2004); as the activity of these proteins is also modulated by binding Ca^{2+} it adds extra complexity to how Ca^{2+} affects the gating of RyR. Several members of the FKBP family of proteins, which bind the immunosuppressant drug FK506 (Marks 1996), have been found to have a potent effect on RyR's activity. FKBP12 and FKBP12.6 associate with RyR1 and RyR2 respectively (Jayaraman et al. 1992; Timerman et al. 1996), stabilizing the channel in its closed state and reducing its sensitivity to Ca^{2+} (Timerman et al. 1993; Xiao et al. 1997). When the respective protein dissociates from the channel it enters a state of subconductance, where it is sensitized to Ca^{2+} again (Brillantes et al. 1994). Similarly, FKBP12 has been found to modulate the activity of IP_3R by affecting their interaction with various other proteins (MacMillan et al. 2005).

Unlike IP_3, which binds directly to its receptor (Ferris et al. 1989; Mignery and Südhof 1990; Yoshikawa et al. 1999); cADPR does not do so to RyR's (Walseth et al. 1993); however it does still act on them by increasing their sensitivity to CICR (Galione et al. 1991), which they

are a major component of (Imagawa et al. 1987). Of the three RyR isoforms (Lanner et al. 2010), cADPR has only been shown to affect the opening of the RyR2 and RyR3 isoforms (Lee 1997), with its activity dependent on the presence of calmodulin (Lee et al. 1994). The actual mechanism by which cADPR potentiates RyR sensitivity to CICR is unknown, with several suggested models. The most basic model is that cADPR increases RyR's sensitivity to the $[Ca^{2+}]_c$; alternatively it may sensitise RyR's by increasing the $[Ca^{2+}]_l$ (Lukyanenko et al. 2001); or it might bind to FKBP12.6, causing its dissociation from RyR's (Tang et al. 2002).

1.1.3.3 NAADP-induced calcium release

While *E*-NAD was quickly identified as cADPR (Lee et al. 1989); the other unknown Ca^{2+} releasing pyridine nucleotide (Clapper et al. 1987), *A*-NADP, proved harder to identify. Lee et al. found commercially available NADP displayed the ability to mobilize Ca^{2+} from sea urchin egg homogenate that had been desensitised to both high concentrations of IP_3 and cADPR with no delay, implying that the active form of NADP was present in the commercial product. A combination of three different chromatographic and spectrographic techniques were used to isolated and identify *A*-NADP from NADP, using the alkaline-activation process used in the previous report to maximise the yield of *A*-NADP. These techniques indicated that the active compound was NAADP (Lee and Aarhus 1995), a compound with a high structural similarity to NADP that only differs in the substitution of a nicotinamide group with a nicotinic acid group. This relatively simple structural substitution was enough to provide Ca^{2+} mobilizing activity, as HPLC purified NADP (which lacks any NAADP contamination) had no activity when applied to sea urchin egg homogenate. Lee et al. suggested the presence of the contaminate NAADP in the commercially available NADP was

due to a simple deamination of some of the NADP, though questioned if this would be the reaction used in the NAADP synthesis pathway *in vivo* or if phosphorylation of NAAD was a more viable alternative.

NAADP's identity was confirmed by a second group (Chini et al. 1995), who also looked at its Ca^{2+} release properties in the sea urchin egg homogenate compared to the other two Ca^{2+} moralizing agents, IP_3 and cADPR. As described in Lee' original paper, repeat applications of NAADP were shown to be auto-desensitizing but have no effect on subsequent applications of cADPR or IP_3. Additionally, while NAADP induced Ca^{2+} release could be blocked by TMB-8 (a non-specific $[Ca^{2+}]_i$ release inhibitor (Chiou and Malagodi 1975)) its activity was insensitive to both heparin and ruthenium red (RR), inhibitors of IP_3 and cADPR-induced release respectively (Taylor and Broad 1998). The group also found thionicotinamaide-NADP (thio-NADP) blocked NAADP induced release, but showed no effect on either IP_3 or cADPR induced Ca^{2+} release. A lack of interaction between the binding of the three Ca^{2+} mobilizing agents to the sea urchin egg homogenate was also observed, as pre-incubation of any of the three did not diminish the subsequent binding of a radio-labelled form of either of the other two messengers.

While the previous work into NAADP's activity had all taken place using either homogenates of sea urchin eggs or microsomes isolated from them, Perez-Terzic et al. used intact eggs and microinjected to introduce the messenger into their cytosols (Perez-Terzic et al. 1995). In these experiments NAADP clearly showed the ability to increase $[Ca^{2+}]_i$ upon its addition and showed the same lack of desensitisation to pre-application of either IP_3 and cADPR observed in the homogenate. Co-application of heparin with NAADP showed no effect on NAADP's activity like it did when co-applied with IP_3; however pre-incubation with thio-NADP inhibited NAADP-induced increases of $[Ca^{2+}]_i$, but did not affect increases induced by the

other messengers. Interestingly the group found that microinjection of NAADP into eggs that were already fertilized showed a much diminished Ca^{2+} response compared to unfertilised cells, similar to how responses are reduced after subsequent applications of NAADP.

While these experiments were far from conclusive they hinted at a possible role for NAADP in fertilisation, which would be the first cellular process linked to NAADP signalling. This function was given further weight upon the discovery that the level of NAADP present in sperm significantly increases when the sperm encounters egg jelly during the acrosome reaction (Churchill et al. 2003), allowing the sperm to deliver a bolus of NAADP into the cytosol of the egg when its membrane and that of the egg fuse. There has been some dispute as to the role of NAADP in fertilisation however; with some advocating that it is not a bolus of NAADP that sperm delivers but an isoform of Phospholipase C (Nomikos et al. 2012). In this model the PLCζ delivered by the sperm converts PIP_2 in the egg's membrane into IP_3, which in turn generates the Ca^{2+} waves seen during fertilisation, implying that NAADP is not required for this cellular process.

The first proof of NAADP being able to induce Ca^{2+} release in mammalian cells was observed using pancreatic acinar cells (PAC) (Cancela et al. 1999), the same cell model used to confirm the role of IP_3 (Streb et al. 1983). This report found that nanomolar concentrations of NAADP induced Ca^{2+} in PAC but showed no effect at higher micromolar concentrations, suggesting the messenger causes rapid receptor desensitisation at these concentrations. While a desensitising concentration of NAADP had no effect on IP_3 or cADPR induced Ca^{2+} spikes, inhibitors of the other messengers blocked responses to NAADP. This implied that the observable response to NAADP was distinct from the activity of IP_3 and cADPR; but did require the involvement of their associated ion channels to increase its response by the process CICR, which both IP_3R and RyR are known to be sensitive to (Santulli and Marks

2015). These results were replicated in the sea urchin egg model (Churchill and Galione 2001) in accordance with the previous finding that, unlike IP_3 and cADPR, NAADP acted on a Ca^{2+} store that was Tg insensitive (Genazzani and Galione 1996). Together this lead to the creation of the 'trigger hypothesis' of NAADP activity; which suggests that NAADP is able to mobilise a small amount of Ca^{2+} from a store distinct from that which both IP_3 and cADPR act on, this initial Ca^{2+} release then acts as a trigger to induce further Ca^{2+} release through IP_3R and RyR via CICR, thus amplifying the size of the response to NAADP.

Density centrifugation of sea urchin egg homogenates showed that NAADP's activity was physically distinct from that of IP_3 and cADPR, corresponding with its insensitivity to Tg. The fraction it showed activity in contained the egg's reserve granules, a type of acidic organelle related to lysosomes in mammalian cells (Churchill et al. 2002). This corresponded with latter findings in several mammalian cell types; where NAADP's activity is also Tg insensitive (Mitchell et al. 2003) , but can be disrupted by either Bafilomycin A1 (Brailoiu et al. 2005) (an inhibitor of the Vacuolar-type H+-ATPase (V-ATPase) used to fill acid organelles with Ca^{2+} (Gagliardi et al. 1999)) or GPN (Collins et al. 2011) (which causes the osmotic lysis of lysosomes (Berg et al. 1994)). These findings heavy imply that NAADP acts on lysosomes in mammalian cells, an argument strengthened by the lysosomal location of several NAADP receptor candidates (Calcraft et al. 2009; Zhang et al. 2009). There is however evidence that addition to acidic stores NAADP can also mobilize some Ca^{2+} from the ER in some types of mammalian cells (Gerasimenko et al. 2003; Gerasimenko, Sherwood, et al. 2006; Steen et al. 2007) and in higher plants (Navazio et al. 2000).

Since Streb et al.'s report, NAADP has been shown to have a signalling function in a diverse range of mammalian cells, e.g. sperm (Churchill et al. 2003), neurones (Brailoiu et al. 2005), cardiac myocytes (Macgregor et al. 2007) and β cells (Mitchell et al. 2003); as well as in

higher plants (Navazio et al. 2000). While NAADP showed the ability to inhibit its own activity in both the sea urchin egg model and in mammalian cells, it showed a different mechanism of auto-inhibition in the two. Sea urchin eggs pre-incubated with a sub-activating concentration of NAADP show no response to subsequent applications of normally activating concentrations of NAADP (Aarhus et al. 1996). However in mammalian cells there is a bell-shaped curve of NAADP induced Ca^{2+} release (Berg et al. 2000); with nanomolar concentrations showing a dose-depended response which then become inhibitory at micromolar concentration with 100 µM NAADP enough to completely inhibit NAADP induced release (Galione et al. 2011). While these patterns of auto-inhibition do differ they both suggest that NAADP acts on its receptor via two separate binding sites, an activating one and an inhibitory one, which have different affinities to NAADP. Evidence for this has been provided pharmacologically, using agents that affect NAADP's activity and ability to bind to its receptor differently (Rosen et al. 2009). Such variance between invertebrate and mammalian signalling may indicate that there has been an evolution event that may have greatly reduced the affinity of the regulatory NAADP-binding site on the mammalian NAADP receptors.

NAADP shows a high degree of structural similarity with NADP, which shows no Ca^{2+} mobilizing activity, with an amino group substituted for a hydroxyl group the only difference between the two compounds (Lee and Aarhus 1995). It is unsurprising therefore that the negative charge the hydroxyl group of the carboxylic acid residue provides, specifically at the 3-position on the pyridine ring, has been found to be a key structural requirement for NAADP's activity (Lee and Aarhus 1997). The 2'-phosphate attached to the ribose and the amino group at the 6-postion of the adenine ring have also been shown influence the messenger's activity, but are less vital than 3-position of the carboxylic acid residue. The

mammalian cell line SKBR3 showed diminished sensitivity when modifications were made to the 4- and 5- position of nicotinic acid, whereas sea urchin eggs only show sensitivity to modifications at the 4- position (Ali et al. 2014).

1.1.3.4 NAADP synthesis

After discovering cADPR and its action mobilizing Ca^{2+} from internal stores Lee and his collaborators wanted to identify how this metabolite of NAD was synthesised in vitro. All previously identified NADases cleaved NAD into nicotinamide and ADPR, meaning that either one of these previously identified enzymes had an alternative activity as a cyclase or a novel enzyme was involved. In a two part study, a novel NADase from the mollusc *Aplysia californica* was identified and purified (Hellmich and Strumwasser 1991; Lee and Aarhus 1991). This enzyme was shown to both synthesis cADPR from NAD, and induce an increase in extracellular Ca^{2+} when microinjected into sea urchin eggs. The enzymes showed a high specificity for β-NAD as a substrate, lacking activity for a range of NAD analogues other than a limited activity for NADH. This also suggested that the reaction the enzyme catalysed was direct and not via an intermediate, e.g. ADP-ribose, as it displayed no activity for these compounds. To distinguish it from the NADases that had been previously characterised it was named ADP-ribosyl cyclase due to its unique cyclase activity.

Using the protein sequence of the new identified enzyme a search of the GenBank library was conducted to identify any possible mammalian homologues (States et al. 1992). This sequence comparison identified CD38 as a candidate, which shares a 69% sequence homology with ADP-ribosyl cyclase. CD38 is a 46kDa type 2 plasmalemma glycoprotein, with its N-terminus forming a transmembrane domain and its C-terminus locating extracellularly. Previously it had been identified as a phenotype marker indicating different

subpopulations of human T and B lymphocytes, appearing on their surfaces during both the early and late, but lacking during the intermediate, stages of their maturation (Jackson and Bell 1990); as well as a cell marker for leukaemia (Deaglio et al. 2008). The two peptides differ in two key aspects: ADP-ribosyl cyclase lacks the transmembrane domain and the four glycosylation sites of CD38, which are likely due to the different cellular locations of the two proteins.

Expression of the C-terminus of CD38, the region with a similar peptide sequence to ADP-ribosyl cyclase, produces a peptide that experimentally can both catalyse the formation and hydrolysis of cADPR (Howard et al. 1993). Additionally glucose-induced insulin secretion by β cells (Takasawa et al. 1993), a process shown to involve cADPR, can be impaired using CD38 autoantibodies (Ikehata et al. 1998). Together these findings indicate that CD38 is the cyclase that catalyses the physiological production (and degradation) of cADPR in mammalian cells.

The initial experiments that discovered the existence of both cADPR and NAADP showed that NAADP could be produced artificially by exposing NADP to an alkaline pre-treatment (Clapper et al. 1987). However, psychologically a different reaction involving the base exchange of NADP's nicotinamide group and nicotinic acid (NA) occurs. Interestingly this reaction can be catalysed by either ADP-ribosyl cyclase or the C-terminus of CD38 (Aarhus et al. 1995); meaning these are multifunctional enzymes involved in the production of two independent secondary Ca^{2+} messengers (*Fig. 1.1.3.4*). This alternative enzymatic function requires a high concentration of NA and an acidic environment, which implies it does not occur under standard cytoplasmic conditions (Casey et al. 2010). It also suggests a common origin for both NAADP and cADPR, as they are both synthesised from nicotinic nucleotides by the same enzyme, possibly originating as a single pathway that diverged into two separate

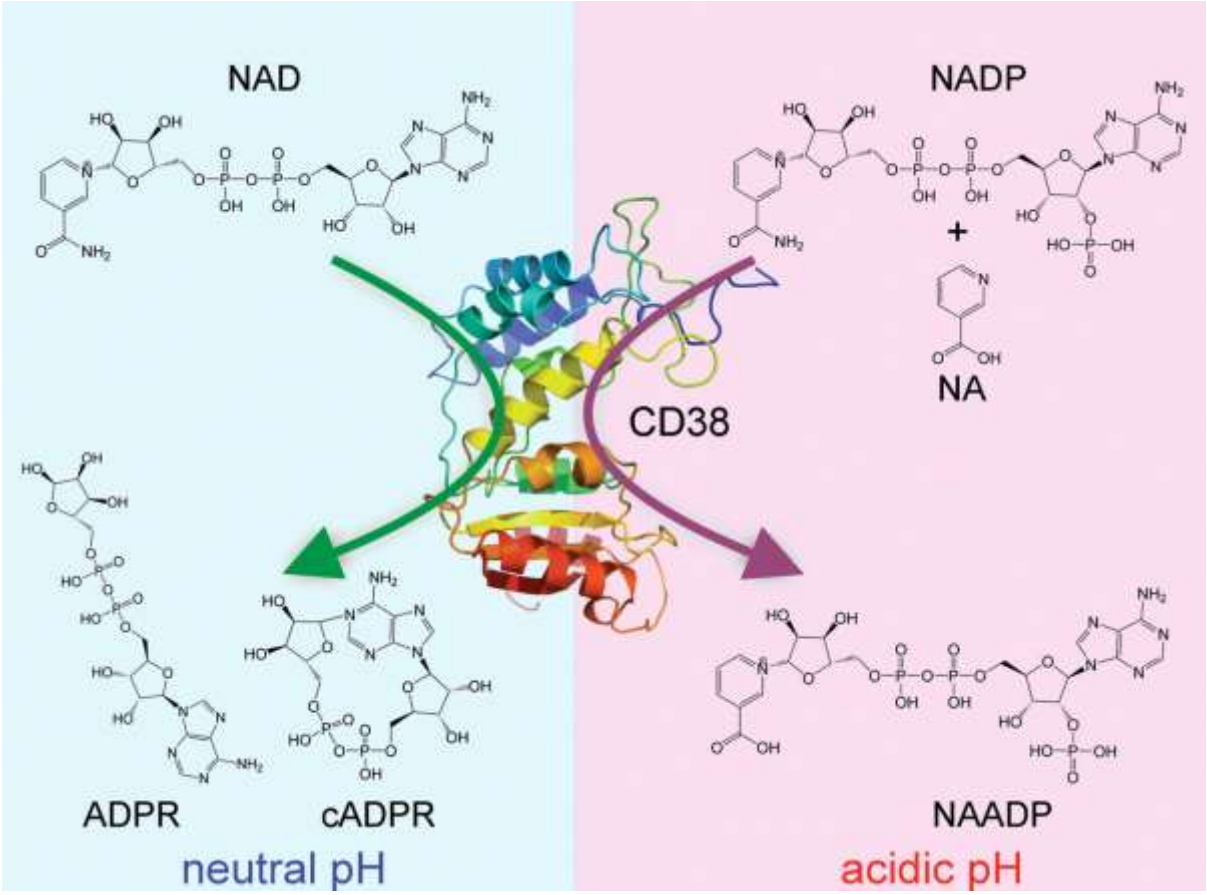

Fig. 1.1.3.4 CD38 is an ectoenzyme that can synthesize both secondary calcium messengers cADPR and NAADP

CD38 can synthesize either cADPR or NAADP from NAD or NADP and nicotinic acid depending on the reaction conditions; the enzyme can also hydrolyze cADPR into ADPR.

Yongjuan Zhao, Richard Graeff and Hon Cheung Lee; Roles of cADPR and NAADP in pancreatic cells; *Acta Biochim Biophys Sin* (Shanghai); 2012; 44 (9): 719-729; by permission of Oxford University Press (Zhao et al. 2012).

signalling pathways.

Despite having been shown to be capable of catalysing the synthesis of both cADPR and NAADP, there is some controversy as to whether CD38 is the endogenous mammalian ADP-ribosyl cyclase. This is due to cataylic domain of CD38 (Howard et al. 1993; Aarhus et al. 1995) existing in the extracellular region of the protein. This creates a 'topological paradox' where the protein's active site is physically isolated from both its substrates and/or the site of its product's activity across a lipid membrane (De Flora et al. 1997).

To try and solve the topological paradox several models have been suggested including a transport model and orientation model. The transport model was proposed for cADPR synthesis, it proposes that the NAD is transported out of the cell by connexin 43 and then the resultant cADPR produced is transported back into the cell by nucleoside transporters (Guida et al. 2002; Tao et al. 2011). Alternatively it has been suggested that polymers of CD38 can form channels that allow NAD and cADPR to cross the membranes (Franco et al. 1998), however this is disputed (da Silva et al. 1998). Several cell lines have been shown to take-up both radiolabelled cADPR and NAADP (Billington et al. 2006); though due to the kinetics of cADPR and NAADP signalling, which are very rapid (especially in the case of NAADP), it is unlikely uptake is physiologically relevant. However, in the case of NAADP it would support the evidence that it can act on several cell types extracellularly (Moreschi et al. 2008; Djerada et al. 2013); which otherwise would require NAADP synthesised intracellularly to be excreted by cells.

The orientation model suggests that a subset of CD38 (that normally exists in a type 2 orientation with its C-terminus located in the lumen during synthesis and transport, or extracellularly at the plasmalemma) has its orientation rotated to type 3 with its C-terminus located in the cytosol. This would allow easy access for either NAD or NADP to CD38's

cyclase active site and would be a better fit for the kinetics of the secondary messengers signalling. There are several studies supporting this model of CD38 activity (Adebanjo et al. 1999; Khoo et al. 2000), one of which shows several mutations to the N-terminus CD38 can affect orientation and activity of CD38 (Zhao et al. 2015). These mutations all reduce the positive charge of the short native intracellular N-terminus region of CD38 either directly by increasing or decreasing the number of negative or positively charge residues respectively, or indirectly by introducing residues prone to phosphorylation; which, following the 'positive-inside rule' (von Heijne 1989), would reverse the topology of the protein. This model is suitable for explaining cADPR synthesis but does not explain how the conditions for NAADP (low pH and high concentration of NA) would occur.

A third model proposes that CD38 can 'escape' from the ER after synthesis via lipid droplets (Ploegh 2007), though this would share the same issues with the orientation model for NAADP signalling and lacks evidence supporting it.

It is possible that synthesis of NAADP occurs in the lumen of one or more type of intracellular organelle that CD38 localises to (Yamada et al. 1997; Orciani et al. 2008). The conditions inside these lumens would be more conducive to the production of NAADP and create a physically distinct way in which it and cADPR are synthesised. However, like the transport model described above, the kinetics of transporting NADP into and NAADP out of the organelles raises doubt as to the viability of this model.

As well as its cyclase active site being located extracellularly, another reason it is disputed that CD38 is the sole ADP-ribosyl cyclase in mammals is the effect observed when its gene is knocked out of cells or animals. In CD38 null mice a reduction in cADPR synthesis is observed in some cell types but not in others (Young et al. 2006) and in CD38 deficient myometrial cells there is no difference in NAADP levels compared to wildtype cells (Soares

et al. 2007). Due to the wide range of cellular process that cADPR and NAADP have been linked to it is unlikely that CD38 is the sole cyclase, otherwise CD38 null mice should not be viable.

Some redundancy in ADP-ribosyl cyclase activity has been observed, with CD157 being shown to contain some activity (Yamamoto-Katayama et al. 2002). Like CD38 this protein is a cell surface antigen and acts as a mediator of neutrophil adhesion and migration (Funaro et al. 2004), as such the two proteins share around high degree of sequence homology (33%) (Ferrero et al. 1999) and a similar structure. The expression of CD157 is limited to a few types of tissue though (Ortolan et al. 2002) and by sharing a structure with CD38 it also shares the same topological paradox in its activity. There is also evidence in neurones from CD38 null mice that there is a separate intracellular ADP-ribosyl cyclase present (Ceni et al. 2003); this may mean there is at least one more protein with the ability to synthesise cADPR and/or NAADP.

1.1.3.5 NAADP receptors

As NAADP Ca^{2+} mobilizing activity was found to be distinct from that of both IP_3 and cADPR (Chini et al. 1995; Lee and Aarhus 1995), it was believed that it would act via a unique 'NAADP receptor'. It was assumed that like IP_3R (Mourey et al. 1990) this unidentified receptor would be a ligand-gated ion channel, which was responsible for both NAADP binding and channel activity. The search for such a receptor has yielded several possible candidates and proven controversial within the field.

1.1.3.5.1 Ryanodine receptors

The initial candidate identified were the RyR family of channels, with NAADP most commonly being associated with the type 1 isoform. This link was established using both cardiac (Mojžišová et al. 2001) and skeletal myocytes (Hohenegger et al. 2002); the first study patched RyR2 from dog cardiac microsomes incorporated into lipid bilayers and observed NAADP increased their opening potential. The probability of an observed RyR2 opening correlated in line with the concentration of NAADP over the range tested and could be blocked by several RyR inhibitors. The second study used preparations of heavy sarcoplasmic reticulum membranes from rabbit white skeletal muscle to produce vesicles containing purified RyR1 and used them to perform a series of florescent and electrophysiological assays. NAADP was observed to increase opening potential of the RyR1 and could mobilised Ca^{2+} from these vesicles, but displayed the same sensitivity to the RyR inhibitors seen in the other study. [^{3}H]ryanodine binding to purified RyR1 has also been shown to increase in the presence of NAADP, though this effect could be blocked by a NAADP antagonist (Dammermann et al. 2009).

Activation of type 1 RyR by NAADP is attractive as it has been suggested that this isoform is insensitive to cADPR (Lee 1997), and therefore would mean that the isoform is still be regulated by a secondary messenger. As cADPR and NADDP display a probable shared evolutionary background (evident in their similar molecular precursors, NAD and NADP (Clapper et al. 1987), and single enzymatic catalyst (Aarhus et al. 1995)), it would be logical that they work on the same family of receptors and potentially could have evolved along with them.

The suggestion of one or more isoforms of RyR acting as a NAADP sensitive ion channel has proven controversial ever since its proposal. RyR are located on the ER/SR of most cells and

not the acidic vesicles that NAADP has been shown to act upon (Churchill et al. 2002), their location on the ER/SR is also incompatible with the insensitivity that NAADP induced Ca^{2+} release shows to Tg (Mitchell et al. 2003). One study has claimed to show that both type 1 and type 2 RyR have no sensitivity to NAADP (Copello et al. 2001); this study also claimed the same for cADPR however, against the general consensus of the field (Venturi et al. 2012), and so its validity is questionable. Other groups have also produced negative data for RyR's when presenting alternative proteins as NAADP sensitive Ca^{2+} channels in order to validate their alternative (Pitt et al. 2010; Zhang et al. 2011).

Despite this controversy there is growing evidence that NAADP can act via RyR in at least some cell types (Mitchell et al. 2003; Langhorst et al. 2004; Jiang et al. 2013), notably PAC (Gerasimenko et al. 2003; Gerasimenko, Sherwood, et al. 2006; Gerasimenko et al. 2015). In this type of secretory cell, in addition to their conventional ER location both RyR and IP_3R are located in the membranes of acidic secretory granules. The first study that showed that NAADP can act upon RyR using this cell type observed that NAADP could mobilise a small observable amount of Ca^{2+} from the nuclear envelope (Gerasimenko et al. 2003), the lumen of which is continuous with that of that of the cell's ER. It is possible that Ca^{2+} release from this store is used to drive the activity of transcription factors and therefore gene expression, which NAADP has shown to do in neurones (Brailoiu et al. 2005). NAADP induced Ca^{2+} release from the nuclear envelope was sensitive to Tg, unlike the acidic store it is classically associated with, and could be blocked by use of either of the RyR inhibitors ryanodine or RR. These factors heavily imply that, at least in the case of this intracellular store, NAADP mobilises Ca^{2+} through RyR. Interestingly a high auto-inhibitory concentration of NAADP did not prevent cADPR induced Ca^{2+} release from this store, this would indicate that either the two messengers act on RyR through different mechanisms or possibly in the isoform

dependent manner previously suggested. In addition to the nuclear store NAADP has been show to mobilise Ca^{2+} from both acidic and ER stores via RyR's under normal physiological conditions in this cell type (Gerasimenko, Sherwood, et al. 2006). A second cell type in which there is strong evidence for NAADP acting on RyR are T cells, whose activation requires transient intracellular Ca^{2+} signals. Knockout of RyRs from the Jurkat cells (an immortalized human T lymphocyte line) (Dammermann and Guse 2005) or RyR1 from primary murine T cells (Wolf et al. 2015) either abated or significantly reduced the NAADP-induced Ca^{2+} signals observed.

1.1.3.5.2 TRP-ML1

Despite RyR being reported as acting as NAADP sensitive intracellular ion channels, the scepticism of some in the field meant that the search for the 'true NAADP receptor' continued. This lead to the identification of a second potential candidate, nonspecific cation channel transient receptor potential mucolipin 1 (TRP-ML1). TRP-ML1 is a nonspecific cation channel located on lysosomal and late endosomal membranes (Waller-Evans and Lloyd-Evans 2015); mutation to which can cause the lysosomal storage disease, mucolipidosis IV (Sun et al. 2000).

Zhang et al. demonstrated its candidacy in a series of papers (Zhang and Li 2007; Zhang et al. 2009; Zhang et al. 2011) using a range of different cell types and several different techniques. The first paper (Zhang and Li 2007) used lysosomes and ER microsomes isolated from the livers of male Sprague Dawley rats and reconstituted into lipid bilayers for patch clamp analysis. The lysosome bilayers could be activated by NAADP in the *cis* solution but not the *trans* and showed the bell shaped dose response to NAADP that it is classically associated with. However, neither IP_3 or a low concentration of ryanodine elicited a response and

blockers of both IP_3R and RyR failed to inhibit a response to NAADP. Several voltage-gated calcium channel antagonists, e.g. nifedipine, which had previously been shown to block NAADP induced Ca^{2+} release in sea urchin eggs; were all capable of reducing the opening potential elicited by NAADP to varying degrees. Alternatively, the ER enriched bilayers showed an increase in opening potential when treated with cADPR, which could be blocked with a high concentration of ryanodine, but not when treated with NAADP. The group reported that a TRP-ML1 polyclonal antibody attenuated the response of the lysosome bilayers to NAADP in a concentration dependent manner, though no evidence was provided to support the specificity of the antibody used. The second paper (Zhang et al. 2009) confirmed the findings of the first using lysosomes purified from coronary atrial myocytes, which showed the same pharmacological profile to the lysosome-lipid bilayers used in the previous report (unresponsive to IP_3 or cADPR, no effect on NAADP induced release by antagonist of the other messengers and blocked to a varying degree by a range of compounds previously shown to reduce NAADP-induced Ca^{2+} release or by a TRP-ML1 Ab in a dose dependent manner). The group's final paper (Zhang et al. 2011) supporting TRP-ML1 as a NAADP sensitive lysosomal ion channel used human fibroblasts to observe the effect of knocking TRP-ML1 out of cells and then restoring its expression. NAADP induced Ca^{2+} release in wild type cells, but had no effect on TRP-$ML1^{-/-}$ cells; restoring the channel's expression to knockout cells rescued NAADP's effect. Interactions between lysosomes and endosomes were observed in WT cells which could be increased by the addition of NAADP, any increase induced by NAADP could be decreased below that of untreated cells by addition of either a Ca^{2+} chelator or NAADP antagonist. KO of TRP-ML1 significantly reduced these interactions compared to unstimulated WT cells, restoring the channel re-established NAADP's ability to stimulate interactions between the organelles.7 A BODIPY-FL C5-LacCer BSA complex was used to measure lipid trafficking, WT cells exposed treated with

the fluorescent lipid showed a small amount of colocalization with lysosomes. This colocalization was significantly increased by the addition of NAADP, whose effect could be reduced by a pre-treatment of its antagonists or bafilomycin A1. Hardly any colocalization was observed in TRP-ML1$^{-/-}$ cells even when treated with NAADP, however a significant increase occurred when the protein was reintroduced and treated with NAADP.

Together these results gave a strong case for TRP-ML1's candidacy as a NAADP sensitive ion channel, as well as providing further scepticism to RyR's also being so. TRP-ML1's lysosomal location, combined with the bell-shaped dose response to NAADP and it response to the various pharmacological agents tested makes it an appealing prospect. Additionally the group's work shows a direct role for NAADP in endocytosis and lipid trafficking; this fits with another group's observation that irregular Ca^{2+} handling by lysosomes occurs in Niemann-Pick disease type C1 (Lloyd-Evans et al. 2008 p.1), another lysosomal storage disease like mucolipidosis IV.

However like with RyR there is evidence to the contrary, over expression of TRP-ML1 neither increases the binding of radiolabelled NAADP in NRK cells (Pryor et al. 2006) or increases release in response to NAADP in SKBR3 cells (Yamaguchi et al. 2011). No significant difference was observed in the response of pancreatic acinar cells from TRP-ML1$^{-/-}$ mice compared to wild type cells to NAADP cells (Yamaguchi et al. 2011). There is evidence supporting TRP-ML1 having an alternative function to that of a NAADP sensitive ion channel. This includes it being a $PI(3,5)P_2$ sensitive Ca^{2+} ion channel instead of a NAADP sensitive one (Dong et al. 2010 p.5) or a lysosomal Ca^{2+} leak channel (Lee et al. 2015). Alternatively it has been suggested that instead of a Ca^{2+} channel it is a proton channel involved in the acidification of the lysosomal lumen (Soyombo et al. 2006), though this has been disputed (Kogot-Levin et al. 2009). There is also evidence for it being an iron channel

(Dong et al. 2008); however as the channel is an unselective cation channel (also known to be permeable to Na^+ and K^+ (Cheng et al. 2010)) it may be multifunctional with a varying ion permeability (dependent on the stimulus and/or the luminal and cytosolic conditions (Xu et al. 2007; Lee et al. 2015)). One possibility is that as TRP-ML1 easily forms complexes with other proteins (Miedel et al. 2006) it may act as a subunit of a NAADP receptor complex, even if this is just a scaffolding role rather than acting as an ion channel. This could explain some of the results that Zhang et al. produced, e.g. an antibody for TPR-ML1 could prevent it from associating with other proteins and therefore prevent formation of receptor complex. This is a possibility as it has been found that while TRP-ML1 and TPCs, the other family of lysosomal ion channels linked to NAADP induced Ca^{2+} release, do not affect each other's activity they do associate with one another (Yamaguchi et al. 2011).

As well as TRP-ML1; two other TRP proteins, both of the TRP melastatin (TRPM) sub family, have been reported as acting as being activated by NAADP. With TRPM2 reported as having NAADP-induced activity in T cells (Beck et al. 2006), neutrophils (Lange et al. 2008), β cells (Lange et al. 2009) and HEK cells (Starkus et al. 2010); additionally NAADP has been reported to activate TRPM4 in HeLa cells (Ronco et al. 2015). Unlike TRP-ML1 however, it has not been suggested that NAADP acts directly on TRPM2 or TRPM4; but instead may do so indirectly by its activity affecting the membrane potential of lysosomes or their luminal pH (Lu et al. 2013), which can affect TRPM channel opening (Starkus et al. 2010). Another possibility is that NAADP could enhance the interaction between the TPRM channels and their endogenous ligands (Lange et al. 2008).

1.1.3.5.3 Two-pore channels

Two-Pore Channels were identified as NAADP sensitive ion channels in reports by three independent research groups released within several months of each other in 2009 (E. Brailoiu et al. 2009; Calcraft et al. 2009; Zong et al. 2009). The family of ion channels was identified when looking for an evolutionary midpoint between the families of voltage-gated Ca^{2+} and Na^{+} channels comprised of four homologous six transmembrane domains and the single domain channels like voltage-activated K^{+}. A channel was cloned from rat kidneys and named TPC1 based on its structure, but no function could be discerned when it was expressed in xenopus oocytes (Ishibashi et al. 2000). Homologues of this protein were found in multiple species of plant, with several paralogs found in some (Hashimoto et al. 2004; Kadota et al. 2004; Kurusu et al. 2004); these channels were localised to the vacuole (an acidic organelle in plants related to the eukaryotic lysosome) and found to act as a Ca^{2+} dependent Ca^{2+} release channels required for several physiological processes in plants (Peiter et al. 2005). Due to the conflicting data surrounding RyR's and TRPM-ML's and their possible roles as NAADP sensitive channels, TPC's made an enticing prospect as an alternative candidate as they had no know function in mammalian cells but had been shown to act as a Ca^{2+} channel in plants and were localised to plant vacuoles (an acidic organelle that is the functional equivalent of lysosomes in mammalian cells (Wink 1993)).

Three members of the TPC family have been have been identified in animals, with equal evolutionary divergence (Calcraft et al. 2009). In primates the expression of TPC3 has been lost as the gene has been truncated, it is also not present in some species of rodent, including mice and rats, where the gene is completely deleted. As some species of rodent do express TPC3, e.g. rabbits and squirrels, and the difference in the type of mutation implies that the it

was lost independently in primates and the rodent species but was redundant in both (Zhu et al. 2010).

Human TPC's are widely expressed throughout the body; with both isoforms being found most types of tissue tested, though with a varied level of expression. Colocalization assays with cell markers showed TPC1 primary with the endosomal marker endo-GFP and to a much lesser degree the lysosomal marker LAMP-1 (E. Brailoiu et al. 2009). TPC2 however only colocalizes with the lysosomal marker; meaning both channels are found in the membranes of the acidic organelles of the endolysosomal system but to distinct components. When TPC3 from chickens was expressed in HEK cells it colocalized with TPC1, alternatively when rabbit TPC3 was expressed in these cells it colocalized with both TPC1 and TPC2 (Ogunbayo et al. 2015). Such colocalization may indicate a possible redundancy of function between the proteins and explain why they are lacking in some species. TPC1 also has been found to have an splice variant that colocalizes with TPC2 rather than to endosomes (Ruas et al. 2014), though the physiological relevance of this variant has not been reported.

NAADP has been heavily implicated in the release Ca^{2+} from lysosomes (Churchill et al. 2002; Yamasaki et al. 2004), and because of TPC2's location exclusively in the membranes of these organelles two of the three groups (Calcraft et al. 2009; Zong et al. 2009) decided to solely investigate the relationship between this channel and NAADP. Alternatively, the third group focused on NAADP's relationship with TPC1 (E. Brailoiu et al. 2009). However, all three groups decided to use a genetic approach to maximise any effect observed.

The two groups investigating TPC2 both decided to heterologously express the channel in HEK293 cells, which express it at low endogenous levels (Galione 2011). Together they found that by increasing the channel's expression there was a corresponding increase in NAADP binding membranes from TPC2 over expressing cells compared to wildtype ones.

Additionally, there was an increase in the size of the NAADP-induced Ca^{2+} response, which varied directly in relation to the level of TPC2 expression. TPC2 overexpressing cells still showed the characteristic bell shaped dose response curve to NAADP and inhibition of signalling by pre-treatment with bafilomycin. Pre-treatment of TPC2 overexpressing cells with shRNA for TPC2 also inhibited the NAADP response. No response was observed when the overexpressing cells were treated with NADP, demonstrating the response is unique to NAADP. The two groups disagreed slightly over the effect of pre-treating cells with Tg, one group saw no effect while the other saw a significant reduction in the Ca^{2+} response to NAADP. It is possible that this difference is due to one group expressing human TPC2 and the other murine; both results however, do demonstrate that Ca^{2+} is being mobilized from a non-ER store in their TPC2 overexpressing cells. To confirm their results from cultured cells one of the groups decided to test a possible physiological role of TPC2 in primary cells by producing $TPC2^{-/-}$ mice and observing its effect on pancreatic β-cells. Previously it had been shown that NAADP-induced Ca^{2+} release in these cells triggers a Ca^{2+}-activated cation current across the plasma membrane (Mitchell et al. 2003; Naylor et al. 2009); when the group looked for these cation currents in β-cells from $TPC2^{-/-}$ mice none could be measured in response to NAADP.

The third group testing TPC1's interaction with NAADP also chose to over express their target protein, however unlike the other groups they decided to use SKBR3 cells, which they had previously used to characterise NAADP effect on (Schrlau et al. 2008). Overexpression of TPC1 produced similar results to over expressing TPC2 (an increase in the response to NAADP which could be inhibited by pre-incubation with bafilomycin or reduced by pre-incubation with either ryanodine or TPC1 shRNA). Targeted mutation of the predicted pore forming region of TPC1 to reduce its permeability of Ca^{2+} also reduced the size of the Ca^{2+} response to NAADP. However, the group expressing murine TPC2 also did express murine

TPC1 in their experiments and observed little to no effect of NAADP on it. It is possible that this is a result between differential channel activity between the two species or because a lack of coupling between TPC1 and the ER via CICR, producing only very small localised increases in $[Ca^{2+}]_c$ compared to the much larger global responses elicited by the TPC2 expressing cells (Zhu et al. 2010).

Expression of TPC3 from the sea urchin *Strongylocentrotus purpuratus* (*Sp*) in mammalian cells has provided conflicting results. In SKBR3 cells a clear Ca^{2+} response to NAADP that was significantly larger than that in WT cells was observed in *Sp*TPC3 transfected cells, though much smaller than that observed in cells transfected with either *Sp*TPC1 or *Sp*TPC2 from the urchin (Brailoiu et al. 2010). When the three proteins were independently expressed in HEK293, both *Sp*TPC1 or *Sp*TPC2 expression resulted in a significant increase in NAADP-induced Ca^{2+} release, however *Sp*TPC3 appeared to inhibit Ca^{2+} release to levels below that of the WT control (Ruas et al. 2010). The differences in results seen may be cell specific or due to the two groups who produced these reports using different constructs of the *Sp*TPC3 gene.

Despite this evidence indicating that TPC's act as a NAADP sensitive Ca^{2+} channel, this function has been questioned (Wang et al. 2012; Cang et al. 2013). In the first of two studies by Ren's & Xu's groups vacuolin-1enlarged endolysosomes were patched and reported to have a $PI(3,5)P_2$ induced Na^+ current, but very limited permeability to Ca^{2+} and no sensitivity to NAADP (Wang et al. 2012). $PI(3,5)P_2$ is a phosphoinositide specific to the membranes of endolysosomes (Di Paolo and De Camilli 2006), which has been linked to Ca^{2+} homeostasis of these organelles (Dong et al. 2010). The activity observed was specific to $PI(3,5)P_2$ but not to a range of other phosphoinositides and was not present when enhanced endolysosomes from TPC double KO mice were patched. NAADP alone elicited no response and had no

effect on the response observed when used in combination with $PI(3,5)P_2$ compared to using the lipid alone. While permeability to Ca^{2+} was observed for hTPC2 it was significantly low to that of Na^+ and Li^+. The Ren group's second study reported that the Na^+ mobilizing activity of TPC's were sensitive to inhibition by ATP via a mTOR dependent process, and forms complexes with the kinase (Cang et al. 2013). TPC's association with mTOR gave them the ability to sense nutrient depletion. This fits with previous findings that mTOR translocates off lysosomal membranes upon nutrient depletion (Sancak et al. 2010; Korolchuk et al. 2011), which would remove its kinase activity from TPC's and therefore their inhibition by ATP.

A key argument presented by Ren & Xu groups against NAADP acting on TPC's was the finding that the response to the secondary messenger was not diminished in *Tpc1*$^{-/-}$*/Tpc2*$^{-/-}$ β cells (Wang et al. 2012). These findings however have been challenged, as it was observed that the knockout cells used to show this apparent lack of TPC sensitivity to NAADP could still express approximately 91% of the protein's structure and still responded to NAADP (Ruas et al. 2015). As such, a new TPCN1/2$^{-/-}$ mouse was produced which demonstrated no expression of either TPC isoform. Cells from these new double knockout animals showed no response to NAADP, but were restored when wild type TPC's were re-expressed in the TPCN1/2$^{-/-}$ cells. β cells from these knockout animals were found to be NAADP insensitive (Arredouani et al. 2015), contradicting Ren & Xu group's findings (*Fig. 1.1.3.5.3.1*). TPC's activity has been reported to be regulated by a range of factors; including $[Mg^{2+}]_c$, NAADP, $PI(3,5)P_2$, its phosphorylation state, luminal pH, $[Ca^{2+}]_l$ and membrane potential (Pitt et al. 2010; Rybalchenko et al. 2012; Jha et al. 2014). They have also been reported as being non-selective cation channels with a permeability order of $H^+ >> K^+ > Na^+ \geq Ca^{2+}$ (Pitt et al. 2014), but physiologically are likely to be selective for Ca^{2+} due to the concentration and

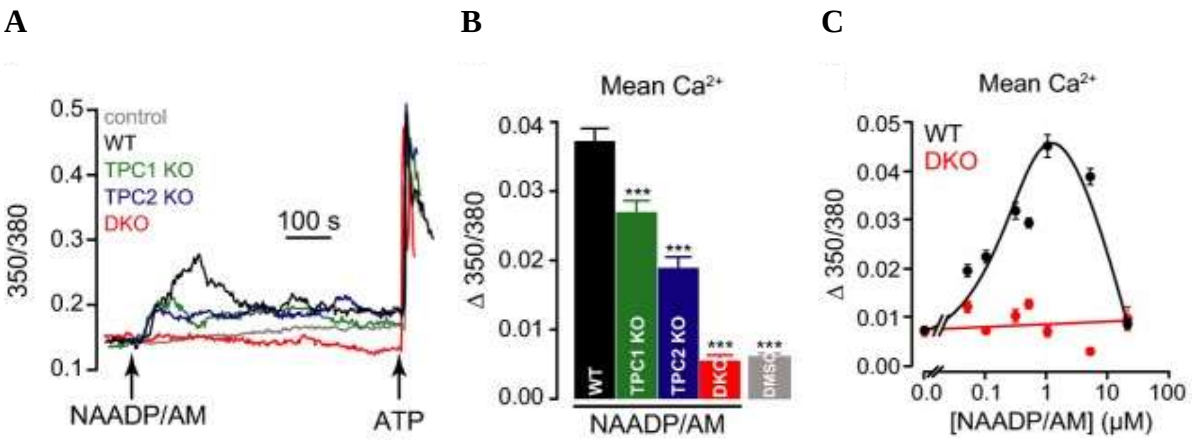

Fig. 1.1.3.5.3.1 TPC 1/2 double knockout mice are insensitive to NAADP

(A) Representative traces of single cell fura-2 recordings of mouse embryonic fibroblasts (MEF) isolated from wild-type (WT), *Tpcn1*$^{-/-}$ (TPC1 KO), *Tpcn2*$^{-/-}$ (TPC2 KO), and *Tpcn1/2*$^{-/-}$ (DKO) animals with the addition of NAADP-AM or DMSO control and ATP positive control. **(B)** Mean calcium release over a 500 s period upon addition of NAADP-AM or DMSO control; n =384-621 cells; ***$P < 0.001$ relative to WT using the ANOVA–Tukey test. **C** Mean calcium response to a range of NAADP-AM concentrations in MEF isolated from WT and DKO cells; n = 41-105 cells.

electrophysiological gradients across lysosomal membranes. Together this evidence has resulted in Ren's group findings that TPC channels are $PI(3,5)P_2$ and ATP sensitive, can be regulated by mTOR and are Na^+ permeable being accepted within the field (Jha et al. 2014); but their assertion that TPC's are NAADP insensitive being rejected (Ruas et al. 2015).

TPC proteins dimerize to form ion channels, and have been shown to form both homo and heterodimers (Rietdorf et al. 2011). TPCs have two domains, each comprised of 6 transmembrane regions; the first 4 transmembrane regions of each of a TPC proteins 2 domains are required for dimerization, while the 5^{th} and 6^{th} are responsible for the pore forming loop (Churamani et al. 2012).

The crystal structure of TPC1 from the plant *Arabidopsis thaliana* has recently been resolved (Guo et al. 2016; Kintzer and Stroud 2016) (*Fig. 1.1.3.5.3.2*), supporting the predicted mammalian structure of TPC. This structure included an EF-hand domain close to the cytosolic C-terminus end of TPC1 with 2 EF-hand motifs, which suggests that Ca^{2+} binding to these motifs may induce a conformational change in the channel. As mammalian TPC1 had previously been reported to be voltage sensitive (Rybalchenko et al. 2012), it was not surprising that the structure contained a voltage sensing domain in the loop between the 1^{st} and 2^{nd} transmembrane regions of each domain; with the channel's voltage sensing ability conferred by the second of the two domains. While the structure of TPC1's ion selectivity filter is similar to the related Na_v and Ca_v channels, it lacks the specific anionic residue known to confer selectivity for either Na^+ or Ca^{2+} (Payandeh et al. 2011; Tang et al. 2014); this matched the predicted *in silico* model (Rahman et al. 2014) and supports the lack of TPC cation specificity (Pitt et al. 2014). In accordance with previous reports of its activity (Cang et al. 2013; Jha et al. 2014), the protein's structure showed multiple possible phosphorylation sites. Interestingly, while *Arabidopsis thaliana* TPC1 (*At*TPC1) has been reported as being

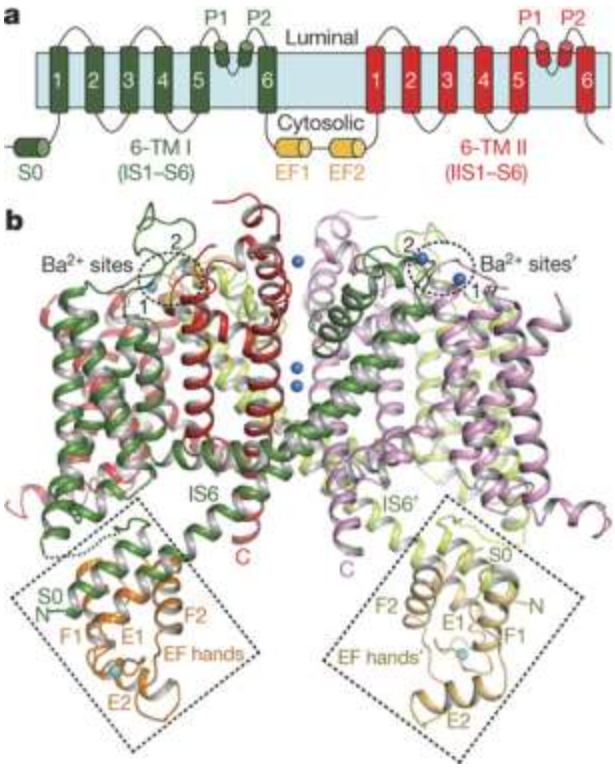

Fig. 1.1.3.5.3.2 X-ray crystallography structure of *Arabidopsis thaliana* TPC1

(A) Topological diagram of a single *Arabidopsis thaliana* TPC1 protein. **(B)** Side view of an *Arabidopsis thaliana* TPC1 channel dimer. The 6-TM I, 6-TM II, and EF hands from one subunit are shown in green, red and orange, respectively; with the other subunit's symmetrical domains shown in lime green, purple and light orange, respectively. The cytosolic EF-hand domains with bound Ca^{2+} (cyan sphere) in EF1 are boxed and the two luminal Ba^{2+} (blue spheres labelled 1 and 2) binding sites are circled.

insensitive to both NAADP and PI(3,5)P_2 (Boccaccio et al. 2014) its structure did show a binding site for *trans*-Ned19, a NAADP specific antagonist that shares a high 3D electrostatic homology to NAADP (Naylor et al. 2009). Ned-19 was found to bind both the pore domains and voltage sensitive domains, allosterically blocking channel activation. It has also been found that the C-terminal end of *At*TPC1 contains a helix forming motif that is required for both the dimerization of TPC proteins and their channel activity (Larisch et al. 2016). The lumenal N-terminal end of both human isoforms of TPC have been found to contain three glycosylation sites (Hooper et al. 2011), site directed mutations that prevent glycosylation enhanced the size of the response to NAADP.

While it was expected that the 'NAADP-receptor' would contain both NAADP-binding and channel activity, this has been found to not be the case for TPC channels. Studies in both sea urchin eggs and mammalian cells using radiolabelled photoprobe 5-azido-NAADP ([^{32}P-5N_3]NAADP) (which has a high affinity for the NAADP receptor and cross links to in under UV light) found no change in probe binding when TPC's were either over expressed or knocked out (Lin-Moshier et al. 2012; Ruas et al. 2015). Western blotting with antibodies for the various TPC isoforms performed using both sea urchin egg homogenate and mammalian cell preparations did not show antibody binding to the same band as the probe, but immunoprecipitation of TPC's did show some co-precipitation with the probe (Walseth et al. 2012). Using radiolabelled NAADP to identify the size of NAADP binding proteins, several different weight bands were labelled in sea urchin egg homogenate (Walseth et al. 2012); with the strongest binding at both 40 and 45 kDa. However in mammalian cells, NAADP was found to bind to a range of low weight peptides both of the S100 cytoplasmic and the P100 membrane fraction, consistently labelling a 22/23kDa (Lin-Moshier et al. 2012; Walseth et al. 2012). The difference in the size between the urchin and mammalian proteins may be related

to the different profiles of activation described previously between the species (Aarhus et al. 1996; Berg et al. 2000)

These finding prove that NAADP does not act directly on TPC channels, but instead associates with TPC via one or more separate binding proteins. The discovery of NAADP binding proteins opens a range of possibilities: are there multiple binding proteins that affect NAADP's activity on a cell specific basis? Will different NAADP-binding proteins associate with different ion channels, meaning there is no single 'NAADP receptor'? Is the two binding site model of NAADP activity still relevant, and if so are the two sites on the same binding protein?

NAADP binding proteins are not the only proteins that have been found to associate with TPC channels, and are likely to form signalling complexes in the membranes of their associated organelles. Both human TPC isoforms have been found to associate with another 'NAADP receptor' candidate, TRP-ML1; though neither isoform of TPC channel was found to affect TRP-ML1's activity and vice versa (Yamaguchi et al. 2011). Based on its ability to locate to lysosomal membranes and its effect on TPC channels it is likely mTOR can associate with any complex TPC's form (Cang et al. 2013). Yeast two hybrid assays have identified the anti-apoptotic protein Hax-1 (Sharp et al. 2002) as binding to the cytoplasmic region of TPC2 (Lam et al. 2013). A 'One-*Strep*' pull down method has also been used to identify proteins that associate with TPC's, creating a TPC 'interactome' (Lin-Moshier et al. 2014). This technique identified 40 different proteins that have been reported to have a range of different functions including Ca^{2+} homeostasis, membrane trafficking/organisation and autophagy regulation. The Rab GTPase Rab7 was found to associate with the N-terminus of TPC2, but not TPC1; together Rab7 and TPC2 were found to cause the proliferation of endolysosomal structures. This association appears to be dependent on the lysosomal pH, as

over expression of TPC2 increases their pH and shows a reduced association with Rab7 (Lu et al. 2013).

While TPC's activity has been shown to be independent of RyR (Brailoiu et al. 2010; Ogunbayo et al. 2011), there is conflicting evidence where TPC can directly couple to IP_3R or RyR and may do so in a cell specific manner (Davis et al. 2012; Jiang et al. 2013).

Despite some reports to the contrary (Wang et al. 2012; Cang et al. 2013), it is now commonly accepted that the TPC family of proteins form NAADP sensitive ion channels, with their sensitivity to NAADP conferred via one or more separate NAADP-binding proteins. TPC's have been shown to have a physiological role in a range of different cell types, including: megakaryoblasts (López et al. 2012), neuronal precursor cells (Zhang et al. 2013), gastric smooth muscle (Pereira et al. 2014), cardiac ventricular myocytes (Capel et al. 2015) and β cells (Arredouani et al. 2015). While activity in such a wide range of different cells highlights the ubiquity of TPC activity, it raises the question of their physiological importance due to the viability of TPC1/2$^{-/-}$ mice (Ruas et al. 2015).

1.1.3.5.4 $P2Y_{11}$

As a secondary messenger NAADP is classically associated as having an intracellular target (Galione et al. 2010), however there is some limited evidence that NAADP may also act extracellularly. Extracellular application of NAADP to 1321N1 human astrocytoma cells induced an increase in $[Ca^{2+}]_i$ in a dose-dependent manner, via a combination of the entry of extracellular Ca^{2+} and the production of intracellular cAMP, IP_3 and cADPR (Moreschi et al. 2008). This response to extracellular NAADP was also observed in human granulocytes, where a similar effect had previously been seen in this cell type in response to NAD via a

$P2Y_{11}$- dependent mechanism had previously been reported (Moreschi et al. 2006). Based on this the $P2Y_{11}$ specific inhibitor NF157 (Ullmann et al. 2005), which had been shown to inhibit the effect of NAD on granulocytes, was tested against NAADP's effect. NF157 had a similar inhibitory effect against the $[Ca^{2+}]_i$ increases induced by extracellular NAADP; implying it also acted via the $P2Y_{11}$ receptor, but as a more potent ligand.

Extracellular NAADP was also found to have a protective effect against ischemia and reperfusion injury in Langendorff perfused rat hearts (Djerada et al. 2013). This cardioprotective effect was inhibited by NF157 and found to be due to the activation of pro-survival protein kinases. In cultured rat cardiomyocytes an increase in intracellular cADPR and NAADP was found in response to extracellular NAADP, NAD or NF546 (a $P2Y_{11}$ agonist (Meis et al. 2010)). The intracellular effects of all 3 extracellular stimuli could be inhibited by NF157; implying extracellular NAADP can induce the production of intracellular NAADP via $P2Y_{11}$ most likely via the activation of CD38.

1.1.3.6 Pharmacological Regulation of NAADP Signalling

Research into NAADP signalling has been greatly facilitated by the development of chemical analogues of the molecule. The first chemical analogue developed was an inactive caged form of the dinucleotide (H. C. Lee et al. 1997), which can be injected into cells and uncaged using ultraviolet light, allowing for precision activation of NAADP signalling (Aarhus et al. 1996). While characterising the structural requirements for NAADP activity several analogues were created that could be used as antagonists, e.g. deA-NAADP (Lee and Aarhus 1997). However, no use of any of these analogues has subsequently been reported; this may be due to them being impermeable to cells and acting via similar a method of desensitisation to NAADP, which unlike the analogues is commercially available. Additionally as a result of

this study several active fluorescent analogues of NAADP were created (Lee and Aarhus 1998), though again no further use has been reported. A radiolabelled form of NAADP, synthesised using ^{32}P, has been used to show the distribution of NAADP binding in whole tissues (Patel et al. 2000). A membrane permeable analogue of NAADP has also been created, via the reversible addition of acetoxymethyl (AM) groups (Parkesh et al. 2008). NAADP-AM is a potent tool as it means NAADP signalling can be visualised in whole colonies of cells rather than in individual cells, and removes the previous intrusive techniques used to apply NAADP to cells.

As it has become apparent that NAADP-regulated Ca^{2+} signalling plays a vital role in a diverse range of mammalian cell there is a need for drugs to regulate abnormal signalling in patients. Such drugs could possibly be used to treat type 2 diabetes by stimulating insulin secretion (Arredouani et al. 2015), thrombosis by preventing platelet activation (López et al. 2006), or help trigger an immune response by activating T-cells (Steen et al. 2007). The first reported antagonist of NAADP's activity was thio-NADP (Chini et al. 1995; Perez-Terzic et al. 1995); however when this compound's activity was analysed in sea urchin egg homogenate it was found to have the same profile as commercial NADP. This combined with HPLC evidence suggests that rather than thio-NADP being an NAADP antagonist, it is in fact an NAADP contaminate in the thio-NADP (similar to how NAADP was discovered as a contaminate of commercial NADP (Lee and Aarhus 1995)) that inhibits its own activity (Dickey et al. 1998). Pharmacological blockers of L-type Ca^{2+}-channels, e.g. Diltiazem, can inhibit NAADP signalling in excitable cells (Genazzani et al. 1997; López et al. 2006), though the effect of these compounds is nonspecific and may not be direct. Triazine dyes have been shown to be NAADP agonists in sea urchin eggs (Billington et al. 2004), though again this effect is nonspecific and has not been shown in mammalian cells.

Recently the existence of membrane permeable antagonists of NAADP-induced Ca^{2+} release have been published (Dammermann et al. 2009; Naylor et al. 2009). The first was identified using *in silico* screening of a library of compounds to identify ones with a similar 3D electrostatic structure to NAADP (Naylor et al. 2009). The 19th ranked hit of this search proved to be both membrane permeable and inhibit both NAADP's activity and its binding to it receptor. Based on the name of the software application used to identify the compound and its hit number it was called NAADP EON Discovered 19 (Ned-19). As the key structural requirement for NAADP's activity is its nicotinic acid residue (Lee and Aarhus 1995; Lee and Aarhus 1997) various chemical analogues of nicotinic acid were synthesised. One of these analogues named BZ194 was found to inhibit the NAADP-dependent proliferation of T cells, as well as NAADP-induced binding of [^{3}H]ryanodine to purified RyR1 (Dammermann et al. 2009). These compounds have both been shown to inhibit responses to NAADP in several different cell types (Cordiglieri et al. 2010; Barceló-Torns et al. 2011; Coxon et al. 2012; Aley et al. 2013; Nebel et al. 2013); with Ned-19 the most commonly used of the two, probably due to its commercial availability.

1.1.4 Store-operated calcium entry

Elevations in the $[Ca^{2+}]_c$ are a ubiquitous signal, driving numerous physiological processes (Berridge et al. 2000); however prolonged elevations in $[Ca^{2+}]_c$ are cytotoxic (Schanne et al. 1979) to cells. This means any elevation in $[Ca^{2+}]_c$ is rapidly dealt with via either extrusion (Brini and Carafoli 2011) or uptake into organelle stores (Prins and Michalak 2011) to return the $[Ca^{2+}]_c$ back to resting levels. The ER comprises the largest Ca^{2+} store in most cells types, and is therefore the major source of Ca^{2+} release within cells (Lam and Galione 2013). Each time this store is stimulated to release Ca^{2+}, some of that Ca^{2+} mobilized is lost via extrusion or uptake into other type of organelle (Berridge et al. 2003). This means without a specific

refilling pathway, the Ca^{2+} content of the ER would diminish, and cellular process driven by Ca^{2+} release from this store would become unviable.

A model for this process based on previously published data was proposed by J Putney in 1986 (Putney 1986); this biphasic model suggested that agonist-activated store depletion initiated rapid entry of extracellular Ca^{2+} into the cell, this influx of Ca^{2+} allowed for the refilling of depleted stores, which in turn terminates the influx of Ca^{2+}. While Putney named the process he described capacitative Ca^{2+} entry (CCE), it has instead become known as store-operated Ca^{2+} entry (SOCE).

SOCE can be reproduced pharmacologically by use of inhibitors of SERCA, e.g. Tg (Takemura et al. 1989); inhibition of SERCA prevents refilling of the ER, this leads to depletion of ER Ca^{2+} content due to loss through Ca^{2+} leak channels (Tu et al. 2006). This loss of ER $[Ca^{2+}]_l$ activates an inward flux of Ca^{2+} through a plasma membrane channel called the Ca^{2+} release-activated channel (CRAC) (Penner et al. 1988; Matthews et al. 1989). The molecular identity of the CRAC channel was initially elusive, but obviously contained several elements: a sensor of ER lumen Ca^{2+} content, a Ca^{2+} permeable channel in the plasma membrane and mechanism to communicate between the two.

The first CRAC channel component identified was the Ca^{2+} sensor, which was shown to be the Stromal interaction molecule 1 (STIM1) (Liou et al. 2005; Roos et al. 2005). This protein had previously been identified by cloning experiments of the novel gene GOK (Parker et al. 1996 p.199), though at the time was of unknown function. STIM1 and its orthologue STIM2, have an ER location and are composed of a single pass transmembrane domain and two Ca^{2+} binding EF hand motifs in its N-terminal luminal region (Roos et al. 2005).

After STIM1 was identified as the Ca^{2+} sensing component of the CRAC channel the plasma membrane channel was also identified (Feske et al. 2006). As T cells from sufferers of severe combined immune deficiency (SCID) syndrome were known to exhibit impaired SOCE, the

genomes of patients with this disorder were mapped to identify the mutation that cause the condition (Feske et al. 2005). A mutation was found in a novel protein that was dubbed Orai1, after the keepers of the gates of heaven in Greek mythology. Expression of wild type Orai1 in SCID T cells was found to restore normal SOCE, and so Orai1 was identified as the CRAC channel's channel. Two other members of the Orai family (Orai2 and Orai3) have since been identified; while Orai1 is considered the major contributor to SOCE (Gwack et al. 2007), both Orai 2 and Orai3 have been shown to be able to form active CRAC channels (Ay et al. 2013; Vaeth et al. 2017) and may provide a developmental or tissue specific role. Each Orai protein has 4 transmembrane domains, and while it has been suggested that they form tetrameric channels (Penna et al. 2008), the crystal structure of *drosophila* Orai1 instead shows that channels are formed of 6 Orai1 subunits (Hou et al. 2012). In addition to the 4 α-helix transmembrane domains, each subunit has another helix after the 4th transmembrane helix (called the M4 extension helix) that probably interact with other proteins to activate the channel.

As well as providing the Ca^{2+} sensing function of CRAC channels, STIM1 also provides the communication mechanism, directly gating Orai1 (Luik et al. 2006). At a resting ER $[Ca^{2+}]_l$ Ca^{2+} is bound to both of STIM1's EF hands, which stabilises the protein in its inactive state. Upon store depletion these bound Ca^{2+} dissociate from STIM1, activating the protein (Zhou et al. 2013). Active STIM1 proteins then dimerize through their luminal SAM motifs, this in turn induces a conformational change through the whole protein (Feske and Prakriya 2013). The result of this conformation change is the elongation of the protein and the extension of the SOAR domain which interacts with the M4 extension helix of Orai1. In addition to inducing a conformational change that allows STIM1 to interact with Orai1, dimerization also induces the STIM1 dimers to migrate through the ER membrane to ER-plasma membrane puncta where Orai1 channels are physically close to the ER (Cahalan 2009) (*Fig.*

1.1.4). It has been suggested that at rest Orai1 proteins are dimers that only form channels upon stimulation by STIM1 (Penna et al. 2008).

CRAC channels show a biphasic form of inactivation, with both a quick and a slow phase (Parekh and Putney 2005). The initial quick phase is Ca^{2+} dependent, and is believed to be the result of Ca^{2+} binding the cytoplasmic 'inactivation domain of STIM1' (ID_{STIM}) domain (Mullins and Lewis 2016). When Ca^{2+} is bound to ID_{STIM} it promotes Orai1 channel inactivation, though the mechanism by which it does this is unknown. Slow inactivation of CRAC channels is the result of ER $[Ca^{2+}]_l$ reaching resting levels (or close to them), and Ca^{2+} rebinding to the lumenal EF hands of STIM1. This then destabilises the active STIM1 dimers, returning STIM1 back to its resting state (Jacob 1990).

As well as being located in the ER membranes, small amounts of STIM1 has been found on the plasma membranes of some cells; though its function there is contentious, with some reports that plasma membrane -STIM1 plays a role in Ca^{2+} (Spassova et al. 2006; Ambily et al. 2014) and others that it does not (Cahalan 2009; Roberts-Thomson et al. 2010 p.).

Before Orai1 was identified it had been suggested that members of the canonical family of Transient receptor potential channels (TRPC) may fulfil the role of the CRAC channel's channel (Yue et al. 2001; Cui et al. 2002; Mori et al. 2002; Philipp et al. 2003). While these channels have been reported to be able to act independently of the STIM1-Orai1 complex (DeHaven et al. 2009); they have also been shown to be directly gated by STIM1 (Huang et al. 2006; Yuan et al. 2007), and to form complexes with Orai1 in the plasma membrane, where they are indirectly activated by the action of STIM1 on Orai1 (Liao et al. 2007). While there is some confusion as to their mechanism of activation; TRPC channels have been shown to play a role in SOCE in some cell types, e.g. the influx of Ca^{2+} during SOCE in PAC from $TRPC3^{-/-}$ mice was found to be reduced to about half that observed in wild type cells (Kim et al. 2009).

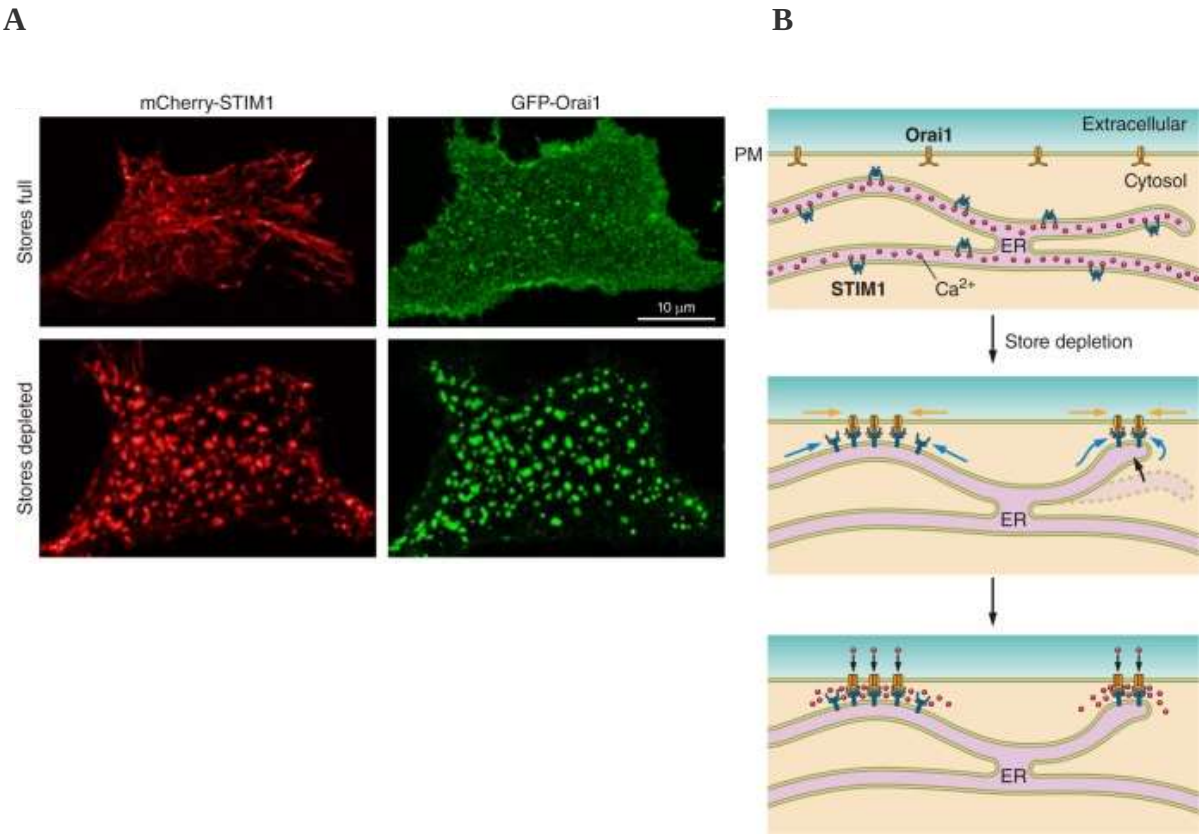

Fig. 1.1.4 STIM1 and Orai1 interact at ER-PM puncta to allow entry of extracellular calcium into the cell

(A) mCherry tagged STIM1 and GFP tagged Orai1 are distributed throughout the ER and PM respectively in resting HEK293 cells (*top*). After thapsigargin-induced depletion of ER calcium content the proteins colocalize with each another (*bottom*). **(B)** When the ER lumen is filled with calcium STIM1 is dispersed throughout the ER membrane in its resting conformation, bound to calcium (*top*). Upon store depletion STIM1 losses its bound calcium, changes into its active conformation and migrates to ER-PM puncta (*middle*). STIM1 activates Orai1, which allows entry of extracellular calcium across the PM into the cytoplasm (*bottom*).

Adapted under terms of use from M Prakriya and S Lewis; *Physiological Reviews*; 2015 (Prakriya and Lewis 2015).

While the function of STIM1 has clearly been identified, the function of its orthologue STIM2 is less clear. Due to overexpression of STIM2 reducing the size of the SOCE response it has been suggested that in may inhibit STIM1's activity (Soboloff et al. 2006), possibly by competing to bind Orai1. However, it has also been suggested that STIM2 might regulate basal levels of Ca^{2+}; sensing smaller changes in $[Ca^{2+}]_l$ than STIM1 and triggering SOCE accordingly (Brandman et al. 2007 p.2). This action would ensure that the ER Ca^{2+} store is kept full under physiological conditions, despite loss of Ca^{2+} through leak channels (Tu et al. 2006).

1.1.5 Visualizing calcium signalling

Real-time visualisations of changes in either the $[Ca^{2+}]_c$ or $[Ca^{2+}]_l$ is possible thanks to the use of florescent Ca^{2+} probes (Paredes et al. 2008). These Ca^{2+} probes are either florescent dyes based on Ca^{2+} chelators or recombinantly expressed Ca^{2+}-sensing fluorescent proteins, which have a combined bioluminescence and Ca^{2+} sensing function.

Probably the most commonly used type of florescent Ca^{2+} probes are fluorescent dyes, due to their ease of use and the varied characteristics (e.g. affinity to Ca^{2+} or absorption/emission spectra) of different dyes (Takahashi et al. 1999; Paredes et al. 2008). Two of the most widely utilized dyes are the Fluo and Fura families of dye, often in their cell permeable AM forms. The Fluo-1, Fluo-2 and Fluo-3 are part of a range of Ca^{2+} dyes created by Roger Tsien's group (Minta et al. 1989), combining the 8-coordinate tetracarboxylate chelating site of 1,2-bis(2-amino-phenoxy)ethane-N,N,N',N'-tetraacetic acid (BAPTA) with a xanthene chromophore. These dyes gain their fluorescence upon binding of Ca^{2+} and have a single excitation and emission wavelength, making them easy to record and correlate to changes in $[Ca^{2+}]$. Several derivatives of the original Fluo dyes have since been created, including Fluo-4 and Fluo-5 (Gee et al. 2000). Fluo-4 is more sensitive to excitation at 488 nm, producing a

brighter fluorescence emission, and shows a higher rate of cell permeation than the original Fluo dyes. Fluo-5 and its analogues have a reduced sensitivity to Ca^{2+}, making them suitable for recoding $[Ca^{2+}]_l$ which is much higher at resting levels than that of the cytosol. This allows for the recording of the depletion of store content in response to a stimulus rather than an increase in $[Ca^{2+}]_c$ (Gerasimenko, Sherwood, et al. 2006).

Tsien group also created the Fura family of dyes; like Fluo dyes, Fura dyes are also based on BAPTA but use a stilbene chromophore rather than a xanthene to confer fluorescence (Grynkiewicz et al. 1985). While 3 Fura dyes were initially created, Fura-2 has proven to be the most popular and is still the most commonly used. These dyes are ratiometric and change excitation wavelength depending on if they are bound to Ca^{2+} or not; with Fura-2's peak absorbance shifting from 340 nm when Ca^{2+} is bound to 380 nm when it is unbound. Both bound and unbound emit light at the same wavelength so a ratio of emission intensities in response to the two different excitation wavelengths can be calculated, giving a more accurate quantification of the Ca^{2+} concentration than single wavelength dyes, eg. Fluo-4. However, ratiometric dyes are sensitive to any background auto-fluorescence and require an excitation source that can switch between wavelengths and a senor that can record emitted light rapidly to make use of them.

The salts of both Fluo and Fura dyes are easily modified with AM groups; removing their charge and making them readily cell permeable. AM versions of dyes do suffer from being compartmentalized into organelles and extruded from cells over prolonged periods of time (Blatter and Wier 1990). Conjugating the dye's salts to dextran prevents loss of cytoplasmic location, but does not confer membrane permeability.

A drawback of using Ca^{2+} dyes is that they only bind free ionic Ca^{2+}, which due to native buffering in the cytosol is about 1 in every 100 ions present in the cytosol. As dyes are based on Ca^{2+} chelators they also have a buffering effect, so further reduce the availability of free

Ca^{2+} in the cytosol, which can affect the kinetics of Ca^{2+} signalling within cells being observed (Takahashi et al. 1999). Another disadvantage of using Ca^{2+} dyes is that they cannot be targeted to specific locations in the cell (Kwon et al. 2016); this has been one of the key reason for the development of recombinantly expressed Ca^{2+}-sensing fluorescent proteins, which do have this ability (Button and Eidsath 1996; Sieberer et al. 2009).

The first type of Ca^{2+}-sensing fluorescent protein discovered was aequorin from the *Aequorea victoria* jellyfish (Shimomura et al. 1962), which is natively activated by Ca^{2+}. A recombinant form of this protein can be expressed in mammalian cells (Shimomura et al. 1990), and unlike Ca^{2+} dyes it does not suffer from extrusion from cells or compartmentalization into organelles. It can sense free Ca^{2+} in the range of 0.1 – 100 µM, and as its fluorescence does not need to be excited there is no chance of auto-fluorescence (Kendall et al. 1996). However, aequorin's fluorescence needs a prosthetic group called coelenterazine, which is irreversibly cleaved upon stimulation by Ca^{2+} (Shimomura 1995). Cells need to be supplemented with this group before imaging, and provided with a continual supply for aequorin to produce more than one emission of light (i.e. to allow real time visualisation of Ca^{2+} levels).

The second type of Ca^{2+}-sensing fluorescent protein was developed from another of *Aequorea victoria*'s proteins GFP (Prasher et al. 1992). In *Aequorea Victoria* Ca^{2+} binds to aquorin causing it to cleave coelenterazine, this results in the release of blue light that excites GFP, which then emits green light (Morise et al. 1974). Experimentally this can be reproduced by stimulating GFP (or one of its alternative coloured variants, e.g. YFP (Aliye et al. 2015)) with the correct wavelength of light to excite its fluorescence. Tsien's group created a ratiometric Ca^{2+} sensing protein based on the Ca^{2+} binding activity of calmodulin with the fluorescence of GFP and its analogues (Miyawaki et al. 1997). This protein named CaMeleon consists of two corresponding GFP derived domains (e.g. BFP and GFP or CFP

and YFP) joined by calmodulin and a M13 link domain. When the protein is in its resting, Ca^{2+} unbound state the two GFP derived domains are far apart and excitation of BFP or CFP results in emission of blue or cyan light that can be recorded. However, when Ca^{2+} binds to calmodulin the protein undergoes a conformational change, with the calmodulin domain wrapping around the M13 domain bringing the two GFP derived domains close together. When the BFP or CFP domain of activated CaMeleon is excited the light it emits then excites the other GFP derived domain (GFP or YFP respectively), which then emits either green or yellow light. This change in the wavelength of emitted light allows for the ratio of CaMeleon that has bound Ca^{2+} and that that does not to be calculated. Several other types of Ca^{2+}-sensing fluorescent protein have been developed from GFP and its derived florescent proteins, including Camgaroos and GCaMP (Whitaker 2010).

1.2 The pancreas

1.2.1 The structure and function of the pancreas

The pancreas is an organ with two distinct functions, endocrine and exocrine, both of a secretory nature. Its structure varies between species; in some species, e.g. rabbits, it is diffusely distributed in the *mesentery* of the small bowel, while in humans and rodents it is compacted into a distinct organ (Tsuchitani et al. 2016). In humans the pancreas weighs between 50 - 100 g; is between 15 - 18 cm long, 2 – 9 cm wide and 2 -3 cm thick; and can be dived into three sections: the head (*caput pancreatis),* a C-shaped part aligned with the upper curvature of duodenum; the body (*corpus pancreatis),* located underneath the stomach; and the tail (*cauda pancreatis),* which touches the hilum of the spleen (Dolenšek et al. 2015). The bulk of the pancreas is given over to its exocrine function, which accounts for 96 -99 % of its total mass. Structurally the exocrine pancreas is lobular; subdividing into lobes, then

lobules and finally grape like structures called acini of pancreatic acinar cells (PAC) (Leung and Ip 2006) (*Fig. 1.2.1B*). These acini connect to intralobular ducts comprised of pancreatic ductal cells; intralobular ducts merge into larger extralobular ducts, which in turn merge to form the main collecting duct (Grapin-Botton 2005). The collecting duct connects with the common bile duct to form the ampulla of Vater, which empties into the duodenum (*Fig. 1.2.1A*). Pancreatic stellate cells are present in the periacinar space, and have protrusions of membrane that encircle acini (Omary et al. 2007). When activated, under physiological conditions it is believed that they synthesise extracellular matrix components, which promote tissue repair, but under pathological conditions are involved in fibrosis of the pancreas.

The endocrine pancreas is formed of clusters of cells called the islets of Langerhans, which are dispersed throughout the volume of the pancreas (*Fig. 1.2.1D*). Islets are comprised of five types of cell: α cells, β cells, δ cells, ε cells and Polypeptide (PP) cells (sometimes referred to as γ cells) (Pelletier 1977; Andralojc et al. 2009); the ratio and distribution of the different cell types within islets varies between species (Elayat et al. 1995).

The organ is surrounded by a fibrous capsule with extensions into the organ's body that delineate the parenchyma into its lobular sutures. Due to its endocrine function the pancreas is highly microvascularised, and receives about 1% of cardiac output (Lewis et al. 1998). It receives blood from both the celiac and the superior mesenteric artery, the first 2 of the 3 major branches of the abdominal aorta; while its venous system drains into the portal vein (Wharton 1932). While only described in rodents, the pancreas has a sparse distribution of lymphatic vessels, that are physically distinct from acini, ducts and islets (O'Morchoe 1997). Intralobular lymphatic vessels join to form interlobular vessels running in the connective tissue between pancreatic lobes, which connect to a series of nodes surrounding the pancreas. The pancreas is also highly innervated by a mixture of sympathetic, parasympathetic and

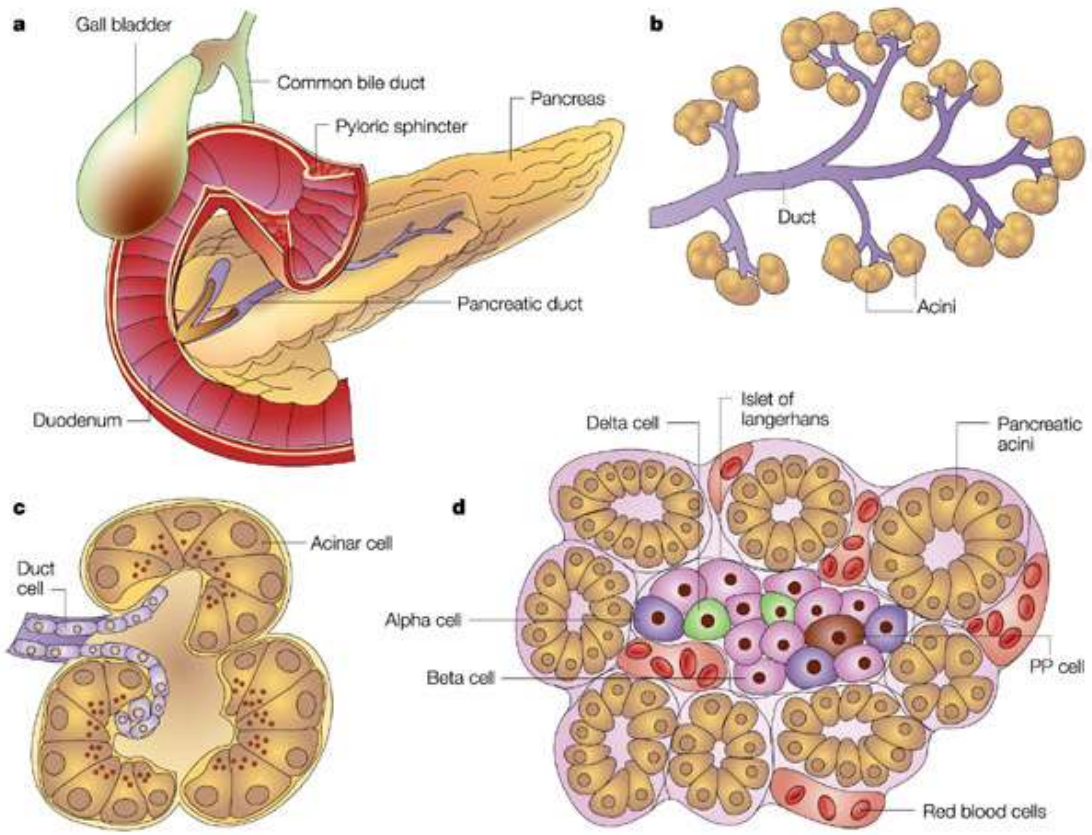

Fig. 1.2.1 Structure of the human pancreas

The pancreas is a secretory organ with two distinct functions, exocrine and endocrine; with the bulk of the pancreas given over to its exocrine function. **(A)** The exocrine pancreas is a branching structure, which joins to form the pancreatic duct. This joins with the common bile duct and empties into the duodenum. **(B)** The exocrine pancreas is organised into bundles of cells called acini that are connected to intralobular ducts, which merge into extralobular ducts. **(C)** Within an acinus structure pancreatic acinar cells are organised with their granular apical region facing the acinar lumen. **(D)** Dispersed throughout the exocrine pancreas are clusters of endocrine cells called islets of Langerhans, comprised of several different types of hormone secreting cells.

afferent neurones, which have a regulatory role for both the exocrine and endocrine pancreas (Ahrén 2000; Love et al. 2007).

The pancreas develops from the endoderm germ layer, via the formation of two distinct buds (Rutter 1980). The dorsal anlagen is formed when the endoderm envaginates into a condensation of mesenchyme that had previously formed on its dorsal side (Gittes 2009). The ventral bud forms laterally from the primitive gut tube, close to the same region of endoderm that the forms the biliary and hepatic ducts (Puri and Hebrok 2010). The dorsal pancreas forms part of the developing head, the body and the tail of the organ, while the ventral pancreas forms part of the devolving head (Tsuchitani et al. 2016). The buds fuse after gut rotation (Kluth et al. 2003) and branch into the surrounding mesenchymal tissue. Both the endocrine and exocrine pancreas share the same linage and develop in tandem (Fishman and Melton 2002), rapidly forming the recognisable architecture of the organ (Pictet et al. 1972). While each type of cell composing the pancreas is highly specialised for its specific function, differentiation does not always appear to be irreversible. PAC have been found to revert to ductal-type cells during the development of pancreatic ductal adenocarcinoma (Rooman and Real 2012). Metaplasia of PAC into hepatocytes has been found to occur *in vivo* during regeneration of the pancreas (Shen et al. 2003). One of the most studied models of this is when rats are fed a copper (Cu^{2+})-deficient diet with Trien (a Cu^{2+}-chelating agent) for 7-9 weeks to induce a near complete loss of PAC, and then returned to normal feed. Using this model, hepatic cells have found to occupy over 60% of the pancreatic volume 6-8 weeks post recovery (Rao et al. 1988). This transdifferentiation is likely due to the shared endodermal origin of both cell types; highlighted by the viability of islets transplanted from healthy donors into the liver of patients with type 1 diabetes (Iwanaga et al. 2006).

The function of the endocrine pancreas is the secretion of various hormones, with each type of cell responsible for the production of a different hormone (Mastracci and Sussel 2012). α

cells and β cells secrete glucagon and insulin respectively, which are involved in blood glucose homeostasis; while δ cells, ε cells and PP cells respectively secrete somatostatin, ghrelin and pancreatic PP, which regulate pancreatic secretions.

The exocrine pancreas' role is the secretion of the digestive enzymes (including trypsin, chymotrypsin, pancreatic amylase and lipase (Case 1978)) required for digestion in the intestines. Enzymes are produced by acinar cells and secreted in their zymogen form, which are then activated in the duodenum. First by the activation of trypsinogen into trypsin by the brush-border glycoprotein peptidase, enterokinase; which in turn cleaves the other proenzymes into their active form (Rinderknecht 1986). Duct cells secret bicarbonate, which aids in the clearance of enzymes through the pancreatic duct system and neutralises the acid pH of the chyme produced by the stomach (Grapin-Botton 2005; Ishiguro et al. 2012). Pancreatic stellate cells normally exist in a quiescent state, however under pathological conditions they activate and are involved in fibrosis (Masamune and Shimosegawa 2013).

1.2.2 Pancreatic acinar cells

1.2.2.1 Structure and function of acinar cells

Acinar cells account for roughly 90% of the total cells in the pancreas; and play the key role of synthesizing, storing and secreting digestive enzymes upon stimulation. Natively they have a pyramidal shape with a highly polarised intracellular layout consisting of an apical granular region and a basolateral region (Petersen and Tepikin 2008). The basolateral region comprised up to 90% of the cells volume and contain its nucleus and the bulk of the ER. When PAC form acini structures their granular regions face the acinar lumen (*Fig. 1.2.1C*); it is this region that contains the specialised secretory vesicles called zymogen granules, which store the digestive enzymes in their inactive proenzyme form (Rindler 2001). The granular and basolateral regions of the cell are separated by a mitochondrial belt; which has been seen

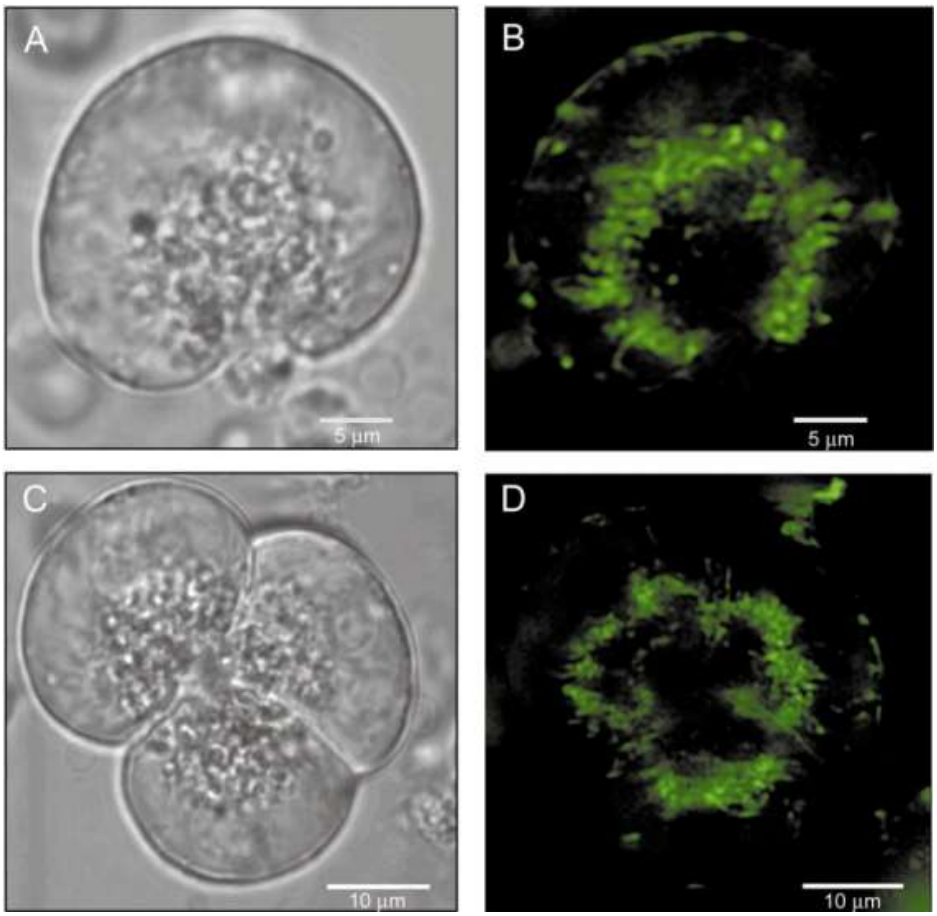

Fig 1.2.2 Pancreatic acinar cells have a highly polarized structure

Bright field images **(A** and **C)** and florescent images **(B** and **C)** of a single pancreatic acinar cell **(A** and **B)** and a cell triplet **(C** and **D)** stained with the mitochondria-specific florescent dye MitoTracker Green. The bright field images show the cells are highly polarised, with a separate granular region at their apical pole. Fluorescence imaging shows a clear clustering of mitochondria into a belt separation cells apical and basal regions.

acting as a 'firewall', preventing Ca^{2+} signals created in the granular region from propagating into the basolateral one (Tinel et al. 1999) (*Fig. 1.2.*2). While the majority of the ER is located in the basolateral region of the cell, extensions of the ER membrane cross the mitochondrial belt into the granular region. A tunnelling effect has been observed in the lumen of the ER, with Ca^{2+} migrating from the basolateral region of the cell into the protrusions in the granular region, keeping them filled (Mogami et al. 1997). Physiological fluid secretion from PAC is stimulated by either the neurotransmitter acetylcholine (ACh) or the digestive hormone cholecystokinin (CCK) (Cancela 2001). These secretagogues induce the production of intracellular secondary Ca^{2+} messengers in PAC, this results in the release of Ca^{2+} from intracellular stores (Low et al. 2010), which in turn drives the process required for secretion of enzymes from the zymogen granules (Söllner 2003; Stojilkovic 2005). Individual PAC cells show extensive coupling with neighbouring PAC via gap junctions (Meda et al. 1983); these cell-cell couplings show the ability to enhance and coordinate responses in connected cells (Michon et al. 2005). Endocrine cells in islets are also connected via gap junctions, which play a similar role as they do in PAC (Bertuzzi et al. 1999). Exocrine and endocrine cells express opposing connexion proteins, and therefore do not appear to form jap junctions between each other (Meda 1996).

1.2.2.2 Physiological calcium signalling in acinar cells

Physiological concentrations of both ACh and CCK typically induce small oscillations in the $[Ca^{2+}]_c$ confined to the granular region of the cell (Li et al. 2014); though occasionally induce a Ca^{2+} wave initiated in the apical region that spread throughout the cell (Pandol et al. 2007; Sutton et al. 2008). It is believed that while Ca^{2+} oscillations induce fluid secretion; the function of Ca^{2+} waves is to trigger gene transcription (Cancela 2001), which can be a Ca^{2+} dependent process (van Haasteren et al. 1999). Supramaximal concentrations of CCK cause

hyperstimulation of PAC, producing a large sustain increase in $[Ca^{2+}]_c$ that are cytotoxic and results in necrosis of PAC (Criddle et al. 2009).

Receptors for both physiological secretagogues are concentrated on the basolateral plasma membrane (Pandol 2010) and are forms of metabotropic G-protein coupled receptors. (Schnefel et al. 1988). Structurally G-protein coupled receptors consist of a extracellular N-terminus that interacts with its ligand, 7 transmembrane domains and an intracellular C-terminus that typically (but not always) associated with a G protein complex (Bockaert and Pin 1999). The type of G protein required for physiological Ca^{2+} in PAC are the G_q class heterotrimers (comprised of a α, a β and a γ subunit) (Williams 2001), which in its inactive state is bound to the receptor and GTP. The associated receptor undergoes a conformational change when it binds its ligand; activating the GTPase activity of the complex, which converts the attached GTP to GDP. The G protein complex releases GDP and dissociates from the receptor, with the α subunit separating from the β and γ subunits, and performing downstream signalling functions.

ACh is released by peripheral nerve endings in the pancreas, and acts on the M3 type muscarinic ACh receptor (M-AChR M3) (Schnefel et al. 1988). Phospholipase C (PLC), which cleaves phosphatidylinositol 4,5-bisphosphate (PIP_2) into IP_3 and diglyceride (DAG) is known to be directly activated by the G_q α subunit (Park et al. 1993).

CCK is secreted by the endocrine cells of the small intestine after food ingestion and by peripheral nerves in the gut (Liddle 1997), it is expressed as a 115 residue precursor and then cleaved into peptides of various length with 8-NH_2-CCK being the most biologically active. There are two types of CCK receptors, CCK_A and CCK_B, though both human and mouse PAC only express CCK_A (Cancela 2001). The receptor has two CCK binding domains; the high affinity site couples CCK to physiological signalling by activation of CD38 via an

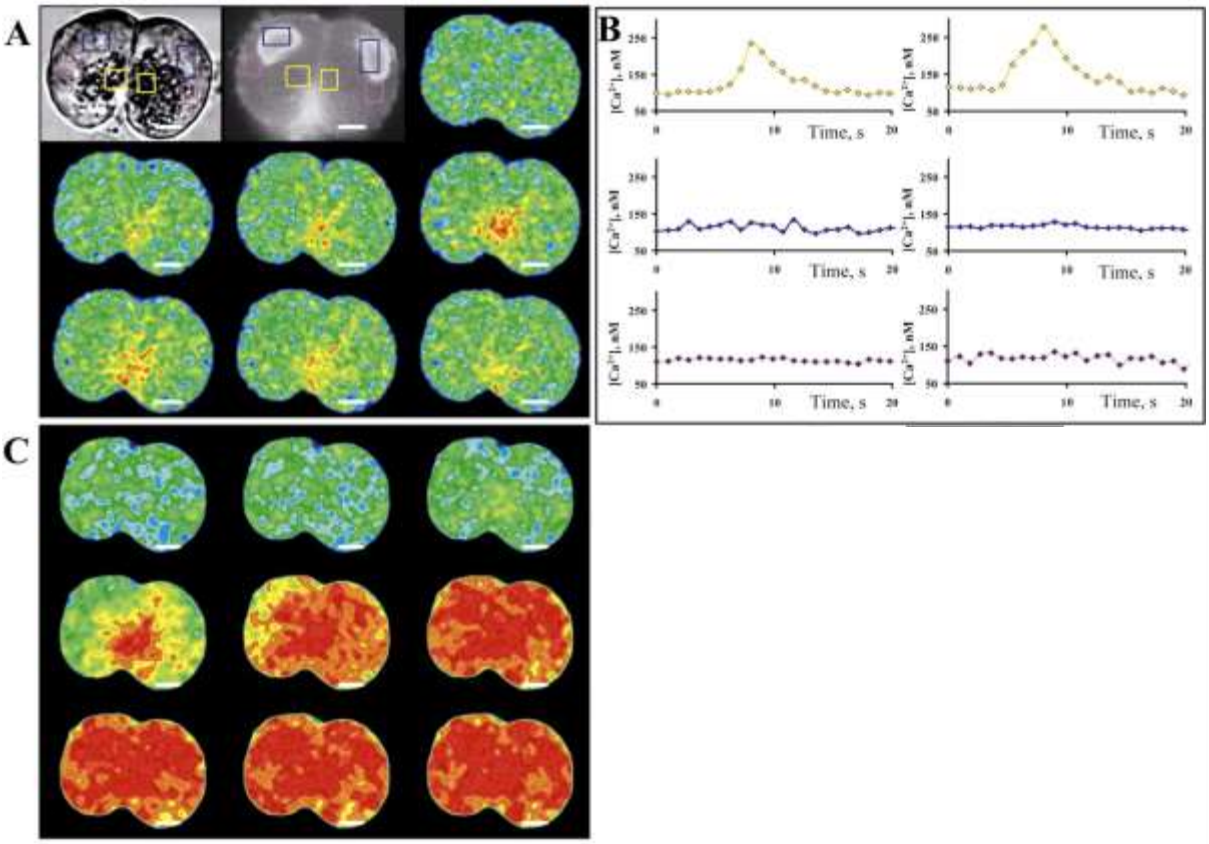

Fig. 1.2.2.2 Stimuli induced cytoplasmic calcium responses in pancreatic acinar cells

(A) Calcium responses in pancreatic acinar cells upon short applications of acetylcholine are confined to the apical granular region. **(B)** Recordings of the apical areas (yellow), basal areas (purple) and nuclei (blue) of the cells in **(A)**. **(C)** Prolonged exposure to ACh induce global calcium responses in the cells.

Adapted with permission from *Journal of Cell Science* (Gerasimenko and Gerasimenko 2004), originally modified with permission of Springer (Gerasimenko et al. 1996).

unknown pathway (Cosker et al. 2010) and the low affinity site has been linked to the production of IP_3 (Matozaki et al. 1990) and pathological signalling (Beil et al. 2002).

Activation of CD38 by CCK produces both cADPR and NAADP (Yamasaki et al. 2005), though there have been conflicting finding as to the importance of each messenger in the Ca^{2+} response induced by CCK. The cADPR specific antagonist 8-NH_2-cADPR inhibits responses to CCK, suggesting cADPR's activity is vital for the response (Cancela and Petersen 1998 p.2). However, 300 µM glucose, which inhibits cADPR-induced Ca^{2+} release in PAC, has no effect on the response to CCK, suggesting cADPR is not vital (Cancela et al. 1998). A high autoinhibitory concentration of NAADP has no effect on cADPR-induced Ca^{2+} release in PAC, but does inhibit their response to CCK, suggesting that NAADP is required for the hormone's activity (Cancela et al. 1999). Based on these results it has been suggested that NAADP may be required to initiate the Ca^{2+} response to CCK, while cADPR plays a role in propagating it.

As ACh and CCK receptors are primarily located on the basolateral membrane and secretory Ca^{2+} is confined to the granular region, it suggests that the secondary messengers produced in response to secretagogues must diffuse through the cell to their target region. PACs express all three isoforms of both IP_3R (M. G. Lee et al. 1997) and RyR (Fitzsimmons et al. 2000). IP_3Rs localise to the granular region of the cell (Thorn et al. 1993; Nathanson et al. 1994), while RyRs show a more dispersed localisation in both regions of the cell (Leite et al. 1999; Straub et al. 2000).

While both IP_3R and RyR are associated with being located in ER membranes in most cell types, antibody staining has shown RyR localized with a zymogen granule marker (Husain et al. 2005). While immunohistochemistry suggests that IP_3R that do not localise to these vesicles (Yule et al. 1997; Husain et al. 2005), IP_3 have been shown to mobilize Ca^{2+} in the

granular region after ER Ca^{2+} is depleted by Tg (Gerasimenko, Sherwood, et al. 2006). All three secondary Ca^{2+} messengers have been shown to be able to mobilise Ca^{2+} from both an ER and acidic store in the granular region of PAC. While not positively confirmed, selective disruption of other candidates implies that it is the zymogen granules that comprise this IP_3/cADPR/NAADP sensitive store. This suggests that IP_3R and RyR are both present and functional in the membranes of zymogen granules, with their non-ER location possibly due to the high rate of ER turnover required to produce and maintain the pool of zymogen granules present in PAC. As zymogen granules are an acidic organelle specific to PAC, present in large numbers concentrated to the granular region they provide a unique large pool of Ca^{2+} that can be mobilized in response to any of the secondary messengers. The expression and localisation of the two TPC isoforms has yet to be shown in PAC.

It is believed that a combination of secondary messenger receptors being concentrated to the granular region, the process of CICR and the mitochondrial belt is the reason that most physiological Ca^{2+} in PAC is confined to their granular region. The high concentration of receptors in the granular region makes it prone to the initiation of Ca^{2+} release by secondary messengers; and also make it susceptible to CICR, which both IP_3R and RyR are known to be sensitive to (Santulli and Marks 2015). This is highlighted in experiments where Ca^{2+} was uncaged in specific areas of the cell (Ashby et al. 2002); uncaging of Ca^{2+} in the granular region initiated a Ca^{2+} wave that spread throughout the cell, whereas uncaging in the basolateral region produced no response. This implies that the basolateral region is not sensitive to CICR, while the granular region is highly sensitive to it. It is possible that the combination of IP_3R and RyR present in the granular region, compared to just RyR in the basolateral region, is the reason for this; suggesting both are a requirement for CICR. The majority of Ca^{2+} signals initiated in the granular region will be confined there due to the

buffering capacity of the mitochondrial belt that separates it from the basolateral region; therefore, for any response to propagate throughout the cell it must be of sufficient size to overcome this barrier.

All three secondary Ca^{2+} messengers are also capable of mobilising Ca^{2+} from the Tg sensitive nuclear envelope (Gerasimenko et al. 2003). While the physiological relevance of this is unknown, there is a probable link to gene transcription. With the same messengers that induce PAC to secrete digestive enzymes, driving the synthesis of new enzymes to replenish the pool.

1.2.3 Diseases of the exocrine pancreas

The three most common diseases of the exocrine pancreas in order of severity are: acute pancreatitis (AP), chronic pancreatitis and pancreatic cancer. AP is the most common of the three conditions, but each is considered a key risk factor in developing the next most severe.

AP is a single inflammatory incidence that often presents rapidly, initial symptoms include severe abdominal pain, nausea and vomiting (Swaroop et al. 2004). 1 out of every 2000 people suffer from the disease annually (Sutton et al. 2003), with key risk factors excessive alcohol consumption and gallstones (Lowenfels et al. 2005). The disease is the result of the pathological activation and secretion of the digestive enzymes stored within PAC (Petersen et al. 2011). The activity of the pathologically activated enzymes then autodigests the pancreas and surrounding tissue (Fagniez and Rotman 2001), causing necrosis and inflammation (*Fig. 1.2.3*). There is no current specific treatment for AP and sufferers often require hospitalisation, with analgesics and prophylactic antibiotics often administered to patients (Johnson 2005) to treat the symptoms; supplementary fluids, nutrition and oxygen are also

sometimes required . Treatment of related complications can have a positive effect; if gallstones are a factor, a cholecystectomy is a possibility, though due to its invasive nature an established set of guidelines for when surgery should be performed have been established (Uhl et al. 2002). Most incidences of AP resolve themselves after a 5-10 day period, however approximately one in five patients develop a more severe form of the disease, with more extensive necrosis and a systemic inflammatory response. This can result in multiple organ failure and about half of patients who develop the severe form of AP die within 2 weeks of the disease's progression (Swaroop et al. 2004).

Between 10-15% of patients who suffer an initial incidence of AP will suffer a recurrence of the disease, with 6.4% progressing to suffer from chronic pancreatitis (Banks et al. 2010). Of the AP patients who progress to a chronic condition, over 65% will have had their initial incident of AP as a result of excessive alcohol consumption, making it a key risk factor for chronic pancreatitis (Joergensen et al. 2010). Alternatively, the chronic condition can have a hereditary link, with mutations to several proteins of varying function reported (Zator and Whitcomb 2017). Patients with the hereditary form of chronic pancreatitis tend to develop the condition much earlier (10-15 years) than is average for sufferers of the disease (35-55 years) (Rosendahl et al. 2007).

Chronic pancreases is characterised by the loss of secretory years) the organ, irreversibly altering its morphology and structure (Brock et al. 2013). Fibrosis is caused by the activation of pancreatic stellate cells under pathological conditions, causing them to synthesise excessive amounts of extracellular matrix components (Haber et al. 1999; Apte et al. 2012). While levels of necrosis and inflammation in chronic pancreases are often low patients can suffer from chronic pain, as well as recurrent episodes of increased severity that mimic AP (Skipworth et al. 2010). Loss of pancreatic parenchyma can result in a range of complications

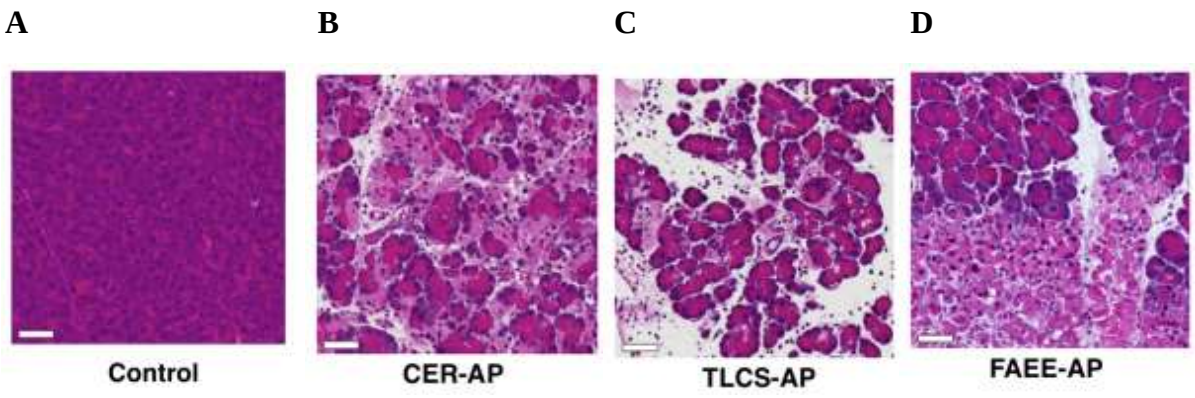

Fig. 1.2.3 Various agents can be used to reproduce acute pancreatitis *in vivo*

Normal pancreatic histology **(A)** and the histopathology in three *in vivo* experimental models of acute pancreatitis: **(B)** hyperstimulation induced by intraperitoneal injections of cerulean (a peptide from the secretions of the Australian green tree frog *Litoria caerulea* that mimics the effect of CCK); **(C)** retrograde pancreatic ductal injection of the bile acid TLC-S; or **(D)** production of FAEEs by intraperitoneal injections of ethanol and palmitoleic acid. All three pathological agents induce inflammation, oedema and necrosis in the pancreatic tissue.

including digestive issues caused by the loss of acini and Type 1 diabetes due to loss of endocrine tissue (Sarles 1992; Ewald and Hardt 2013), which occurs in 50-60% of chronic pancreatitis sufferers.

As with AP there is no true treatment for chronic pancreatitis; with management of symptoms (e.g. analgesics, pancreatic enzyme supplements, insulin injections) often all that is possible (Nair et al. 2007). Half of all patients with chronic pancreatitis undergo some form of surgery to try and treat their condition (Steer et al. 1995), with a lateral pancreaticojejunostomy the most common. This where all but the head of the pancreas is removed and the remaining pancreatic tissue attached to the duodenum with a duct-to-mucosa connection made so that pancreatic juices can drain directly from the common bile duct into the duodenum. A recently developed technique is a complete pancreatectomy with autotransplantation of islets into the liver (Ong et al. 2009). There is a clear correlation between chronic pancreatitis and pancreatic cancer (Raimondi et al. 2010); with sufferers of chronic pancreatitis 13.3 times more likely to develop pancreatic cancer than non-suffers (Yadav and Lowenfels 2013). Sufferers of hereditary chronic pancreatitis have a significantly increased risk of developing cancer over those with other forms of the disease, and tend to develop tumours at younger cancer over those with other forms of the disease, and tend to develop tumours at younger ages (Lowenfels et al. 1997).

While there is variation of rates of pancreatic cancer between populations (Ilic and Ilic 2016), it is generally more prevalent in western populations (7.4 per 100,000 people in Northern America and 7.3 per 100,000 people in Western Europe), believed to be due to lifestyle in these regions. Men have a higher risk of the disease than women, though both genders show an increased risk with age (Yadav and Lowenfels 2013). It is the 11th most common form of cancer worldwide, and has the lowest survival rate of 1% over 5 years (Jura et al. 2005). The

early symptoms of pancreatic cancer are nonspecific (e.g. diffuse abdominal pain, vomiting, diarrhoea and constipation), meaning the condition is often only diagnosed when it has progressed in severity and symptoms like acute abdominal pain, jaundice and significant weight loss (Malhotra et al. 2015).

The majority of growths arise in the exocrine pancreas, with pancreatic ductal adenocarcinoma (PDAC) accounting for about 95% of all pancreatic tumours (Amundadottir 2016). Due to their morphology PDAC had historically been though to solely originate from duct cells; however with the finding that PAC can be stimulated to revert to a pre-ductal like state (Wagner et al. 1998) it appears that these cells also play are role in tumorigenesis. Kras is mutated in most incidences of PDAC within the $Kras^{G12D}$ mutation found in the majority of tumours (Kolodecik et al. 2014). Mutation to Kras alone is not enough to develop PDAC, but it is believed to be the first step in pancreatic intraepithelial neoplasia, with mutations to several other genes required for the transformation into PDAC (Murtaugh 2014). Pancreatic stellate cells are activated in pancreatic cancer, where they help establish the tumour microenvironment by producing its stroma and possible signalling to PDAC cells in a protumorigenic manner (Apte et al. 2012; Haqq et al. 2014)

While no direct cause of PDAC has been identified, a range of risk factors that significantly increase the probability of developing the disease have been identified. These risk factors include: smoking, obesity, diabetes, excessive alcohol consumption, diet, pancreatitis (especially the chronic form of the disease) (Ilic and Ilic 2016); infection by the *Helicobacter pylori* bacteria has been cited by some as potential risk factor (Maisonneuve and Lowenfels 2015), though this has been disputed (X.-Z. Chen et al. 2016).

When tumours arise in the tail of the organ they can effectively be removed surgically; however as about 70% of tumours develop in the head of the pancreas they are often

inoperable due to the late stage of diagnosis (Malhotra et al. 2015). When surgery is viable it requires removal of the pancreatic head, common bile duct to above the ampulla of Vater and the attached section of the duodenum; with the remaining pancreatic tissue and bile duct reconnected to what is left of the duodenum (Ghaneh et al. 2007). PDAC shows a high resistance to traditional chemotherapy drugs, though use of Gemcitabine alone or in combination with other agents has shown positive effects (Teague et al. 2015). Modern therapeutic techniques targeting pathological signalling linked to growth of PDAC cells, e.g. inhibition of Epidermal growth factor receptor (EGFR) activity by antibodies, are currently being trialled (Fjällskog et al. 2003).

All three diseases of the exocrine pancreas can be fatal, and currently there is no specific treatment for any of them. Due to the potential for each disease to progress to a more severe condition, the creation of a treatment for AP should reduce the incidence of all three.

1.2.3.1 Acute pancreatitis

1.2.3.1.1 Causes of acute pancreatitis

AP can be the result of a number of causes, though 23.3% of cases are idiopathic (Joergensen et al. 2010). The mnemonic taught to medical students to remember the causes of AP (roughly in their order of incidence) is aptly I. G.E.T. S.M.A.S.H.E.D.; standing for: Idiopathic, Gallstones, Ethanol, Trauma, Steroids, Mumps, Autoimmune, Scorpion stings or Spider bites, Hyperlipidaemia or Hypercalcaemia, Endoscopic retrograde cholangiopancreatography, and Drugs. Smoking has previously described as an exacerbating factor in combination with known causes of AP, e.g. alcohol, however recently it has been

suggested as cause in and of itself (Barreto 2016). Of the known causes of AP, gallstones and alcohol together contribute over half of all incidences of the disease (Joergensen et al. 2010).

Claude Bernard first suggested that reflux of bile into the pancreas's main colleting duct could cause AP in 1856 (Wang et al. 2009). When in 1901 Opie described the case of a patient who had died and was found to have gallstone blocking the ampulla of Vater, he proposed that such a blockade might result in such a reflux of bile. Gallstones are formed from condensates of various components of the bile and are often highly calcified; the two most common types are primarily formed from either bilirubin or cholesterol (and its catabolites) and are referred to as black and brown pigment stones respectively (Trotman 1991).

While bile is known to contain a mixture of substances (including Bilirubin, excess heavy metals and phospholipids), bile acids (sometimes referred to as bile salts) make up about 61% of its composition (Kristiansen et al. 2007). Bile Acids have been shown to induce large sustained pathological increases in $[Ca^{2+}]_c$ within PAC (Voronina et al. 2002 p.202; Gerasimenko, Flowerdew, et al. 2006) and resulting in necrosis of cells (Kim et al. 2002; Orabi et al. 2013). They have also been shown to cause necrosis in both pancreatic duct and stellate cells (Alvarez et al. 1997; Ferdek et al. 2016), implying they have a pathogenic effect throughout the exocrine pancreas. AP can be recreated experimentally *in vitro* by either ligation of the ampulla of Vater to recreate the gallstone blockage, or by injection of bile acids into the main colleting duct to simulate their reflux (Hue Su et al. 2006). PAC have also been shown to express active bile acid transporters, indicating some function for bile acid uptake in these cells (Kim et al. 2002).

This has been disputed though as less than 10% of patients with symptomatic gallstone disease suffer an incident of AP (Armstrong et al. 1985). It has also been suggested that the

pressure built up in the common bile duct in response to its blockage is insufficient to cause reflux into the pancreas (Armstrong and Taylor 1986) and that the common duct is too short to allow efficient reflux to occur (Vonlaufen et al. 2008). This means despite a clear and obvious link between patients with AP and gallstones, the underlying pathological mechanism is yet to be definitively proven.

Alcohol consumption also has a clear correlation to AP, with a linear relationship observed between the risk of contracting the disease and level of alcohol intake (Durbec et al. 1981). However only a small number of alcoholics develop AP (Steinberg and Tenner 1994); also intact PAC show a tolerance to high concentration of ethanol (Criddle et al. 2004) and long-term intraperitoneal administration of ethanol does not induce AP (Lerch and Gorelick 2013). These findings suggest that it is not directly ethanol itself that is pathological in alcohol-related AP.

Elevated concentrations of fatty acid ethyl esters (FAEE) were observe.d in serum and pancreatic tissue of rats that displayed symptoms of AP after infusion of ethanol (Werner et al. 2002). FAEEs are nonoxidative metabolites of ethanol and can be produce in the pancreas via one of two pathways: oxidative or non-oxidative (Wilson and Apte 2003). The oxidative path way utilizes alcohol dehydrogenase (ADH) and possibly cytochrome P4502E1 to produce acetaldehyde, and is the major route for ethanol metabolism in the pancreas. Alternatively, the non-oxidative produces the FAEE linked to AP from ethanol and fatty acids (FA) via the enzyme FAEE synthases. Rats on a high-fat supplemented diet with a continuous intragastric infusion of ethanol were found to develop AP (and in some cases chronic pancreatitis) (Tsukamoto et al. 1988), indicating the importance of both fat and alcohol in the development of alcohol-related AP.

Like bile acids, FAEE's are able to induce a pathological Ca^{2+} response in PAC (Criddle et al. 2004) via an IP_3R dependent action (Criddle, Murphy, et al. 2006). Within PAC, FAEEs can be converted back to FAs; which have their own Ca^{2+} mobilizing activity (which is not sensitive to IP_3R inhibition like FAEE's) and disrupt ATP syntheses (Criddle, Sutton, et al. 2006), which will affect the cells Ca^{2+} homeostasis. FAEEs have also been linked with an increased fragility of both lysosomes and zymogen granules (Haber et al. 1993; Haber et al. 1994) and the activation of pro-inflammatory transcription factors, e.g NF-κB (Gukovskaya et al. 2002); all of which would have a pro-AP effect.

Ethanol metabolites also seem to have an effect on pancreatic stellate cells, which have been shown to have ADH activity (Wilson and Apte 2003). Increased levels of extracellular matrix proteins have been observed in pancreases after exposure to FAEEs (Lugea et al. 2003), suggesting the activity of stellate cells, which synthesise these proteins (Robinson et al. 2016).

Both bile acids and FAEE have been shown to induce the death of PAC by inducing a sustained rise in $[Ca^{2+}]_c$ at cytotoxic levels (Wen et al. 2015). The form that that death takes however can vary; in mild AP cells mainly have an apoptotic fate, and in severe AP a necrotic one (Klöppel and Maillet 1993). With the balance between pro-apoptotic and pro-necrotic factors determining which form of cell death occurs, and hence the severity of the disease (Bhatia 2004). Several mechanisms have been observed in PAC, e.g. production of reactive oxygen species (ROS) in response to bile acids, where by the cell is steered toward an apoptotic fate (Bhatia et al. 1998; Booth et al. 2011). Recent attempts have been made to subdivide cell death into multiple categories, beyond that of just apoptosis and necrosis (Kroemer et al. 2009). One example is necrosis (which had typically been thought of as an uncontrolled pro-inflammatory process), now subdivided into necrosis (retaining its original

definition) and necroptosis (Feoktistova and Leverkus 2015). Necroptosis is effectively a controlled pro-inflammatory process; believed to occur when initiating a localised immune repose is advantageous, e.g. when a cell is viral infected. There is some evidence that necroptosis can occur in PAC during AP (Wang et al. 2016); like apoptosis this might be an attempt by PAC undergo a less harmful form of death than necrosis, and so be relevant for mild AP. It seems unlikely however, that necroptosis is involved in the severe form of AP due to the amount of inflammation and extent of damage to the pancreas that occurs.

1.2.3.1.2 Bile acids

Bile acids are a group of amphipathic steroids (Lefebvre et al. 2009) that play a key role in digestion acting as detergents and emulsifiers; they also act as surfactants to aid in the absorption of lipids and lipid-soluble vitamins (Insull 2006) by forming cylindrical micelles with them (Hjelm et al. 1995; Hofmann 1999).

The majority of bile acids are synthesised by hepatocytes from cholesterol via one of two catabolic pathways (Chiang 2009); over 90% of bile acids are synthesised via the neutral classic pathway, though a small amount are synthesized via an acidic alternative pathway (Duane and Javitt 1999). The initial stage in conversion of cholesterol into 7-hydroxy-Cholesterol by 7 α-hydroxylase (CYP7A1) is the only rate limiting step of bile acid synthesis (Chiang 2009). 7-hydroxy-Cholesterol can then follow one of two metabolic pathways (*Fig. 1.2.3.1.2.1*): continued activity by CYP7A1 produces Chenodeoxycholic acid (CDCA) or by 12α-hydroxylase (CYP8B1), which produces cholic acid (CA) (also referred to as cholate). The amount of CA and CDCA (collectively referred to as primary bile acids) synthesised by hepatocytes is about equal (Hofmann 1999). Most of the resultant CA and CDCA is then conjugated with either glycine or taurine by CoA:amino acid N-acyltransferase (Falany et al.

1994), with taurine conjugation the predominate form in mice (over 95% of all bile acids). Conjugation has several effects; it increases the solubility of bile acids (reducing their membrane permeability), makes them less suitable to Ca^{2+} precipitation and resistant to cleavage by pancreatic carboxypeptidases (Chiang 2013). Hepatocytes secrete bile acids into bile canaliculi, these are the smallest branch of the hepatic duct system, which eventually join up to form the common hepatic duct (Castaing 2008). From this duct bile components are taken up, concentrated and stored by the gallbladder ready to be secreted when stimulated by CCK (Housset et al. 2016). During this concentrating step the concentration and composition of the bile can change, meaning that the biliary bile excreted by the gallbladder is different to the hepatic bile secreted by the liver (Keulemans et al. 1998).

Secondary bile acids are produced in the distal intestine; here they are unconjugated and CA is converted to lithocholic acid (LCA) and CDCA to Deoxycholic acid (DCA) by bacterial 7α-dehydroxylase (Ridlon et al. 2014). About 95% of bile acids are reabsorbed by ileocytes (ileal enterocytes), with the rest eliminated in the faeces (Staels and Fonseca 2009). LCA is quite toxic, but induces its own detoxification by promoting expression of a sulfotransferase, which conjugated the bile acid by sulfation to reduce its toxicity (Hofmann 2004). Secondary bile acids are then recycled to the liver via the portal venous system for reuse, where they are either directed straight into the bile via uptake/extrusion by cholangiocytes or taken back up by hepatocytes for reconjugation to glycine or taurine (Chiang 2013).

While most secondary bile acids are directly recycled (about 95% are reabsorbed in the ileum), some do enter the general circulatory system and are transported around the body. Bile acids can act as signalling compounds, via interaction with specific bile acid receptors; e.g. bile acids act on a farnesoid X receptor (FXR) in the lungs to activate lung fibroblasts (B. Chen et al. 2016). Circulating bile acids are reabsorbed in the kidneys (St-Pierre et al. 2001)

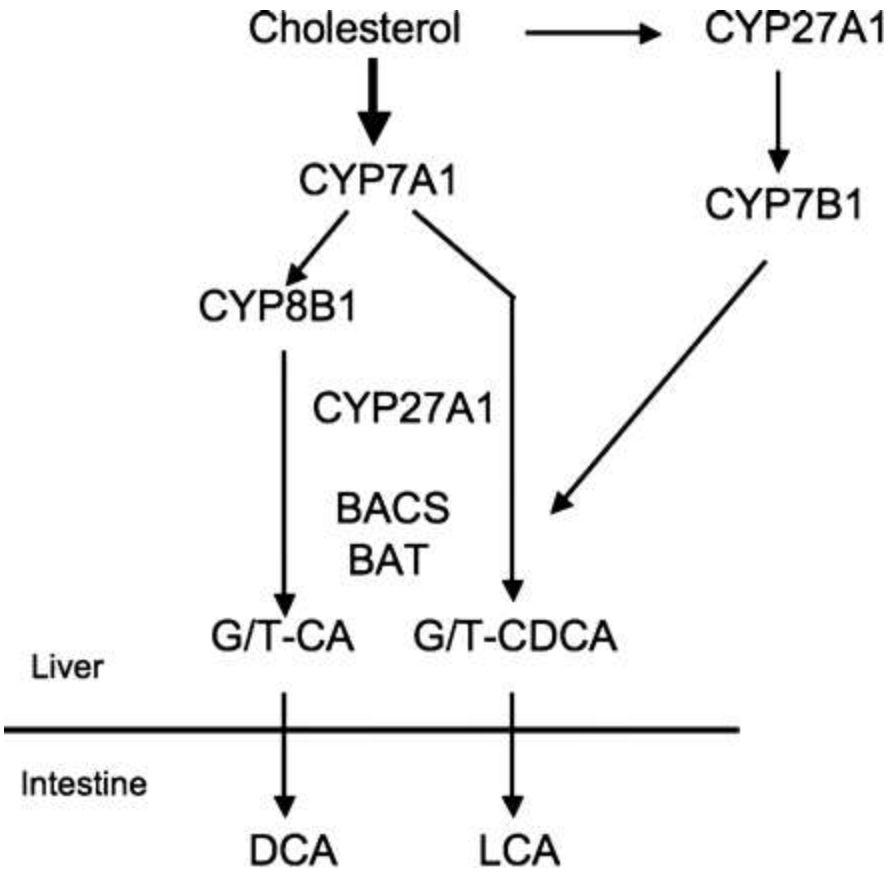

Fig. 1.2.3.1.2.1 Bile acid synthesis

The key enzymes in the synthesis of primary bile acids from cholesterol in the human liver. CYP7A1 is the first enzyme in the classic (neutral) biosynthesis pathway, and therefore its activity is the rate limiting step of the pathway. The alternative (acidic) pathway occurs in the liver or macrophages and is initiated by the activity of CYP27A1. BACS and BAT are the key enzymes required for bile acid conjugation. In the intestine bile acids are deconjugated and converted into secondary bile acids by the activity of the intestinal flora.

and returned to the liver through portal venous circulation. This system of circulation of bile from the liver to the intestines and back to the liver (with overflow being returned to the liver by the kidneys) is called enterohepatic circulation (Fitzsimmons et al. 2000) (Fig. 1.2.3.1.2.2).

As enterohepatic circulation creates an (almost) enclosed system there is need for homeostasis so energy is not wasted producing potentially toxic excesses of bile acids. This is achieved by feedback regulation of CYP7A1 expression. Bile acids act via a FXR called NR1H4 to supress CYP7A1 expression, while cholesterol acts via NR1H3 to induce it. (Redinger 2003). This ratio of pro- and anti-expression signalling controls the overall level of CYP7A1 expressed (and therefore rate of bile acids synthesised), as it catalyses the rate limiting step of their creation.

As conjugated bile acids and secondary bile acids are not membrane permeable they have to be transferred into and out of cells. Multiple bile acid transporters have been identified (St-Pierre et al. 2001) with evidence their expression is regulated by bile acid signalling (Dawson et al. 2009). Due to the polarized nature of epithelial cells different types of bile acid transporters can be separated between the apical and basal membrane to create directional flow of bile acids through the cell. At the apical membranes of enterocytes, cholangiocytes and renal proximal tubular cells bile acids are take-up into the cell via Na^+ dependant transporters, using the Na^+ gradient to facilitate movement of bile acids against their own concentration gradient. On the basal membrane Na^+ independent organic anion transporters allow the transfer out of cells of bile acids along their concentration gradient. While in hepatocytes bile acid uptake occurs via a Na^+ transporter; extrusion is performed by the bile salt export pump (BSEP), an ATPase used to actively remove bile acids from the cell (Stieger 2010). Bile acid transporters have been found on other cell types not involved in

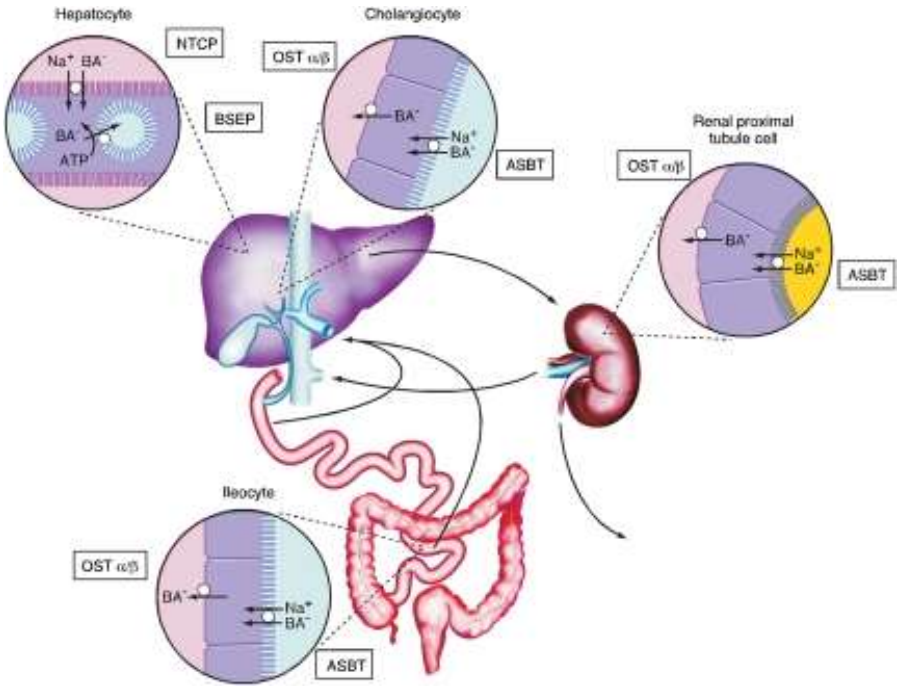

Fig. 1.2.3.1.2.2 Enterohepatic circulation of bile acids

While some bile acids are lost in the faeces, most are reabsorbed from the intestinal lumen by ileocytes. Reabsorbed unconjugated secondary bile acids are then transported by the portal venous system where they can be directly returned to the biliary track by cholangiocytes or taken back up by hepatocytes to be reconjugated. Some bile acids enter the general circulatory system, where they are reabsorbed by renal proximal tubule cells and returned to the portal venous system. All cell types involved in bile acid reabsorption and transport show polarised transport, utilizing sodium cotransporters to move bile acids against their concentration gradients into the cell. Cholangiocytes, renal proximal tubule cells and ileocytes then use Na^+ independent organic anion transporters to extrude bile acids, while hepatocytes use a ATPase to actively transport them out of the cell.

Reproduced under terms of free use from P Dawson; *The Journal of Lipid Research*; 2009 (Dawson et al. 2009).

enterohepatic circulation, e.g. PAC cells express both Na^+ dependant and Na^+ independent bile acid transporters (Kim et al. 2002), while pancreatic stellate cells express Na^+ dependent ones (Ferdek et al. 2016).

1.2.3.1.3 Pathological calcium signalling of bile acids in acinar cells

Taurolithocholic acid 3-sulfate (TLC-S) was the first bile acid shown to induce an increase in $[Ca^{2+}]_c$ in PAC (Voronina et al. 2002), and while others have been shown to have a similar effect (e.g. taurocholate (TC) and taurodeoxycholate (TDC)), the mechanisms by which TLC-S achieves this remains the best described.

Lower concentrations of TLC-S induce cytoplasmic Ca^{2+} transients, while higher ones' result in a single sustained elevation in $[Ca^{2+}]_c$ (Husain et al. 2005). In both cases TLC-S induces these responses by inducing the release of Ca^{2+} from both ER and acidic intracellular stores in PAC, utilizing both IP_3Rs and RyRs to do so (Gerasimenko, Flowerdew, et al. 2006). Ca^{2+} induced by higher concentrations of TLC-S deplete organelle stores of their Ca^{2+} content, triggering an influx of extracellular Ca^{2+} via SOCE (Kim et al. 2002; Wen et al. 2015). Bile acids can directly inhibit SERCA pumps, preventing ER refilling and therefore the slow inactivation of SOCE; together this creates the sustained Ca^{2+} response observed.

TLC-S's Ca^{2+} mobilizing effect (and by extension its necrotic effect) has been shown to be CD38 dependent, as a loss of response to TLC-S in $CD38^{-/-}$ mice (Orabi et al. 2013). This implies TLC-S's effect is via the production of the secondary messengers cADPR and NAADP, in a similar manner as hyperstimulation with CCK. This corresponds with the response to TLC-S being diminished in the presence of either a high autoinhibitory concentration of NAADP or the cADPR specific antagonist 8-Br-cADPR (though

interestingly not in the presence of 8-NH_2-cADPR). It is unknown how TLC-S activates the cyclase activity of CD38 and if it has the same effect on PLC to produce IP_3; otherwise IP_3Rs involvement in the response to TLC-S could be purely due to CICR in response to Ca^{2+} mobilized by cADPR and NAADP. There is also evidence that the related bile acid TC can directly gate RyR1 that have been purified and incorporated into a lipid bilayer (Geyer et al. 2015).

Release of Ca^{2+} from zymogen granules can affect the proenzymes they contain, which require a high $[Ca^{2+}]_i$ to remain in stable inactive state (Petersen and Sutton 2006). The activity of bile aids cause an increase in $[Na^{2+}]_i$ (Voronina et al. 2005) and zymogen granules are believed to contain a K^+/Ca^{2+} exchanger (Yang et al. 2007). This means that because of the localised release of Ca^{2+} from zymogen granules there would be favourable conditions for the uptake of K^+ into granules. The lumenal matrix of granules is a highly efficient exchanger of Ca^{2+} and K^+ (Nguyen et al. 1998); therefore it could exchange its H^+ and Ca^{2+} content for K^+, which would create conditions for the auto-activation of trypsinogen to trypsin (Moreland and Sanyal 1985).

Ca^{2+} increases in PAC, to either physiological or pathological stimuli, result in an increase in mitochondrial Ca^{2+} content, inducing the production of ROS (Booth et al. 2011). A combination of ROS and elevated mitochondrial Ca^{2+} induces opening of the mitochondrial Permeability Transition Pore (mPTP) and the release of cytochrome c into the cytosol (Baumgartner et al. 2009; Odinokova et al. 2009). Combined with TLC-S induced caspase activation (Criddle et al. 2007), this pushes the cell toward a controlled apoptotic death before conditions are favourable for a necrotic one.

Sustained mitochondrial Ca^{2+} levels induced by TLC-S result in the depolarization of the mitochondrial membrane (Voronina et al. 2004). Prolonged depolarization of the membrane

impairs ATP production and creates a switch from an apoptotic fate to a necrotic one (Nicotera et al. 1998; Tsujimoto 1997). The prolonged cytotoxic levels of Ca^{2+} caused by TLC-S activates calcineurin (Muili, Wang, et al. 2013), which in turn activates NF-κB (Muili, Jin, et al. 2013), one of several inflammation associated signals caused by bile acids (Kim et al. 2002). Ultimately PAC undergo necrosis, lose their membrane integrity and release pro-inflammatory factors (Hoque et al. 2012); triggering an inflammatory response (Kang et al. 2014).

1.3 Aims of the study

The main aim of this study is to use the recent advancements in the field of NAADP research to better characterise the mechanism of NAADP-induced Ca^{2+} in PAC, and that role that it plays in both physiological and pathological Ca^{2+} in these cells.

In PAC NAADP has been shown to act on both acidic and ER Ca^{2+} stores, mobilising Ca^{2+} in a RyR dependent manner (Gerasimenko et al. 2003; Gerasimenko, Sherwood, et al. 2006). TPC channels have recently been identified as NAADP-sensitive ion channels (E. Brailoiu et al. 2009; Calcraft et al. 2009; Zong et al. 2009) but their activity in PAC has yet to be characterised. Therefore, this study aims to determine the requirements for both TPC and RyR in NAADP-induced Ca^{2+} release in PAC. Use of knockout animals and isoform specific antibodies will allow for the targeted inhibition of individual isoforms of TPC and RyR and discern their relative requirements for NAADP's activity.

Both ACh and CCK act on PAC as physiological secretagogues, though only CCK activity has been shown to contain an NAADP component (Cancela 2001). It has been suggested that this NAADP component is required to initiate the response to CCK, which is then sustained

by its cADPR component (Cancela et al. 1999). Using the recently discovered NAADP specific-antagonists Ned-19 (Naylor et al. 2009) and BZ194 (Dammermann et al. 2009), this study aims to identify the importance of the NAADP component in the CCK-induced Ca^{2+} response in PAC.

Ca^{2+} responses to the bile acid TLC-S in PAC have been shown to contain a NAADP-sensitive component (Gerasimenko, Flowerdew, et al. 2006), and both TLC-S induced Ca^{2+} release and necrosis have been shown to involve the activity of the NAADP synthesis enzyme CD38 (Orabi et al. 2013). Based on these previous findings, this study aims to investigate if either of the NAADP-specific antagonists can protect against the pathological effects of TLC-S.

While the harmful effects of a range of bile acids towards PAC have been reported (Kim et al. 2002; Voronina et al. 2002), the effect of the primary bile acid cholate has yet to be tested. As such, this study aims to characterise the effect of cholate on PAC and test to see if it, like TLC-S, contains a NAADP-sensitive component.

Finally, this study also aims to investigate the effect of knocking out the TPC2 protein, which forms NAADP-sensitive Ca^{2+} channels, has on Ca^{2+} release in PAC in response to both physiological and pathological stimuli.

CHAPTER 2:
MATERIALS AND METHODS

Chapter 2: Materials and Methods

2.1 Reagents

The following compounds were purchased from Sigma-Aldrich, Gillingham, UK: CCK-8 (Cat. C2175), ACh (Cat. A6625), NAADP (Cat. N5655), cADPR (Cat. C7344), IP_3 (Cat. I9766), taurolithocholic acid 3-sulfate (Cat. T0512), sodium cholate hydrate (Cat. C6445); TPEN (Cat. P4413), Ryanodine (Cat. SML1106) and FFP-18 K^+ salt (Cat. 17089).

Fluorescent dyes for calcium measurement: Fluo-4-AM (Cat. F14201), Fluo-5N-AM (Cat. F14204), Fura-2-AM (Cat. F1221), Texas Red® dextran (Cat. D1863) and Propidium Iodide (Cat. P3566) for cell death assays were obtained from ThermoFisher Scientific, Loughborough, UK.

Type V Collagenase came from Worthington Biochemical Corporation (Cat. LS004194), Lakewood, NJ, USA.

Trans-Ned-19 was purchased from Tocris Bioscience, Bristol, UK (Cat. 3954).

Rabbit Anti-TPC1 (Cat. LS-C95184) and Anti-TPC2 (Cat. LS-C95187) polyclonal antibodies were obtained from LifeSpan BioSciences, Nottingham, UK.

Rabbit Anti-RyR1 (Cat. AB9078, Anti-RyR2 (Cat. AB9080) and Anti-RyR3 (Cat. AB9082) polyclonal antibodies; Mouse IgG Negative Control antibody (Cat. CBL600B); and the compounds Thapsigargin (Cat. 586005) and ATP (Cat. 130124) were purchased from Merck Millipore, Watford, UK.

Caffeine (Cat. 205548) was purchased from Calbiochem, Nottingham, UK.

Molecular biology dH_2O (Cat. M830C), dNTPs Mix 10 mM (Cat. U151B), 5x GoTaq reaction buffer (Cat. M791B) and GoTaq DNA Polymerase (Cat. M830C) were purchased from Promega, Southampton, UK.

Custom TPC2 primers were sourced from Eurofins Genomics, Ebersberg, Germany.

GSK-7975A was provided by GlaxoSmithKline, Stevenage, United Kingdom; and is compound 36 from patent WO 2010/1222089.

BZ194 was kind gift from Prof Barry Potter, University of Bath, and was synthesised as previously described (Dammermann et al. 2009).

Unless otherwise stated all other chemicals were supplied by Sigma-Aldrich, Gillingham, UK. All stock solutions were created in either NaHEPES solution without supplemental Ca^{2+} or in DMSO depending on their solubility and stored at either -80, -20 or 4°C, when required stock solutions were protected from light. Unless stated all active solutions were prepared from stock solutions in NaHEPES solution supplemented with 1 mM Ca^{2+}, active solutions made from stocks solutions in DMSO had a final DMSO concentration of 0.1% or less. Sodium cholate hydrate was made up on day of use.

2.2 Animals

Wild type male C57BL6/J mice were purchased from Charles Rivers, UK; and maintained under low barrier conditions on a 12 h light cycle on a standard rodent chow diet with free access to water.

TPC2 knockout mice were a gift from Dr. John Parrington, Oxford University, and were created as previously described (Calcraft et al. 2009) using a gene trap strategy (Stryke et al. 2003). A colony of $TPCN2^{-/-}$ mice produced from those supplied was maintained in-house

under low barrier conditions on a 12 h light cycle on a standard rodent chow diet with free access to water. Female TPCN2$^{-/-}$ mice were found to occasionally develop abdominal or uterine fluid filled cysts; both genders are also prone to over-grooming, resulting in areas of discoloured fur or bald patches (*Fig. 2.2.1*). After several generations the number of litters produced by the colony significantly decreased, suggesting fertility issues; to increase the yield several breeding pairs of wild type male C57BL6/J mice crossed with female TPCN2$^{-/-}$ mice (which are from a C57BL6/J back ground) were established. The resultant male heterozygous offspring were then crossed with female TPCN2$^{-/-}$ mice to produce homozygous knockout offspring, these new TPCN2$^{-/-}$ mice showed no loss of breeding capacity. The genotype of each mouse in the colony was confirmed by PCR reaction, using specifically designed primers.

RyR3 knockout mice were provided by Dr. K. Mikoshiba's Lab, Riken Brain Science Institute, Japan; and were created as previously described (Futatsugi et al. 1999).

2.3 Genotyping

Tissue samples were taken from mice in the TPCN2$^{-/-}$ colony by ear punching and stored at -20˚C until use. A PureLink® Genomic Mini Kit (ThermoFisher Scientific, Loughborough, UK; Cat. K182001), was used as described in the manufacturer's manual to isolate DNA from the samples taken. 3 µl of DNA per sample was combined in a PCR tube with 34.25 µl Molecular biology dH_2O, 10 µl DreamTaq Green Buffer, 1 µl dNTPs, 5 µl primer 1 (CTTCGGAGCCTTCTTTCCTT), 5 µl primer 2 (CTGTCCCTGACGAGTGGTTT), 5 µl primer 3 (GTCGGGGCTGGCTTAACTATG) and 0.25 µl Taq polymerase. A TC-312 Thermal Cycler A (Techne, Stone, UK) was programed to 5 min at 94 °C, then 30 cycles of 94 °C for 15 s, 56 °C for 30 °C and 72 °C for 1 min; and finally 6 min at 72 °C. The

A **B**

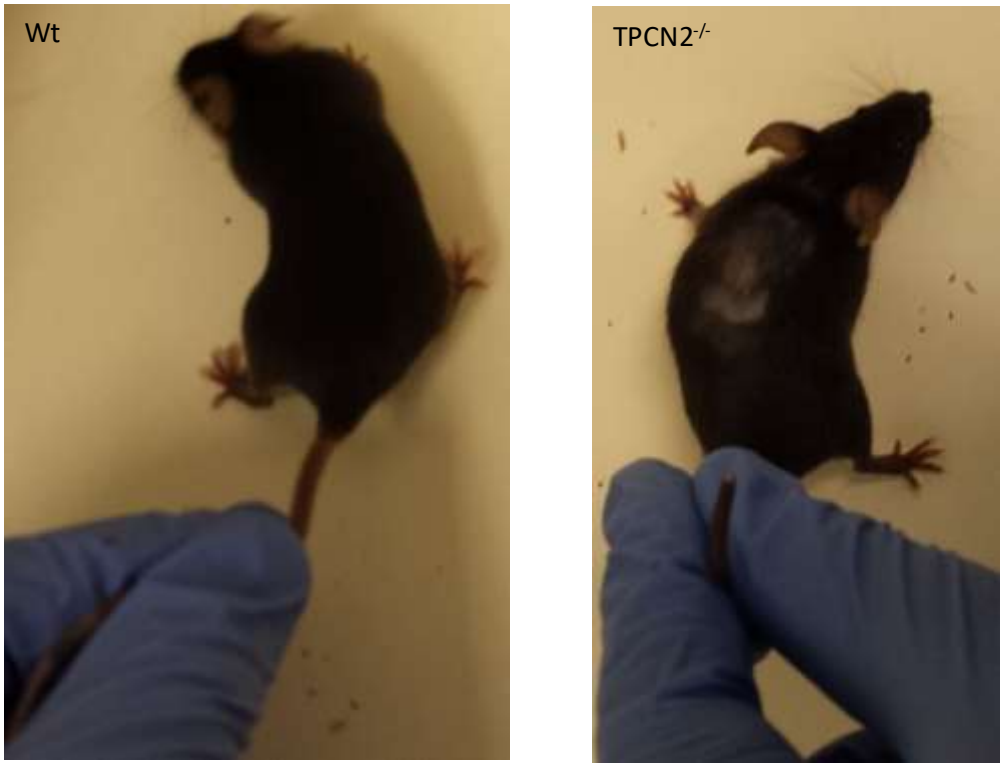

Fig. 2.2.1 Wild type and TPC2 knockout mice

(A) Male wild type C57BL6/J mouse. **(B)** Male TPC2 knockout mouse (C57BL6/J background) with signs of over-grooming.

amplified DNA was resolved on a 1% agarose gel for 30 min at 90 V and then photographed using a ChemiDoc™ XRS+ System (Bio-Rad Laboratories, Hercules, CA, USA). Mice were identified as wild type, heterozygous or TPCN2 null based on the number and location of bands on the gel (Fig. 2.3.1).

2.4 Preparation of NaHEPES solution

A standard extracellular buffered solution of 'NaHEPES' was prepared as follows: 140 mM sodium chloride; 4.7 mM potassium chloride 10 mM HEPES, free acid; 10 mM D(+)-Glucose; 1 mM magnesium chloride. The pH was adjusted to 7.2 with sodium hydroxide. Unless otherwise stated 1 mM calcium chloride was added before use. The buffer solution was stored at 4°C and used within a week.

2.5 Preparation of K-HEPES solution

A standard intracellular buffered solution of 'K-HEPES' was prepared for use in permeabilization experiments as follows: 20 mM sodium chloride; 127 mM potassium chloride 10 mM HEPES, free acid; 2 mM ATP; 1 mM magnesium chloride; 0.1 mM EGTA; 0.05 mM calcium chloride. The pH was adjusted to 7.2 with sodium hydroxide. The buffer solution prepared on the day of its use.

2.6 Preparation of Collagenase

4000 U stock of type V collagenase was diluted with 20 ml of freshly prepared NaHEPES solution supplemented with 1 mM Ca^{2+} to produce a 200 U/ml solution, which was used to

A

		Female	
		-	-
Male	+	+/-	+/-
	-	-/-	-/-

B

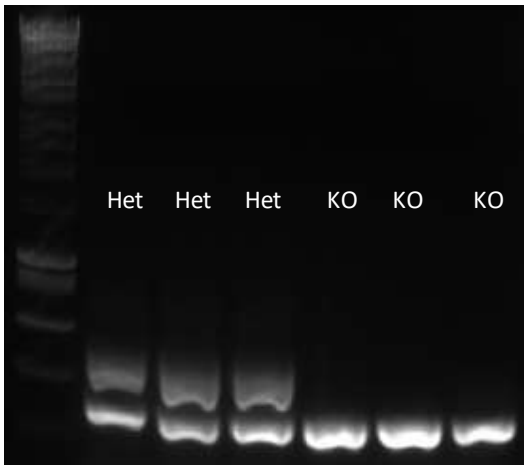

Fig. 2.3.1 Genotyping results for the offspring of a Male TPC2 heterozygous and female TPC2 null homozygous breeding pair

(A) Mendelian cross for the breeding pair used. **(B)** Gel electrophoresis image displaying the genotyping result for the resultant litter; two bands represent heterozygous offspring, while one band in the lower position represent TPC2 null offspring.

create 1 ml aliquots, which were stored at -20°C. The activity of each batch of collagenase was tested to ensure it was used optimally.

2.7 Preparation of fluorescent calcium indicators

2 mM stock solutions of all three Ca^{2+} indicators (Fluo-4-AM, Fluo-5N-AM and Fura-2-AM) were prepared in DMSO and divided into 5 µl aliquots for Fluo-5N-AM and Fura-2-AM, and 4 µl aliquots for Fluo-4-AM. Stocks of the Ca^{2+} indicators protected from light and stored at -20°C.

2.8 Isolation of pancreatic acinar cells

Preparations of acinar cells (single, or clusters of two or three cells) were isolated from the pancreases' of wild type or knockout mice aged 1.5-3 months as previously described (Thorn et al. 1993). Mice were sacrificed in accordance with Schedule 1 of the Animal (Scientific Procedure) Ac, 1986, by cervical dislocation, and the pancreas was immediately excised. The organ was washed twice in Ca^{2+} supplemented NaHEPES solution, then injected with 1 ml of the type V collagenase stock. The pancreas and any excess collagenase solution was then placed in a snap-top tube and left to be digested for 15-17 min (dependant on the assayed activity of the specific batch of collagenase) in a water bath with an in-built shaker set to 37°C and a low speed. Gentle pipetting was used to mechanically separate the tissue; isolated cells and clusters were then removed by separating the top fraction, with no visible fragments of tissue, into a 15 ml polystyrene tube from Sarstedt, Leicester, UK (Cat. 62.553.041). This was repeated several times, each time replacing the fraction removed with fresh NaHEPES solution, until several ml of cell solution was collected. The isolated cells were then pelleted

in a centrifuge for 1 min at 1200 g twice; replacing the supernatant with fresh buffer and resuspending the pellet between the spins. The final pellet was resuspended in 2 ml NaHEPES buffer for calcium measurement experiments and 3 ml buffer for necrosis assays.

2.9 Calcium measurements in intact cells

Freshly isolated acinar cells were loaded using the membrane permeable AM form of either of the calcium sensitive dyes Fluo-4 or Fura-2. The final concentrations of the dyes were 4 µM Fluo-4 or 5 µM Fura-2 in DMSO (4 or 5 µl of 2 mM stock into 2 ml of cell suspension, respectively). Cells were incubated with the dye for 45 min at room temperature on an orbital shaker set to a low speed, whilst protected from light.

After the incubation, loaded cells were pelleted in a centrifuge for 1 min at 1200 g and resuspended in 2ml of fresh NaHEPES buffer. The loaded cells were kept at room temperature, protected from light and used within 3-4 h of loading.

For imaging experiments, 20 µl of loaded cell solution was placed on a 32 x 32 mm thickness No 1 glass coverslip purchased from VWR international, Lutterworth, UK (Cat. 631-0129) secured to a custom-made cell bath by silicone grease. During imaging experiments, reagents made up in NaHEPES buffer were perfused over cells using a custom-made gravity-fed perfusion system.

2.10 Calcium measurements in permeabilized cells

Freshly isolated acinar cells were loaded using the membrane preamble AM form of the calcium sensitive dye Fluo-5N. The final concentration of the dye was 5 µM Fluo-5N in

DMSO (5 µl of a 2 mM stock into 2 ml of cell suspension). Cells were incubated with the dye for 50 min in a water bath with an in-built shaker set to 37°C and a low speed, whilst protected from light. Under these loading conditions the dye preferentially accumulates within organelles, allowing for depletion of the calcium content of their lumens to be visualised.

After the incubation, loaded cells were pelleted in a centrifuge for 1 min at 1200 g and resuspended in 2ml of fresh Na-HEPES buffer. The loaded cells were kept at room temperature, protected from light and used within 3-4 h of loading.

20 µl of loaded cell solution was placed on a 32 x 32 mm thickness No 1 glass coverslip secured to a custom- made cell bath by silicone grease. Cells were permeabilized by two-photon laser; then perfused by reagents made up in K-HEPES solution using a custom made gravity-feed perfusion system during imaging. Localised permeabilization of the plasma membrane results in loss of cytosolic content, including any dye not taken up by organelles, which is replaced by K-HEPES solution; intracellular stores remain intact and are loaded with Fluo-5N.

For antibody blocking experiments, permeabilized cells were preincubated with the relevant antibody/antibodies for 20 min at a dilution of 1:100.

2.11 Two-photon permeabilization

The technique of two-photon permeabilization of pancreatic acinar cells was developed by our research group (Gerasimenko, Sherwood, et al. 2006) from a previously described protocol to temporarily perforate mammalian cells for *in vitro* transfection of foreign DNA (Tirlapur and König 2002). Before the cells were permeabilized they were perfused with K-

HEPES to replace the NaHEPES they were prepared in; and then incubated with 1 µM of the 'near membrane' Ca^{2+} indicator FFP-18 for 5 min prior to permeabilization to help pore formation. A small area, preferentially in the apical region of the cell, was then selected and exposed to a high intensity two-photon laser beam from a Mai Tai two-photon laser (Spectraphysics, Didcot, UK) in pulse mode at between 720-760 nm with a 100 fs width for 1-3 frames. Creation of a membrane pore by permeabilization was confirmed by monitoring the uptake of fluorescence of the membrane impermeable dye Texas Red dextran added to the extracellular medium. Conformation of the pore's stability was then confirmed by washing the dextran dye out of the cell by perfusion.

2.12 Cell death assay

Levels of necrosis were assessed as previously described (Ferdek et al. 2012). Post isolation, the cell preparation produced was separated in 0.5 ml volumes and exposed to selected reagents at their required concentrations for a 1 h period at room temperature on orbital shaker set to a low speed or in a water bath with an in-built shaker set to 37°C and low speed. The start of each treatment was staggered by 15 min from the previous to allow for imaging of the previous treatment. 6 µM Propidium Iodide was added and mixed by gentle pipetting directly before imaging. 20 µl of cell solution was place on a 32 x32 mm thickness No 1 glass coverslip secured to a custom made cell bath by silicone grease. Multiple pictures were taken over a 10 min period with a minimum of 20 pictures taken per treatment.

2.13 Equipment

Cell imaging and cytosolic calcium measurements with Fluo-4 were performed using: (1) a

Leica SP5 MP inverted confocal microscope system (Leica Microsystems AG, Wetzlar, Germany) with a x63 1.2 NA water objective using the Leica software, LAS X. (2) a Leica DMI 4000B inverted confocal microscope with a x63 1.2 NA oil objective using the Leica software, LAS X. (3) a custom built Carl Ziess ZEN 2011 TIRF System with Axio Observer.Z1 inverted microscope, CSU-X1 Spinning Disc Unit (Carl Zeiss Ltd., Cambridge, UK), an Evolve 512 Delta EMCCD camera (Photometrics, Tucson, AZ, USA) and a x63 1.2 NA oil objective using the Ziess software, Zen blue. For all systems fluorescence was excited at 488 nm and emission collected between 510-640 nm.

Cell imaging and cytosolic calcium measurements with Fluo-5N were performed using a Leica SP5 MP inverted confocal microscope system with a x63 1.2 NA water objective using the Leica software, LAS X. Fluorescence was excited at 476 nm and emission collected between 500-600 nm.

Cell imaging and cytosolic calcium measurements with Fura-2 were performed using a Nikon Diaphot 200 inverted microscope system (Nikon Instruments, Kingston-Upon-Thames, UK) with a x40 oil objective using Image-Pro software (Media Cybernetics, Rockville, MA, USA). Cells were excited at 355 and 385 nm and emission recorded between 510-550 nm.

Necrosis experiments were performed using a Carl Zeiss ZEN 2011 TIRF System with Axio Observer Z1 Inverted Microscope, CSU-X1 Spinning Disc Unit, an Evolve 512 Delta EMCCD camera (Photometrics, Tucson, AZ, USA) and a x63 1.2 NA oil objective using the Zeiss software, Zen blue. Propidium Iodide was excited at 514 nm and emission was recorded at 629 nm, additionally a bright-field image was taken.

2.14 Data analysis

To allow for comparison between experiments; all calcium measurements were conducted using identical laser power, photomultiplier sensitivity and were processed using identical values for contrast and brightness.

For experiments conducted using Fluo-4 or Fluo-5N the data produced was normalised by dividing the fluorescence by the initial fluorescence (F/F_0). When using Fura-2 the ratio of fluorescence when cells were excited at 355 nm and at 385 nm was calculated (F_{355}:F_{385}) and then normalised by dividing by the initial fluorescence ratio (which can be simplified to R/R_0).

For comparative analysis of Ca^{2+} responses, areas under individual traces recorded between the periods stated in the text were calculated and then averaged (for experiments using Fluo-5N values were multiplied by -1 to obtain a positive value) and presented as bar charts with standard errors.

For cell death assays, a minimum of three experiments using cells isolated from different animals were performed, with a maximum of five treatments tested per experiment. The number of viable and necrotic cells were then counted by eye based on the Propidium iodide staining observed, and the percentage of necrotic cells in each treatment for every experiment was calculated. Average values and standard errors of the mean were calculated and results presented as bar charts.

Statistical analysis was performed using ANOVA or Student's *t*-test, with two-tailed distribution and two-sample unequal variance (heteroscedastic) as its parameters. The significance threshold was set at 0.05. Where applicable, *n* indicates the total number of individual cells recorded/counted for the data displayed.

2.15 Software

LAS X, Zen blue and Image-Pro software were used with their respective microscope systems to program experiments; collect recordings of fluorescence in real time and calculate the intensity of regions of interest; and take fluorescent and bright field images.

Microsoft Word 2016 was used to write and edit this report. Microsoft Excel 2013 and 2016, and GraphPad Prism version 7.03 were used to view and edit data, prepare graphs and charts, make calculations and perform statistical analysis. Microsoft PowerPoint 2016 was used to produce and edit some images. The free referencing software Zotero version 4.0.29.17 was used to insert references and compile the bibliography with the addition of the 'Cardiff University – Harvard' referencing format application; the required plugins for Word and the Google Chrome web browser were installed.

CHAPTER 3:

NAADP-INDUCED CALCIUM RELEASE FROM INTRACELLULAR ORGANELLE STORES REQUIRES THE ACTIVITY OF BOTH RYANODINE RECEPTORS AND TWO-PORE CHANNELS

Chapter 3: NAADP-induced calcium release from intracellular organelle stores requires the activity of both ryanodine receptors and two-pore channels

3.1: Overview of NAADP-induced calcium release in pancreatic acinar cells

The function of PAC is to synthesise digestive enzymes in their inactive proenzyme form, store them in zymogen granules and then secrete them when required. Secretion is triggered by either of the external signals, the neurotransmitter ACh or the hormone CCK binding to their respective cell surface receptors (Mukherjee et al. 2008). These external signallers are then converted into an internal one via the production of intracellular secondary calcium messengers (Zhao et al. 2012). IP_3 is produced in response to ACh by the activation of phospholipase C, while CCK stimulates the production of both cADPR and NAADP via an ADPR cyclase believed to be CD38. The secondary messengers then trigger the release of Ca^{2+} from organelle stores, which in turn drives the secretion process.

IP_3 and cADPR are known to act on IP_3R and RyR respectively, mobilising Ca^{2+} stored in the lumen of the ER. The action of NAADP has been harder to characterise however, with several different channels identified as possible candidates (Hohenegger et al. 2002; Calcraft et al. 2009; Zhang et al. 2009). Though the suitability of each of these candidates fulfilling the role of a NAADP-sensitive Ca^{2+} channel has been questioned (Copello et al. 2001; Pryor et al. 2006; Wang et al. 2012), leading to disagreement within the field. The most recently identified candidate, the TPC family of proteins (Calcraft et al. 2009), is currently believed by many to fulfil the role. However, it has been shown that these channels do not interact directly with NAADP (Lin-Moshier et al. 2012), but instead must do so via one or more separate NAADP-binding proteins.

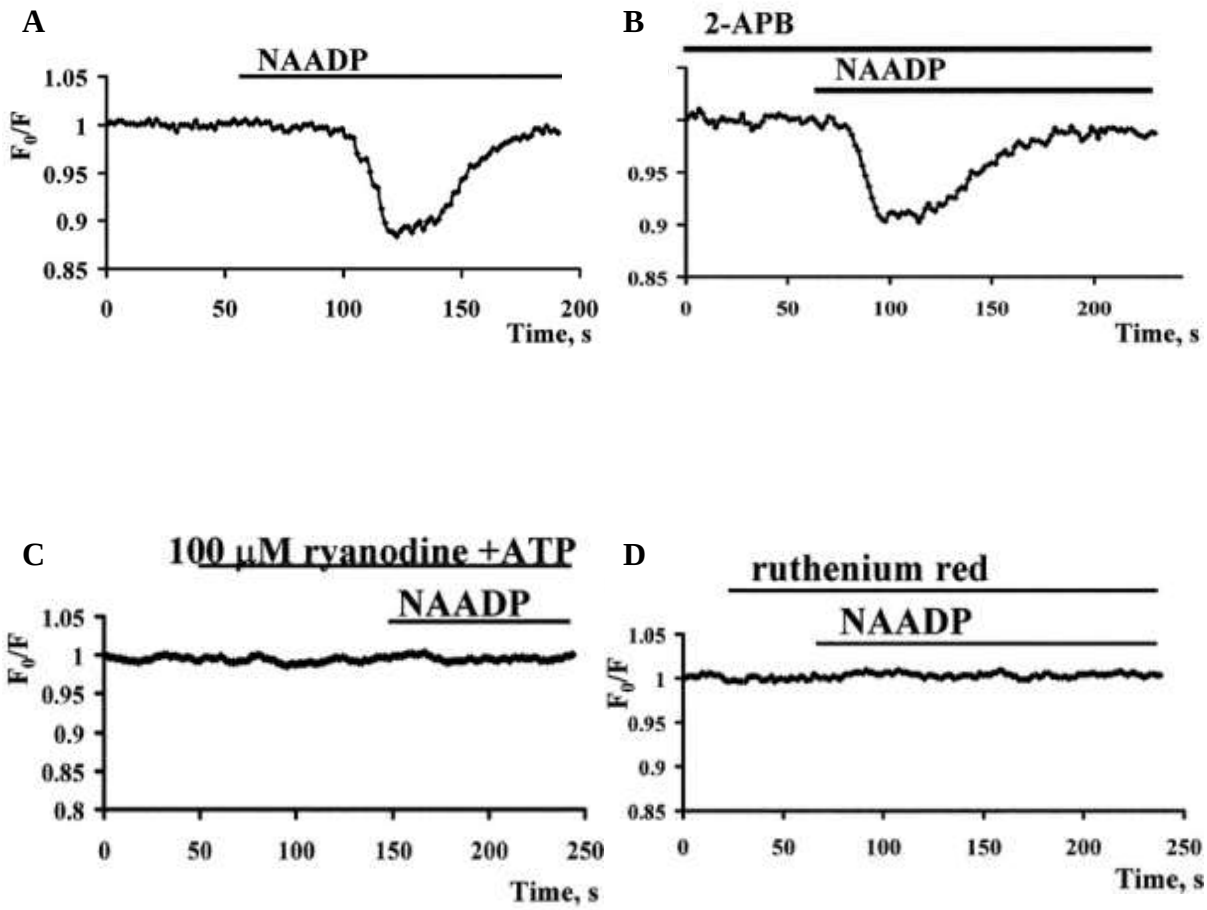

Fig 3.1.1 NAADP induced calcium release from a calcium store in the nuclear envelope of isolate nuclei from pancreatic acinar cells

(A) Representative trace showing NAADP induces the release of calcium from the nuclear envelope, depleting the stores calcium content. **(B)** Representative trace showing the IP_3R antagonist 2-APB has no effect on NAADP's ability to mobilise calcium from the nuclear envelope. **(C)** and **(D)** Representative traces showing inhibition of RyR by either ryanodine or ruthenium red prevented NAADP-induced calcium release from the nuclear envelope.

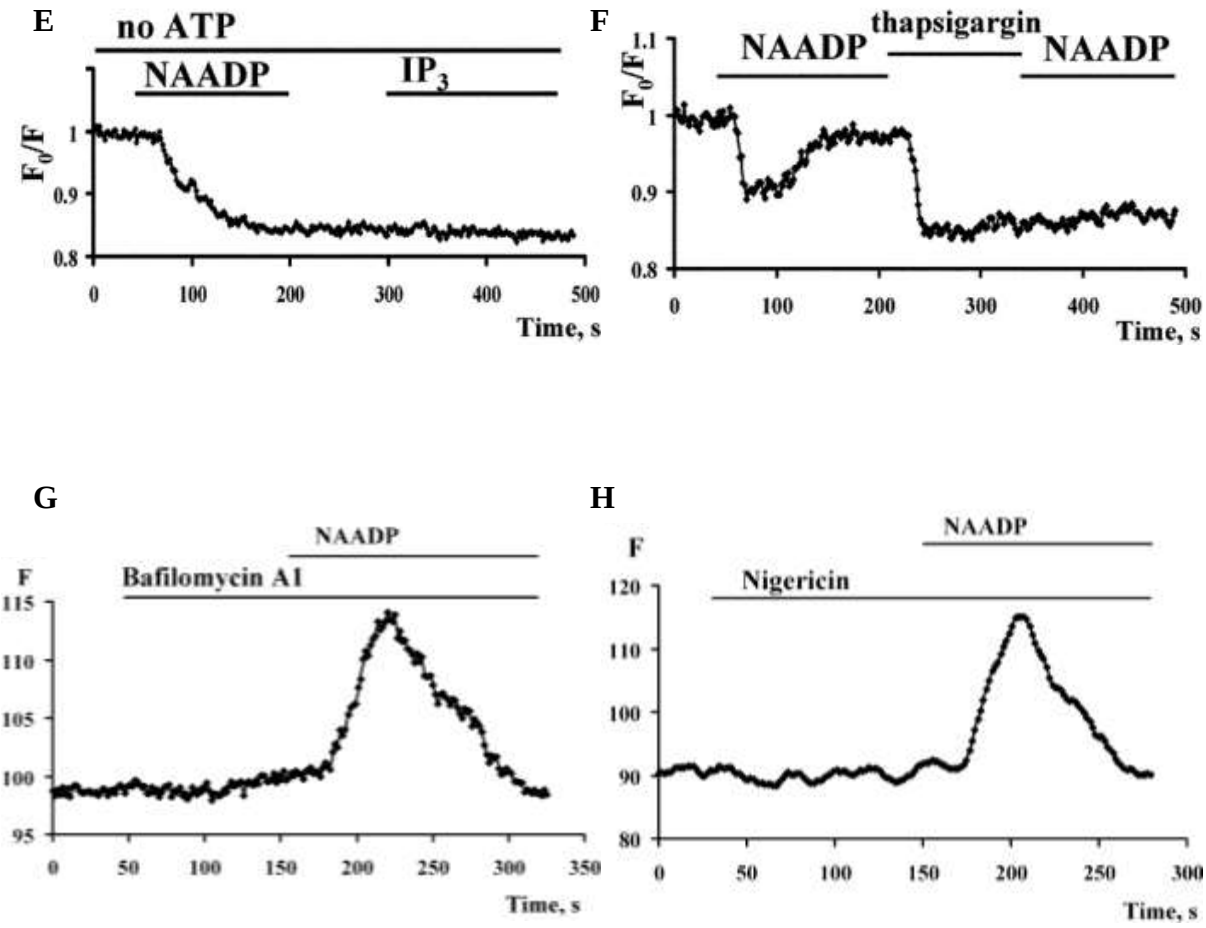

Fig 3.1.1 (*continued*)

(E) Representative trace showing refiling of the nuclear envelope store was inhibited in the absence of ATP, as IP_3 failed to elicit a response after NAADP was removed. **(F)** Representative trace showing NAADP failed to induce a secondary response after the nuclear envelope store was depleted by Tg. **(G)** and **(H)** Representative traces showing NAADP was able to induce an increase in the amount of calcium in the nucleoplasm even after acidic stores were disrupted by the use of either bafilomycin A1 or nigericin.

This requirement for a separate NAADP-binding protein opens the possibility for a greater complexity to NAADP signalling than if it acted directly on an ion channel. Potentially there could be multiple such binding proteins and therefore cell specific expression and interactions with more than one type of ion channel is conceivable. Such a possibility would explain the findings of Gerasimenko et al., who have shown that NAADP can mobilise Ca^{2+} through RyR (Gerasimenko et al. 2003) and from the ER (Gerasimenko, Sherwood, et al. 2006).

In one study Gerasimenko et al. used centrifugation to isolate nuclei from PAC to study the effect of NAADP on the organelle (Gerasimenko et al. 2003). Nuclei were loaded with Mag-Fura Red, a low affinity Ca^{2+} sensitive dye, to visualise depletion of Ca^{2+} from within the nuclear envelope or with Fluo-4 dextran to visualise Ca^{2+} increases in the nucleoplasm. Like the other secondary messengers NAADP was able to deplete the $[Ca^{2+}]_l$ (*Fig 3.1.1A*), though showed auto-inhibition when its concentration exceeded 10 μM. The presence of an auto-inhibitory concentration of NAADP did not block release of Ca^{2+} from the nuclear envelope induced by either IP_3 or cADPR. NAADP-induced depletion of the envelope store was insensitive to the IP_3R inhibitor 2-APB (*Fig 3.1.1B*), but was sensitive to both ryanodine and ruthenium red (*Fig 3.1.1C* and *D*), inhibitors of RyR. These results imply that NAADP mobilises Ca^{2+} from the lumen of the nuclear envelope via RyR; though via a mechanism distinct from cADPR, which also acts on these channels.

Reloading of the envelope store after NAADP-induced depletion was inhibited in the absence of ATP (*Fig 3.1.1E*) and NAADP failed to elicit a response after the store was emptied by Tg (*Fig 3.1.1F*); indicating that NAADP's effect on the nuclear envelope is dependent on the activity of the SERCA Ca^{2+} pump. Bafilomycin A1, an inhibitor of the vacuolar H^+ ATPase, and the protonophore nigericin both disrupt acidic Ca^{2+} stores and are known to inhibit NAADP-induced Ca^{2+} release in some cell types (Davis et al. 2012). However neither of

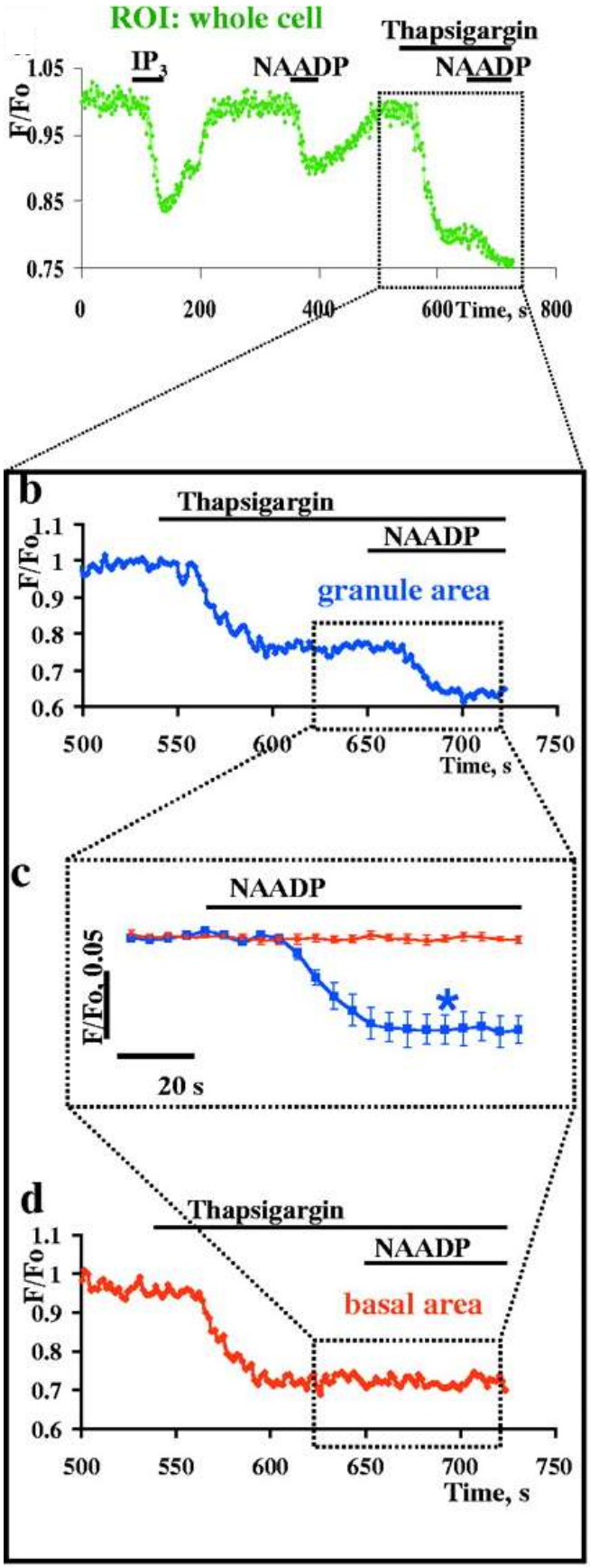

Fig 3.1.2 NAADP only induces alcium release form the apical granule area of permeabilized pancreatic acinar cells after the ER store is depleted by thapsigargin

(A) Representative trace of a whole cell recoding showing NAADP induced calcium release was substantially reduced after the ER calcium store was depleted by Tg. **(B)** The corresponding trace of the highlighted time period on trace **(A)** when the region of interest (ROI) was solely place in the apical granular region. **(C)** Average trances from the highlighted final 100 s period of traces **(B)** and **(D)** (n = 20). **(D)** The corresponding trace of the highlighted time period on trace **(A)** when the ROI was solely place in the basal region.

Adapted with permission from JV Gerasimenko; *Journal Cell Science*; 2006 (Gerasimenko, Sherwood, et al. 2006).

these agents had any effect on NAADP's ability to mobilise Ca^{2+} from the nuclear envelope (*Fig 3.1.1G* and *H*). These results conflict with the belief held by some that NAADP can only induce Ca^{2+} release from a non-ER, Tg-insensitive acidic store (Galione and Churchill 2002). The outer nuclear envelope is continuous with the ER membrane, containing the same Ca^{2+} channels and pumps, and therefore should act in a similar manner to the ER. As NAADP induced release from the isolated nuclei was insensitive to inhibitors of Ca^{2+} release from acidic stores any argument of a native acidic store or contamination by a non-nuclei acid store can be dismissed. The function of a Ca^{2+} store within the nuclear envelope that is sensitive to the activity of secondary messengers, is likely to drive gene transcription by inducing localised increases of Ca^{2+} within the nucleoplasm. As these messengers are produced in response to secretagogues it is possible that this would trigger the synthesis of new digestive enzymes to replace those secreted by the cell in response to the same incident of cell stimulation.

In a second study Gerasimenko et al. (Gerasimenko, Sherwood, et al. 2006) examined the activity of all three secondary Ca^{2+} messengers on release from both the ER and acidic stores in PAC. The acidic store can be isolated from the ER one by first depleting the ER store using Tg and then applying a stimulus after a new baseline is established. Under such circumstances all three secondary messengers were still able to mobilize a small amount of Ca^{2+}, with NAADP having a greater effect than the other two messengers. NAADP induced release was specific to the apical granular region of the cell, with none observed in the basal region (*Fig 3.1.2*). Conversely the ER store can be isolated in a similar manner using either bafilomycin A1 or nigericin to deplete the cells acidic stores. Under such conditions both NAADP and IP_3 were still able to mobilize Ca^{2+} (*Fig 3.1.3A* and *B*); however, when Tg was used in combination with either bafilomycin A1 or nigericin neither messenger had any effect

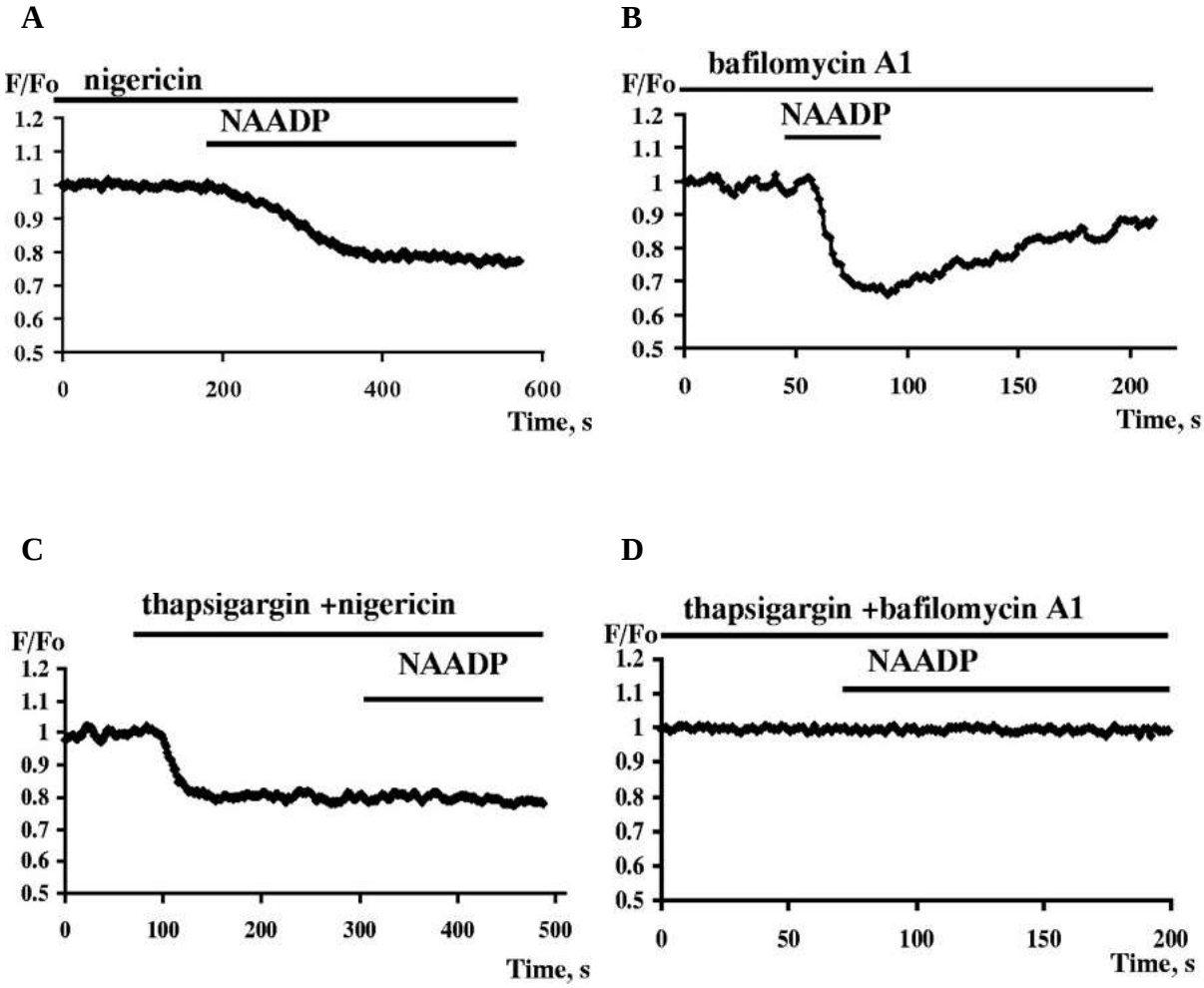

Fig 3.1.3 NAADP can induce calcium release from a none acidic calcium store in permeabilized pancreatic acinar cells

(A) and **(B)** Representative traces of whole cell recordings showing NAADP was able to induce a release of calcium from a none acidic store after the acid store was disrupted by the use of either nigericin or bafilomycin A1. **(C)** and **(D)** Representative traces of whole cell recordings showing that depletion of both the ER and acidic calcium stores by thapsigargin with either nigericin or bafilomycin A1 inhibited NAADP-induced calcium release.

Adapted with permission from JV Gerasimenko; *Journal Cell Science*; 2006 (Gerasimenko, Sherwood, et al. 2006)

(*Fig 3.1.3C* and *D*).

Use of GPN or brefeldin A to disrupt lysosomes and the Golgi body respectively, in combination with thapsigargin had no effect on NAADP-induced Ca^{2+} release. This suggests that neither of these type of acidic organelle is the store that NAADP acts on. The most probable candidate for the store is therefore the secretory zymogen granules, a type of organelle specific to PAC that is present only in the apical region of the cell and in a suitably large number to explain the size of the acidic pool in this region of the cell. These results indicate that in PAC all three secondary Ca^{2+} messengers can mobilize Ca^{2+} from both the ER and an acidic store. This contradicts the conventional model of secondary messenger induced Ca^{2+} release, where IP_3 and cADPR only release Ca^{2+} from the ER while NAADP acts on a separate acidic store, believed to be lysosomes. This pattern of signalling reported might be unique to PAC due to their large pool of a type of acidc organelle specific to this cell type, the zymogen granules. IP_3R and RyR, which typically exhibit an ER location, could be present on these unique PAC organelles due to the high rate of ER turnover required to produce the large number of these vesicles. Combined with the potential for there being NAADP binding proteins specifically expressed in PAC, this would explain any contradiction is secondary messenger activity.

NAADP-induced Ca^{2+} releases in the apical region of the cell was completely abolished in the presence of ryanodine or RR (*Fig 3.1.4A* and *B*), indicating a key role for RyR in this process. When the Ca^{2+} concentration was clamped to prevent CICR, NAADP was unable to induce a response in the presence of thapsigargin (*Fig 3.1.4D*), while IP_3 and cADPR were still able to. In the absence of thapsigargin NAADP was still able to mobilize Ca^{2+} (*Fig 3.1.4C*); this suggests NAADP acts via different mechanisms on the two stores, with release from the acidic stores dependent on CICR. Like the Ca^{2+} release seen from the nuclear

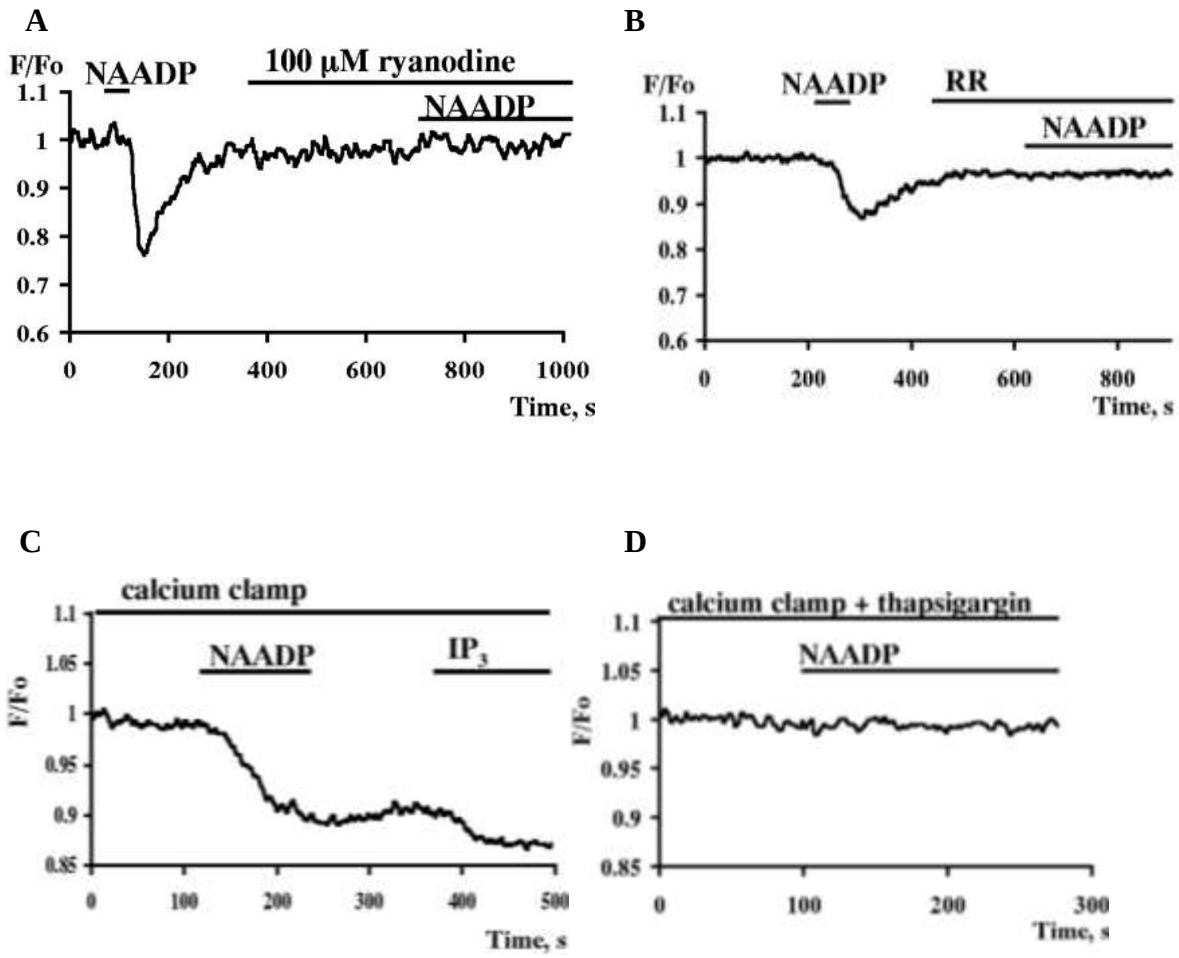

Fig 3.1.4 NAADP-induced calcium release in permeabilized pancreatic acinar cells utilizes ryanodine receptors and calcium-induced calcium release

(A) and **(B)** Representative traces of the granular area showing NAADP-induced calcium release was inhibited by ryanodine and ruthenium red, both inhibitors of RyR. **(C)** Representative trace of a whole cell recording showing NAADP is still able to mobalise calcium when the calcium concentration was clamped at 100 nM using a calcium/BAPTA mixture with a high concentration of BAPTA to prevent calcium-induced calcium release. **(D)** Representative trace of a whole cell recording showing NAADP is unable to mobilise calcium when the ER store is depleted by thapsigargin and calcium concentration clamped at 100 nM.

Adapted with permission from JV Gerasimenko; *Journal Cell Science*; 2006 (Gerasimenko, Sherwood, et al. 2006)

envelope, NAADP and cADPR release from the acid store suggests the two messengers employ different mechanisms of action despite both involving RyR, as cADPR-induced release was not dependent on CICR.

Calibration experiments using ionomycin to estimate the size of the two stores suggest that while in the whole cell the ER store is twice the size of the acidic one (Gerasimenko, Sherwood, et al. 2006), in the apical region where the majority of secondary messenger signalling is thought to occur the size of the two stores is larger than the ER one. A large acidic Ca^{2+} store in the apical region of PAC that is sensitive to all three secondary Ca^{2+} messengers would be useful in this cell type; localised Ca^{2+} release from these organelles could drive the migration, docking and membrane fusion required for them to secrete the pro-enzymes they contain. Since these two studies, the TPC family of ion channels located with the endolysosome system have been identified as potential NAADP sensitive Ca^{2+} channels. While disruption of lysosomes with GPN was found to have no effect on NAADP-induced Ca^{2+} release from the acidic store in PAC (Gerasimenko, Sherwood, et al. 2006) it is important to clarify if these ion channels play a role in PACs response to NAADP.

3.2 TPC and RyR isoform requirements for NAADP activity in pancreatic acinar cells

PACs from either wild type or knockout animals were loaded with Fluo-5N and permeabilized via a two-photon laser to visualise the amount of Ca^{2+} within organelle stores. As previously shown NAADP induced a decrease in intensity corresponding to a reduction in the amount of Ca^{2+} within stores (*Fig 3.2.1A*). In the presence of the NAADP specific antagonist Ned-19 this release was significantly reduced, down to 32.2% compared to when Ned-19 was not present, though a complete inhibition was not observed (*Fig 3.2.1B*). As expected due to Ned-19's specificity, it had no significant effect on either cADPR or IP_3-

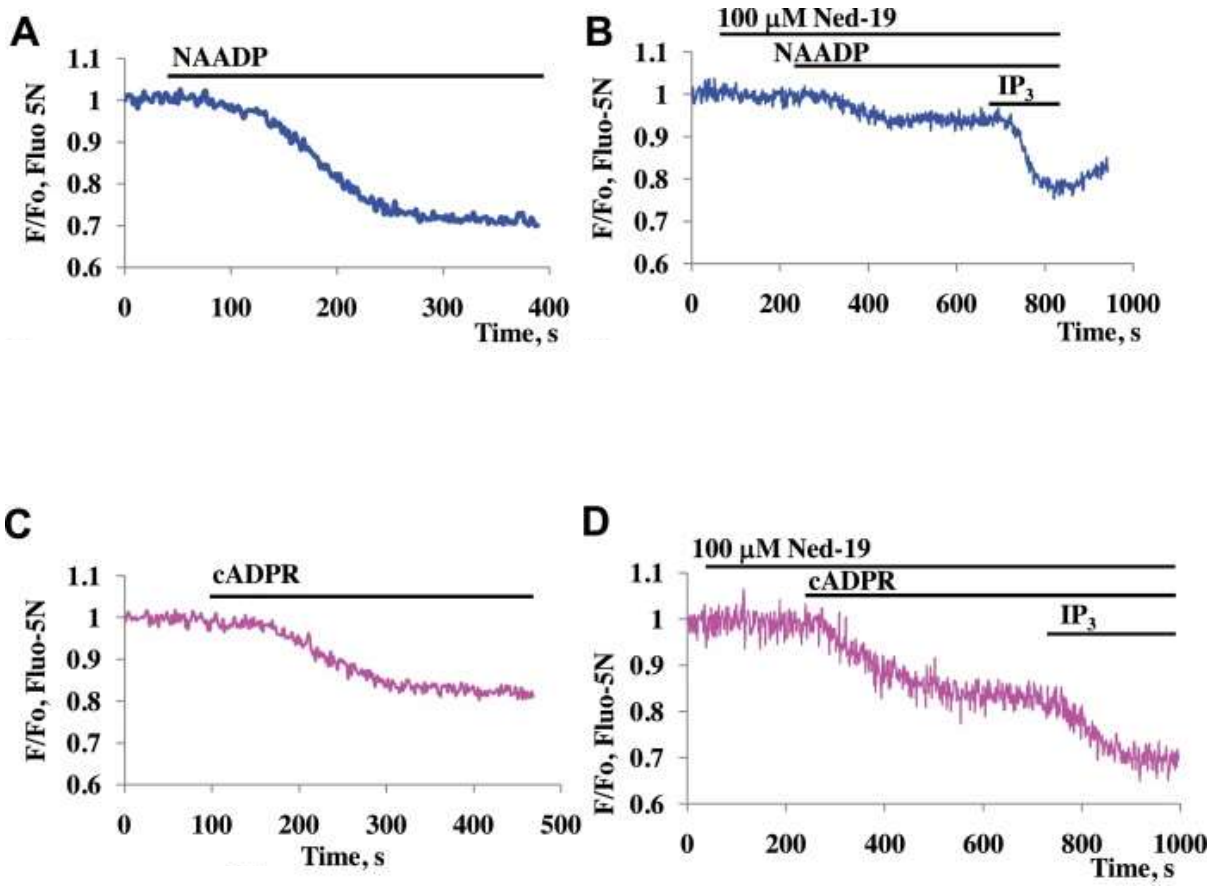

Fig 3.2.1 The effect of Ned-19 on secondary messenger induced calcium release in permeabilized pancreatic acinar cells

(A) Representative trace of the effect of 100 nM NAADP on store calcium in permeabilized pancreatic acinar cells. **(B)** Representative trace of the effect of 100 nM NAADP followed by 10 µM IP_3 on store calcium in permeabilized pancreatic acinar cells in the presence of 100 µM Ned-19. **(C)** Representative trace of the effect of 10 µM cADPR on store calcium in permeabilized pancreatic acinar cells. **(D)** Representative trace of the effect of 10 µM cADPR followed by 10 µM IP_3 on store calcium in permeabilized pancreatic acinar cells in the presence of 100 µM Ned-19.

Modified under terms of free use as author from JV Gerasimenko; *Cell Calcium*; 2015 (Gerasimenko et al. 2015).

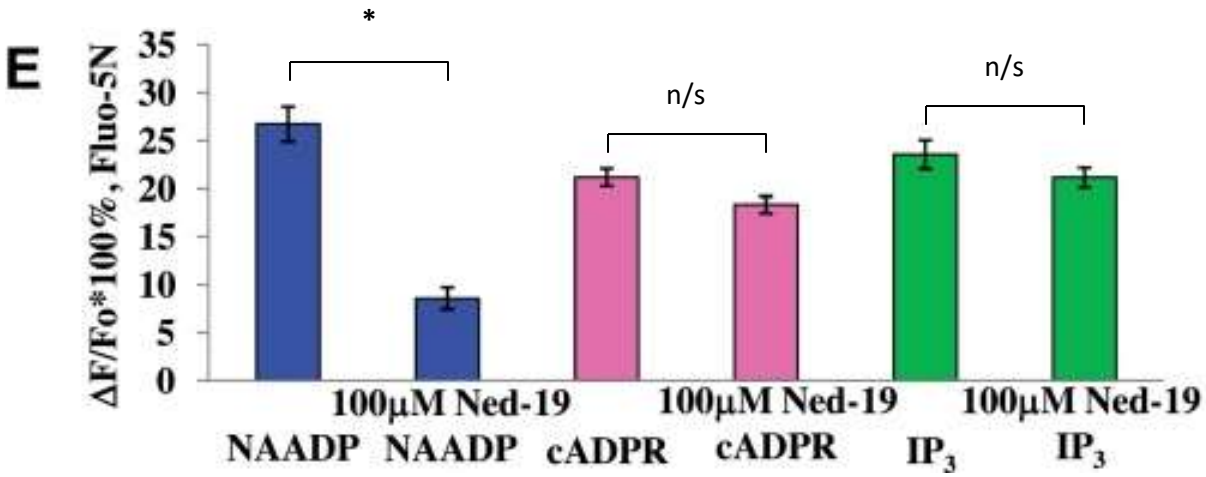

Fig 3.2.1 (*continued*)

(E) Summary of data comparison of secondary messenger induced calcium release from stores in permeabilized pancreatic acinar cells with and without the presence of Ned-19. NAADP (control 26.7 ± 1.8%, n = 13; with Ned-19 8.6 ± 1.1, n = 5, p = 0.00002), cADPR (control 21.2 ± 0.9%, n = 10; with Ned-19 18.3 ± 0.9%, n = 4; p = 0.1) or IP_3 (control 23.6 ± 1.5%, n = 11; with Ned-19 21.2 ± 1.1%, n = 6, p = 0.3) Error bars represent ± SEM.

Modified under terms of free use as author from JV Gerasimenko; *Cell Calcium*; 2015 (Gerasimenko et al. 2015).

induced Ca^{2+} release (*Fig 3.2.1D* and *E*).

The importance of TPC channels in the response to NAADP was tested by inhibiting their activity via either allosteric inhibition via pore targeted antibodies or the use of PAC from $TPCN2^{-/-}$ mice. The response to NAADP in $TPCN2^{-/-}$ cells (*Fig 3.2.2B*) was 36% the size of that in wild type cells (*Fig 3.2.2 A*), a similar decrease of 72% was observed in wild type cells preincubated with a TPC2 antibody after permeabilization (*Fig 3.2.2C*). The antibody's blocking activity was specific against NAADP-induced Ca^{2+} release as it had no significant effect on IP_3 or cADPR's ability to mobilize Ca^{2+} (*Fig 3.2.2E*). Inhibition of TPC1 by its antibody produced a less drastic effect, reducing the NAADP response to 75.5% of the control (*Fig 3.2.2D*). Use of the TPC1 antibody either in combination with the TPC2 antibody or $TPCN2^{-/-}$ cells resulted in a similar level of inhibition down to 19.4% and 14.3% respectively (*Fig 3.2.2F*). These results suggest that while both TPC isoforms form part of the PAC's response to NAADP, there is a much greater requirement of the TPC2 isoform.

As TPC proteins have been shown to be expressed on acidic organelles, the ER's Ca^{2+} content was depleted by thapsigargin to prevent CICR enhancing responses from acidic stores. Under such conditions antibody blockade of TPC1 resulted in a non-significant reduction in the NAADP response from the control, however blockage of TPC2 reduced the response to 19.1% of the control (*Fig 3.2.2G*). Inhibition of both TPC isoforms by antibodies further reduced the response to 7% of the control; confirming the previous findings that NAADP can moblise Ca^{2+} via TPC channels in PAC, with TPC2 having a much greater role than TPC1.

As NAADP activity displayed different requirements for the two TPC isoforms it was decided if there was a similar varying requirement of the three isoforms of RyR; which have previously shown to play a key role in NAADP induced Ca^{2+} release in PAC. Cells from

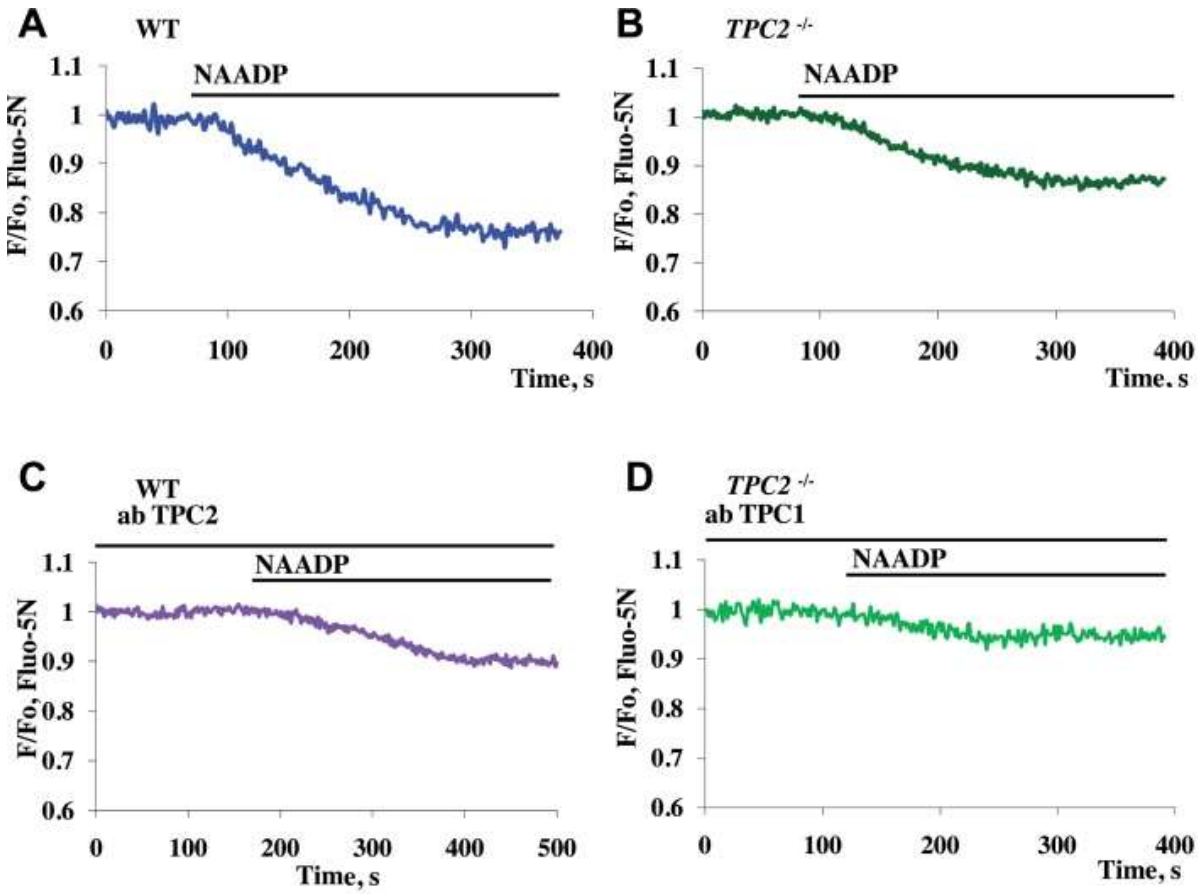

Fig 3.2.2 TPC channels are involved in NAADP-induced calcium release in permeabilized pancreatic acinar cells

(A) Representative trace of the effect of 100 nM NAADP on permeabilized pancreatic acinar cells from wild type mice (n = 13). **(B)** Representative trace of the effect of 100 nM NAADP on permeabilized pancreatic acinar cells from TPC2 knockout mice (n = 5). **(C)** Representative trace of the effect of 100 nM NAADP on permeabilized pancreatic acinar cells from wild type mice after pre-treatment with a TPC2 antibody (20 min 1:100) (n = 8). **(D)** Representative trace of the effect of 100 nM NAADP on permeabilized pancreatic acinar cells from TPCN2 Knockout mice after pre-treatment with a TPC1 antibody (20 min 1:100) (n = 11).

Modified under terms of free use as author from JV Gerasimenko; *Cell Calcium*; 2015 (Gerasimenko et al. 2015).

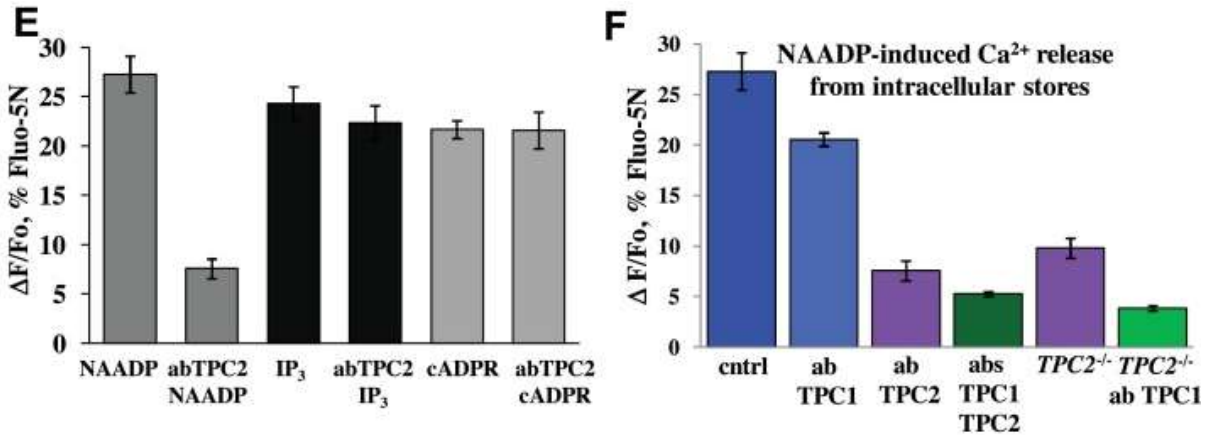

Fig 3.2.2 (*continued*)

(E) Summary of data comparison of the amplitudes of responses to secondary calcium messengers in permeabilized pancreatic acinar cells with and without the presence of the TPC2 antibody. 100 nM NAADP (n = 13 control; n = 8 with TPC2 antibody treatment), 10 μM IP_3 (n = 9 control; n = 8 with TPC2 antibody treatment) or 10 μM cADPR (n = 9 control; n = 5 with TPC2 antibody treatment). **(F)** Summary of the role the two TPC isoforms play in NAADP-induced calcium release in permeabilized pancreatic acinar cells. A TPC1 antibody (20.6 ± 0.7%, n = 11) or TPC2 antibody (7.6 ± 1%, SEM, n = 8) were used alone or in a mixture of the two (5.3 ± 0.2%, n = 4), in cells from wild type mice compared to responses in permeabilized cells isolated from TPC2 KO mice and treated (3.9 ± 0.3%, n = 7) or non-treated with TPC1 antibody (9.8 ± 1.0%, n = 5).

Modified under terms of free use as author from JV Gerasimenko; *Cell Calcium*; 2015 (Gerasimenko et al. 2015).

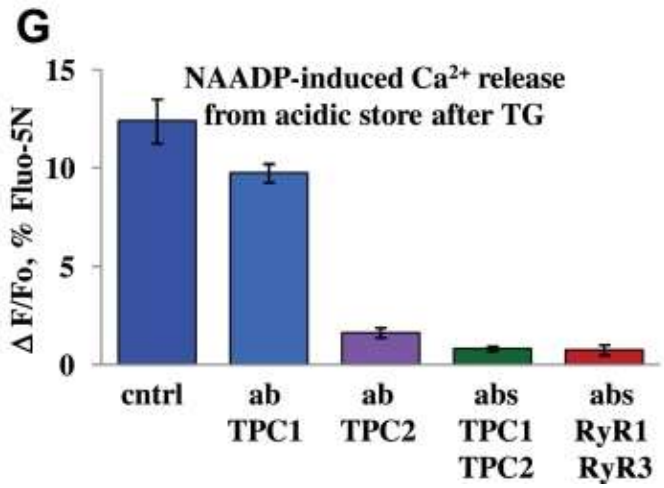

Fig 3.2.2 (*continued*)

(G) Summary of the role the two TPC isoforms play in NAADP-induced calcium release after ER store depletion by 10 µM thapsigargin in permeabilized pancreatic acinar cells; in the presence of a TPC1 antibody (9.8 ± 0.5%, $n = 5$, $p > 0.08$), or aTPC2 antibody (1.63 ± 0.3%, $n = 6$), or a mixture of both (0.83 ± 0.1%, $n = 6$), or a mixture of antibodies against RyR1 and RyR3 (0.75 ± 0.1%, $n = 5$) as compared to control NAADP responses (12.4 ± 1.1%, $n = 5$). Error bars represent ± SEM. Cells were loaded with Fluo-5N in AM form.

Modified under terms of free use as author from JV Gerasimenko; *Cell Calcium*; 2015 (Gerasimenko et al. 2015).

RyR3$^{-/-}$ mice show a reduction of about 52% compared to wild type cells (*Fig 3.2.3B*), and when used in combination with a RyR1 pore-blocking antibody increased this inhibition to 90% (*Fig 3.2.3C*). Use of the RyR1 alone resulted in the NAADP response being reduced to approximately 18.7% of the control (*Fig 3.2.3E*). Antibody blockade of RyR3 produced a less significant inhibition of the NAADP response (*Fig 3.2.4C*), while doing so for RyR2 had no significant effect (*Fig 3.2.4C*). Combining antibodies for RyR1 and RyR2 showed no additional inhibition compared to using the RyR1 antibody alone (*Fig 3.2.4G*), reducing the response to 17.4% of the control. A combination of RyR1 and RyR3 did however show an additive effect, with a 93.0% reduction compared to the control (*Fig 3.2.4G*). This inhibition was only slightly enhanced to 95.2% when all antibodies for all three RyR isoforms were utilised (*Fig 3.2.4G*). Use of antibodies for RyR1 and RyR3 after the ER was depleted by thapsigargin showed a 94% inhibition of the control NAADP response (*Fig 3.2.2G*), a level nearly identical to when both TPC1 and TPC2 were blocked. These results suggest that there is a variable requirement of RyR isoforms for NAADP induced Ca^{2+} release in PAC with the type 1 isoform the most important and type 2 having minimal involvement.

As NAADP's Ca^{2+} mobilizing activity had displayed a clear preference for certain RyR isoform it is logical that cADPR, which also has been shown to act via this family of ion channels, might do so. Blocking RyR1 had a much less significant effect against cADPR than NAADP, with a response 70.0% of the control observed (*Fig 3.2.3E*). The effect of blocking RyR2 was much more significant for cADPR, inhibiting the response by about 54.8% (*Fig 3.2.4D*). The combination of RyR1 and RyR3 antibodies that was most effective against NAADP only produced a 49.3% inhibition against cADPR (*Fig 3.2.4G*), with a similar 49% inhibition seen when RyR3$^{-/-}$ cells were used in combination with the RyR1 antibody (*Fig 3.2.3D*). The combination of RyR1 and RyR2 antibodies proved highly effective, displaying

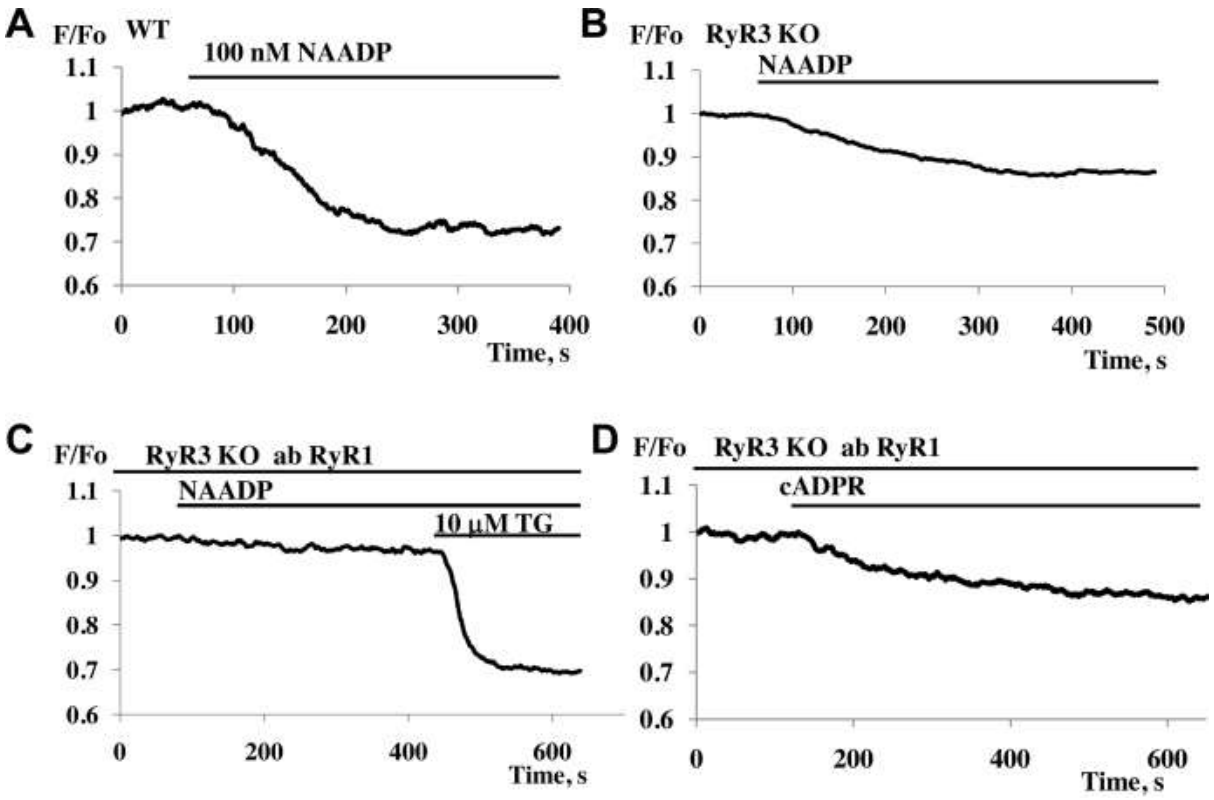

Fig 3.2.3 NAADP-induced calcium release is reduced in permeabilized pancreatic acinar cells isolated from RyR3 knockout mice

(A) Representative trace of the effect of 100 nM NAADP on permeabilized pancreatic acinar cells from wild type mice (n = 12). **(B)** Representative trace of the effect of 100 nM NAADP on permeabilized pancreatic acinar cells from RyR3 knockout mice (n = 8). **(C)** Representative trace of the effect of 100 nM NAADP on permeabilized pancreatic acinar cells RyR3 knockout mice after pre-treatment with a RyR1 antibody (20 min 1:100) (n = 10). **(D)** Representative trace of the effect of 10 µM cADPR on permeabilized pancreatic acinar cells from RyR3 knockout mice after pre-treatment with a RyR1 antibody (20 min 1:100) (n = 9).

Modified under terms of free use as author from JV Gerasimenko; *Cell Calcium*; 2015 (Gerasimenko et al. 2015).

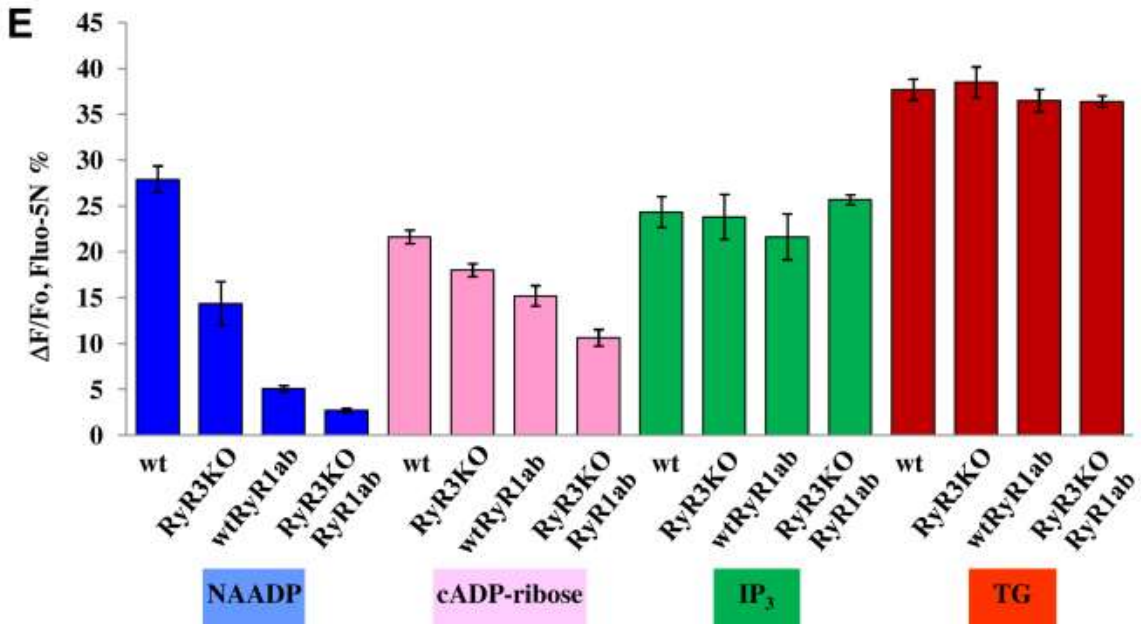

Fig 3.2.3 (*continued*)

(E) Summary of data comparison of the amplitudes of responses to secondary calcium messengers and thapsigargin (10 µM) in permeabilized pancreatic acinar cells from wild type and RyR3 knockout mice, with and without RyR1 antibody pre-treatment ($n > 4$ for each group). Data represent mean values ± SEM.

Modified under terms of free use as author from JV Gerasimenko; *Cell Calcium*; 2015 (Gerasimenko et al. 2015).

an 83.4% inhibition (*Fig 3.2.4G*). Antibody blocking of all three RyR isoforms had the greatest effect, reducing the response to 10.6% of the control (*Fig 3.2.4B*). Together these results suggest that cADPR-induced Ca^{2+} release in PAC is highly dependent on the type 2 isoform of RyR, with a small involvement of the type 1 and minimal involvement of the type 3 isoforms. This would mean that despite both NAADP and cADPR utilising all three isoforms of RyR there is a clear segregation of the two messenger's effects by the respective involvements of the various isoforms.

Genetic knockout of RyR3 or inhibition of any of the three RyR isoforms had no significant effect on IP_3's ability to mobilize Ca^{2+} from stores within PAC (*Fig 3.2.3E* and *Fig 3.2.4G*). Neither did they have any effect on the amount of Ca^{2+} within organelle stores, observed by emptying them by using either thapsigargin (*Fig 3.2.3E*) or TPEN (*Fig 3.2.4G*).

To compare the relative importance of RyR and TPC proteins in PAC's response to NAADP their activity was blocked; ryanodine or antibodies for all three RyR isoforms were used to inhibit RyR activity, and a combination of antibodies for both TPC isoforms or $TPC2^{-/-}$ cells with TPC1 antibodies was used to inhibit the activity of TPC channels (*Fig 3.2.5*). Inhibition of RyR by either method had a greater effect than inhibition of TPC channels, with the RyR antibody mixture displaying a 95% inhibition of NAADP-induced release. A smaller effect was observed when both TPCs were inhibited; using antibodies alone produced an 80% inhibition and the combination of TPC1 antibody and $TPCN2^{-/-}$ cells an 86% inhibition. These results show that while inhibiting TPCs significantly reduces the response to NAADP in PAC, inhibition of RyR causes a near complete inhibition. This could be due to RyR potentially acting as both an NAADP sensitive ion channel and being able to enhance any response to NAADP through CICR, while TPC's act only as a NAADP sensitive channel. Interestingly 100 µM Ned-19, a concentration shown to inhibit NAADP responses in several

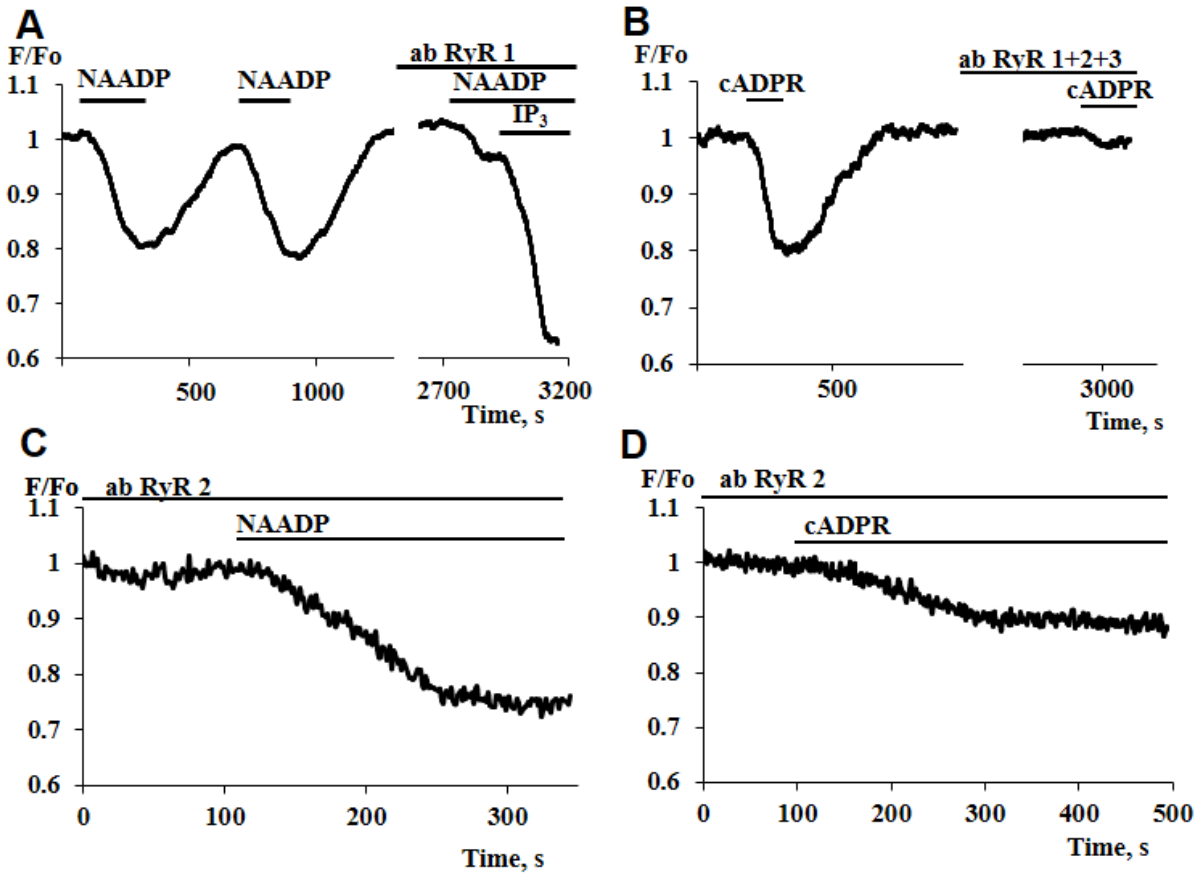

Fig 3.2.4 NAADP and cADPR-induced calcium release in permeabilized pancreatic acinar cells is inhibited by antibodies for different RyR isoforms

(A) Representative trace of the effect of 100 nM NAADP in the presence or absence of a RyR1 antibody (20 min 1:100) followed by 10 µM IP_3 (n = 5). **(B)** Representative trace of the effect of 10 µM cADPR in the presence or absence of a mixture of antibodies for all three RyR isoforms (20 min 1:100) (n = 3). **(C)** Representative trace of the effect of 100 nM NAADP after pre-treatment with a RyR2 antibody (20 min 1:100) (n = 6). **(D)** Representative trace of the effect of 10 µM cADPR after pre-treatment with a RyR2 (20 min 1:100) (n = 5).

Modified under terms of free use as author from JV Gerasimenko; *Cell Calcium*; 2015 (Gerasimenko et al. 2015).

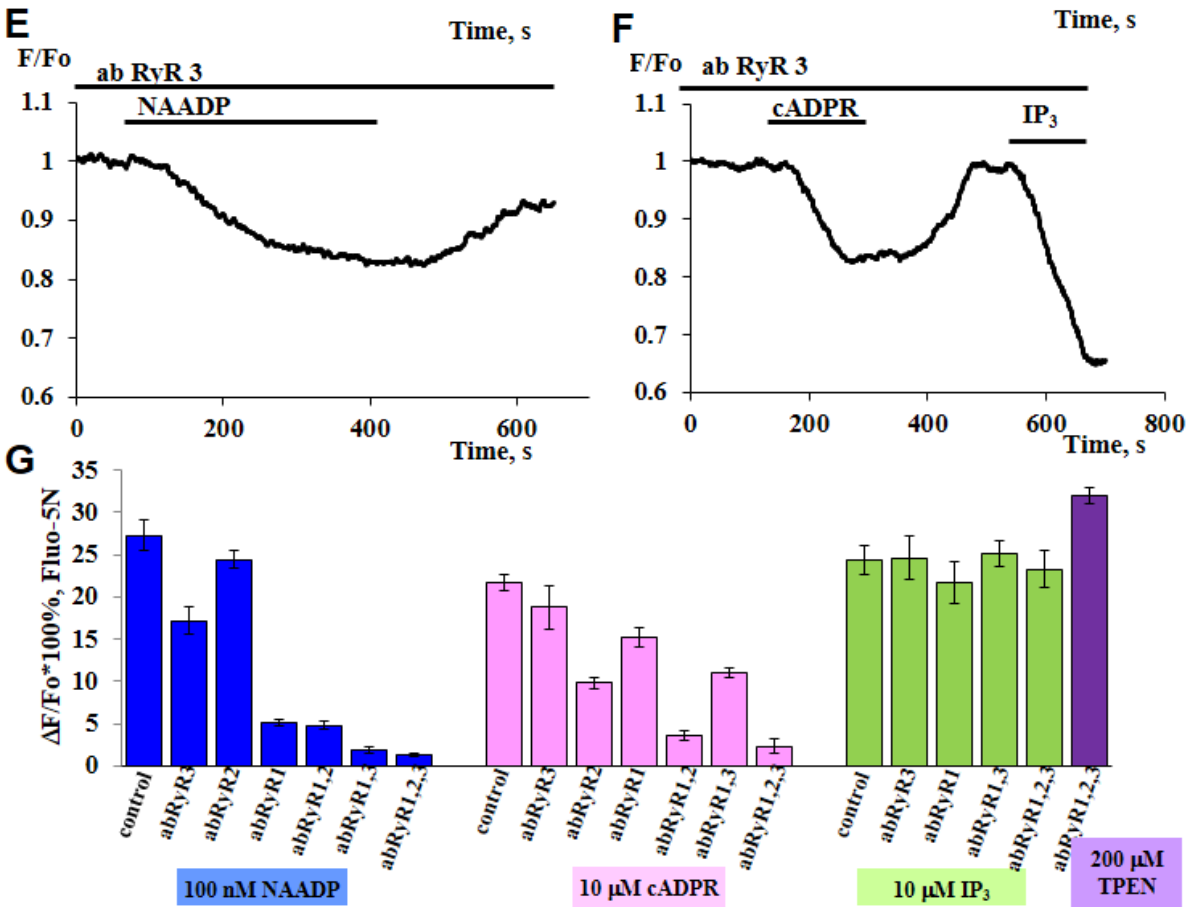

Fig 3.2.4 (*continued*)

(E) Representative trace of the effect of 100 nM NAADP after pre-treatment with a RyR3 antibody (20 min 1:100) (n = 5). **(F)** Representative trace of the effect of 10 µM cADPR followed by 10 µM IP_3 after pre-treatment with a RyR2 (20 min 1:100) (n = 4). **(E)** Summary of data comparison of the amplitudes of responses to secondary calcium messengers and TPEN (200 µM) in permeabilized pancreatic acinar cells from wild type and mice, with and without pre-treatment using antibodies for the three RyR isoforms applied either alone or in combination ($n > 4$ for each group). Data represent mean values ± SEM.

Modified under terms of free use as author from JV Gerasimenko; *Cell Calcium*; 2015 (Gerasimenko et al. 2015).

cell types, only showed a 68% inhibition, and was therefore less effective than inhibiting either family of ion channel.

3.3 Discussion

NAADP is produced by PAC in response to the external stimulus CCK and drives fluid secretion in this cell type (Mukherjee et al. 2008). Classically, it has been believed that NAADP can only mobilise Ca^{2+} from a small acidic store distinct from the ER, this initial release then triggers the release of Ca^{2+} from the larger ER store via CICR amplifying the response to NAADP (Churchill and Galione 2001). Gerasimenko et al. have previously shown that this might not be the case in PAC, where they have previously shown NAADP induced release independent of acidic stores (Gerasimenko, Sherwood, et al. 2006) and in a RyR dependent manner (Gerasimenko et al. 2003).

The results above expand on this and show the involvement of the TPC family of ion channels in NAADP-induced Ca^{2+} release within PAC, with a much greater involvement of the TPC2 isoform than the TPC1 isoform (*Fig 3.2.2*). The activity of these channels is unique to the response to NAADP, and show no involvement in either IP_3 or cADPR induced release. The previous finding that RyRs play a key role in NAADP's activity (Gerasimenko, Sherwood, et al. 2006) are also supported, again in an isoform specific manner (*Fig 3.2.3* and *Fig 3.2.4*). Inhibition of either TPC channels or RyR failed to produce a complete inhibition of NAADP activity, though a combined inhibition of both families of ion channel was not tested and may provide a complete inhibition. While inhibition of TPC channels was found to provide a near complete inhibition of NAADP-induced release from acidic stores (*Fig 3.2.2G*), blocking their activity only showed a maximum of an 86% inhibition of the whole cells response to NAADP (*Fig 3.2.5*). This suggests that while these channels play a key role

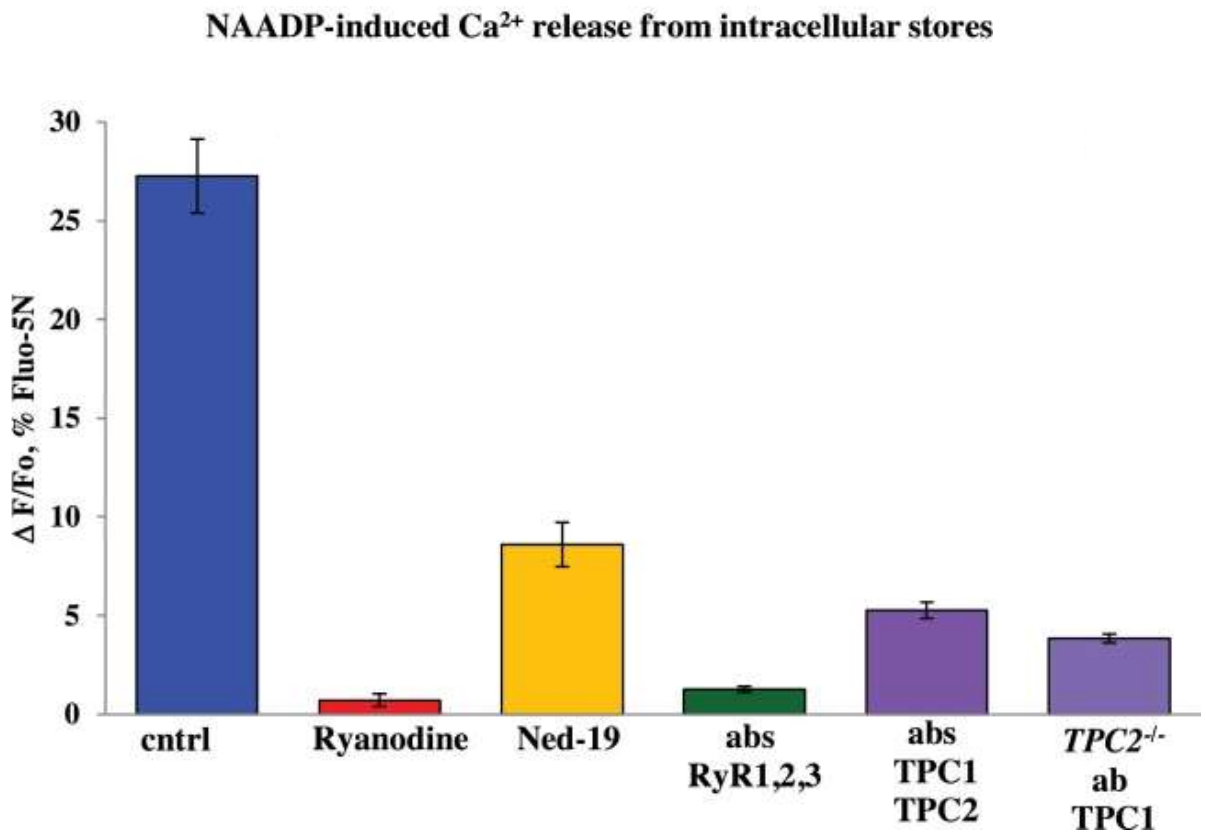

Fig 3.2.5 Comparison of the relative importance of the RyR and TPC families of ion channels for NAADP-induced calcium release in permeabilized pancreatic acinar cells

Calcium responses were measured in permeabilized pancreatic acinar cells from wild type mice were exposed to either NAADP alone (27.3 ± 1.8%, *n* = 12); in presence of either 100 μM Ryanodine (0.71 ± 0.30%, *n* = 7) or Ned-19 (8.6 ± 1.12%, *n* = 5); or after pre-treatment with a mixture of antibodies for either all three RyR isoform (1.27 ± 0.15%, *n* = 3) or both TPC isoform (5.3 ± 0.24%, *n* = 7). Calcium responses were also measured in permeabilized pancreatic acinar cells from TPC2 knockout mice after pre-treatment with a TPC1 antibody (3.9 ± 0.27%, *n* = 7). Error bars show ± SEM.

in NAADP's activity there is a separate independent mechanism through which NAADP can act on a none acidic store. This would support previous findings that NAADP can directly mobilise Ca^{2+} from the ER in PAC (Gerasimenko, Sherwood, et al. 2006) and T-cells via RyR (Dammermann and Guse 2005). Futher corroboration could be provided by examining the effect of blocking RyR's after emptying acidic stores using either bafilomycin A1 or nigericin. Blockade of RyR1 and RyR3 also provided a near complete inhibition of NAADP-induced Ca^{2+} release from acidic stores, this would suggest that any Ca^{2+} mobilized via TPC channels is further enhanced via CICR through RyR's present in the membranes of the acidic zymogen granules.

When inhibiting the activity of both TPC channels a greater inhibition was observed when cells from $TPCN2^{-/-}$ mice were used in combination with a TPC1 pore-targeted antibody compared to when antibodies for both isoforms were used in wild type PACs (*Fig 3.2.2F* and *Fig 3.2.5*). This difference is possibly because knocking the channel out physically removes it from the cell, thereby completely preventing its activity; whereas treatment with pore-targeted antibodies may not provide a complete inhibition, as not all of the target channels may be bound by antibodies. Therefore, an improvement to the techniques utilised in this study would have been to have used PAC cells from $TPCN1^{-/-}$ mice (Ruas et al. 2014) and from the $TPCN1/2^{-/-}$ double knockout mouse (Ruas et al. 2015). Use of cells from these mice would ensure the most efficient inhibition of the target channels activity was achieved. It should be noted that, due to the diverse range of cellular functions NAADP had been shown to play a role in (Lee 2001), the viability of $TPCN1/2^{-/-}$ double knockout mice suggests that NAADP may also be able to act via a TPC independent process, like observed in PACs.

The size of the response to cADPR in PAC (*Fig 3.2.4G*) was 79.5% the size of that of the NAADP (*Fig 3.2.3A*). This could be the result of NAADP-induced Ca^{2+} release involveing

both TPC and RyR, while cADPR-induced release involves only RyR. Alternatively, it could be because Ca^{2+} release induced by the two secondary messengers has differing involvements of the three RyR isoforms. Gerasimenko et al. had previously described that the two messengers did not act in the same manner despite their responses both utilising RyR. cADPR-induced release from the nuclear envelope was insensitive to an auto-inhibitory concentration of NAADP; and while no response to NAADP was seen from acidic stores when CICR was blocked by clamping the $[Ca^{2+}]_i$, cADPR still induced a response. These previous findings could suggest that cADPR acts directly on RyR and NAADP does not, or could be due to the differences seen in the involvement of the various RyR isoforms. RT-qPCR could be used to measure the different expression levels of the various isoforms in PAC and antibody staining of the various isoforms could identify their relative locations within PAC. Together these experiments would identify any segregation of isoforms within the cell and see if a particular isoform has a greater expression than the other, which could enhance the response to a particular secondary messenger over another.

Similarly, while TPC channels have been shown to be expressed on endolysosomes (Calcraft et al. 2009) it would be useful to perform antibody staining for TPC channels to identify their location in PAC; especially as the role of lysosomes in NAADP-induced Ca^{2+} release in these cells has previously been questioned via the use of GPN (Gerasimenko, Sherwood, et al. 2006). As zymogen granules create the largest acid store in PAC's, and are believed to contain other Ca^{2+} not normally found on acidic organelles, it would be interesting to discover if they also contain TPC channels. NAADP-induced Ca^{2+} release from acidic stores via TPC channels is enhanced by CICR via RyR, therefore an antibody based FRET technique to identify puncta between the two types of channel could identify potential domains where CICR occurs. CICR can also occur via IP_3R, and while the involvement of

this type of channel was ruled out of NAADP-induced Ca^{2+} release from the nuclear envelope by the use of 2-APB, it would be useful to repeat some of the previous whole cell experiments in the presence of a more specific IP_3R inhibitor e.g. Xestospongins (Gafni et al. 1997). If either NAADP or cADPR induced release was shown to be affected by an IP_3R inhibitor, similar experiments to dissect the involvement of the various IP_3R isoforms and identify puncta between them and the other channels involved in response to the messenger would be required.

Based on the results above, NAADP can mobilize calcium from lysosomes and endosomes via TPC2, and Zymogen granules or the ER via RyR1 and RyR3 isoforms. Whereas cADPR acts only on the Zymogen granules or the ER stores, mobilizing calcium through RyR2 and RyR1 isoforms. Responses to either messengers would then be amplified by CICR from the zymogen granules and the ER via RyRs and IP_3Rs.

Together these findings can be used to describe a more complex picture of NAADP-induced Ca^{2+} release in PAC than the standard 'trigger hypothesis' (Churchill et al. 2002). In these cells NAADP can mobilise Ca^{2+} from endo-lysosomal stores though TPC channels, predominantly TPC2. This response is then enhanced by CICR from either zymogen granules or the ER via RyRs, with RyR1 having the greatest involvement assisted by RyR3. NAADP is likely to also act directly on these RyR isoforms, especially to mobilise Ca^{2+} from the ER store (*Fig 3.3.2*). Conversely, cADPR acts only on RyR; mobilising calcium from both the ER and zymogen granules or the ER predominantly through RyR2, and to a lesser extent RyR1.

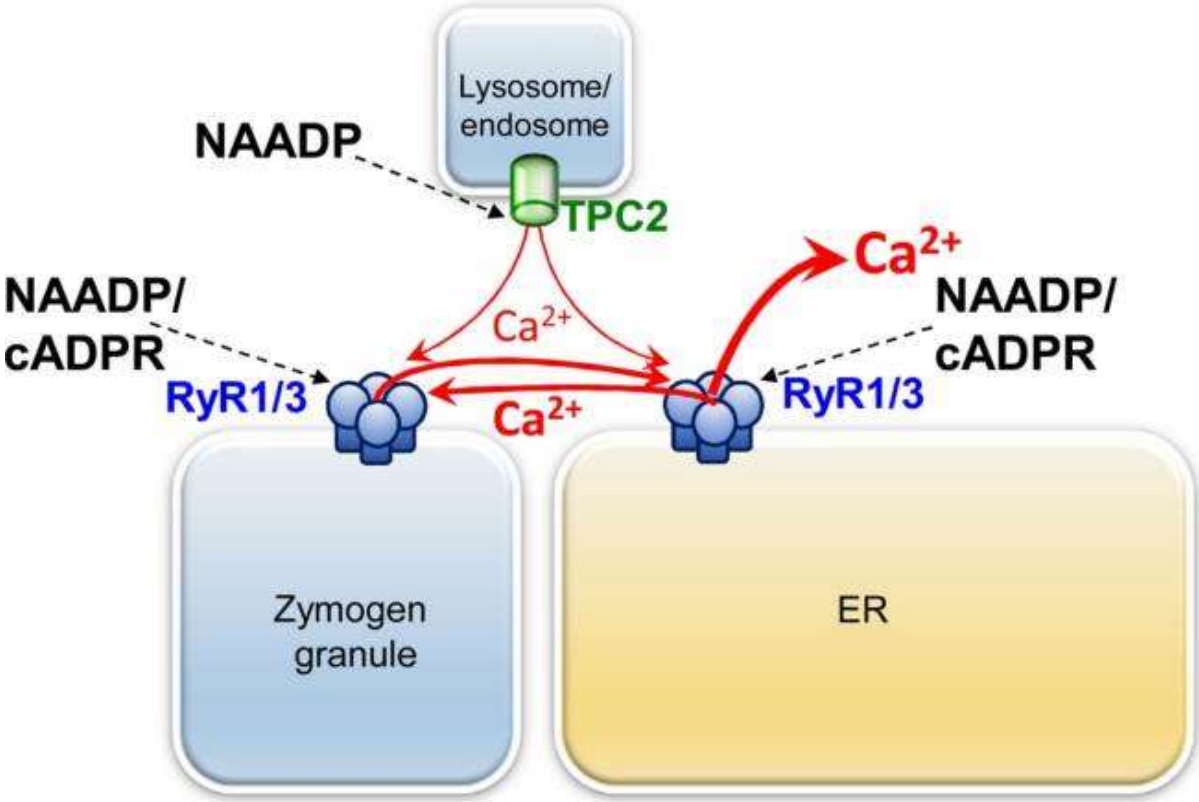

Fig 3.3 Graphical representation of NAADP and cADPR induced calcium release from organelle stores in pancreatic acinar cells

Reproduced under terms of free use as author from JV Gerasimenko; *Cell Calcium*; 2015 (Gerasimenko et al. 2015).

CHAPTER 4:

THE NAADP ANTAGONIST NED-19 HAS AN INHIBITORY EFFECT ON CHOLECYSTOKININ-INDUCED CALCIUM RELEASE IN PANCREATIC ACINAR CELLS

Chapter 4: The NAADP antagonist ned-19 has an inhibitory effect on cholecystokinin-induced calcium release in pancreatic acinar cells

4.1 Overview of the effect of Ned-19

Use of pharmacological agents that alter the activities of individual components of physiological signalling pathways have greatly aided out understanding of their roles in these pathways and the cellular processes they are involved in. These agents can highlight a signalling molecule's function either by blocking its activity or enhancing it. As well as increasing our physiological knowledge these compounds can play a potential therapeutic role, either in their existing state or acting as lead compound for development.

The three intracellular secondary calcium messengers IP_3, cADPR and NAADP are produced within cells in response to external stimuli to mobilise Ca^{2+} from intracellular organelle stores (Gerasimenko, Sherwood, et al. 2006). Their activity has been shown to be required in a wide range of cellular process as diverse as fertilisation (Moccia et al. 2004), neuronal plasticity (Sarkisov and Wang 2008) and muscle contraction (Ge et al. 2003). However, studying their activity can be difficult due to all of their structures carrying a large negative net charge meaning they are not membrane permeable. As they are both synthesized and act on ion channels within the cell, their charged structures are an advantage for these molecules' physiological activity; as it prevents them from diffusing out of the cell or into organelles, maximising their activity within the cytosol. But this also means to discern their effect on cells they either need to be either microinjected into cells (James and Freedman 1977), applied to permeabilized or homogenised cells (Gerasimenko, Sherwood, et al. 2006; Morgan and Galione 2014) or converted into a membrane-permeable analogue (Rosen et al. 2012).

This increases the need for membrane permeable pharmacological agents specific to the activity of these molecules to study them in intact cell and whole organism levels.

Traditionally such compounds may be developed by modifying the structure of the active compound, e.g. creating an inhibitor by modifying the compound so that it still binds to its receptor, but is functionally inactive. While such techniques have been used for NAADP (Lee and Aarhus 1997), their cell permeability was not considered at the time and so still have the large negative charge that makes NAADP membrane impermeable. As increasing NAADP's membrane permeability would require removing multiple negatively charge groups, several of which are required for its binding and activity, it is a poor lead compound for a structural modification approach. Modern *in silico* techniques are a possible alternative solution; rather than altering the existing structure they allow potential compounds of interest to be identified via high throughput screening of libraries of large numbers of compounds that conform to specific criteria, e.g. a neutral net charge but contain a specific active group in a specific conformation.

One such compound identified using *in silico* screening, is the membrane permeable NAADP specific antagonist Ned-19 (Naylor et al. 2009). Naylor et al. used the ZINC (Zinc Is Not Commercial) database (Irwin and Shoichet 2005), which is only comprised of commercially available compounds with biological relevant representations of the molecules, in combination with the free-to-use OpenEye software (Nicholls et al. 2004; Rush et al. 2005), to generate and compare 3D structures. NAADP's 3D structure was used as a starting point; though as its bioactive 3D conformation is currently unknown, 40 possible conformations had to be generated using The OpenEye Omega application. This application was also used to produce up to 100 possible conformations for each compound in the ZINC library. The 3D conformations of the ZINC compounds were then screened against those generated for

A

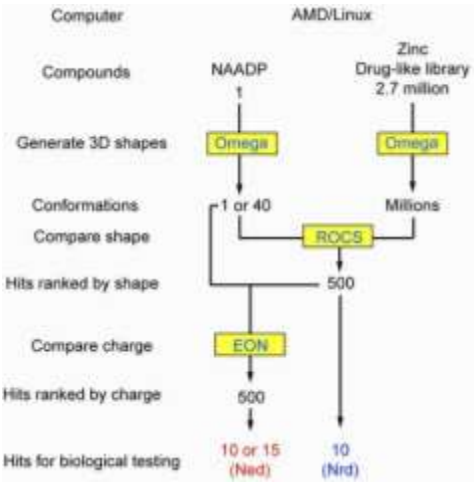

B

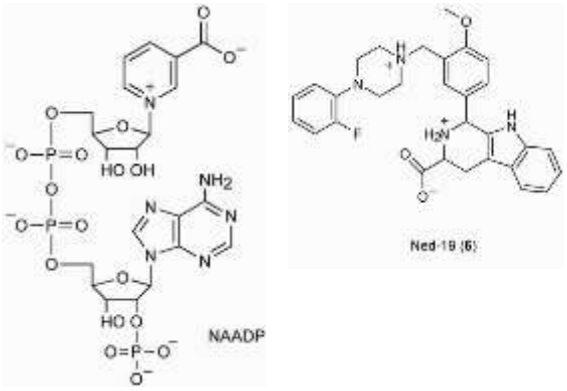

C

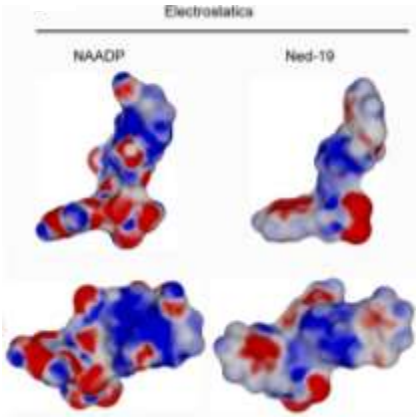

D

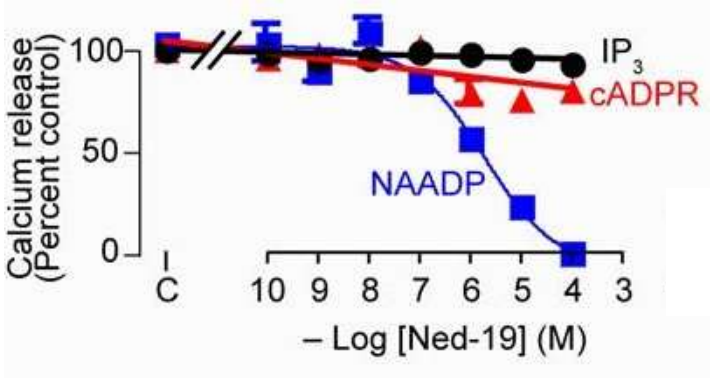

Fig. 4.1.1 Ned-19 has a similar electrostatic structure to NAADP and can inhibit its activity

(A) Schematic of the *in silico* process used to identify compounds similar 3D or electrostatic structures to NAADP. **(B)** The two-dimensional chemical structures of NAADP and Ned-19. **(C)** 3D electrostatic surface representations of NAADP and Ned-19, red represents areas of negative charge and blue those of positive charge. (D) Ned-19 inhibits NAADP-induce calcium release, but not IP_3 or cAPDR-induced release in sea urchin egg homogenate.

NAADP using OpenEye's ROCS (Rapid Overlay of Chemical Structures) application and ranked based on their Tanimoto score. The top 500 ranked compounds from the ROCS comparison were then compared to NAADP again using the EON application, which compared compounds based on their 3D electrostatic structures, and ranked again based on this second comparison. Compounds from the ROCS search were referred to as Nrd (NAADP ROCS Discovered) compounds and those from the EON search Ned (NAADP EON Discovered) compounds; all compounds were given a number based on their ranking, e.g. Nrd-6 was the 6th highest ranked compound in the ROCS comparison. The activity of the 10 highest ranked Nrd and 15 highest ranked Ned available for purchase were then tested *in vitro*.

The compounds purchased were tested in a plate reader assay to test their effect on NAADP's ability to induce Ca^{2+} release from sea urchin egg homogenate. 4 of the 25 compounds provided a significant inhibition against NAADP-induced Ca^{2+} release, with Ned-19 having the most potent effect. When used at a concentration of 100 µM it provided a 94.6 ± 1.0% inhibition against NAADP, but had no significant effect against either cADPR or IP_3-induced release. Conflicting data was produced as to Ned-19's mechanism of inhibition against NAADP, though the kinetics of its dissociation from homogenates suggested it was a functionally irreversible non-competitive inhibitor. Ned-19 exists as two diastereomers (and was initially used as a mixture of the two), with the *trans* form of Ned-19 showing a much greater inhibitory effect than the *cis* form. It is this *trans* form that has since been utilized by multiple groups in subsequent studies and is generally referred to as just Ned-19 (Coxon et al. 2012; Aley et al. 2013; Ali et al. 2016). Significantly, Ned-19's effect on NAADP-induced Ca^{2+} release in intact cells was demonstrated in two ways; pre-incubation with Ned-19 blocked NAADP-induced responses when the messenger was microinjected into either intact

sea urchin eggs or murine pancreatic β cells. Naylor et al. highlighted the usefulness of Ned-19 by showing that at a sufficient concentration it could inhibit glucose-induced Ca^{2+} oscillations in isolate murine pancreatic islets when either applied as a pre-treatment or acutely, further implying NAADP plays a role in glucose sensing (Johnson and Misler 2002; Masgrau et al. 2003; Mitchell et al. 2003). As a tryptophan derivative, Ned-19 is fluorescent and shows a second possible use as it can label NAADP binding sites within cells; which in pancreatic β cells was found to co-localise with Lysotracker red fluorescence (Naylor et al. 2009).

Since Ned-19's discovery as a membrane-permeable NAADP antagonist it has been used in multiple mammalian cell systems to inhibit NAADP-induced Ca^{2+} release and thereby highlight the physiological role that the secondary messenger plays in those cell types (Esposito et al. 2011; Arndt et al. 2014; Khalaf and Babiker 2016; Pereira et al. 2016). As well as being used to highlight NAADP role in cells by inhibiting its activity Ned-19 has been used to provide experimental data supporting the long held belief within the field that the 'NAADP receptor's' activity is regulated by two NAADP-binding sites. In Sea urchin eggs the application of a sub-activating concentration of NAADP is auto-inhibitory to a subsequently applied activating concentration of NAADP (Aarhus et al. 1996; Genazzani et al. 1996). Alternatively, in mammalian cells NAADP shows a bell-shaped activation curve, inducing Ca^{2+} release from intracellular cells until a threshold is reached where it becomes auto-inhibitory (Cancela et al. 1999; Berg et al. 2000). Together these mechanism of auto-inhibition both suggest that the 'NAADP receptor' has two separate NAADP-binding sites, with one inducing channel opening and the other inhibiting it.

Using the sea urchin egg homogenate model, Rosen et al. examined the effect of Ned-19 and the two closely related compounds Ned-20 and Ned-19.4 on NAADP's binding to its receptor

A

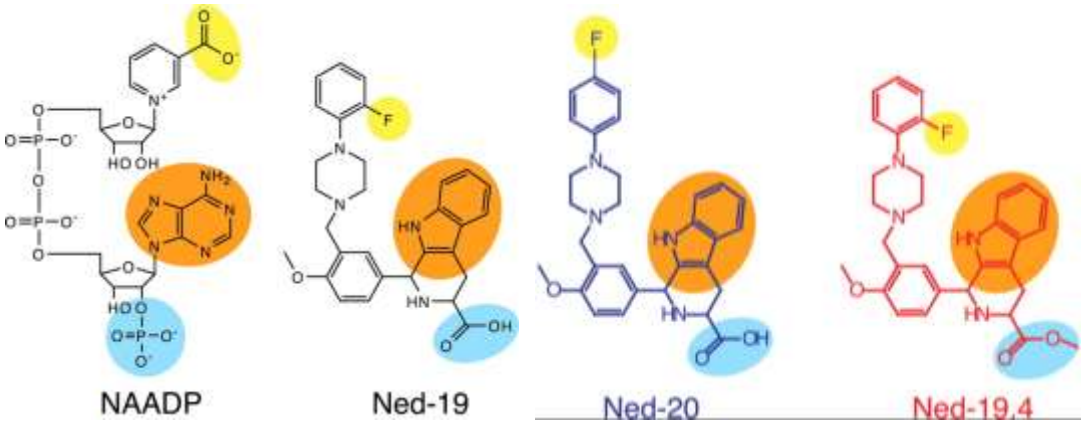

B **C**

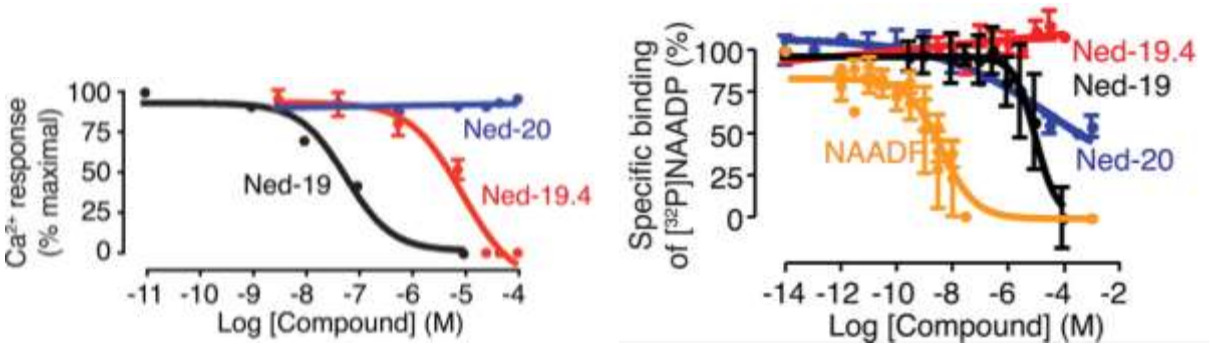

Fig. 4.1.2 Analogues of Ned-19 have varying effects on NAADP-induced Ca^{2+} release and binding

(A) Comparison of the two-dimensional chemical structures of NAADP; Ned-19 and its structural analogues, Ned-19.4 and Ned-20. Regions with share structural similarity are highlighted in the same colours. **(B)** Comparisons of the effect of Ned-19 and its analogues on NAADP-induced calcium release from sea urchin egg homogenate. **(C)** Comparisons of the effect of Ned-19 and its analogues on NAADP binding to its receptor in sea urchin egg homogenate.

and ability to induce Ca^{2+} release (Rosen et al. 2009). Both these compounds are identical to Ned-19's except for one structural modification, the carboxylic acid group substituted for a methyl ester group in Ned-19.4 and Ned-20 has its fluorine atom in the *para* rather than the *ortho* position. As previously shown by Naylor et al. (Naylor et al. 2009), Ned-19 is able to inhibit both NAADP's ability to bind to its receptor and NAADP-included Ca^{2+} release. Ned-19.4 was able to inhibit NAADP-induced Ca^{2+} release, though to a lesser extent than Ned-19, but had no effect on its binding. Conversely Ned-20 had no effect on Ca^{2+} release but did affect binding in a pattern constant with allosteric displacement (Christopoulos and Kenakin 2002). These results suggest that the Ned-19's inhibition of NAADP-induced Ca^{2+} release is independent of its ability to disrupt its binding and vice versa. Unlike Ned-19 and Ned-19.4, pre-incubation with Ned-20 blocked auto-inhibition by a sub-activating concentration of NAADP.

Together with the previous findings this lead Rosen et al. to propose a three state model of the 'NAADP receptor', based on it having both a low affinity orthosteric and a high affinity allosteric for NAADP. In the absence of NAADP the receptor exists in a close resting state; addition of a sub-activating concentration of NAADP will lock the channel in it closed state by binding to the allosteric site, preventing the effect of a second application of a normally activating concentration. An initial application of an activating concentration of NAADP will instead bind to the orthosteric site, which induces channel opening. The experimental data suggests Ned-20 prevents NAADP from binding to the allosteric site, thus preventing the formation of the channel's locked state. Ned-19.4 instead prevents the channel changing from its inactive state to active open state when NAADP is bound to the orthosteric site. How Ned-19 interacted with the 'NAADP receptor' could not be deduced from this study, with Rosen et al. suggesting how it could act on either site independently or both.

There is no data published on the effects of Ned-20 and Ned-19.4 in mammalian cells to build a model of NAADP's activity; although based on its bell shaped activation curve (Cancela et al. 1999; Berg et al. 2000) it can be speculated that a mutation has led to the affinity of the allosteric site to decrease below that of the orthosteric site. Such a mutation would increase the required concentration of NAADP for it to bind to the allosteric site and produce its bell shaped activation curve. However, this would mean that the 'NAADP receptor' in mammalian cells can change between its open and locked states without transitioning through its resting state.

The discovery that TPC channels form NAADP sensitive ion channels (E. Brailoiu et al. 2009; Calcraft et al. 2009; Zong et al. 2009) has added an extra degree of complication to NAADP's activity; since it has been shown that in neither sea urchin eggs or mammalian cells does the messenger act directly on these channels (Lin-Moshier et al. 2012; Walseth et al. 2012), but instead must do so via one or more as yet unidentifed NAADP-binding proteins. How these binding proteins interact with the channel forming ones, if more than one NAADP binding protein exists, and if both the orthosteric and allosteric site are on the same binding protein are all currently unknown and increase the complexity of NAADP-induced Ca^{2+} release. Identification of TPC channels has allowed for a better insight into Ned-19's activity, as at sub-inhibitory concentrations it has been shown to induce the opening of recombinant TPC2 expressed in lipid bylayers (Pitt et al. 2010). This suggest that Ned-19 may act in a similar manner to NAADP, activating TPC channels at low concentrations and inhibiting them at high concentrations.

PAC have been shown to produce both the intracellular secondary Ca^{2+} messengers cADPR and NAADP in response to the physiological secretagogue CCK (Yamasaki et al. 2005). This is understandable as both messengers are produced by the same ADPR cyclase, the

ectoenzyme CD38 (Malavasi et al. 2008); the knockout of which is known to abolish the presence of cADPR in PAC (Fukushi et al. 2001). Interestingly microinjection of a high auto-inhibitory concentration of NAADP into PAC is able to inhibit CCK-induced Ca^{2+} responses but not cADPR-induced responses (Cancela et al. 1999). This suggests that NAADP may be key to the creation of CCK-induced Ca^{2+} release, acting upstream of cADPR; with cADPR aiding in the amplification of the initial response induced by NAADP by reducing the requirement of CICR.

If NAADP is the initial messenger required for the generation of CCK-induced Ca^{2+} release in PAC, it was predicted that the membrane permeable NAADP-specific antagonist Ned-19 would have an inhibitory effect against formation of the response. It was also predicted that Ned-19 might show a protective effect against necrosis in the CCK hyperstimulation model of acute pancreatitis (Han et al. 2001).

4.2. The effect of Ned-19 on CCK-induced calcium oscillations in pancreatic acinar cells

The response of PAC to a physiological concentration of either of the secretagogues ACh or CCK is well characterised (Cancela 2001) (*Fig. 4.2.1 A-B).* An extracellular application of either stimulant triggers a series of Ca^{2+} oscillations in the cytoplasm of the cell, localised to the apical region of the cell (Thorn et al. 1993; Park et al. 2001). These short lived repetitive increases in $[Ca^{2+}]_c$ initiate the migration of zygomorphic granules to the plasmalemma; upon reaching the cell membrane granules will fuse with it, releasing the proenzymes they contain into a intralobular duct (Williams 2010). Removal of the secretagogue from the extracellular solution results in the rapid cessation of the Ca^{2+} oscillations it initiated (*Fig. 4.2.1 B),* thus ending secretion from the cell. An immediate resumption of oscillations occurs upon reapplication of the secretagogue, implying there is no desensitisation of the cell to the

A

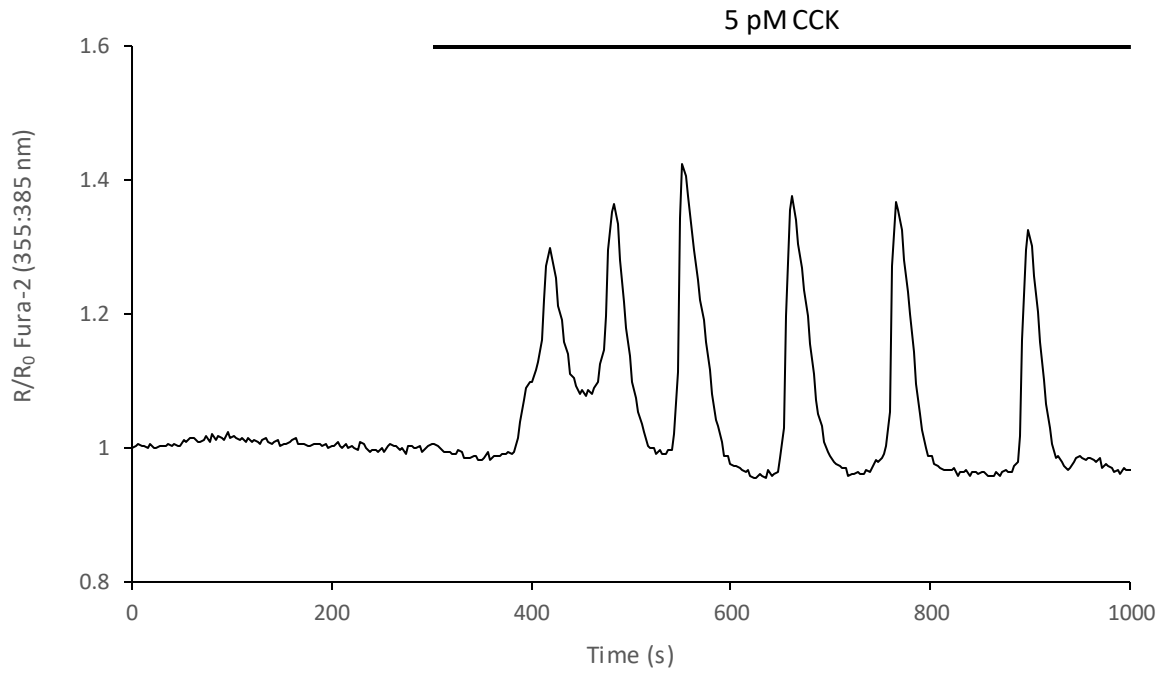

B

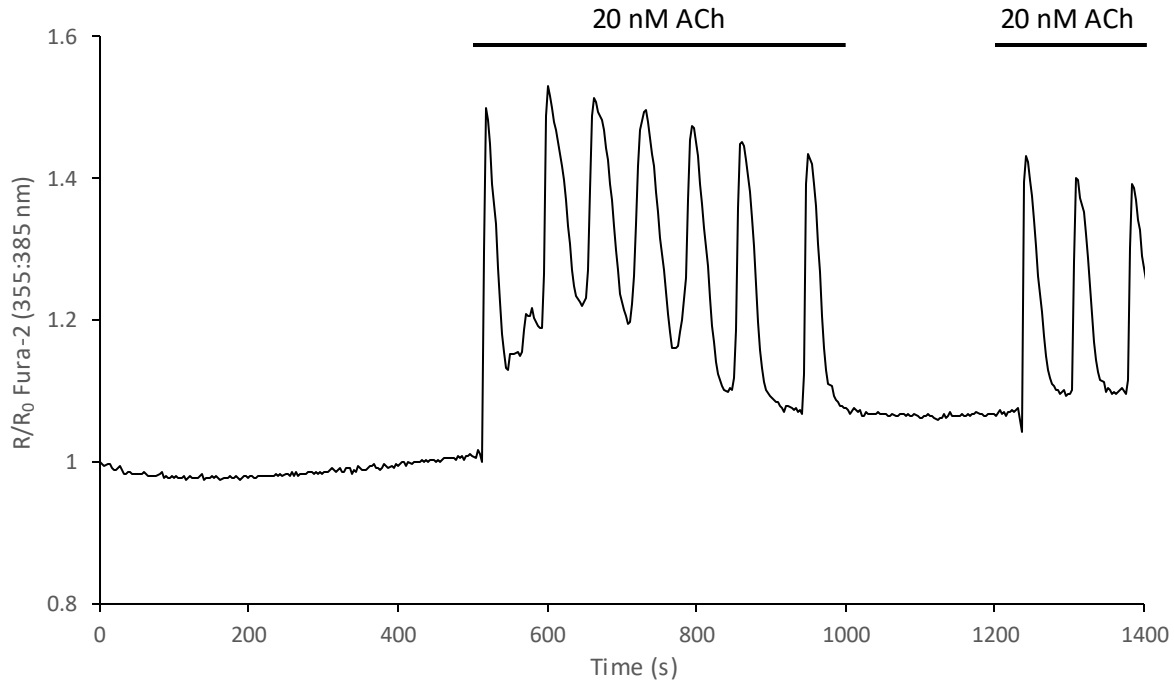

Fig. 4.2.1 CCK and ACh-induced calcium responses

Representative traces obtained upon treatment of pancreatic acinar cells with: **(A)** 5 pM CCK (n = 11) and **(B)** 20 pM Ach, including wash-off and reapplication of ACh (n = 6).

C

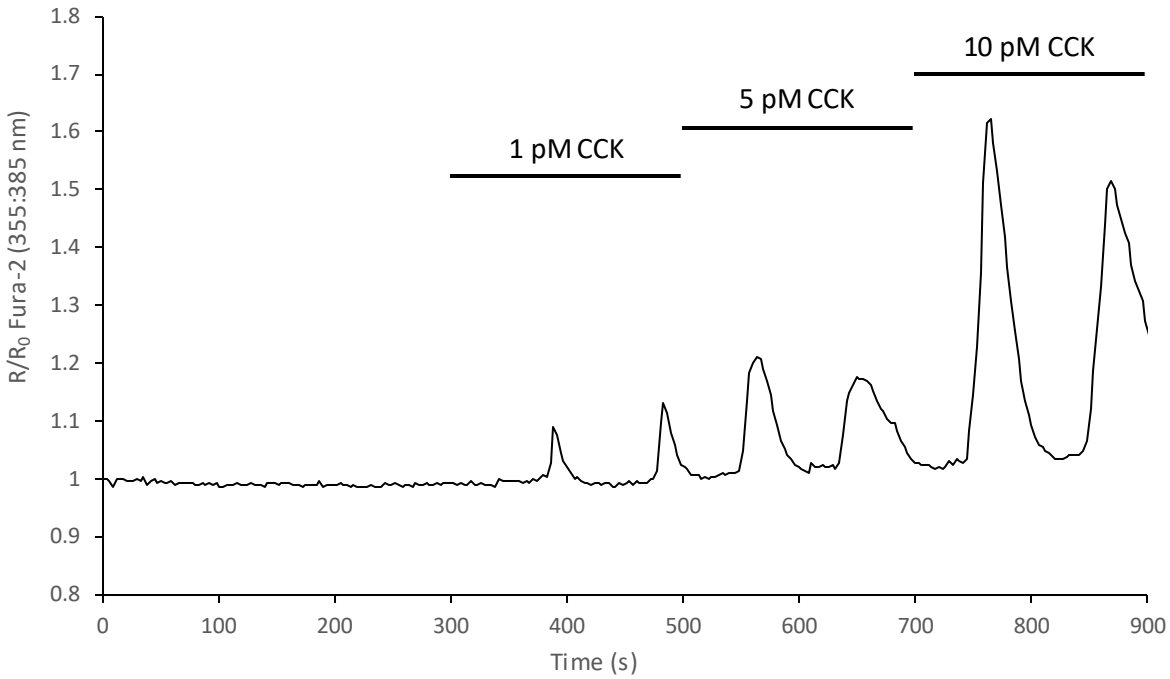

D

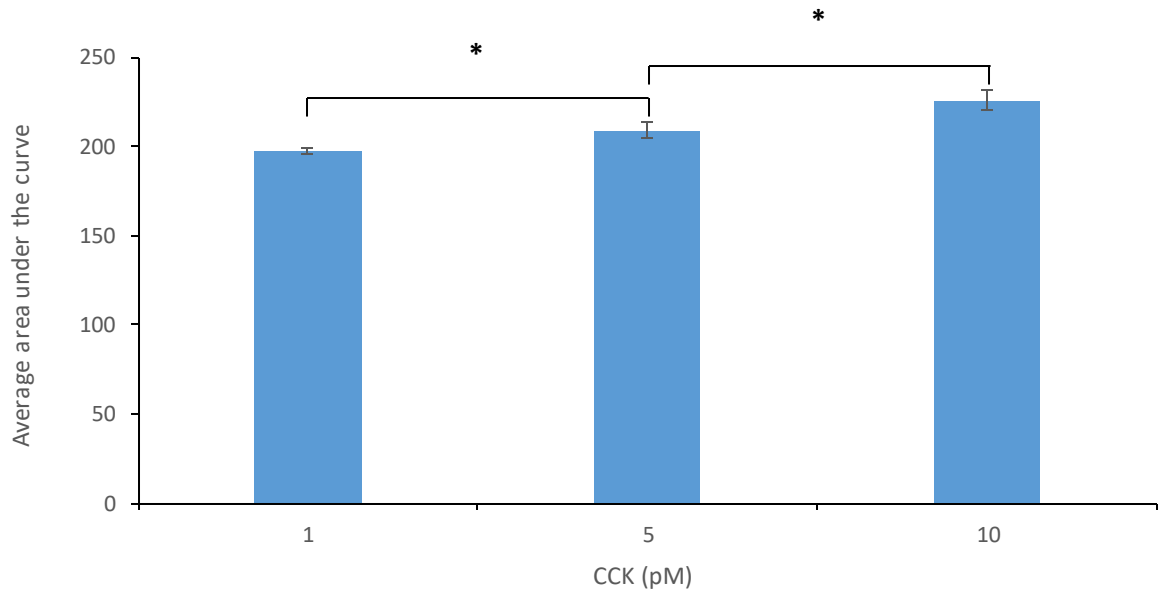

Fig. 4.2.1 *(continued)*

(C) Representative trace of pancreatic acinar cells responding to an increasing concentration (1, 5 and 10 pM) of CCK (n = 8). **(D)** Bar Chart showing the average area under the trace for the cells sampled (Data represents mean ± SEM, n = 8; *, $P \leq 0.05$).

E

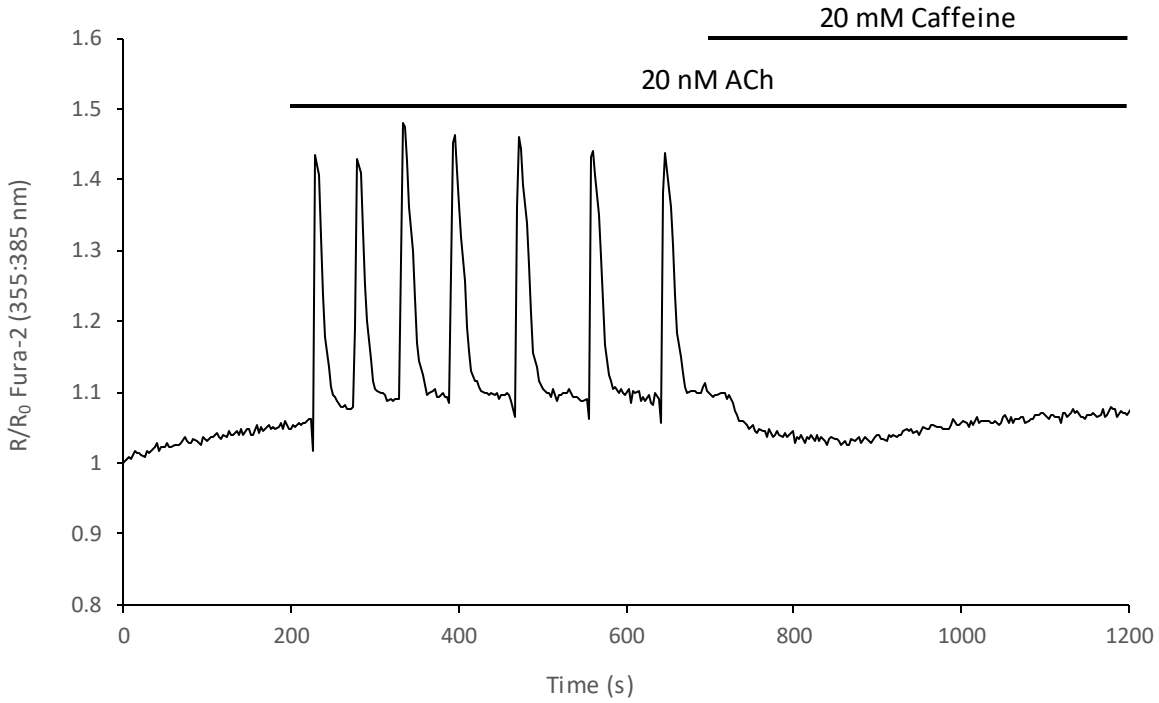

Fig. 4.2.1 *(continued)*

(E) Representative trace of the effect of a high concentration of caffeine (20 mM) on the Ach response in pancreatic acinar cells (n = 12).

stimulant after the first application.

The size of the Ca^{2+} response observed within a cell corresponds to the amount of the secretagogue applied to it (*Fig. 4.2.1 C)*. Across a physiological range of CCK concentrations (1-10 pM) tested, all elicited a measurable Ca^{2+} response, with an apparent increase in the intensity and length of the response in accordance with the increasing concentration. Quantification of the responses observed by calculating the area under the curve (*Fig. 4.2.1 D)* confirms the increases observed on the trace. A student's *t*-test for each change in concentration shows that each increase is significant ($p = 0.02$ between 1 pM and 5 pM, and $p = 0.03$ between 5 pM and 10 pM), indicating a clear dose-response relationship.

An increase in $[Ca^{2+}]_c$ can come from one of two sources: an influx of extracellular Ca^{2+} across the plasmalemma or by release of Ca^{2+} stored in the lumen of one or more of the cell's organelles. ACh mobilizes Ca^{2+} from organelle stores via the production of IP_3 and therefore the increase in $[Ca^{2+}]_c$ it induces can be blocked by caffeine (*Fig. 4.2.1 E)*, which at high concentrations is an inhibitor of IP_3R channel activity (Parker and Ivorra 1991).

100 µM Ned-19 has been shown to inhibit NAADP-induced Ca^{2+} release in several different mammalian cell types (Naylor et al. 2009; Barceló-Torns et al. 2011; Coxon et al. 2012); therefore it was decided to test the effects of concentration against secretagogue induced Ca^{2+} release in PAC. Addition of Ned-19 on top of a CCK-induced Ca^{2+} response causes a complete abolition of the Ca^{2+} oscillations (*Fig. 4.2.2 A)*. This effect is temporary, as when both Ned-19 and CCK were washed out of the cells the reapplication resulted in a resumption of Ca^{2+} oscillations. Unlike for CCK-induced Ca^{2+} oscillations, Ned-19 had no effect on ACh-induced responses (*Fig. 4.2.2 B)*.

The experiments using the ratiometric Ca^{2+} sensitive dye Fura-2 (*Fig. 4.2.1* and *Fig. 4.2.2*) were conducted using an LED microscope system taking whole cell recordings of intact PAC.

A

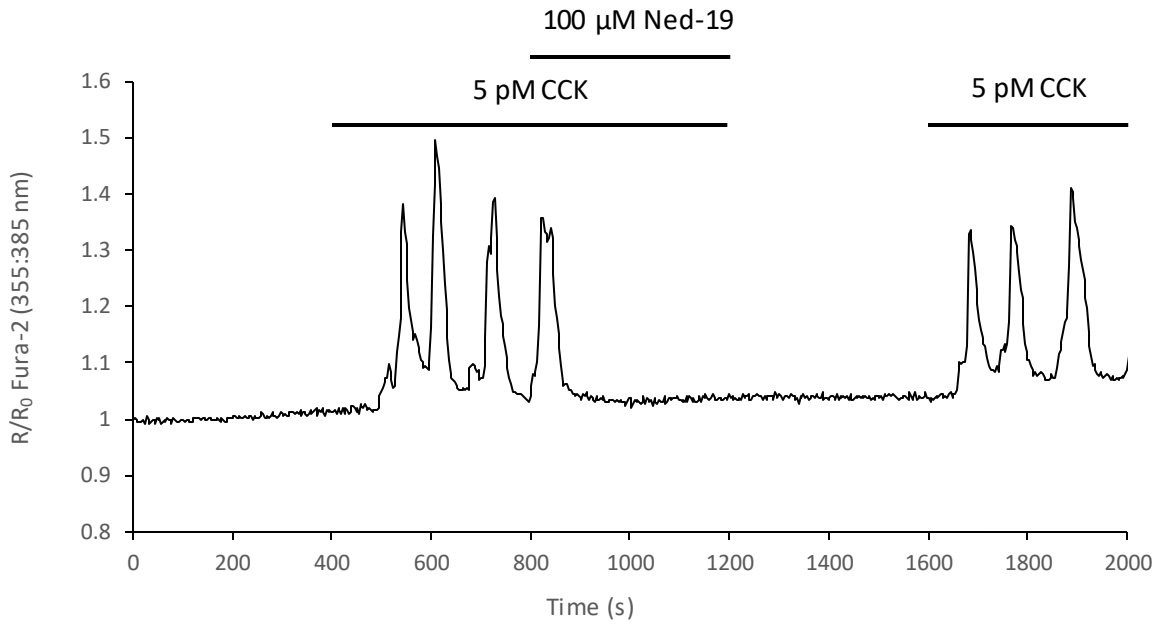

B

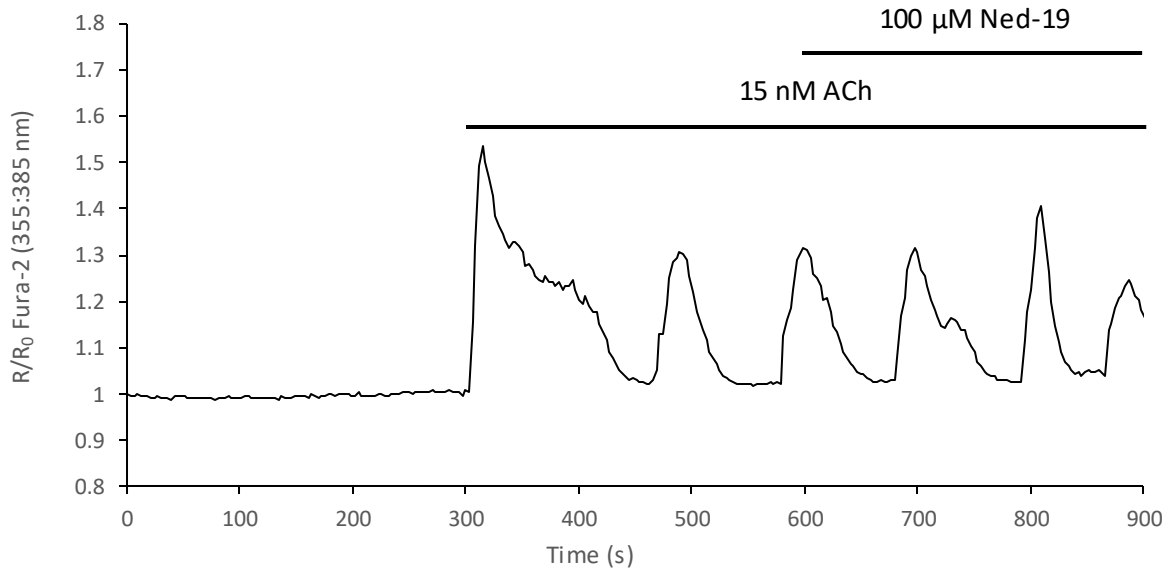

Fig. 4.2.2 The effect of Ned-19 on physiological calcium signalling in pancreatic acinar cells

(A) Representative trace showing the effect of exposing pancreatic acinar cells to 5 pM CCK followed by 100 µM Ned-19, both agents were removed from the bath solution and then CCK was reapplied (n = 10). **(B)** Representative trace showing the effect of exposing pancreatic acinar cells to 15 nM ACh followed by 100 µM Ned-19 (n = 21).

As the apical granular region is where physiological secondary messenger signalling in PAC is initiated (Thorn et al. 1993; Park et al. 2001), the Ned-19 experiments were repeated using a confocal microscope and the non-ratiometric Ca^{2+} dye Fluo-4. This allowed for imaging of PAC at a higher resolution and for recordings to accurately be taken specifically from the granular region. These results showed an identical pattern to those previously observed; alone 5 pM CCK induces an oscillation in the $[Ca^{2+}]_c$ in PAC, however when 100 µM Ned-19 was applied acutely onto of these oscillations they were completely inhibited (*Fig. 4.2.3A*). Alternatively, when 20 nM ACh was used to induce Ca^{2+} oscillations acute application of Ned-19 had no visible effect (*Fig. 4.2.3B*). The average areas under the curve for the 300 s periods that cells were exposed to CCK or ACh alone and with Ned-19 (*Fig. 4.2.3C-D*). These areas were compared using a Student's *t*-test, which showed a significant difference in the response to CCK in the presence and absence on Ned-19 ($p < 0.01$), but no significant difference for the response to ACh ($p = 0.78$).

As Ned-19 was able to inhibit the Ca^{2+} response induced by a physiological concentration of CCK, it is possible that it would be able to do so against a pathological concentration of the secretagogue. Supramaximal concentrations of CCK cause hyperstimulation of PAC, resulting in sustained cytotoxic increases in $[Ca^{2+}]_c$ and resulting in pro-inflammatory necrotic cell death (Mukherjee et al. 2016). Cell were exposed to 10 nM CCK with and without 100 µM Ned-19 at room temperature for 1 hour and then 6 µM PI was added before multiple images of cells were taken. The total amount of necrosis for a particular treatment was then calculated as the percentage of cells showing PI staining (Kaiser et al. 1995) compared to the total number of number of cells imaged. Under these conditions there was 6.6 ± 0.58% necrosis observed for the untreated control cells; in the presence of 10 nM CCK this was increased to 10.5 ± 1.29%, which was not deemed significant by ANOVA

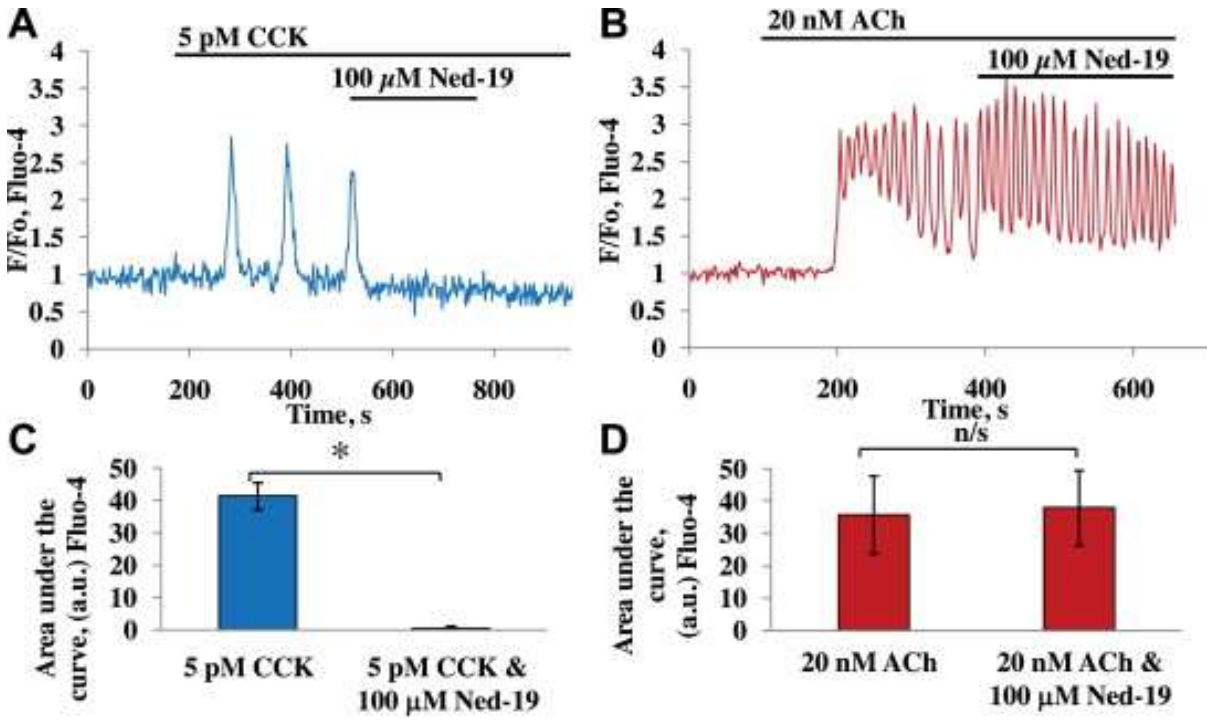

Fig. 4.2.3 Ned-19 inhibits CCK but not ACh-induced calcium release in pancreatic acinar cells

Representative traces of responses to **(A)** 5 pM CCK (n = 9) or **(B)** 20 nM ACh (n = 14) in pancreatic acinar cells with subsequent application of 100 μM Ned-19. **(C-D)** Quantification of the area under the curve for the experiments shown in **(A)** and **(B)** for the two 300 s periods where cells were exposed to CCK or ACh alone, and in the presence of Ned-19 (41.3 ± 4.2 a.u. for 5 pM CCK, and 0.5 ± 0.6 a.u. for 5 pM CCK and 100 μM Ned-19; 35.7 ± 12 a.u. for 20 nM ACh, and 37.9 ± 11.6 a.u. for 20 nM ACh and 100 μM Ned-19). Data represents mean ± SEM; *, $P \leq 0.05$; n/s, not significant.

comparison ($p = 0.0448$). When 100 µM Ned-19 was also present with CCK, only 6.8 ± 0.50% of cells showed PI staining, however this was not deemed significant ($p = 0.0558$). There was no significant difference between the amount of necrosis observed in the control cells and those treated with both CCK and Ned-19 ($p = 0.9826$); therefore, it surprising that Ned-19 did not significantly reduce the amount of necrosis induced by CCK. It is possible that this is a result of the relatively low amount of necrosis induced by the supramaximal concentration of CCK used.

When tested using the assay described, 100 µM Ned-19 showed no toxic effect to PAC (*Fig. 4.2.4D*). This corresponds with previous reports that the compound was not cytotoxic at this concentration in human platelets (Coxon et al. 2012) or *in vivo* in mice (Favia et al. 2016).

As the amount of necrosis induced by 10 nM CCK was very low (*Fig. 4.2.4B*), the toxicity assay was repeated with the incubation step occurring in a water bath at 37°C (*Fig. 4.2.4C*) to induce a higher level of necrosis in response to CCK. Under such conditions the amount of necrosis observed was increased for all treatments, with the lowest amount of necrosis observed in the cells treated with CCK and Ned-19. In these experiments the amount of necrosis in the cells treated with CKK and Ned-19 was deemed significantly different to those treated with CKK alone by ANOVA comparison ($p = 0.0018$), but not significantly different from the untreated control cells ($p = 0.9488$). These results strongly indicate that Ned-19 has a protective effect against the toxic effect of a supramaximal concentration of CCK.

Permeabilized PAC from TPCN2$^{-/-}$ mice showed a reduced response to NAADP compared to PAC from wild type animals, with the amount of Ca^{2+} mobilized from intracellular stores reduced by 64% (Gerasimenko et al. 2015). While this reduction in the size of the response was significant, it does also show that there is reasonable amount of the NAADP response in

A

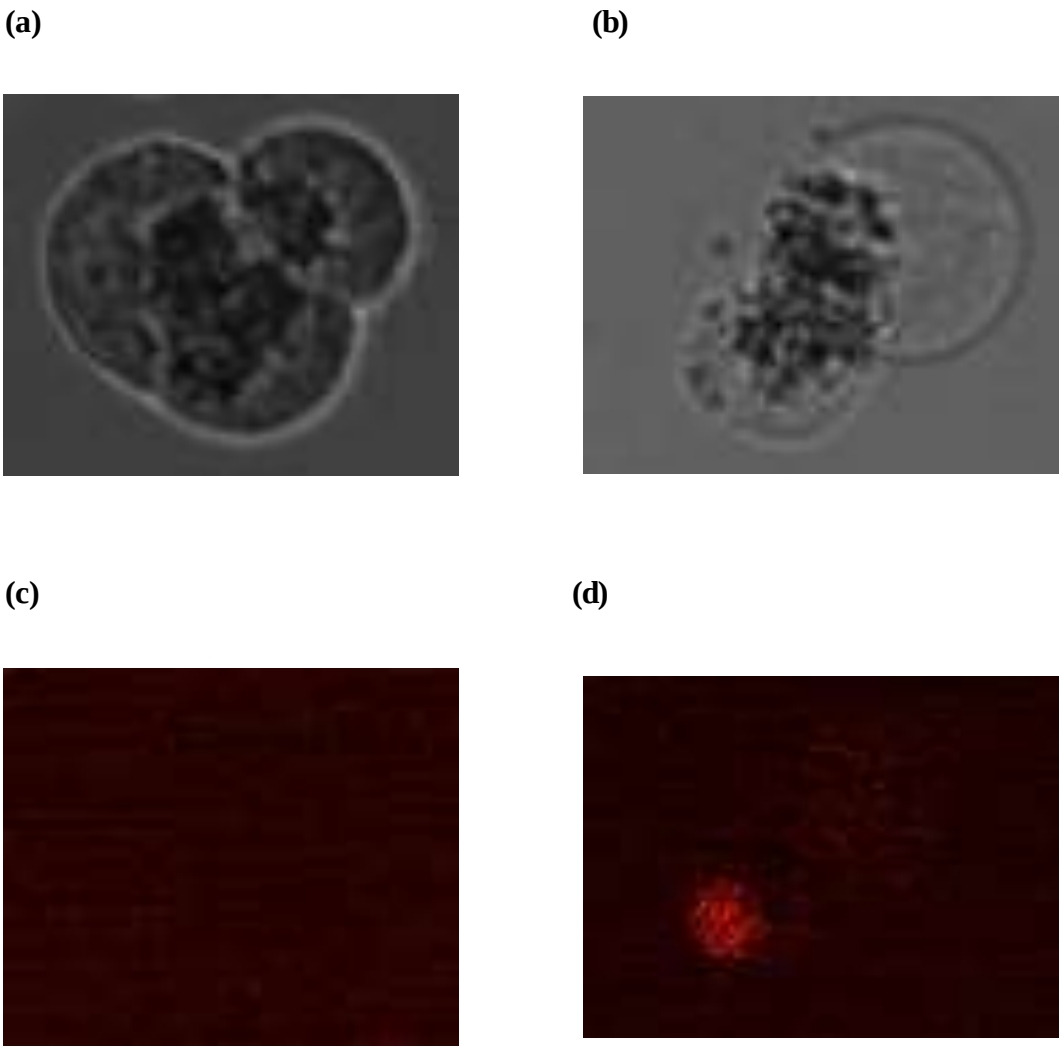

Fig. 4.2.4 Effect of Ned-19 on CCK-induced cell death in acinar cells

(A) Brightlight image, **(a)** and **(b)**, and image of emission at 629 nm, **(c)** and **(d)**, representative of PI staining. **(a)** Untreated control cells show a clearly define plasma membrane and distinct granular region. **(b)** Necrotic cells exposed to pathological agents like 10 nM CCK have poorly defined plasma membranes and dispersed granules. **(c)** Viable cells have no loss of plasma membrane integrity and as such display no PI staining. **(d)** Necrotic cells loss plasma membrane integrity; allowing PI to stain DNA, hence the intense nuclear staining.

B

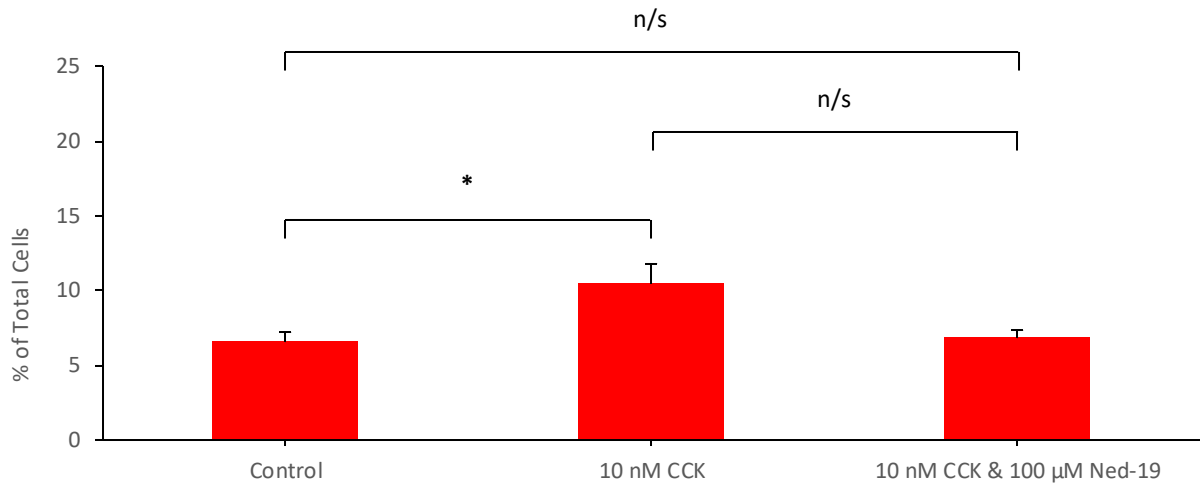

C

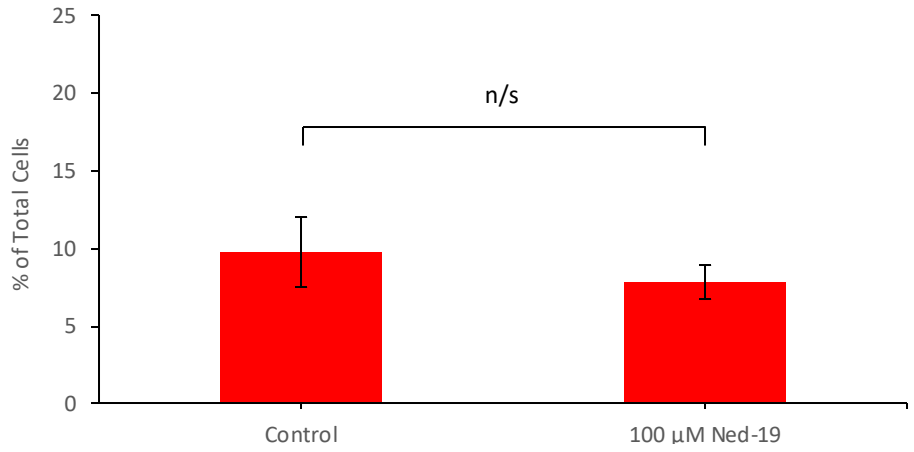

Fig. 4.2.4 (*continued*)

(B) The results of cell death assays performed on pancreatic acinar cells treated with 10 nM CCK alone or in the presence of 100 µM Ned-19 for 1 hour at room temperature. Data represents the number of necrotic cells as a percentage of the total number of cells counted for that specific treatment (Data represents mean ± SEM, n = 3888 cells; n/s, not significant). **(C)** The results of cell death assays performed on pancreatic acinar cells treated with 100 µM Ned-19 for 1 hour at room temperature (Data represents mean ± SEM, n = 881 cells; *, $P \leq 0.05$; n/s, not significant).

D

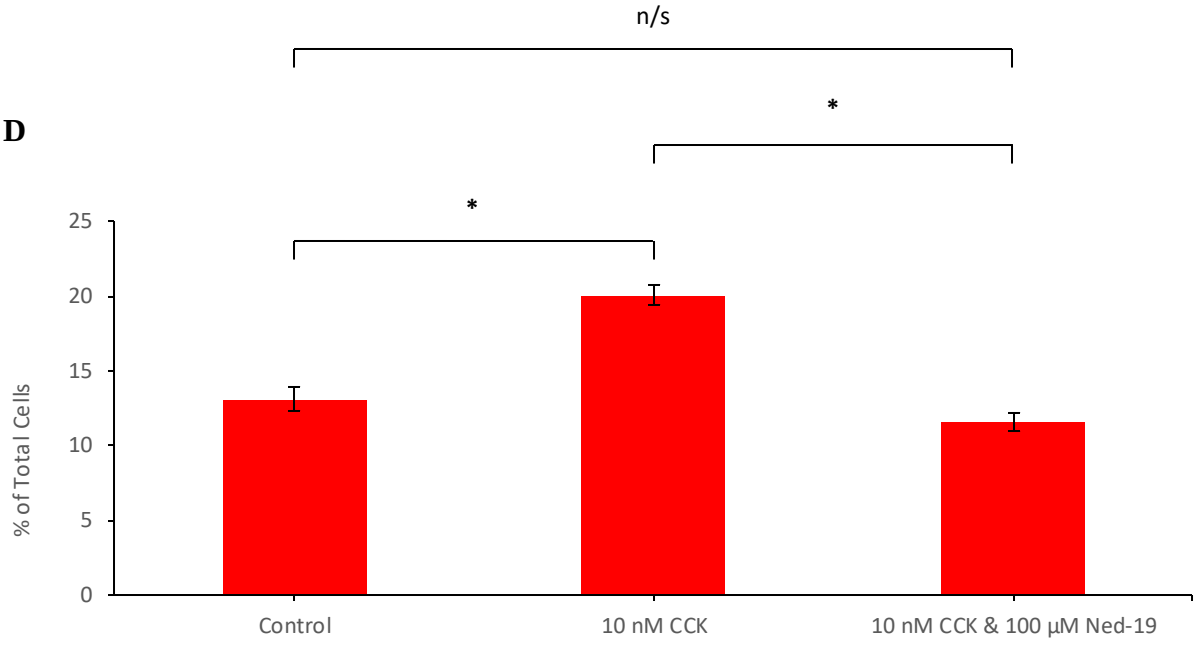

Fig. 4.2.4 (*continued*)

(D) The Results of cell death assays performed on pancreatic acinar cells treated with 10 nM CCK alone or in the presence of 100 µM Ned-19 for 1 hour at 37°C. Data represents the number of necrotic cells as a percentage of the total number of cells counted for that specific treatment (Data represents mean ± SEM, n = 9192 cells; *, $P \leq 0.05$; n/s, not significant).

PAC that is independent of TPC2 channels. To test the impact on physiological signalling, PAC from the same TPCN2$^{-/-}$ mice were tested for responses to 5 pM CCK.

As in wild type PAC cells, 5 pM CCK induced visible Ca^{2+} oscillations in all the cells sampled (*Fig. 4.2.5A*). Indicating the remaining NAADP sensitive element of the CCK response in TPCN2$^{-/-}$ PAC is enough to induce the classic physiological Ca^{2+} response to CCK. There is evidence that NAADP signalling is these cells involves both types of TPC channel and all three RyR channels as well, with a varying importance of each channel's isoform and signs of overlapping function between the two channels; therefore, there is enough redundancy between these channels to compensate for the loss of TPC2's activity.

CCK-induced Ca^{2+} oscillations in TPCN2$^{-/-}$ PAC also showed the same sensitivity to Ned-19 as wild type PAC, with a complete inhibition of oscillations when 100 µM Ned-19 was applied acutely (*Fig. 4.2.5B-C*). This shows that the inhibitory effect of Ned-19 is not dependent on the inhibition of TPC2 activity and it must also act on whichever channels are responsible for the NAADP-induced Ca^{2+} release in TPCN$^{-/-}$ PAC.

Together these results show that loss of TPC2 activity alone is not enough to inhibit physiological CCK signalling in PAC, and that one or more other NAADP sensitive channels must be involved in the response to CCK.

4.3 Discussion

Upon stimulation with CCK PAC are known to produce both of the intracellular secondary Ca^{2+} messengers, cADPR and NAADP (Yamasaki et al. 2005). Cancela et al. observed that a high autoinhibitory concentration of NAADP applied by patch pipette could inhibit CCK induced Ca^{2+} spikes, but had no effect on those induced by cADPR (Cancela et al. 1999).

A

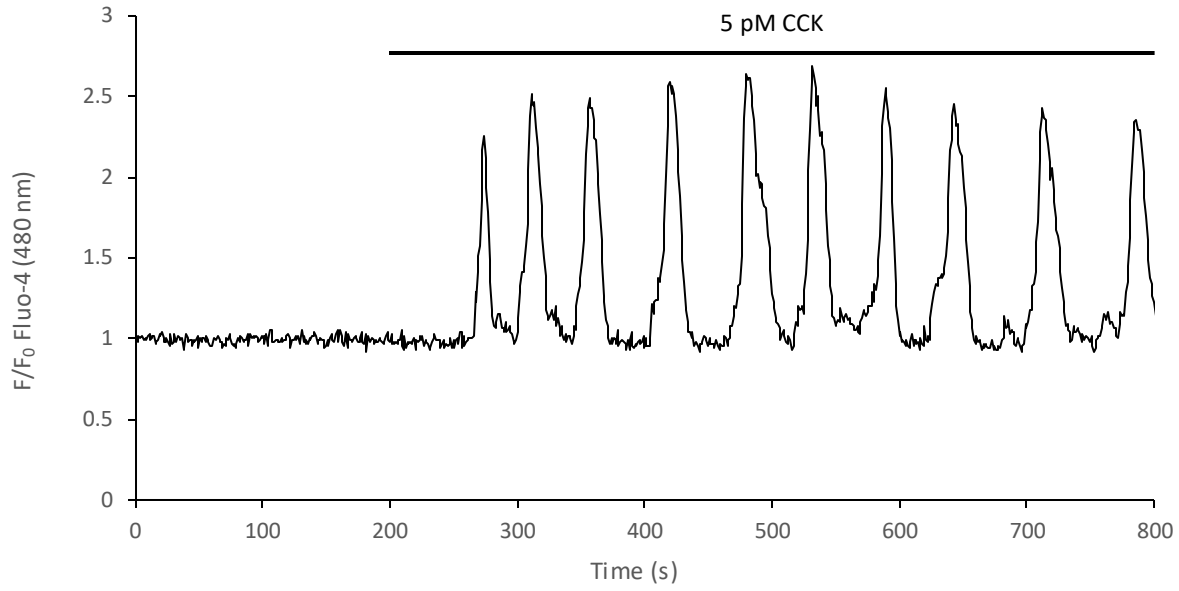

B

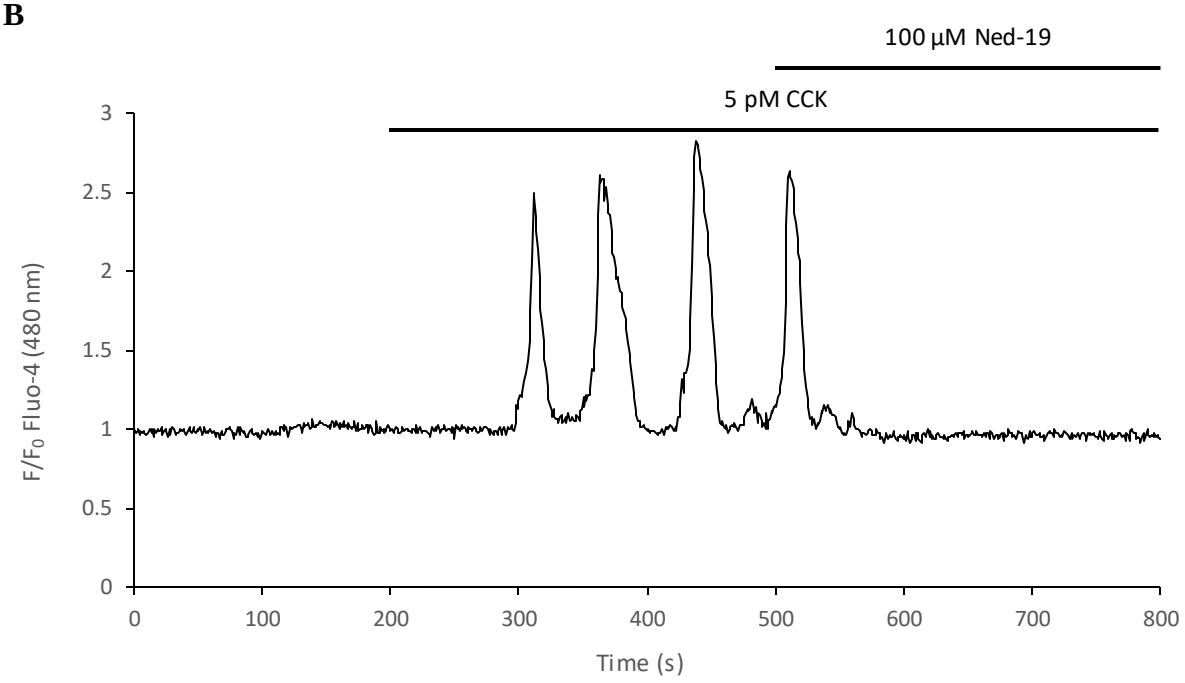

Fig. 4.2.5 The effect of TPC2 knockout on CCK induced calcium oscillations in pancreatic acinar cells

(A) Representative trace of the CCK response in pancreatic acinar cells isolated from TPCN2$^{-/-}$ mice. **(B)** Representative trace of the effect of 100 µM of Ned-19 on the CCK response in pancreatic acinar cells isolated from TPCN2$^{-/-}$ mice.

C

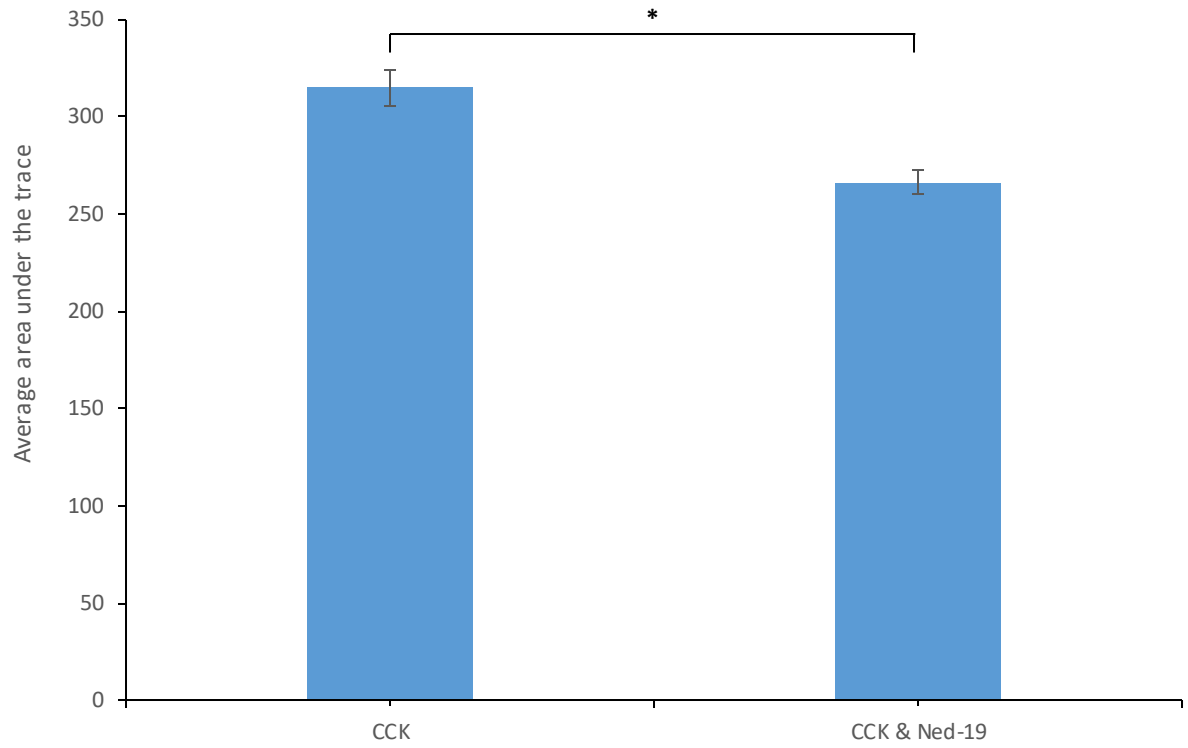

Fig. 4.2.5 (*continued*)

(C) Bar Chart showing the average area under the trace for the cells sampled; CCK between 200 s and 500 s and CCK & Ned-19 between 500 s and 800s (Data represents mean ± SEM, n = 26; *, $P \leq 0.05$).

This led them to hypothesis that NAADP may be the vital element required to induce the response to CCK in PAC; with cADPR acting on RyR to reduce the requirement for CICR, which would enhance the size and length of the initial response induced by NAADP.

The NAADP specific antagonist Ned-19 (Naylor et al. 2009) showed the ability to completely inhibit CCK-induced cytoplasmic Ca^{2+} oscillations in PAC when applied acutely (*Fig. 4.2.2* and *Fig. 4.2.3*) at a concentration known to inhibit NAADP-induced Ca^{2+} release in several different mammalian cell types (Naylor et al. 2009; Barceló-Torns et al. 2011; Coxon et al. 2012). Like previously shown in sea urchin eggs (Naylor et al. 2009), Ned-19 was found to have no significant impact on either cADPR or IP_3 induced Ca^{2+} release in this cell type (*Fig. 3.2.1E*). As the effect of Ned-19 is specific to NAADP-induced release, this means the inhibition of this specific component of the CCK response is enough to inhibit the Ca^{2+} oscillations induced by the secretagogue, and therefore secretion of the digestive enzymes stored within the cell (Petersen and Ueda 1976).

While this does in part support the hypothesis of Cancela et al. that the activity of NAADP is required to generate the response to CCK, it also indicates that the secondary messenger's activity is also required to sustain the response to CCK due to its acute effect. If NAADP's activity was only required to initiate CCK-induced Ca^{2+} oscillations, then the acute application of Ned-19 to pre-existing oscillations would have little to no effect. This would suggest that it also plays a role in the continued response to CCK; and as seen, inhibiting its activity is enough to terminate the response to CCK in PAC.

The cADPR antagonist 8-NH_2-cADPR has been shown to have a similar inhibitory effect on CCK induced Ca^{2+} release to that of Ned-19 (Cancela and Petersen 1998), which may suggest that cADPR's activity is also vital for CCK-induced Ca^{2+} oscillations in PAC. However, as Cancela et al. found NAADP induced Ca^{2+} spikes were inhibited by this compound (Cancela

et al. 1999) the importance cADPR can be questioned. Inhibition of NAADP-induced Ca^{2+} spikes by 8-NH_2-cADPR, suggests that the compound is an inhibitor of RyR activity rather than a specific antagonist of cADPR activity like previously suggested (Walseth and Lee 1993). Inhibition of RyR activity has been shown to significantly reduce the amount of Ca^{2+} mobilized in response to NAADP in PAC (Gerasimenko et al. 2015); this could suggest the inhibition of CCK-induced Ca^{2+} spikes by 8-NH_2-cADPR was the result of the compound blocking Ca^{2+} release via RyR stimulated by NAADP, rather than the activity of cADPR on these channels. While NAADP and cADPR-induced Ca^{2+} release was shown to involve the different RyR isoforms to different extents, cADPR-induced release was shown to involve all three and therefore it is likely 8-NH_2-cADPR could inhibit the activity of all three isoforms.

There is the suggestion that NAADP may act directly on RyR in PAC and induce the opening of this family of ion channels (Gerasimenko et al. 2003; Gerasimenko, Sherwood, et al. 2006; Gerasimenko et al. 2015). If NAADP and cADPR act on these channels in a similar manner, then it is possible that a specific antagonist for one of these messengers may inhibit the activity of both. If this is true then the suggestion would be that it is the activity of RyR, rather than that of a specific secondary messenger, that is the key requirement for CCK induced Ca^{2+} oscillations in PAC. Due to the synthesis of the two messengers occurring via the same enzyme (Chini et al. 2002) and the overlapping nature of their signalling mechanisms (Gerasimenko et al. 2015) untangling the activity of the two messengers is near impossible without an antagonist for cADPR whose specificity has definitively been proven.

The overlap in synthesis of NAADP and cADPR may also suggest another mechanism that Ned-19 could inhibit NAADP signalling other than by preventing its Ca^{2+} mobilizing activity. Ned-19 was unable to provide a complete inhibition of NAADP-induced Ca^{2+} release in permeabilized cells (*Fig. 3.2.5*), but was able to completely inhibit the CCK

response in intact cells (*Fig. 4.2.3*) which involves both NAADP and cADPR. This could indicate an inhibitory role for Ned-19 upstream of both NAADP and cADPR's Ca^{2+} mobilizing activates. Ned-19 was identified due to its 3D electrostatic homology to NAADP (Naylor et al. 2009), therefore there is a chance that under physiological conditions it may interact with and inhibit the enzyme involved with NAADP's metabolism due to its structural homology. If this is the case it could also inhibit cADPR production, due to the synthesis of these two messengers sharing a single enzyme (Zhao et al. 2012), but would not inhibit cADPR's activity when it was directly added to cells (*Fig. 3.2.1*). Alternatively, if Ned-19 were to disrupt the degradation of NAADP by competitive inhibition of its catabolic enzyme it could cause a 'build-up' of the messenger, increasing the concentration of NAADP until it reached a level which is auto-inhibitory (Aarhus et al. 1996).

The potential inhibition of CD38 by Ned-19 is an interesting prospect as it would explain several inconsistencies in the effect of Ned-19. Firstly, as it would occur upstream of the synthesis of cADPR and NAADP it would explain how Ned-19 can inhibit CCK-induced Ca^{2+}ossicalitons, which involves both messengers and so should have a cADPR component that is insensitive to Ned-19. Secondly, it could provide a reason for why it failed to provide a complete inhibition against NAADP-induced Ca^{2+} release in permeabilized cells but did so against CCK. If Ned-19 is only an effective NAADP antagonist against certain NAADP sensitive ion channels it would mean that the channels insensitive to Ned-19 provided the NAADP-induced Ca^{2+} release observed with Ned-19 present in permeabilized PAC. However, in the case of CCK signalling in intact cells Ned-19 would be able to inhibit both the channels sensitive to its action and CD38, reducing the amount of NAADP produced below that required to activate the channels sensitive to its action. Conformation of this conjecture would require analysis of the amount of NAADP and cADPR synthesised by

CD38 (Yamasaki et al. 2005) under both biochemical and physiological conditions in the presence and absence of Ned-19 .

Heparin, which inhibits IP_3R (Ghosh et al. 1988), showed a similar inhibitory effect to 8-NH_2-cADPR on NAADP-induced Ca^{2+} spikes (Cancela et al. 1999). IP_3 has been shown to only be involved in the response to high concentrations of CCK (Sjödin and Gylfe 2000), rather than the low physiological ones used in this study. This could potentially highlight the importance of the cADPR component of CCK-induced Ca^{2+} release. CICR occurs via both IP_3R and RyR (Finch et al. 1991; Endo 2009), blockade of just IP_3R activity shows the ability to inhibit NAADP-induced release, despite RyR still being capable of being activated by this process.

PAC from $TPCN2^{-/-}$ mice showed no obvious loss of sensitivity to CCK (*Fig. 4.2.5*) despite loss of this channels activity being shown to significantly inhibit the amount of Ca^{2+} mobilised in response to NAADP (*Fig. 3.2.2*). This suggests that small amount of Ca^{2+} mobilised in response to NAADP independent of TPC2 is enough to induce the Ca^{2+} oscillations observed (*Fig. 4.2.5A*). This release could either occur via TPC1 channels, by the TPC independent release observed (*Fig. 5.2.5*) (believed to be the result of NAADP activating RyR), or a combination of the two. This reduced amount of Ca^{2+} in $TPCN2^{-/-}$ cells would then still be amplified by CICR, producing the Ca^{2+} oscillations observed and compensating for the loss of TPC2 activity. This again could highlight the importance of the cADPR produced in response to CCK, as lowering the requirement for CICR could be key to this process occurring in response to the reduced amount of Ca^{2+} mobilised in response to NAADP. These knockout cells also still showed a sensitivity to Ned-19, which supports the theory that NAADP induced release is key for the initiation and propagation of CCK-induced Ca^{2+} oscillations. Even though the amount of Ca^{2+} mobilised in response to NAADP in the

knockout cells is already substantially reduced, inhibiting it enough to completely inhibit CCK-induced Ca^{2+} oscillations.

While TPCN2$^{-/-}$ cells show no loss in their ability to produce Ca^{2+} oscillations in response to CCK, the amount of Ca^{2+} mobilized in the knockout cells could potentially be reduced. This can be calculated by permeabilizing cells post experiment with ionomycin and then calibrating the recording fluorescence with the Ca^{2+} concentration using EGTA (Schoutteten et al. 1999). Also testing the effect of CCK on PAC from TPCN1/2$^{-/-}$ mice could be used to see if CCK induced Ca^{2+} can occur independent of TPC activity. Loss of a response to CCK in these double knockout cells would not only show that TPC channels are essential for responses to this secretagogue, but would confirm that NAADP and not cADPR is vital for initiation of the response. Similarly, if there was still a response and it showed sensitivity to Ned-19 it would definitely prove the existence of a TPC independent method of NAADP-induced Ca^{2+} release in PAC.

As well as inhibiting the effect of a physiological concentration of CCK, Ned-19 showed the ability to inhibit the pathological effects of a supramaximal concentration of the secretagogue (*Fig. 4.2.4*). This shows that NAADP plays a key role in this process and can have a protective effect against CCK hyperstimulation. When the necrosis assay was conducted at room temperature a small, but significant increase in necrosis was observed when cells were exposed to CCK alone. Co-incubation with Ned-19 reduced the amount of necrosis in the CCK exposed cells to a level not significantly different to the control; however, this reduction was not deemed significant. As this was believed to due to the small increase in necrosis observed in response to CCK, rather than a lack of protective effect by Ned-19, the experiment was repeated with the incubation step of the assay in a water bath set to 37 °C to replicate body temperature. While the amount of necrosis observed was higher in all three

treatments, the effect was most prominent in the cells treated with CCK alone. As with the experiments conducted at room temperature, co-incubation of CCK with Ned-19 reduced the number of necrotic cells counted, however this time the effect was deemed significant. This suggests than Ned-19 could be used therapeutically against AP, though this would need to be tested against more physiologically relevant models of AP (Su et al. 2006).

Together this work highlights the key role that the intracellular secondary Ca^{2+} messenger NAADP plays in the response to the hormone CCK in PAC. Acute application of the membrane permeable NAADP antagonist Ned-19 is capable of completely inhibiting CCK-induced Ca^{2+} oscillations. This supports the previous suggestion that NAADP-induced Ca^{2+} release is vital for the response to CCK, but also suggest that it plays a key role in propagating this response. The CCK-response was unaltered in $TPCN2^{-/-}$ PAC, despite them having been shown to produce a significantly diminished response to NAADP. CCK responses in these knockout cells were still sensitive to Ned-19, showing that there was still a functional NAADP-dependent component left in them. Hyperstimulation of PAC by a supramaximal concentration of CCK was reduced by Ned-19, indicating a key role for NAADP in this process and a potential role for Ned-19 in preventing AP.

CHAPTER 5:

THE NAADP ANTAGONIST NED-19 HAS AN INHIBITORY EFFECT ON PATHOLOGICAL CALCIUM RELEASE INDUCED BY THE BILE ACID TLC-S IN PANCREATIC ACINAR CELLS

Chapter 5: The NAADP antagonist Ned-19 has an inhibitory effect on pathological calcium release induced by the bile acid TLC-S in pancreatic acinar cells

5.1: Overview of TLC-S-induced calcium release in pancreatic acinar cells

Gallstones are solid masses formed in the gallbladder from various components of bile; they are mainly composed of cholesterol, bilirubin and calcium (Schafmayer et al. 2006). They are believed to be one of the leading causes of AP, and that by physically blocking the ampulla of Vater they cause a reflux of bile into the pancreas. Bile acids are catabolic products of the metabolism cholesterol (Russell DW 2003), synthesised by various hepatic enzymes in a variety of distinct pathways and together comprise the major component of bile (Farina et al. 2009). They have been shown to induce severe AP experimentally (Lerch et al. 1993; Kim et al. 2002), therefore there has been much interest into their effects on PAC and how they induce necrosis in this cell type.

While bile acids have been shown to have several effects in PAC, including increasing the intracellular concentration of Na^+ (Voronina et al. 2005) and depolarizating of the inner mitochondrial membrane (Voronina et al. 2004), it has been suggested their major pathological effect is the ability to induce sustained pathological increases in $[Ca^{2+}]_i$ (Voronina et al. 2002; Gerasimenko, Flowerdew, et al. 2006; Orabi et al. 2013). These Ca^{2+} increases initiate a cascade of events including the vacuolization of zymogen granules (Raraty et al. 2000; Sherwood et al. 2007; Mareninova et al. 2009) and premature activation of the proenzymes stored within them (Krüger et al. 2000; Husain et al. 2005), characteristic of AP. This leads to the expression of pro-inflammatory cytokines (Han and Logsdon 2000; Muili, Jin, et al. 2013), loss of ATP production due to mitochondrial depolarization

(Voronina et al. 2004; Criddle, Murphy, et al. 2006), the loss of plasmalemma integrity (Orabi et al. 2010) and ultimately death of PAC.

Bile acids have been shown to induce increases in $[Ca^{2+}]_i$ initially via the release of Ca^{2+} from intracellular stores (Gerasimenko, Flowerdew, et al. 2006; Orabi et al. 2013) and then subsequently via the entry of extracellular Ca^{2+} through CRAC channels as a result of SOCE (Kim et al. 2002). It has also been suggested that bile acids may allow the entry of extracellular Ca^{2+} either by disrupting the plasmalemma by acting as a detergent (Kim et al. 2002) or by creating pores in it by forming oligomers (Zimniak et al. 1991).

Taurolithocholic acid 3-sulfate (TLC-S) is bile acid that is often used experimentally to represent bile acids and study their effects on PAC (Voronina et al. 2002; Gerasimenko, Flowerdew, et al. 2006; Muili, Jin, et al. 2013; Orabi et al. 2013; Lewarchik et al. 2014; Wen et al. 2015; Huang et al. 2017). Gerasimenko et al. found that in permeabilized PAC TLC-S caused the release of Ca^{2+} in comparable levels to the secondary messengers IP_3 and cADPR (Gerasimenko, Flowerdew, et al. 2006) (*Fig. 5.1.1A*). Application of a combination of TLC-S and cADPR elicited no greater effect than TLC-S alone; while 8-amino-cADPR, a cADPR antagonist, had no effect. These results indicate TLC-S induces a maximal Ca^{2+} response, hence no additive effect when coapplied with cADPR, and that its effect is independent of cADPR. Inhibition of IP_3R by either caffeine or 2-APB, or of RyR by RR caused a significant reduction in the amount of Ca^{2+} released in response to TLC-S; indicating both types of channel play a key role in Ca^{2+} release. A close to total inhibition of TLC-S-induced release was seen when both types of receptor were inhibited by a combination of 2-APB and RR. Both IP_3R (Huang et al. 2017) and RyR (Lewarchik et al. 2014) have subsequently been shown to directly play a role in TLC-S induced AP as well as Ca^{2+} release induced by the bile acid.

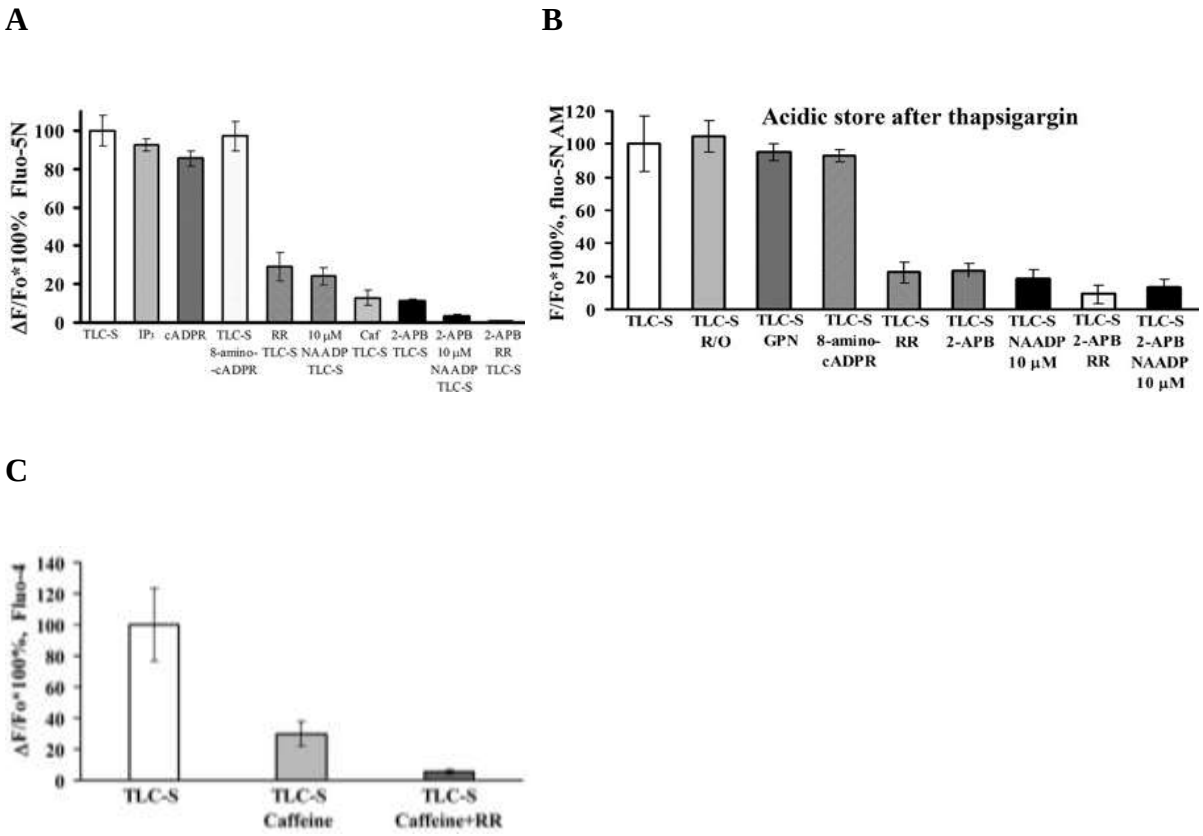

Fig. 5.1.1 Inhibition of TLC-S-induced calcium release in pancreatic acinar cells

(A) Summary of Ca^{2+} responses relative to 200 μM TLC-S alone (100%) in permeabilized pancreatic acinar cells; concentrations of other compounds used were: 10 μM IP_3, 10 μM cADPR, 10 μM 8-amino-cADPR, 10 μM RR, 100 μM 2-APB, 10 mM caffeine or 10 μM NAADP. **(B)** Summary of Ca^{2+} responses relative to 200 μM TLC-S alone (100%) in permeabilized pancreatic acinar cells after treatment with Tg; concentrations of 8-amino-cADPR, RR, 2-APB, caffeine and NAADP used were the same as before; 50 μM GPN or 1 μM rotenone and 1 μM oligomycin were used to disrupt lysosomes and mitochondria respectively. **(C)** Summary of Ca^{2+} responses relative to 200 μM TLC-S alone (100%) in presence of 20mM caffeine with and without 10 μM RR in intact pancreatic acinar cells.

At the time of Gerasimenko et al.'s report TPC channels had yet to be identified as NAADP-sensitive ion channels, so their role in the TLC-S response is unknown. However a high autoinhibitory concentration of NAADP (Aarhus et al. 1996) did reduce the amount of Ca^{2+} released in response to TLC-S, with a near total inhibition reached when a combination of NAADP and 2-APB was applied. These results suggest that TPC's may be sensitive to the activity of TLC-S, as both RyR and TPC channels have been shown to be involved in the response to NAADP in PAC (Gerasimenko et al. 2015). As there is currently no NAADP antagonist whose activity is TPC specific, a similar pharmacological approach to study the effect of TLC-S on these channels is not possible. However, through use of knockout mice for either TPC isoform (Calcraft et al. 2009; Hooper et al. 2015) or the TPC double knockout mice (Ruas et al. 2015), their importance can be investigated.

Using a similar pharmacological approach in permeabilized PAC after depletion of ER Ca^{2+} by Tg Gerasimenko et al. found that TLC-S can mobilize Ca^{2+} from acidic organelles via both IP_3R and RyR (*Fig. 5.1.1B*). PAC cells are known to express both types of Ca^{2+} channel on acidic organelles; meaning, unlike other cell types, some Ca^{2+} can be mobilized through these channels in a Tg-insensitive manner (Gerasimenko, Sherwood, et al. 2006). NAADP-induced Ca^{2+} is characterised by being Tg insensitive, therefore understandably a high concentration of NAADP was also inhibitory after treatment with Tg (Genazzani et al. 1996). As before combining 2-APB with either RR or a high concentration of NAADP provided a further inhibition than any of the 3 antagonists alone, though in neither case total inhibition was achieved.

Various candidates for the IP_3 and cADPR sensitive acidic store in PAC have been ruled out by selective pharmacological disruption; with TLC-S still inducing an increase in $[Ca^{2+}]_i$ after disruption of lysosomes with GPN, mitochondria with rotenone and oligomycin or the Golgi

A

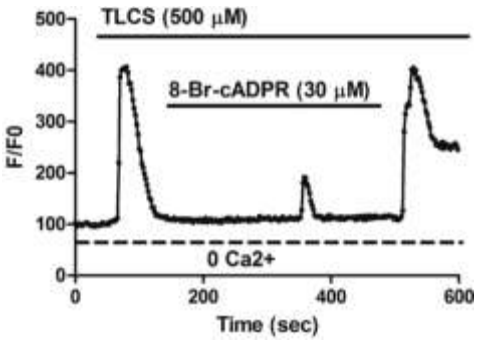

B

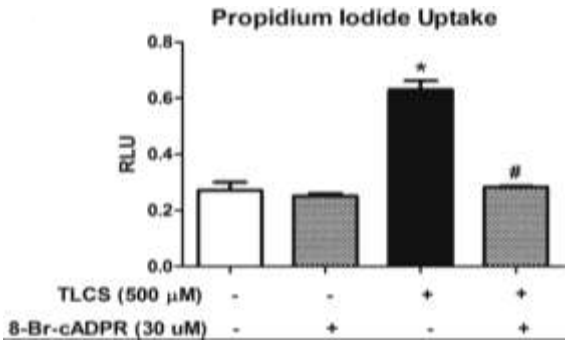

C

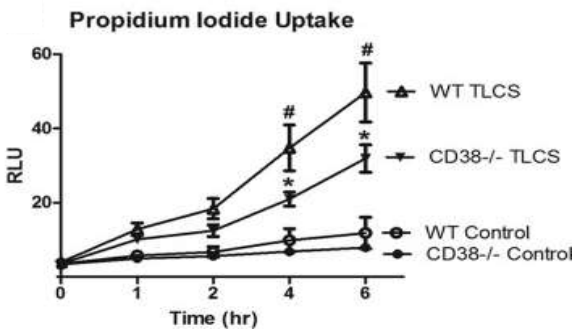

Fig. 5.1.2 Use of a cADPR antagonist or knockout of CD38 protects against TLC-S-induced cell death in pancreatic acinar cells

(A) Representative trace of the effect of 8-Br-cADPR on TLC-S induced calcium release in pancreatic acinar cells. **(B)** Summary of the protective effect of 8-Br-cADPR against TLC-S induced PI uptake as a measure of cell death in pancreatic acinar cells; for * and # $p < 0.05$ compared with the control and TLC-S alone respectively. *RLU*, relative light units (n =3). **(C)** Summary of TLC-S induced PI uptake as a measure of cell death in pancreatic acinar cells isolated from either wild type of CD38 null mice; for * and # $p < 0.05$ compared with the control and TLC-S alone respectively. *RLU*, relative light units (n =3).

body with brefeldin A. By process of elimination it is therefore believed that identity of this unique Ca^{2+} store in PAC is the zymogen granules, specialist organelles characteristic of the exocrine pancreas. In intact PAC, caffeine still reduced the amount of Ca^{2+} released in response to TLC-S (*Fig. 5.1.1C*) and a further reduction was seen when RR was applied in addition to caffeine. These results are important as it shows that the findings in the permeabilized cell model are relevant under more physiological conditions and that preventing the release of Ca^{2+} from organelles stores can prevent the non-physiological levels of $[Ca^{2+}]_i$ seen in AP.

Recently Orabi et al. has shown that PAC isolated from $CD38^{-/-}$ mice are protected against TLC-S-induced necrosis (Orabi et al. 2013) (*Fig 4.1.2C*); indicating that TLC-S mobilizes Ca^{2+} indirectly via the production of secondary messengers like NAADP, rather than acting directly on Ca^{2+} channels itself. CD38 is known to be able to catalyse the synthesis of both the secondary messengers NAADP and cADPR, dependent on the conditions (Aarhus et al. 1995). Previously Gerasimenko et al. had found that the cADPR antagonist 8-NH_2-cADPR had no effect on TLC-S-induced Ca^{2+} release (Gerasimenko, Flowerdew, et al. 2006), concluding that cADPR had no role in PAC's response to TLC-S. Conversely Orabi et al. found an alternative antagonist 8-Br-cADPR both reduced TLC-S induced Ca^{2+} release and cell death (Orabi et al. 2013) (*Fig. 5.1.2A-B*). Combined with the $CD38^{-/-}$ data, this suggests that in PAC CD38 does in fact produce cADPR in response to TLC-S. This discrepancy could be either due to the different types of antagonist used or because the second study used 3 times the concentration of antagonist the first did. Whether TLC-S-induced Ca^{2+} release via IP_3R is the result of it stimulating the synthesis of IP_3 via PLC, CICR, or TLC-S directly activating the channels is unknown.

Currently there is no form of direct treatment for AP, with pain relief the only solution for patients suffering from an incident until it resolves itself. Some compounds used experimentally to investigate the effects of bile acids like TLC-S have low membrane permeability or nonspecific effects, meaning they unsuitable for clinical use. Therefore, it is important to identify compounds that may both have a protective effect against biliary AP and be clinically relevant. One example of this is the CRAC channel blocker GSK-7975A, which prevents SOCE by inhibiting Orai1 and has also been shown to have a protective effect against several models of AP, including a TLC-S-induced biliary model (Wen et al. 2015).

The cell permeable NAADP antagonist Ned-19 has been shown to inhibit CCK-induced Ca^{2+} release in PAC (Gerasimenko et al. 2015), though its effect on TLC-S-induced Ca^{2+} release is unknown. Because TLC-S induced release is known to contain a NAADP sensitive component it is probable that Ned-19 with have a protective effect against the bile acid and requires investigating.

5.2: The effect of Ned-19 on TLC-S-induced calcium release in pancreatic acinar cells

As TLC-S-induced Ca^{2+} release in PAC has been shown to contain an NAADP sensitive element (Gerasimenko, Flowerdew, et al. 2006), it was predicted that the recently discovered NAADP antagonist Ned-19 would have an inhibitory effect on the amount of Ca^{2+} released in response to TLC-S. As 100 µM Ned-19 had an inhibitory effect against CCK-induced Ca^{2+} release (Gerasimenko et al. 2015) it was decided to use this concentration against 200 µM TLC-S, the concentration used by Gerasimenko et al. in their previous study (Gerasimenko, Flowerdew, et al. 2006).

As previously described when PAC are exposed to TLC-S it either induces Ca^{2+} oscillations

A

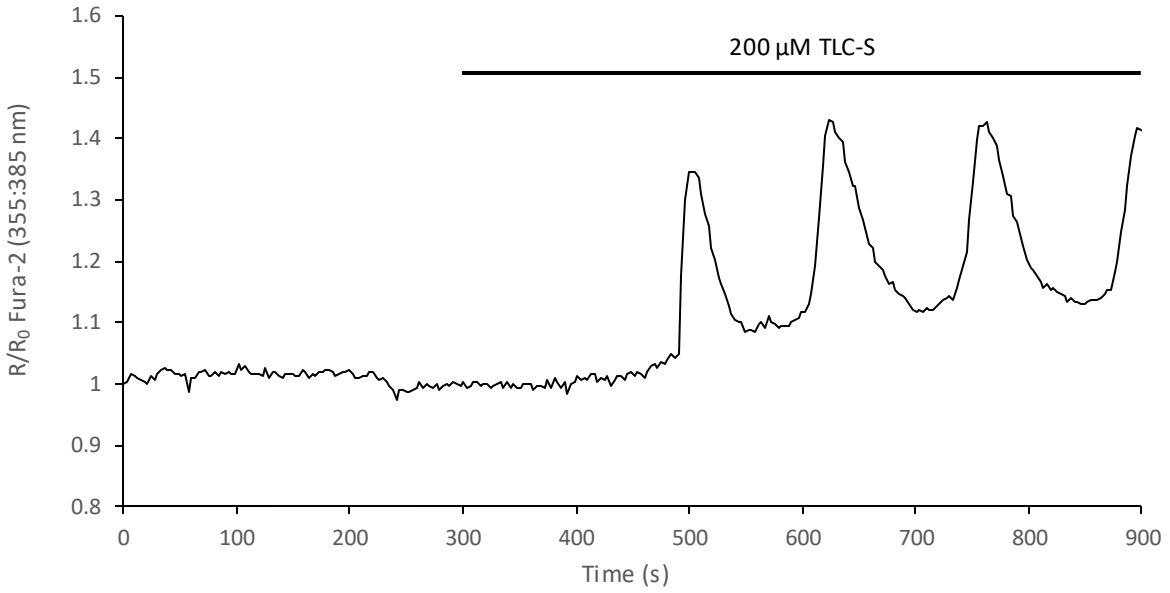

B

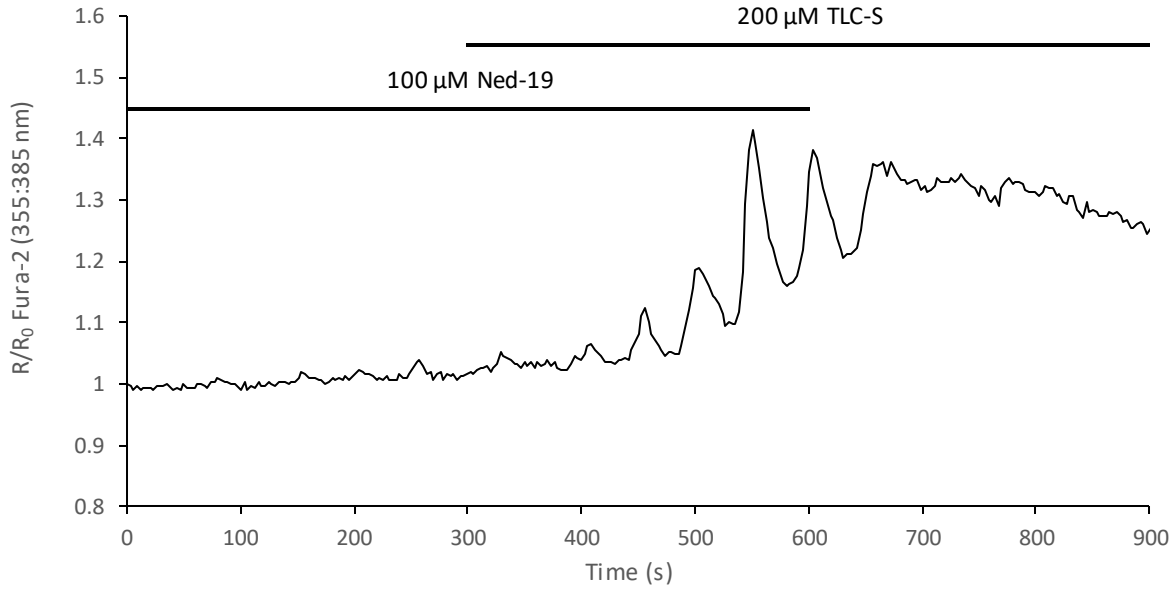

Fig. 5.2.1 The effect of Ned-19 pre-treatment on TLC-S induced calcium release in pancreatic acinar cells

(A) Representative trace showing the cytoplasmic calcium response to 200 µM TLC-S in pancreatic acinar cells. **(B)** Representative trace of the effect pre-treatment with 100 µM Ned-19 on the response to 200 µM TLC-S in pancreatic acinar cells.

C

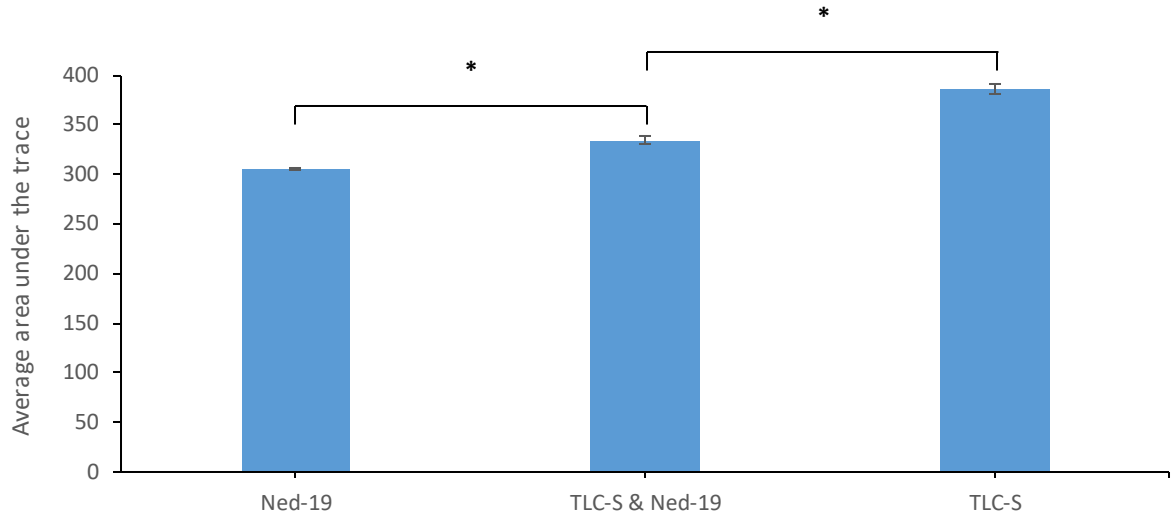

D

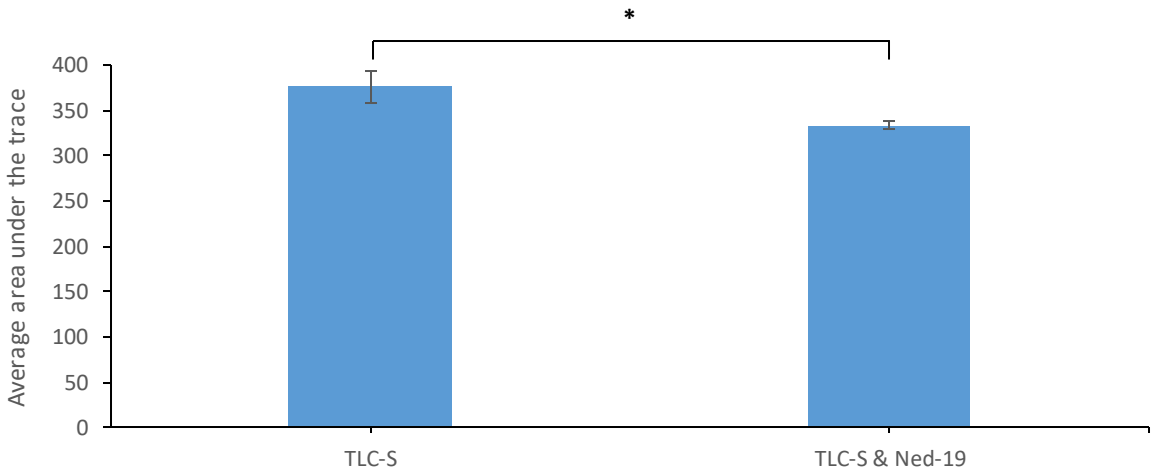

Fig. 5.2.1 (*continued*)

(C) Bar Chart showing the average area under the trace for the cells sampled in **(B)**; Ned-19 between 0 s and 300 s, TLC-S & Ned-19 between 300 s and 600 s, and TLC-S between 600 s and 900s (Data represents mean ± SEM, n = 35; *, $P \leq 0.05$). **(D)** Bar Chart showing the Ned-19 was added to PAC there was no Ca^{2+} response, however when TLC-S was also added average area under the trace for the 300 s after addition of TLC-S (between 300 s and 600 s) for the cells sampled in **(A)** and **(B)** (Data represents mean ± SEM, n = 8 for TLC-S alone and n = 35 for TLC-S and Ned-19; *, $P \leq 0.05$).

(*Fig. 5.2.1A*) or a sustained increase in $[Ca^{2+}]_I$ (Voronina et al. 2002); the latter of which would be cytotoxic and induce the pathological effects associated with bile acids. To test if Ned-19 could prevent TLC-S-induced Ca^{2+} release, cells were first exposed to Ned-19 alone for 300 s, before the addition of TLC-S; after another 300 s interval Ned-19 was removed to expose cells to TLC-S alone for a final 300 s period (*Fig. 5.2.1B*). When PAC were perfused with just Ned-19 there was no visible effect. Addition of TLC-S to the perfusion solution in the continued presence of Ned-19 27 of the 35 cells observed responded with an increase in $[Ca^{2+}]_i$. After Ned-19 was removed there was a sustained increase in $[Ca^{2+}]_i$ observed in 34 of the 35 cells sampled, indicating that Ned-19 may provide a protective effect against TLC-S. The average area under the trace was calculated for the three 300 s periods where cells were exposed to Ned-19 alone, both Ned-19 and TLC-S, and TLC-S alone (*Fig. 5.2.1C*). A significant increase in area was seen in each subsequent period as determined by a Student's *t*-test, $p < 0.01$ for both; implying that Ned-19 has a significant effect on the amount of Ca^{2+} release in response to TLC-S, even though a significant increase in the $[Ca^{2+}]_i$ is still observed. To confirm this observation, the average area under the trace was calculated for the initial 300 s period after TLC-S was applied either alone or in the presence of Ned-19 (*Fig. 5.2.1D*). A Student's *t*-test determined a significant reduction in the amount of Ca^{2+} released in response to TLC-S when Ned-19 is present, $p = 0.04$.

Together these results show that Ned-19 reduced the amount of Ca^{2+} released by PAC from organelle stores in response to TLC-S.

As Ned-19 significantly reduced the TLC-S-induced Ca^{2+} response it is possible that it will provide a protective effect against TLC-S-induced cell death in PAC; as has been seen for other compounds that reduce the amount of Ca^{2+} released in response to TLC-S (Wen et al. 2015 p.1; Huang et al. 2017). As before (*Fig. 4.2.4C*), incubation with 100 µM Ned-19 for 1

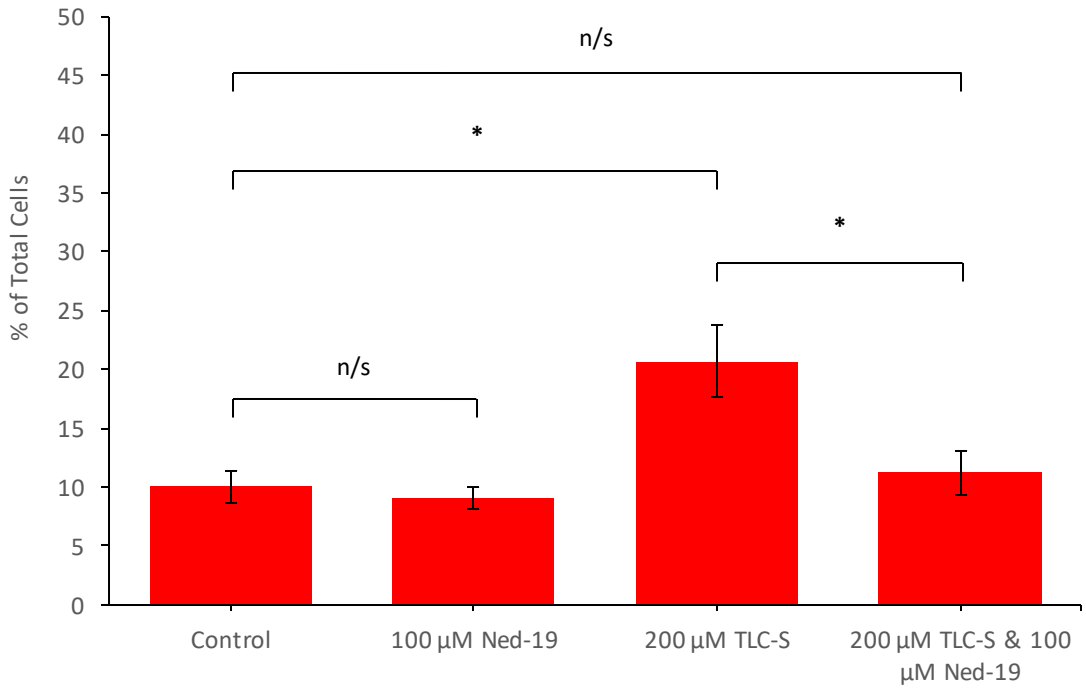

Fig. 5.2.2 Effect of Ned-19 on TLC-S-induced cell death in acinar cells

The results of cell death assays performed on pancreatic acinar cells treated with 200 µM TLC-S and/or 100 µM Ned-19 for 1 hour. Data represents the number of necrotic cells as a percentage of the total number of cells counted for that specific treatment (Data represents mean ± SEM, n = 7093 cells; *, $P \leq 0.05$; n/s, not significant).

hour caused no significant difference in the number of necrotic cells according to a ANOVA comparison ($p = 0.9745$). Incubation for the same time with 200 µM TLC-S however, doubles the amount of necrosis, which is deemed significant ($p = 0.0045$). The amount of necrosis observed when TLC-S and Ned-19 were co-incubated together is a significantly smaller than that observed when TLC-S applied alone ($p = 0.0082$); down to a level not significantly different from that seen in the control ($p = 0.991$).

Both caffeine, which at high concentrations block Ca^{2+} release via IP_3R (Wakui et al. 1990), and GSK-7975A, which prevents SOCE by blocking Orai1's channel pore (Derler et al. 2013), have been shown to have a protective effect against TLC-S-induced cell death (Wen et al. 2015; Huang et al. 2017). It was decided to compare the protective effects of these two compounds to Ned-19 and test if they provided any further effect when used in combination with Ned-19.

Like in the previous experiment (*Fig. 5.2.2*) TLC-S induced an increase in necrosis, deemed significant by ANOVA comparison ($p = 0.005$ and $p = 0.0008$ for the caffeine and GSK-7975A experiments respectively). For both sets of experiments Ned-19 showed a significant protective effect against TLC-S induced necrosis ($p = 0.04$ and $p = 0.0189$ for the caffeine and GSK-7975A experiments respectively). Both caffeine (*Fig. 5.2.3*) and GSK-7975A (*Fig. 5.2.4*) alone had a significant protective effect against TLC-S ($p = 0.0048$ and $p = 0.0053$ respectively); with both reducing the amount of necrosis observed below that when Ned-19 was used, though neither decrease was deemed significant. Use of caffeine and Ned-19 together appeared to have an additive protective effect, reducing the number of necrotic cells close to that of the untreated control, however this extra protection was not deemed significant compared to using either Ned-19 or caffeine alone. A combination of GSK-7975A and Ned-19 produced no further decrease in necrosis compared to using GSK-7975A alone.

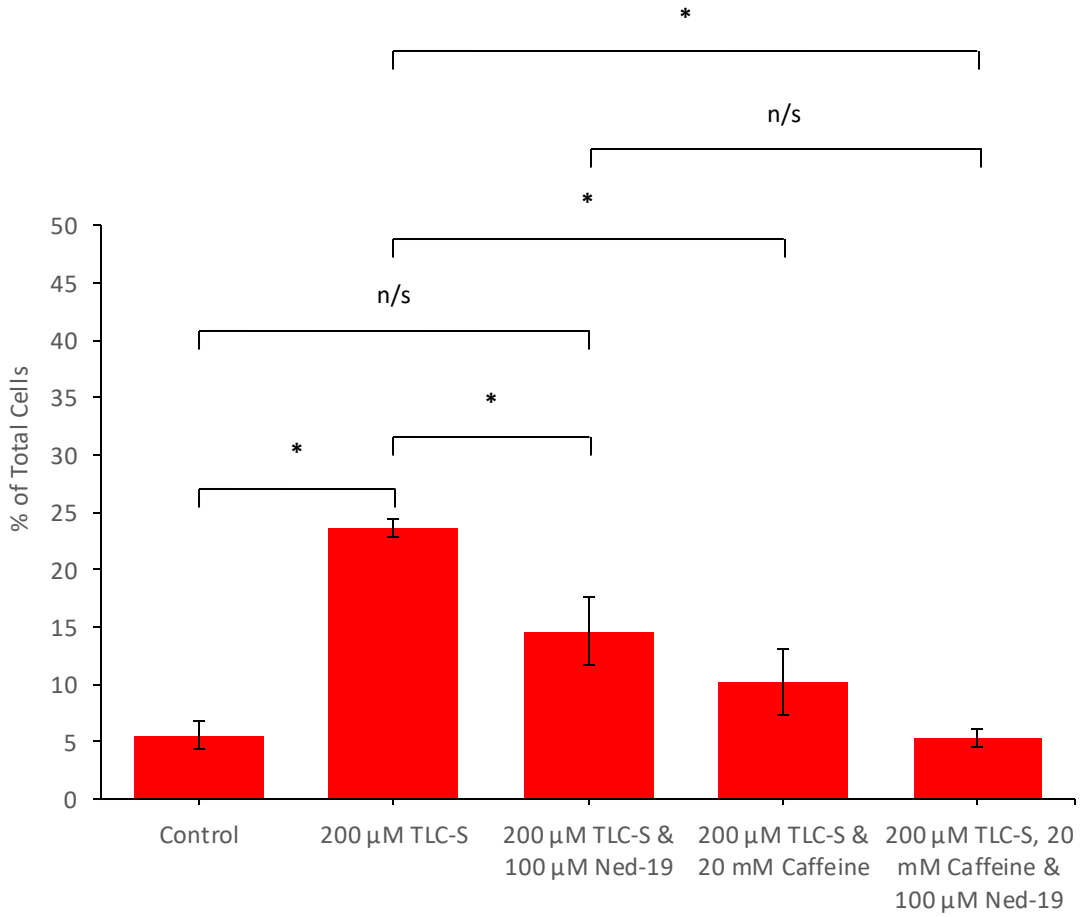

Fig. 5.2.3 Effect of Ned-19 and caffeine on TLC-S-induced cell death in acinar cells

The results of cell death assays performed on pancreatic acinar cells treated with 200 µM TLC-S, 100 µM Ned-19 and/or 20 mM caffeine for 1 hour. Data represents the number of necrotic cells as a percentage of the total number of cells counted for that specific treatment (Data represents mean ± SEM, n = 3632 cells; *, $P \leq 0.05$; n/s, not significant).

While there was no obvious difference in CCK-induced Ca^{2+} oscillations in PAC isolated form TPCN2$^{-/-}$ mice (*Fig. 4.2.5*), the knockout of this ion channels function may provide a protective effect against TLC-S toxicity. As such the level of necrosis in PAC preparations from both wild type and TPCN2$^{-/-}$ mice exposed to TLC-S were compared to examine if loss of TPC2 activity had any effect on TLC-S induced necrosis.

Despite the preparations from TPCN2$^{-/-}$ mice showing a slightly lower amount of necrosis than that in wild type preparations for all treatments tested (*Fig 5.2.5*), none of them was deemed as significantly different by a student's *t*-test (control $p = 0.997$, Ned-19 $p > 0.9999$, TLC-S $p = 0.999$, and TLC-S & Ned-19 $p = 0.9897$). As such the TPCN2$^{-/-}$ preparation showed the same significant increase in necrosis when treated with TLC-S ($p = 0.0006$) which was significantly reduced when Ned-19 was also present ($p = 0.0005$). Therefore; knockout of TPC2 has no significant effect on TLC-S's ability to induce a toxic $[Ca^{2+}]_c$ in PAC, despite this involving an NAADP component. As against CCK-induced Ca^{2+} oscillations, TPCN2$^{-/-}$ cells showed no loss of sensitivity towards Ned-19, which displayed a protective effect against the toxic effects of TLC-S.

5.3 Discussion

The primary bile acid TLC-S is known to mobilize Ca^{2+} in PAC from both the ER and a separate acid store believed to be the zymogen granules (Gerasimenko, Flowerdew, et al. 2006) (*Fig. 5.1.1*). TLC-S-induced Ca^{2+} release has been shown to involve the ectoenzyme CD38 (Orabi et al. 2013) (*Fig. 5.1.2*) and be sensitive to a high autoinhibitory concentration of NAADP in permeabilized cells (Aarhus et al. 1996). Inhibition of IP_3R and RyR reduces the amount of Ca^{2+} released in response to TLC-S, as does use of 8-Br-cADPR, an inhibitor of cADPR induced Ca^{2+} release.

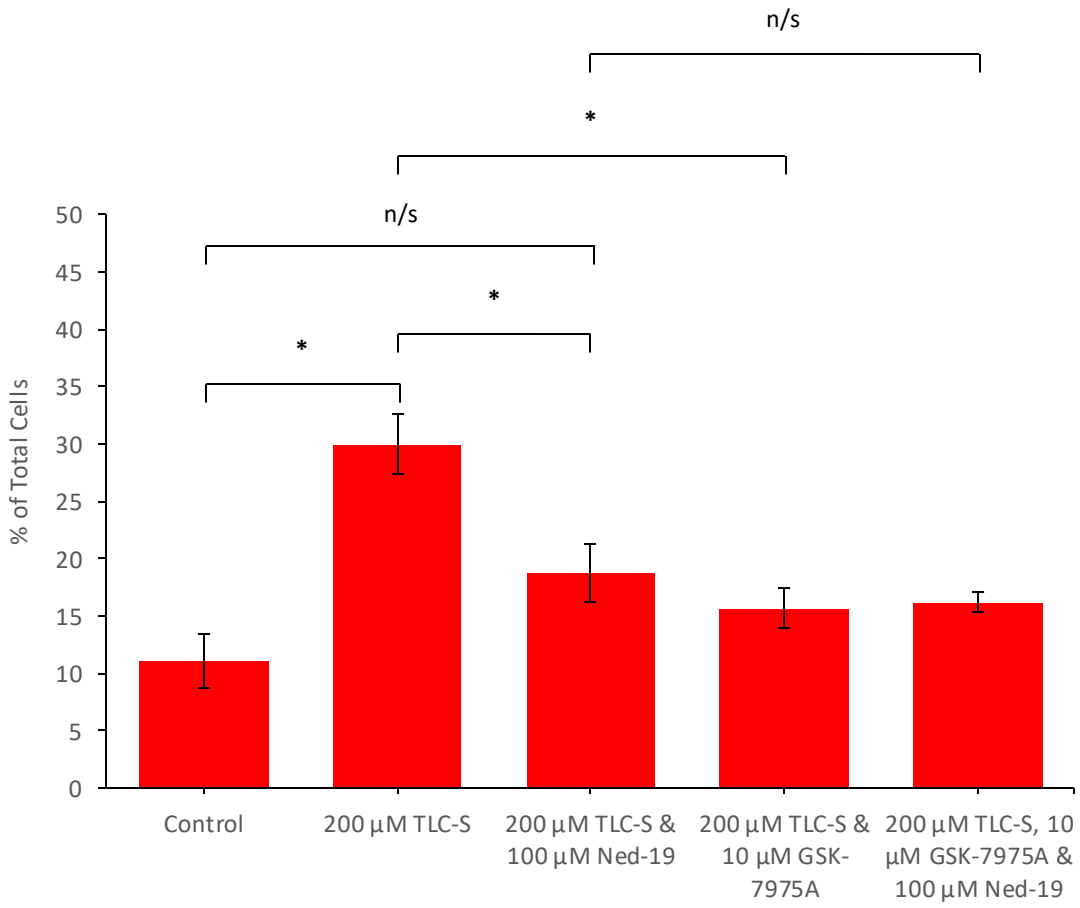

Fig. 5.2.4 Effect of Ned-19 and GSK-7975A on TLC-S-induced cell death in acinar cells

The results of cell death assays performed on pancreatic acinar cells treated with 200 µM TLC-S, 100 µM Ned-19 and/or 10 µM GSK-7975A for 1 hour. Data represents the number of necrotic cells as a percentage of the total number of cells counted for that specific treatment (Data represents mean ± SEM, n = 5099 cells; *, $P \leq 0.05$; n/s, not significant).

As predicted the NAADP antagonist Ned-19 (Naylor et al. 2009) significantly reduced the amount of Ca^{2+} released in response to TLC-S compared to when Ned-19 was not present (*Fig. 5.2.1D*). The increase in Ca^{2+} induced by TLC-S observed in the presence of Ned-19 was deemed as significant, but was also significantly smaller than that observed when Ned-19 was removed (*Fig. 5.2.1C*). As a high autoinhibitory concentration of NAADP was only reported as being capable of achieving a partial inhibition of TLC-S-induced release, it was not expected for Ned-19 to achieve a complete inhibition. In permeabilized PAC the same concentration of Ned-19 did not show a complete inhibition of NAADP-induced Ca^{2+} release (Gerasimenko et al. 2015), suggesting there is component of NAADP induced Ca^{2+} release that is Ned-19 insensitive, at least at a concentration of 100 µM.

Ned-19 does not need to completely inhibit TLC-S-induced Ca^{2+} to have a protective effect against TLC-S induced necrosis, so long as it reduces the amount of Ca^{2+} released in response to TLC-S below a cytotoxic amount (Festjens et al. 2006). This was seen in the case of caffeine; where Gerasimenko et al. only observed a partial inhibition of TLC-S-induced Ca^{2+} release by caffeine (Gerasimenko, Flowerdew, et al. 2006), but it has been found to have a protective effect against another model of AP induced by caerulein (Huang et al. 2017). Applying Ned-19 acutely on top of a TLC-S-induced Ca^{2+} response would be useful for visualising any protective effect it may have; as in a therapeutic setting any drug to treat AP would be given to a patient who is already suffering from a pathological incident.

The initial cell death experiments with Ned-19 showed that application of Ned-19 and TLC-S significantly reduced the amount of necrosis compared to when cells were incubated with TLC-S alone (*Fig. 5.2.2*). This was also the case in both the experiments with caffeine (*Fig. 5.2.3*) and the CRAC channel blocker GSK-7975A (Derler et al. 2013) (*Fig. 5.2.4*). Together these experiments show that NAADP-induced Ca^{2+} release plays a key part in the

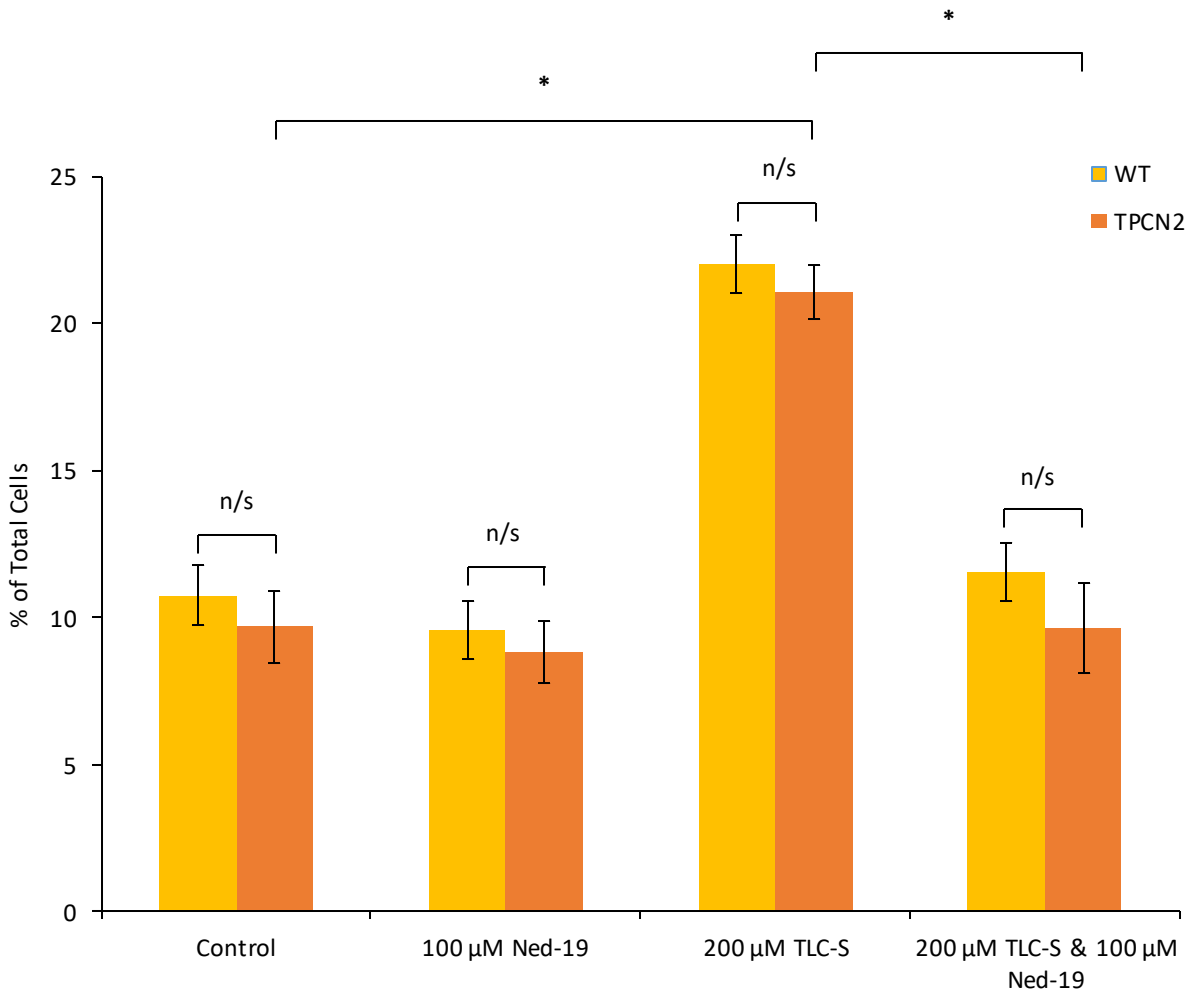

Fig. 5.2.5 Effect of TPC2 knockout on TLC-S-induced necrosis in acinar cells

The necrosis results of cell death assay performed on pancreatic acinar cells isolated form wild type and TPC2 knockout mice treated with 100 µM Ned-19 and/or 200 µM TLC-S for 1 hour where applicable. Yellow bars represent the necrosis observed in wild type cells as a percentage of the total number of cells counted for that specific treatment and orange represent the necrosis observed in TPCN2$^{-/-}$ cells as a percentage of the total number of cells counted for that specific treatment (Data represents mean ± SEM, n = 7093 WT cells and n = 9529 TPCN2 cells; *, $P \leq 0.05$; n/s, not significant).

pathological response to TLC-S, and that Ned-19 can provide a significant protective against the bile acids effect.

Either caffeine or GSK-7975A alone had a greater protective effect against TLC-S-induced necrosis than Ned-19, though neither's effect was significantly greater than Ned-19's. Using caffeine and Ned-19 together further reduced the amount of necrosis observed compared to using either of them alone; although the additional decrease was not significant compared to using either compound alone. This could be due to either compound reducing the amount of necrosis observed down to an amount not statistically significant from the control. This additive effect corresponds to Gerasimenko et al.'s findings that TLC-S-induced Ca^{2+} release involves the components of all three intracellular secondary Ca^{2+} messengers signalling pathways, and that blocking release via the channels involved in two messages signalling has a greater effect on amount of Ca^{2+} released in response to TLC-S than just blocking one (Gerasimenko, Flowerdew, et al. 2006) (*Fig. 5.1.1*).

Despite displaying a slightly stronger protective effect than Ned-19 when used alone, GSK-7975A had no additive effect when used in combination with Ned-19. This could suggest that the effects of Ned-19 and GSK-7975A are overlapping rather than additive, as was the case with caffeine. The NAADP sensitive ion channel TPC2 (Calcraft et al. 2009) has been shown to modulate SOCE via interaction with the CRAC channel proteins STIM1 and Orai1 (López et al. 2012), though the effect of Ned-19 on SOCE has not yet been reported. It is possible that inhibition of NAADP-induced Ca^{2+} via TPC2 with Ned-19 could disrupt the channel's interactions with the CRAC channel components and have an inhibitory effect on SOCE. This would explain the lack of additional inhibition by use of both Ned-19 and GSK-7975A, though this would need confirming by testing Ned-19's effect on Ca^{2+} entry. Alternatively, the inhibition of the NAADP sensitive component of TLC-S-induced Ca^{2+} release by Ned-19

could be reducing the amount of Ca^{2+} mobilized from organelle stores bellow the amount that triggers SOCE; or at least reduces it to a level that inhibiting it with GSK-7975A has a minimal effect.

As Ned-19 has shown the ability to reduce TLC-S induced necrosis, its protective effects should be tested against other models of AP, e.g. alcohol metabolites (Gerasimenko et al. 2013). It may also be beneficial to test how effective Ned-19 is at preventing Ca^{2+} release and necrosis induced by other bile acids, which may prove to act in a more NAADP independent manner. If Ned-19 does prove to exhibit a protective effect against a wide range of cell models of AP, it would be desirable to progress it to animal models of the disease.

The greatest protective effects may be provided when Ned-19 is used in combination with compounds that affect other elements of intracellular Ca^{2+} release than just NAADP, as was seen when it was coapplied with caffeine. Caffeine blocks Ca^{2+} release via IP_3R, which can be activated by either IP_3 itself or Ca^{2+} via CICR (Taylor and Tovey 2010); though it is not known which is the case in TLC-S-induced Ca^{2+} release. TLC-S activity involves the activity of CD38, indicating it acts via the production of secondary messengers rather than direct interaction with intracellular Ca^{2+} channels itself. Testing if TLC-S-induced Ca^{2+} release is also mediated by PLC, e.g. by inhibition with U-73122 (Bleasdale et al. 1990; Smith et al. 1990), would help resolve if this is true. Identifying compounds other than caffeine that have an additive effect with Ned-19 could be useful, as caffeine when used at a high concentration is known to have a range of side effects (Blanchard and Sawers 1983; Mahmud and Feely 2001; Rapuri et al. 2001; Winston et al. 2005).

NAADP induced Ca^{2+} release has been shown to involve the activity of both TPC and RyR channels (Gerasimenko et al. 2015); with RyR1 providing a larger contribution for NAADP induced release and RyR2 doing so for cADPR induced release. This would suggest that

Dantrolene, which specificly inhibits RyR1 and RyR3 (Zhao et al. 2001) and that has been shown to protect against caerulein-induced AP (Orabi et al. 2010), would not have an additive effect if used in conjunction with Ned-19. However, combining Ned-19 with an inhibitor of RyR2, e.g. flecainide (Mehra et al. 2014), may do so, as both NAADP and cADPR induced Ca^{2+} release would be inhibited. A similar effect may be possible independent of Ned-19 by inhibiting CD38 directly, and preventing the formation of the two secondary messengers rather than their activity. Recently it was shown the antibacterial agent Rhein inhibited CD38 dependent glioma progression by preventing microglia activation (Blacher et al. 2015), and therefore could be a useful compound to test against TLC-S-induced Ca^{2+} release and necrosis.

The toxic levels of cytoplasmic Ca^{2+} released in response to TLC-S involves all three secondary Ca^{2+} messenger pathways (Gerasimenko, Flowerdew, et al. 2006). Therefore, it is unsurprising that knocking out TPC2 had no significant effect on the amount of necrosis induced by TLC-S (*Fig. 5.2.5*) because of the multiple sources of Ca^{2+} release still available. However as pharmacological inhibition of one or more of these pathways did diminish the amount of necrosis observed in wild type cell in response to TLC-S (Huang et al. 2017), it was possible that $TPCN2^{-/-}$ cells would be less sensitive to TLC-S's toxic effects. Due to there being no loss of sensitivity to TLC-S in the knockout cells it would be assumed that Ned-19's protective effect would be conserved, as was seen in the case of CCK-induced Ca^{2+} oscillations (*Fig. 3.2.5*). The NAADP antagonist obviously affects enough other elements of NAADP signalling that is effect is not dependent on TPC2.

The results in the chapter show that Ned-19 protects against TLC-S-induced necrosis by reducing the amount of Ca^{2+} mobilized in response to the bile acid. Similar protective effects were observed when IP_3R were inhibited with caffeine or SOCE was blocked by GSK-

7975A, though neither of these compounds when used in combination with Ned-19 had a significant additive protective effect. Genetic knockout of TPC2 channels, which has been shown to significantly reduce the amount of Ca^{2+} mobilized in PAC in response to NAADP, had no effect on TLC-S-induced necrosis or on the protective effect of Ned-19. This further suggests that PAC have enough NAADP-sensitive ion channels to compensate for the loss of TPC2 activity in both physiological and pathological Ca^{2+} signalling.

CHAPTER 6:

INHIBITION OF PANCREATIC ACINAR CELL NECROSIS INDUCED BY THE BILE ACID CHOLATE REQUIRES INHIBITION OF BOTH NAADP-INDUCED CALCIUM RELEASE AND STORE OPERATED CALCIUM ENTRY

Chapter 6: Inhibition of pancreatic acinar cell necrosis induced by the bile acid cholate requires inhibition of both NAADP-induced calcium release and store operated calcium entry

6.1: Overview of calcium entry and GSK-7975A

As non-excitable cells, PAC are known to utilise the process of SOCE to allow for refilling of the ER organelle store after it has been depleted by release of Ca^{2+} induced by secondary messengers (Krause et al. 1996). This process is required to refill the store as not all of the Ca^{2+} released from the ER is taken back up into its lumen via SERCA pumps (Ponnappa et al. 1981), but instead is either taken up by other organelles (Okorokov et al. 2001) or transported outside the cell by the PMCA and NCX (Muallem et al. 1988).

The loss of Ca^{2+} from the ER lumen is detected by the protein STIM1 (Liou et al. 2005); which at resting $[Ca^{2+}]_l$ binds Ca^{2+} to its lumenal domain, but loses these bound ions when the $[Ca^{2+}]_l$ is depleted by secondary messenger-induced release. When STIM1 loses its bound Ca^{2+} it oligomerizes (Luik et al. 2008), inducing a conformational change in the protein (Zhou et al. 2013) and causes it to migrate to regions of the ER membrane that are physically close to the plasmalemma (Zhang et al. 2005). At these ER-PM puncta, STIM1 interacts with Orai1 channels in the plasmalemma (Rothberg et al. 2013) forming a CRAC channel complex and inducing the opening of these channels, allowing extracellular Ca^{2+} to enter the cell (Zhou et al. 2010). Entry of external Ca^{2+} increases the $[Ca^{2+}]_c$, allowing for refilling of the ER, increasing the $[Ca^{2+}]_l$ back to resting levels and causing Ca^{2+} to rebind to STIM1 (Soboloff et al. 2012). Once it has bound Ca^{2+} again STIM1 reverts back to its resting state, causing dissociation of the CRAC channel complex and an end to Ca^{2+} entry.

Several other types of ion channel have been shown to affect SOCE, including several members of the TRPC family located in the plasma membrane (Salido et al. 2009). It has been suggested that these channels form complexes with Orai channels where the TRPC components are activated by the Orai ones after stimulation by STIM (Liao et al. 2007). PAC isolated from TRPC3$^{-/-}$ mice showed a substantial reduction in the amount of Ca^{2+} that entered the cell upon store depletion down about 50% compared to wild type cells (Kim et al. 2009). The NAADP sensitive ion channel TPC2 has also been shown to affect SOCE in MEG01 and HEK293 cells (López et al. 2012). Knockout of TPC2, but not TPC1, reduced the rate and extent of SOCE in both cell types upon ER depletion by Tg, or stimulation of MEG01 cells by thrombin. While no co- immunoprecipitation was observed in resting MEG01 cells; after store depletion TPC2 was found to associate with both Orai1 and STIM1, while TPC1 was not. Interestingly TPC2 showed no association with TRPC1 in depleted MEG01 cells, silencing expression of this gene in MEG01 cells with ShRNA has been shown to reduce the size of the SOCE response (López et al. 2013). These results suggest that TPC2, but not TPC1, can regulate SOCE in these cell types independent of TRPC1; it also links the acidic Ca^{2+} store to a process commonly associated with only the ER store. In PAC there is evidence of two 'pools' of Orai1; a basolateral pool that interacts with STIM1 and an apical pool that interacts with IP_3R (shown by co-localization and co-immunoprecipitation of IP_3R and Orai1), with some evidence that IP_3R activation can have an inhibitory effect on SOCE. (Lur et al. 2011)

The process of SOCE is highly important in PAC, as it is the process through which the large sustained increases in cytoplasmic Ca^{2+} associated with pathological agents occurs through (Wen et al. 2015). Under physiological conditions SOCE results in refilling of the ER, causing STIM to rebind Ca^{2+} and terminate Ca^{2+} entry (Soboloff et al. 2012). In the case of

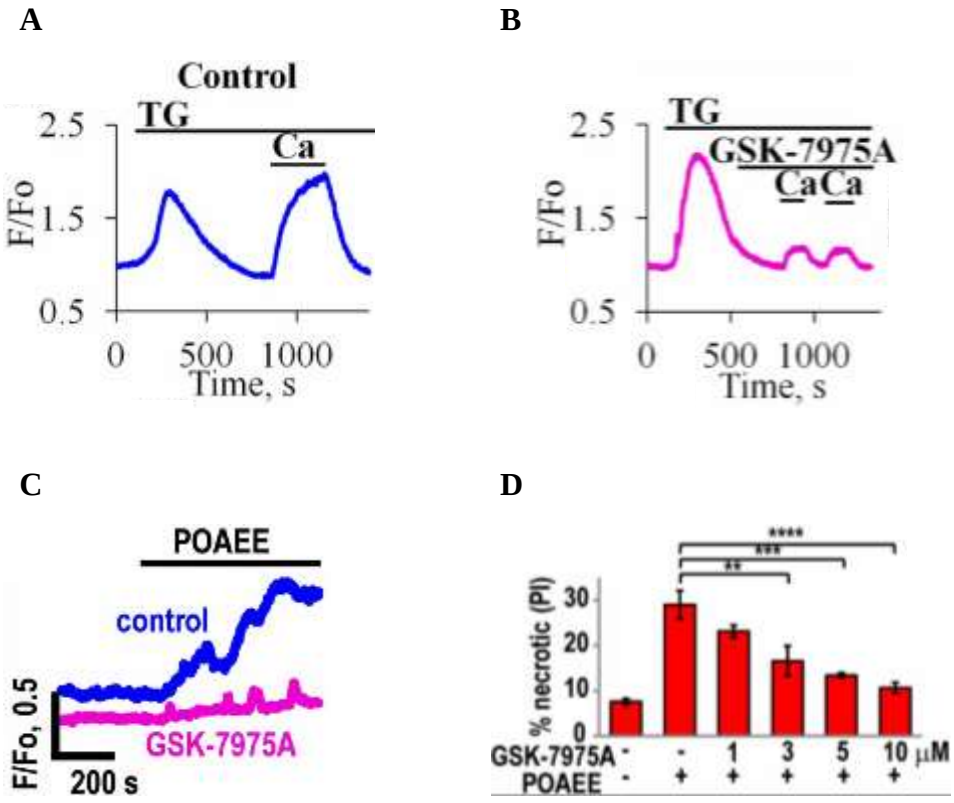

Fig. 6.1.1 The Effect of the CRAC channel blocker GSK-7975A on store-operated calcium entry in pancreatic acinar cells

(A) Representative trace of SOCE in pancreatic acinar cells after depletion of ER calcium content by Tg in calcium free conditions (n = 5). **(B)** Representative trace of SOCE in pancreatic acinar cells in the presence of 10 μM GSK-7975A after depletion of ER calcium content by Tg in calcium free conditions (n = 5). **(C)** Representative trace of intracellular calcium responses to 100 μM POAEE in pancreatic acinar cells in the absence (n = 8) or presence of 10 μM GSK-7975A (n =12). **(D)** GSK-7975A reduced the amount of necrosis induced by 100 μM POAEE (Data represents mean ± SEM; n = 3 series of experiments with the number of tested cells in each group >350). Inhibition of necrosis was significant for 3 μM GSK-7975A (***P* < 0.02) and highly significant for 5 and 10 μM GSK-7975A (****P* < 0.003 and *****P* < 0.001).

Modified under terms of free use from J Gerasimenko et al.; *PNAS*; 2013 (*Gerasimenko et al. 2013*).

bile acids, it has been shown that these pathological agents disrupt this process by preventing refilling of the ER via inhibition of SERCA pumps; either through direct interaction (Kim et al. 2002) or indirectly by disrupting ATP production (Voronina et al. 2010). Due to the involvement of SOCE in the pathogenesis of pancreatitis it had previously been suggested that this refilling pathway might prove to be a potential therapeutic target (Li et al. 2014).

Validation of this hypothesis was proven using the selective CRAC channel blocker GSK-7975A; which blocks Ca^{2+} entry by inhibiting Orai1 channels (Derler et al. 2013; Rice et al. 2013). Gerasimenko et al. found that this compound blocked Ca^{2+} entry in PAC induced by both Tg (*Fig. 6.1.1A-B*) and the pathological agent palmitoleic acid ethyl ester (POAEE) (*Fig. 6.1.1C*) in a dose-dependent manner (Gerasimenko et al. 2013). POAEE is a fatty acid ethyl ester; metabolite products of fatty acids and ethanol that have been shown to induce AP (Criddle et al. 2004). The inhibition of SOCE by GSK-7975A was enough to provide a protective effect against POAEE (*Fig. 6.1.1D*), with concentrations above 3 µM having a significant effect and 10 µM reducing the amount of necrosis observed to a level not significantly different from the control (Gerasimenko et al. 2013). Further confirmation was provided by Wen et al.; who used GSK-7975A and another CRAC channel blocker CM_128 to show similar reductions in SOCE by both TLC-S and of supramaximal concentration of CCK (Wen et al. 2015). Additionally, they tested the effects of these compounds against 3 different models of AP (Bile acid, ethanol metabolite and cerulean) and found a protective effect against all three models.

6.2: The effect of the bile acid cholate on pancreatic acinar cells

As the relationship between cholate and necrosis in PAC has not been characterised it is important to find the ideal concentration of cholate to characterise its effect in them. Bile

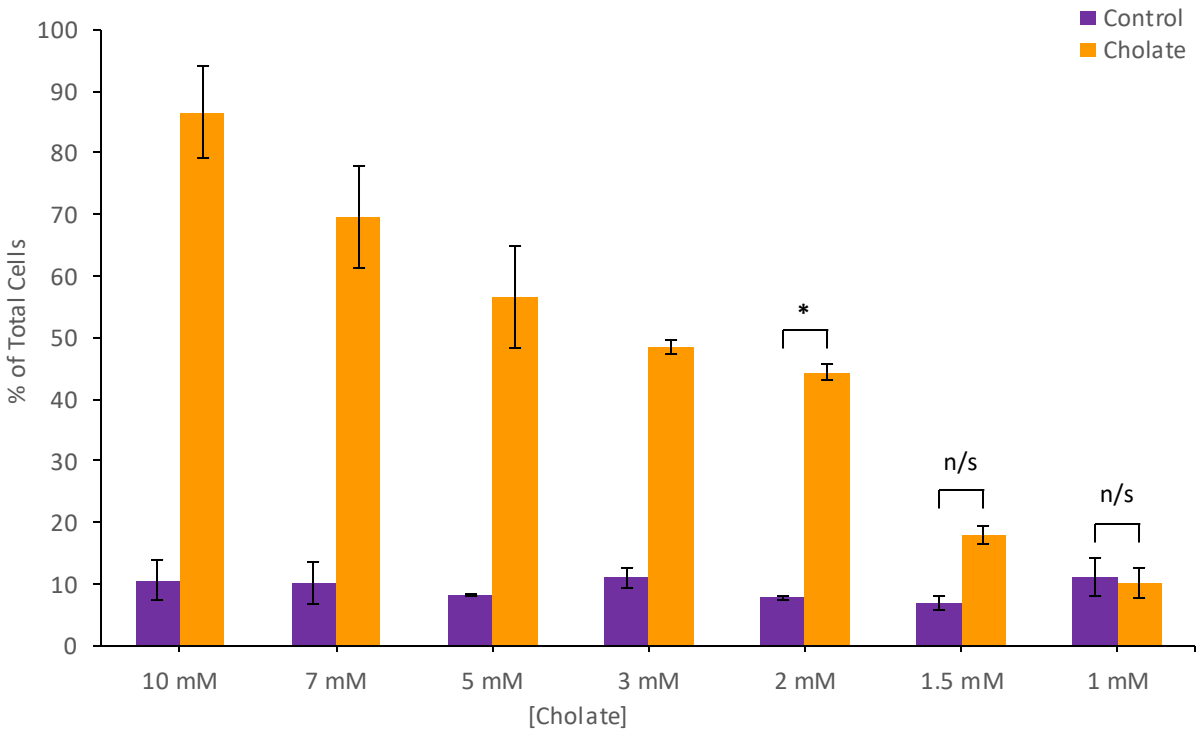

Fig. 6.2.1 Necrosis dose response to cholate by pancreatic acinar cells

Compiled results of cell death assays performed on pancreatic acinar cells treated with a varying concentration of cholate for 1 hour with their corresponding controls. Purple bars represent the number of necrotic cells as a percentage of the total number of cells counted for untreated control samples, and orange bars represent the number of necrotic cells as a percentage of the total number of cells counted when treated with a specific concentration of cholate (Data represents mean ± SEM; n = 1054 cells for 10 mM, n = 846 cells for 7 mM, n = 5305 cells for 5 mM, n = 2031 cells for 3 mM, n = 3771 cells for 2 mM, n = 4646 cells for 1.5 mM and n = 1866 cells for 1 mM; *, $P \leq 0.05$; n/s, not significant).

acids in biliary bile have been reported as reaching the low millimolar (Gerasimenko, Flowerdew, et al. 2006) range, a selection of cholate concentrations between 1 and 10 mM were tested (*Fig. 6.2.1*). The data displayed is the compiled results of multiple different experiments so each concentration of cholate is displayed with its corresponding control, which vary between 6.8 and 11.1 % necrotic cells. While the highest control value is slightly above the maximum desirable background level of 10 % necrotic cells, it is not enough to be concerned and there is no significant difference between any of the control sets of data.

A clear pattern of an increase in the concentration of cholate resulting in an increase in the amount of necrosis can be observed. 1 mM induced a comparable level of necrosis to that in its untreated control cells, 10.2 % compared to 11.1 %, which was not deemed significant by ANOVA comparison ($p > 0.999$). While increasing the cholate concentration to 1.5 mM almost doubled the amount of necrosis observed to 18.0 %, this was not deemed significant compared to its control ($p = 0.89$). A large increase was seen when the concentration was increased by another 0.5 mM to 2 mM, with 44.3 % of cells labelled with PI, an amount deemed significant to its control ($p < 0.0001$). Increasing the cholate concentration above 2 mM resulted in further increases in the amount of necrosis observed, however none of the increases were deemed as significant compared to the amount of necrosis in the previous concentration used.

The ideal amount of necrotic cells for these experiments is between 30 and 40% of the total cells counted. A level of necrosis below this might mean any reduction caused by a pharmacological agent is not large enough to be deemed significant as the positive control is too similar to the negative control (as was seen in *Fig. 4.2.4.B*). Alternatively, an excessive amount of necrosis may produce in unspecific effects or occur too rapidly for a pharmacological agent to have a protective effect. The results for both 2 mM and 1.5 mM

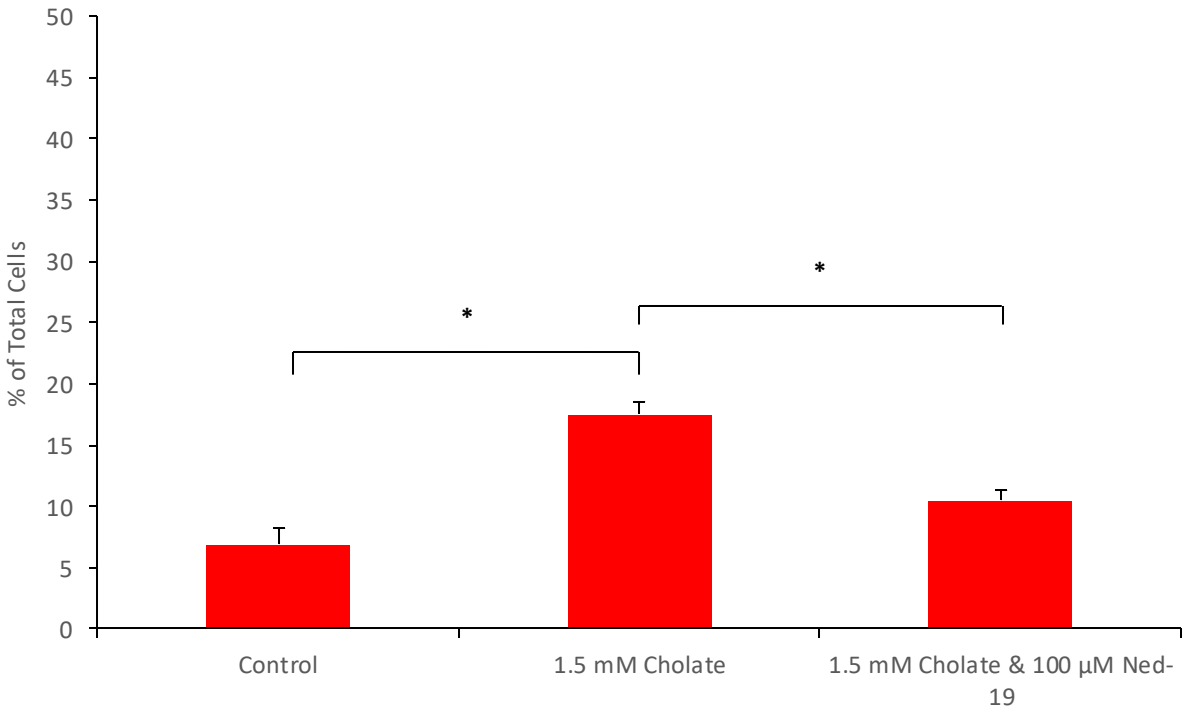

Fig. 6.2.2 Effect of Ned-19 on cell death in acinar cells induced by 1.5 mM Cholate

The results of cell death assays performed on pancreatic acinar cells treated with 2 mM cholate with and without 100 µM Ned-19 for 1 hour. Data represents the number of necrotic cells as a percentage of the total number of cells counted for that specific treatment (Data represents mean ± SEM, n = 6742 cells; *, $P \leq 0.05$).

cholate are outside of this range, with the level of necrosis induced by 1.5 mM 12 % below the lower bound and 2 mM 4.3 % above the upper bound. As neither concentration was within the desired range the effect of 100 µM Ned-19 was tested against both of them.

ANOVA comparison of the 1.5 mM cholate experiment (*Fig. 6.2.2*) deemed the response to the bile acid alone was significantly higher than the untreated control ($p = 0.0013$). When the effects of Ned-19 were tested against 1.5 mM cholate a significant reduction in necrosis was observed ($p = 0.0117$). However, when its effect was tested against 2 mM cholate (*Fig. 6.2.3*) a nonsignificant reduction was observed ($p = 0.4368$). It should be noted in these experiments the average amount of necrosis induced by 2 mM cholate was slightly lower than seen in the dose response experiments; down to 38.9 % of the total cells counted for that treatment, a value within the desired range of necrosis.

As Ned-19 was unable to significantly reduce the amount of necrosis induced by the higher concentration of cholate the inhibitor of SOCE, GSK-7975A, was tested. SOCE is the process by which a pathological $[Ca^{2+}]_c$ is sustained in PAC after store depletion, and inhibition of this process has been shown to have a protective effect against various models of AP (Wen et al. 2015). When PAC were incubated with cholate and GSK-7975A (like with Ned-19) a reduction in necrosis was observed compared to cholate alone, however this reduction was also not deemed as significant ($p = 0.2776$).

Despite GSK-7975A not showing an additive protective effect when used in combination with Ned-19 against necrosis induced by 200 µM of the bile acid TLC-S, a combination of the two compounds was tested against 2 mM cholate. When used in combination a lower level of necrosis was observed compared to either GSK-7975A or Ned-19 alone, down to 18.62 ± 3.86 %. This reduction was deemed significant compared to cholate alone ($p = 0.0496$) unlike when either of the compounds were used separately. Despite the amount of

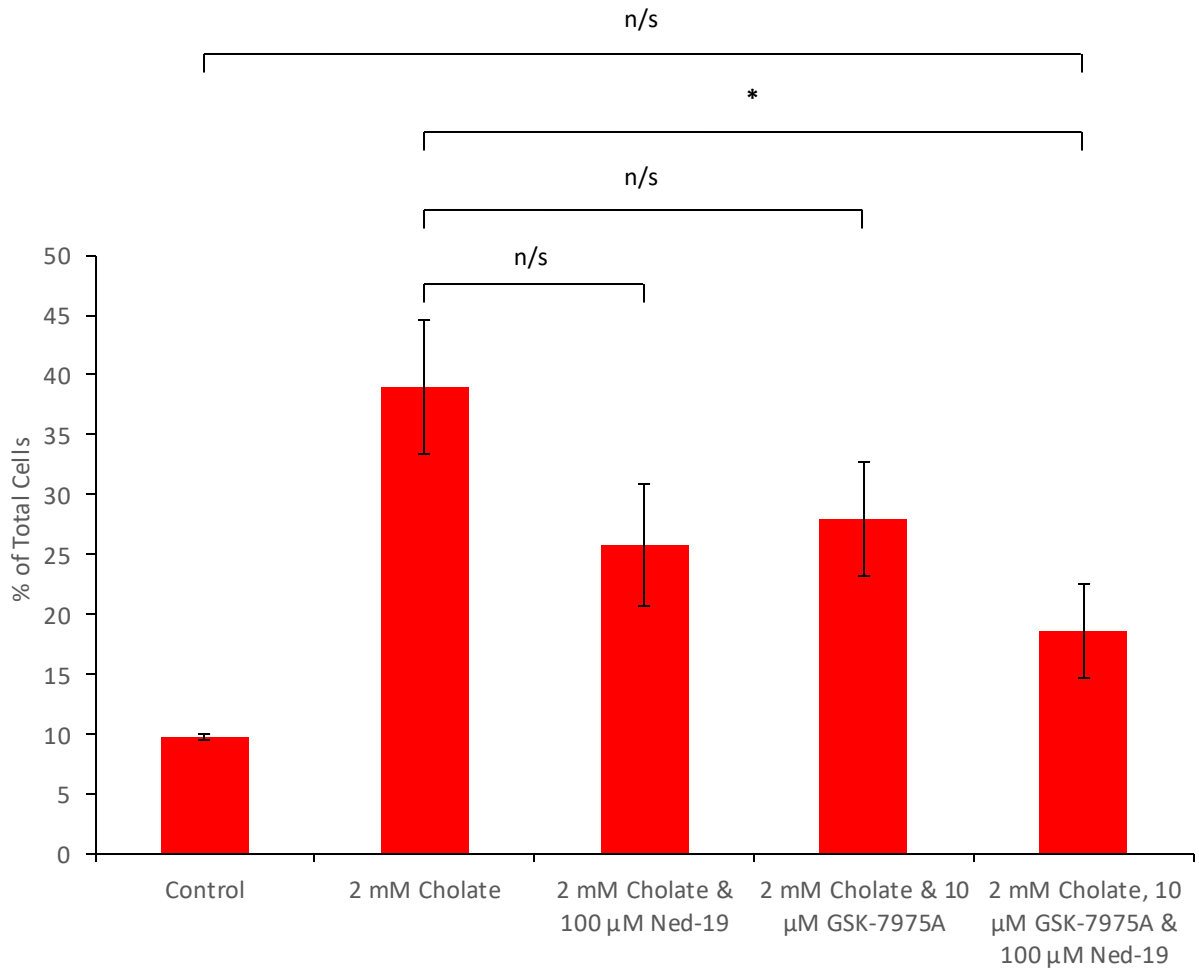

Fig. 6.2.3 Effect of Ned-19 and GSK-7975A on cell death in acinar cells induced by 2 mM Cholate

The results of cell death assays performed on pancreatic acinar cells treated with 2 mM cholate, 100 µM Ned-19 and/or 10 µM GSK-7975A for 1 hour. Data represents the number of necrotic cells as a percentage of the total number of cells counted for that specific treatment (Data represents mean ± SEM, n = 7675 cells; *, $P \leq 0.05$; n/s, not significant).

necrosis being about double that seen in the control of 9.77 ± 0.21 %, this difference was not deemed significant by ANOVA comparison ($p = 0.6204$).

To visualise the protective effects of using a combination of Ned-19 and GSK-7975A, imaging experiments were performed with conditions similar to those in the necrosis experiments. PAC were either perfused with NaHEPES solution for 15 min and then 2 mM cholate for the same hour period of the necrosis experiments; or pre-treated for 15 min with 100 µM Ned-19 and 10 µM GSK-7975A, then continued to be exposed to these compounds as well as 2 mM Cholate for an hour. Additionally, some control experiments were performed where cells were perfused with NaHEPES for 75 min. After some of the experiments Propidium Iodide was added to the cells and the number of necrotic and viable cells calculated.

In all 18 of the recorded cells exposed to Cholate alone (*Fig. 6.2.3A*) there was a large increase in $[Ca^{2+}]_c$ followed by a rapid decrease below the baseline (believed to be the result of the loss of plasmalemma integrity). The onset of this phenomenon differed between cells, varying between about 20 and 55 min after the addition of the bile acid. While it was also seen in the majority of the recorded cells also treated with Ned-19 and GSK-7975A (*Fig. 6.2.3B*), it was not observed in a third of them (8 out of 25 cells). In the cells it did occur in, it was only observed in the final 10 minutes of the recording; suggesting that while the combination of compounds might not have prevented cell death in all of the cells observed, it may have delayed it in those cells. Of the 9 observed control cells, none displayed the rise and loss of fluorescence seen in all of the cells exposed to cholate alone, implying that it is caused by the bile acid and not the cells being exposed to the light source for that time period.

After imaging, when the amount of necrosis was calculated by addition of Propidium Iodide (*Fig. 6.2.3C*), the bile acid alone was observed to induced a significantly higher amount of

A

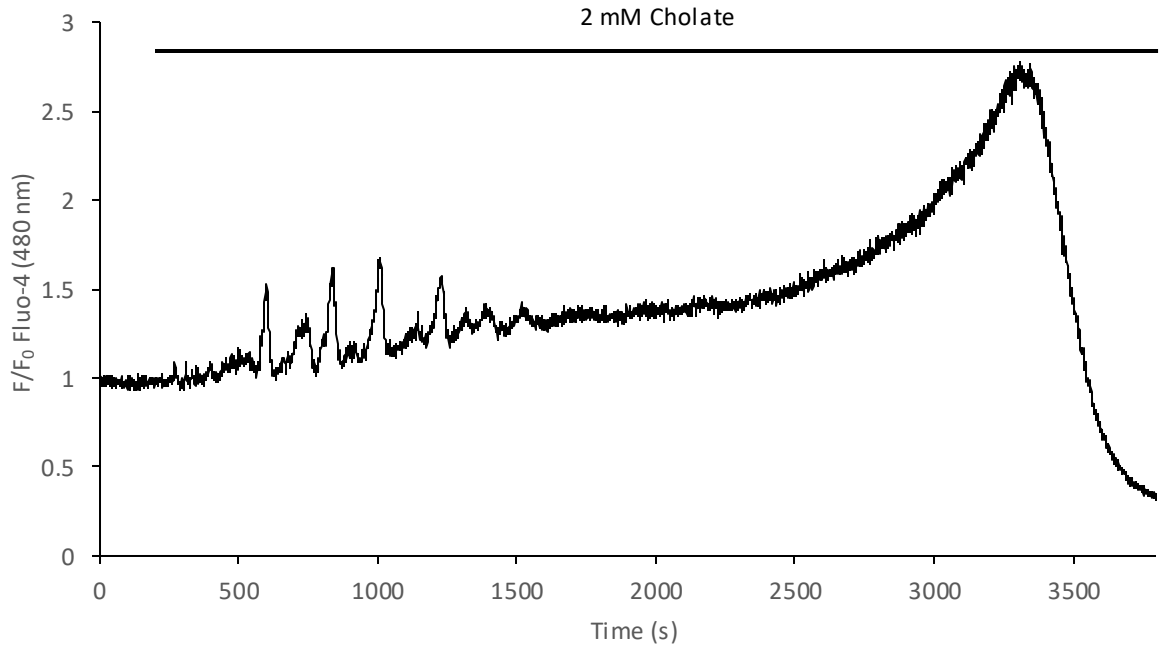

B

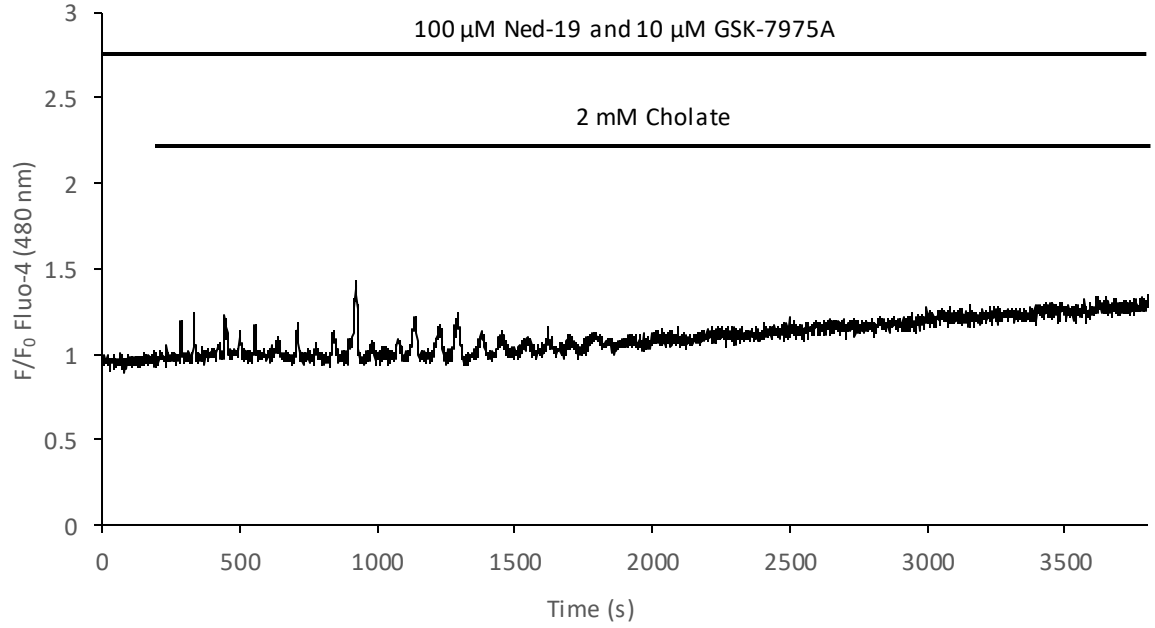

Fig. 6.2.4 The effect of 2 mM cholate on pancreatic acinar cells

(A) Representative trace of the effect of 2 mM cholate on cytoplasmic calcium in pancreatic acinar cells. **(B)** Representative trace of the effect of 2 mM cholate on cytoplasmic calcium in pancreatic acinar cells in the presence of 100 µM Ned-19 and 10 µM GSK-7975A.

C

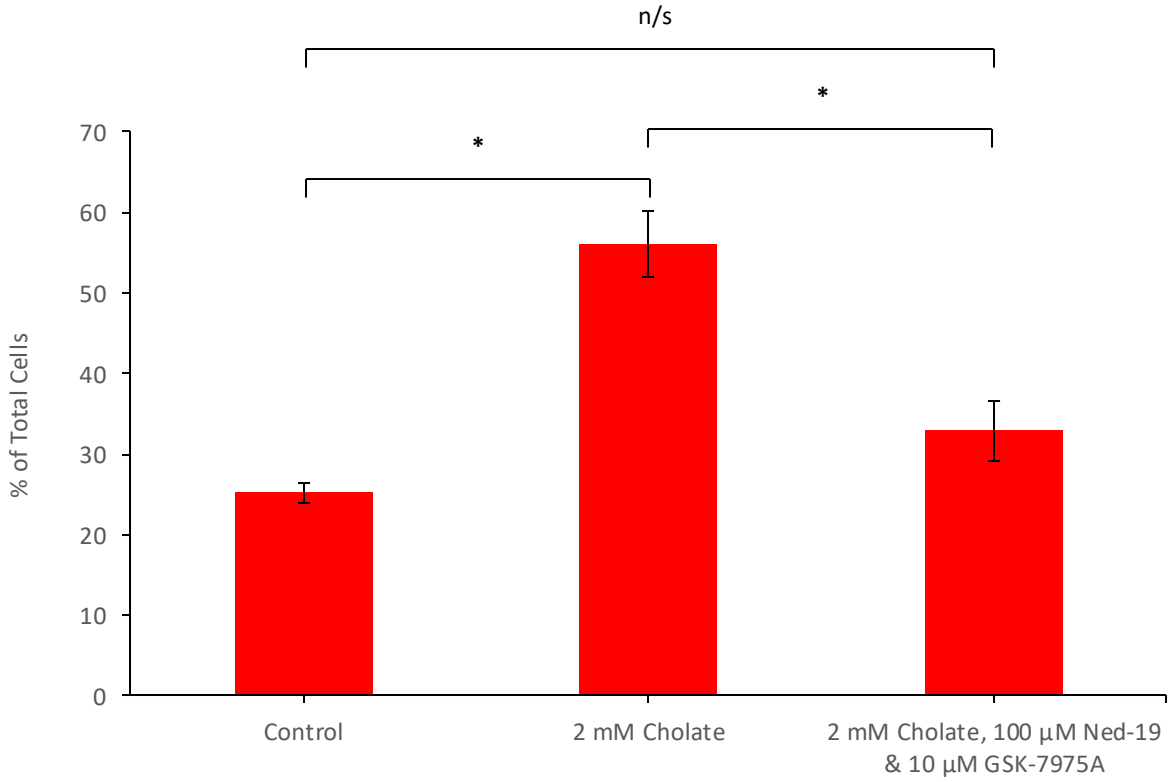

Fig. 6.2.4 (*continued)*

(C) The results of cell death assays performed on pancreatic acinar cells after imaging by the addition of 2 µM PI, during imaging cells were exposed to 2 mM Cholate in the presence or absence of 100 µM Ned-19 and 10 µM GSK-7975A for 1 hour. Data represents the number of necrotic cells as a percentage of the total number of cells counted for that specific treatment (Data represents mean ± SEM, n = 3562 cells; *, $P \leq 0.05$; n/s, not significant).

necrosis than either the control or when also exposed to Ned-19 and GSK-7975A. While the amount of necrosis was higher in the cells treated with cholate, Ned-19 and GSK-7975A than the untreated control cells; there was no significant difference between the two sets of cells ($p = 0.292$).

6.3 Discussion

While various bile acids have been shown to induce increases in cytoplasmic Ca^{2+} in PAC and/or their death (Kim et al. 2002; Voronina et al. 2002), the effect of cholate on them has yet to be characterised. Like other bile acids, cholate was also found to induce necrosis in PAC. However, this required a concentration in the millimolar range rather than the 100 micromolar range for the better characterised bile acid TLC-S. As TLC-S is a derivative of cholate it would suggest the chemical modifications that changes cholate's structure into TLC-S's increases the potency of its effect on PAC.

The lowest concentration of cholate tested, 1 mM, showed no effect on the amount of necrosis compared to the untreated control. While increasing the cholate concentration to 1.5 mM doubled the amount of necrosis, this was not deemed significant compared to its control. Another increase of 0.5 mM to 2 mM had a similar effect, roughly doubling the amount of necrosis; while further increases in the concentration of cholate increased the number of necrotic cells counted, none of these increases was as dramatic. This suggests that there is a narrow range between 1 and 2 mM of cholate where the bile acid becomes toxic to PAC. Based on the well characterised effects of another bile acid, TLC-S; it will be in this concentration range that cholate changes from inducing harmless transient changes in $[Ca^{2+}]_c$ to a pathological sustained increase.

For experimental purposes a desired amount of necrosis is between 30 % and 40 % of the total cells when studying the effects of pharmacological agents. In the cholate concentration response results (*Fig. 6.2.1*) none of the concentrations tested produced an amount of necrosis within the desired range. With 1.5 and 2 mM cholate producing values either side of the desired range, Ned-19 was tested against both of them. While Ned-19 reduced the amount of necrosis induced by concentrations of cholate it was only deemed significant when used against the lower concentration (which in this incidence induced a significant increase in necrosis compared to its control). It is possible that while 100 µM Ned-19 is a high concentration of the compound, it might not be sufficient to significantly inhibit the effects of cholate at higher concentrations. Alternatively, at higher concentrations the NAADP-independent effects of cholate could be enhanced, minimising the Ned-19's ability to inhibit them. Therefore, it could be useful to test the effect of higher concentrations of Ned-19 against 2 mM cholate to see if they have a significant protective effect.

With Ned-19 showing no significant reduction against the necrotic effect of 2 mM cholate the effects of GSK-7975A were tested. Similar to Ned-19, GSK-7975A produced a nonsignificant reduction in cholate-induced necrosis. Like with Ned-19 it would be useful to test higher concentrations of GSK-7975A to discover if 10 µM is a sub-optimal concentration of the compound.

While inhibiton of either NAADP-induced Ca^{2+} release or SOCE alone by Ned-19 or GSK-7975A respectively did not produce a significant reduction in necrosis, applying both both compounds together did produce a significant protective effect. These results could suggest that when used alone, neither compound was applied at a sufficient concentration to prevent the $[Ca^{2+}]_i$ from reaching cytotoxic levels in enough cells to significantly reduce the amount of necrosis observed. Alternatively, it could indicate that the inhibition of multiple elements

of the cell's 'Ca^{2+} signalling toolkit' is required to sufficiently protect PAC against cholate-induced necrosis. If use of increased concentrations of either Ned-19 or GSK-7975A alone has no increased inhibitory effect on cholate-induced necrosis it would suggest that a 'multidrug' approach is required. Under such circumstance the response of either Ned-19 or GSK-7975A and inhibitors for other elements of Ca^{2+}, e.g. caffeine to block IP_3 sensitive Ca^{2+} release (Wakui et al. 1990), should be tested as may have greater protective effect than the combination of Ned-19 and GSK-7975A.

When Ned-19 and GSK-7975A were used together against 200 µM TLC-S, they showed no additive protective effect against the amount of necrosis induced compared to either of them individually. However, the combination of Ned-19 and GSK-7975A did show an additive protective effect against 2 mM cholate. This could be due the lower level of necrosis seen in the positive controls (when the bile acids were used alone) for TLC-S compared to cholate. As Ned-19 alone was enough to significantly reduce the necrotic effect of TLC-S, it might reduce the amount of Ca^{2+} released in response to TLC-S below that required to trigger SOCE, which in turn would mean GSK-7975A would have no additional protective effect. This implies that either 100 µM Ned-19 is not a sufficient concentration to achieve a similar effect against 2mM cholate; or that at this concentration of bile acid there is NAADP-independent Ca^{2+} release occurring, which is sufficient to initiate SOCE. Testing if higher concentrations of Ned-19 can significantly reduce the amount of necrosis induced by 2 mM cholate (like 100 µM Ned-19 did against 1.5 mM cholate) could help resolve which of these possibilities is true. It may also be interesting to see if 100 µM of Ned-19 still has a significant protective effect against a higher concentration of TLC-S that induces a comparable amount of necrosis to 2 mM cholate; and if not if addition of 10 µM GSK-7975A has an additive effect.

Fluorescent Ca^{2+} imaging was used to corroborate the findings of the initial necrosis experiments and give a greater idea of the pattern of cholate-induced cell death. The majority of cells recorded initially showed an oscillatory pattern in response to cholate reminiscent of physiological secretagogue-induced signalling. This signalling was not inhibited by the combination of Ned-19 and GSK-7975A, though did appear to be reduced in size. The pattern of this Ca^{2+} response suggests that it is the result of the release of Ca^{2+} from organelle stores via secondary messenger's pathways and its, at least partial, insensitivity to Ned-19 suggests an NAADP-independent component to this release. As such characterising whether this component is either IP_3 and/or cADPR sensitive would aid in identifying inhibitors that could be used in combination with Ned-19 and/or GSK-7975A to provide a more effective inhibition of cholate-induced necrosis of PAC.

Within the hour exposure to 2 mM cholate alone, all of the cells whose Ca^{2+} responses were recorded showed a clear loss of plasma membrane integrity characteristic of a cell dying. This pattern was also observed in two thirds of the cells recorded when Ned-19 and GSK-7975A were also present. As GSK-7975A has a protective effect against cholate it is likely that the death observed is the result of a sustained cytotoxic concentration of Ca^{2+} occurring via SOCE. This would have several pro-necrotic effects, such as the opening of the mPTP and disruption of ATP production via loss of the inner mitochondrial membrane's potential.

Addition of 6 µM PI post-imaging allowed for the number of necrotic cells to be counted. The same pattern as the initial necrosis experiments was observed, though with a roughly 15 % higher average amount of necrosis for all treatments. This confirmed the previous necrosis results; but demonstrated one of the drawbacks of the preparation used, the time dependence of its use. From the time the PAC cells are isolated their quality declines, limiting its use to a few hours. As the number of necrotic cells in the imaging experiments were counted one to

two hours later than those in the initial necrosis experiments the extra necrosis observed was a result of this phenomenon.

As TPC2 has been shown to affect SOCE in some cell types (López et al. 2012) it would be interesting to see if PAC isolated from TPCN2$^{-/-}$ mice show reduced levels of Ca^{2+} entry in response to store depletion compared to wild type cells. If this was the case these knockout cells might have an additional resistance to cholate induced necrosis, at least at lower concentrations of the bile acid due to the reduced amount of Ca^{2+} entry occurring in them.

Together with the results for the bile acid TLC-S this work demonstrates that inhibition of NAADP-sensitive Ca^{2+} release by the NAADP antagonist Ned-19 can have a protective effect in a cellular model of biliary AP. Testing its protective potential against the necrotic effects of other bile acids, especially those derived from the other initial bile chenodeoxycholic acid rather than from cholate, would help strengthen this conclusion. As would testing if it can inhibit other forms of necrosis, most notably ethanol and its metabolites like fatty acid ethyl esters. Additionally, progression from cellular models of the disease to animal models would demonstrate if Ned-19 has future clinical applications.

CHAPTER 7:

THE SYNTHETIC NAADP ANTAGONIST BZ194 SHOWS NO EFFECT IN PANCREATIC ACINAR CELLS

Chapter 7: The synthetic NAADP antagonist BZ194 shows no effect in pancreatic acinar cells

7.1: Overview of BZ194

The intracellular secondary signalling molecule NAADP has been shown to induce the release of Ca^{2+} from intracellular stores in a wide range of both mammalian (G. C. Brailoiu et al. 2009; Aley et al. 2010; Sánchez-Tusie et al. 2014) and non-mammalian cells (Galione et al. 2000; Navazio et al. 2000). It is structurally identical to its chemical precursor NADP other than the substitution of a nicotinic acid moiety for a nicotinamide one (Aarhus et al. 1995), this exchanges an amide anion for a hydroxide anion (*Fig. 7.1.1*). This change reduces the molecule's net charge by -1 down to -4 and confers the Ca^{2+} mobilising activity that NADP lacks; implying the nicotinic acid moiety is the key structural requirement for NAADP's activity (Lee and Aarhus 1997).

It is known that high concentrations of NAADP are auto inhibitory in mammalian cells, exhibiting a bell-shaped response curve (Berg et al. 2000). Additionally, coapplication of nicotinic acid with NAADP via microinjection into T cells, greatly reduces the increase in $[Ca^{2+}]$ observed; an effect lacking when nicotinamide instead is coapplied (Dammermann et al. 2009). Together these results imply that nicotinic acid, either as a molecule or as a moiety in NAADP, is producing this inhibitory effect. However due to their polar nature both NAADP and nicotinic acid have a low membrane permeability, limiting their use as pharmacological agents in research.

Dammermann et al. decided to design a small molecule inhibitor of NAADP's activity (Dammermann et al. 2009) using nicotinic acid as a lead compound rather than NAADP itself due to its lower net charge (-1 compared to -4). They performed a screen of a library of

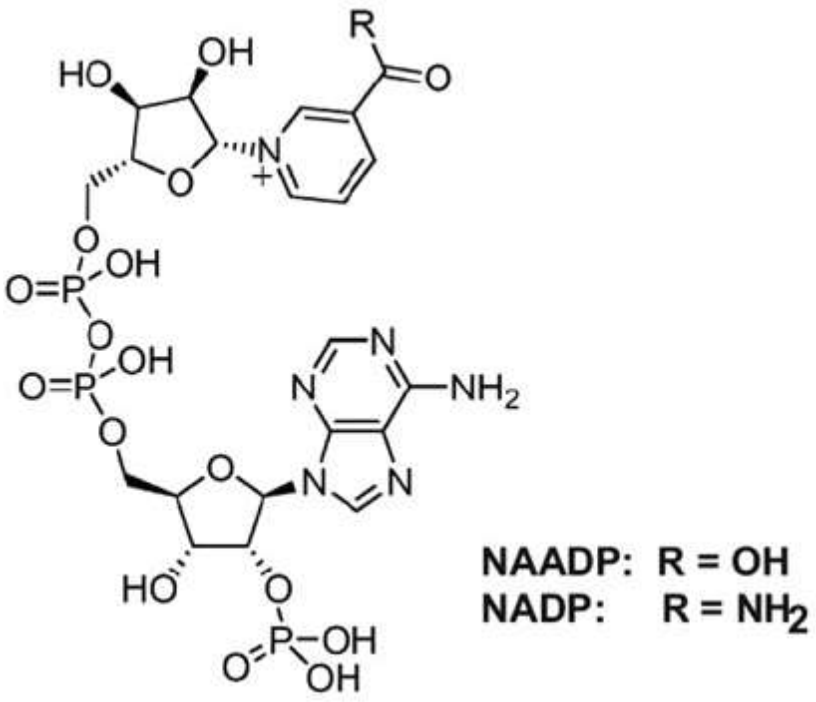

Fig. 7.1.1 Structures of NAADP and NADP

The skeletal formulas of the dinucleotides NAADP and NADP.

Reproduced under terms of free use from W Dammermann et al.; *PNAS*; 2009 (Dammermann et al. 2009).

alkylated nicotinic acid derivatives, examining their ability to block T-cell proliferation (a measure of their activation, which is regulated by NAADP signalling). This identified a *N*-alkylated 8-carbon side chain derivative of nicotinic acid as the most efficient antagonist of effector T cell proliferation. The compound (*Fig. 7.1.2A*), 3-carboxyl-1-octylcarbamoylmethyl-pyridinium (BZ194), when coinjected with NAADP was able to reduce the increase in $[Ca^{2+}]_c$ observed in a concentration-dependent manner (*Fig. 7.1.2B*), with an IC_{50} below 10 µM (*Fig 7.1.2C*). This effect was specific to NAADP's activity; showing no significant effect on the Ca^{2+} mobilizing capacity of either IP_3 or cADPR the other Ca^{2+} mobilizing secondary messengers (*Fig. 7.1.2D*).

As well as reducing the Ca^{2+} response to NAADP directly; BZ194 was able to reduce the increase in $[Ca^{2+}]_c$ observed in primary T cells activated by either the Myelin basic protein (MBP) antigen or by CD3 antibodies. Both the phases of the Ca^{2+} response, the initial peak and sustained plateau, were diminished when T cells were preincubated with BZ194. While only a partial reduction in the $[Ca^{2+}]_c$ upon T cell activation is observed in the presence of BZ194 (likely a result of several secondary messengers being involved in such a response, as is the case of the response to CCK in PAC (Cancela 2001)), this reduction is enough to suppress several downstream events of Ca^{2+} signalling in T cells. Both nuclear translocation of nuclear factor of T cells" (NFAT) and antigen-induced production of interleukin-2 was significantly reduced when BZ194 was present, restimulation of cells after removal of the compound resulted in expression of the cytokine. A similar effect was observed on T cell proliferation; preincubation with BZ194 before stimulation suppressed proliferation, removal and reapplication of an antigen resulted in a normal response.

Previously, the group had shown that NAADP increased binding of [^{3}H]ryanodine to purified RyR1 receptors (the binding of which is proportional to channel opening). BZ194 showed no

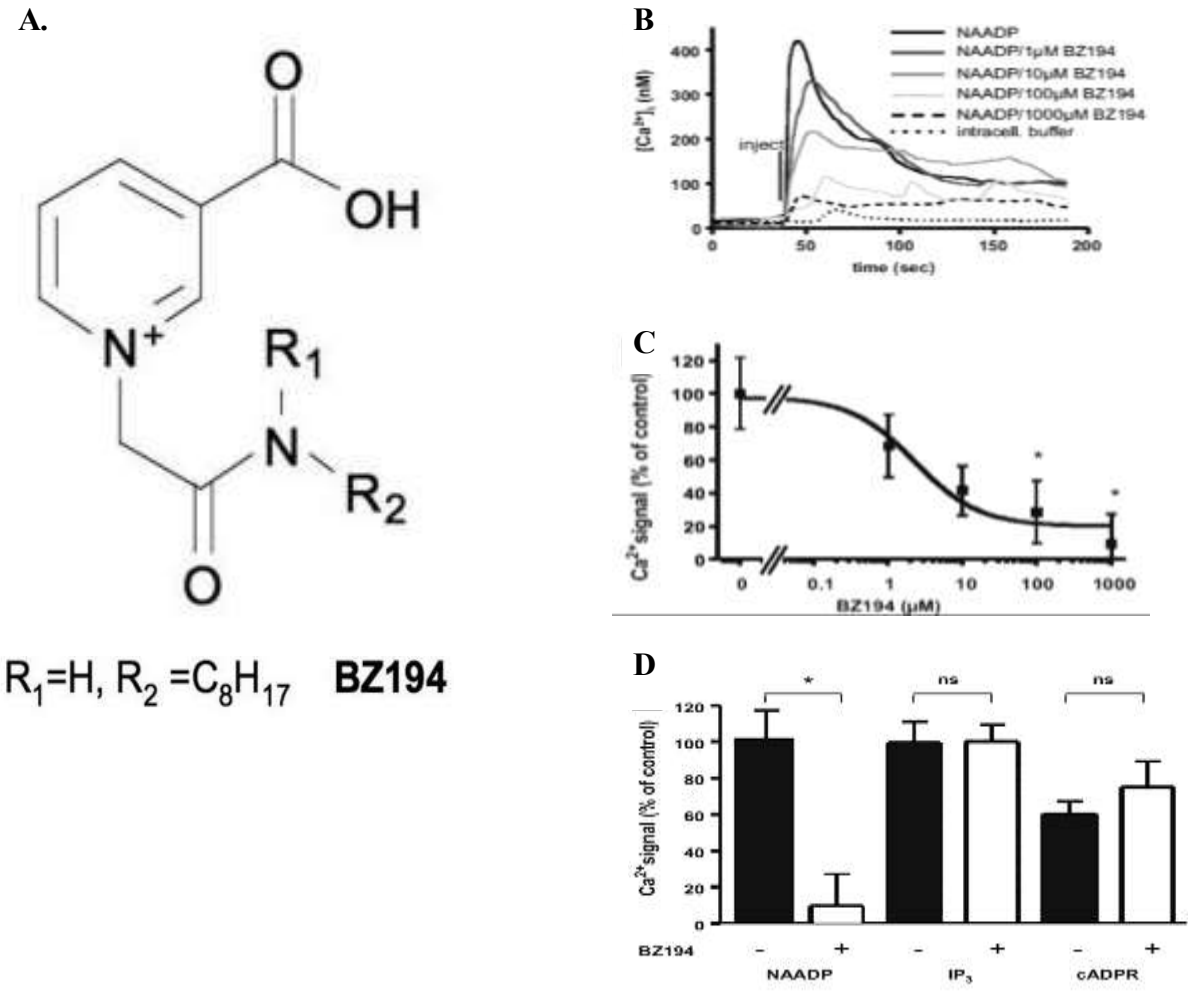

Fig. 7.1.2 Structure of BZ194 and its effect on NAADP signalling

(A) The skeletal formula of the shared structure used in Dammermann et al.'s screen of nicotinic acid analogues and variable groups for BZ194. **(B)** Inhibition of Ca^{2+} signals induced by coinjection of 100 nM NAADP in Jurkat T cells with a variable concentration of BZ194, traces represent the mean data of 5-13 experiments. **(C)** Concentration-response curve of NAADP-induced $[Ca^{2+}]_c$ with BZ194 (mean ± SEM, n = 5-13; *, $P \leq 0.05$). (D) Effect of NAADP (100 nM), IP_3 (4 µM) or cADPR (100 µM) microinjection on Jurkat T cells with or with coapplication of 1 mM BZ194 (Data represents mean ± SEM, n = 5-13; *, $P \leq 0.05$; ns, not significant).

Modified under terms of free from W Dammermann et al.; *PNAS*; 2009 (Dammermann et al. 2009).

ability to disrupt basal binding of [^{3}H]ryanodine to the receptor, but did block the increased binding induced by NAADP. This effect is also concentration-dependent, with a comparable IC_{50} value to its ability to block NAADP induced Ca^{2+} release. As BZ194 was observed promoting the dissociation of NAADP, but not [^{3}H]ryanodine from reactivated RyR1, it is most likely via allosteric regulation.

Together this work showed that BZ194 is a cell permeable specific inhibitor of NAADP's Ca^{2+} releasing activity via RyR1. Subsequently it has been used in several studies to examine NAADP's role in cellular processes; including experimental autoimmune encephalomyelitis (Cordiglieri et al. 2010), isoproterenol-induced cardiac arrhythmias (Nebel et al. 2013), and T cell shape and migration (Nebel et al. 2015). However, Ali et al. found BZ194 had no effect on the proliferation of naïve CD4 T Cells, but Ned-19 did (Ali et al. 2016); and suggested that BZ194 effect may be cell specific.

Another study by Ali et. al showed that co-injection of 100 µM BZ194 with NAADP into SKBR3 cells diminished Ca^{2+} responses compared to NAADP alone (Ali et al. 2014), but had no effect on either NAADP-induced Ca^{2+} release or NAADP binding in sea urchin egg homogenate. They also found no effect of Ned-19 on NAADP's activity and binding in the homogenate; directly contradicting previous findings in this model, showing Ned-19 affecting both (Naylor et al. 2009). While Ali et al. concluded this shows a difference in specificity between human and urchin NAADP receptors for BZ194, the Ned-19 urchin results do raise doubts about the validity of this conclusion.

As well as disrupting NAADP's ability to release Ca^{2+} via RyR's, BZ194 could have an additional effect on NAADP signalling by affecting its synthesis. NAADP is produced as part of an intracellular signalling cascade in response to a cell receiving an external stimulus (Cosker et al. 2010). It is synthesised from NADP and nicotinic acid via a base-exchange

catalysed by the enzyme CD38. As BZ194 is based on the structure of nicotinic acid, it could potentially compete with nicotinic acid in CD38's binding site, blocking the base-exchange with NADP due to the extra acyl group present on BZ194.

The ability of RyR's to act as NAADP sensitive Ca^{2+} channels has been disputed, due to both their ER/SR subcellular location in most cells and some experimental evidence (Copello et al. 2001; Wagner et al. 2014). However there is compelling evidence that it can do so both in isolation (Mojžišová et al. 2001; Hohenegger et al. 2002) and in whole cells (Gerasimenko et al. 2003; Mitchell et al. 2003; Steen et al. 2007).

It was recently suggested in PAC that NAADP-induced Ca^{2+} release can occur by either TPC and RyR channels (Gerasimenko et al. 2015), with disruption to either type of channel resulting in a large reduction in the size of the Ca^{2+} response to NAADP. As PAC have been shown to mobilize Ca^{2+} (at least in part) via RyR's, with RyR1 providing the bulk of this response, it is likely that BZ194 should have an inhibitory effect on NAADP signalling in PAC.

7.2: The effect of BZ194 in pancreatic acinar cells

5 pM CCK was applied to intact PAC to induce a typical oscillatory Ca^{2+} response and then a high inhibitory concentration of BZ194 (Dammermann et al. 2009) was applied acutely to the cells, as previously done with Ned-19 (Gerasimenko et al. 2015). After 300 s of CCK alone, BZ194 was added in the continued presence of CCK for 300 s. Addition of BZ194 appeared to cause a small reduction in the amplitude of the Ca^{2+} oscillations observed (*Fig. 7.2.1A*); but not a total inhibition, like that observed for Ned-19. The average area under the trace was calculated for the two 300 s periods that CCK was applied to the cells with and without

A

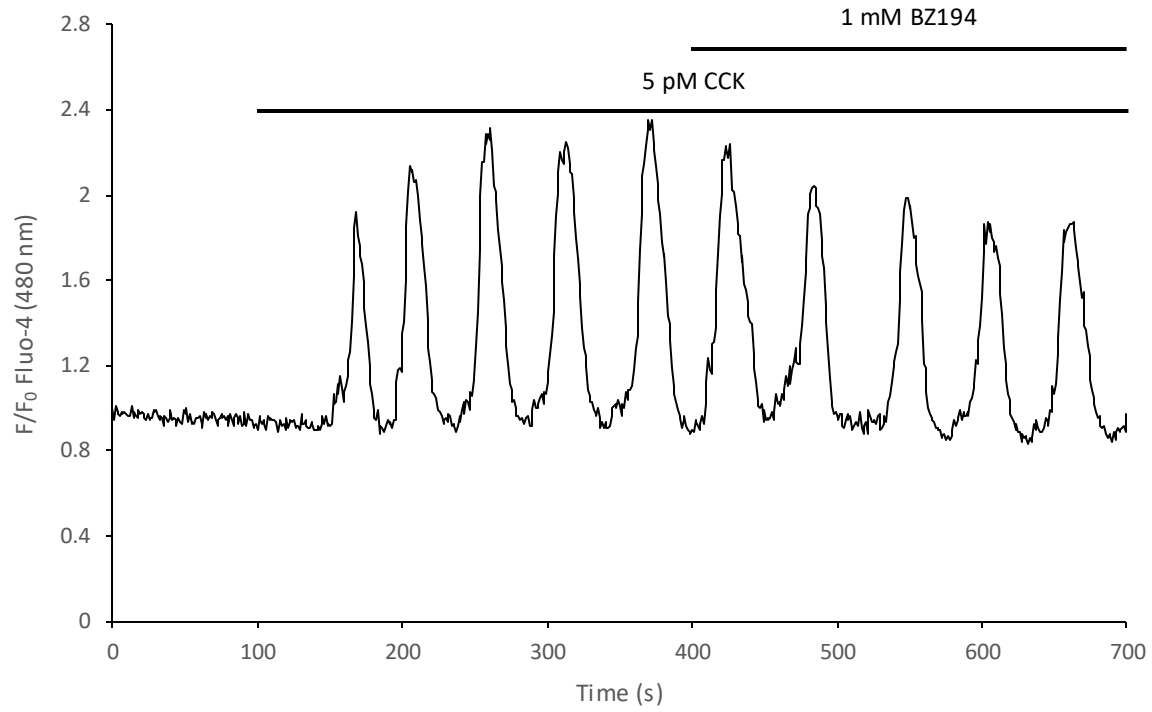

B

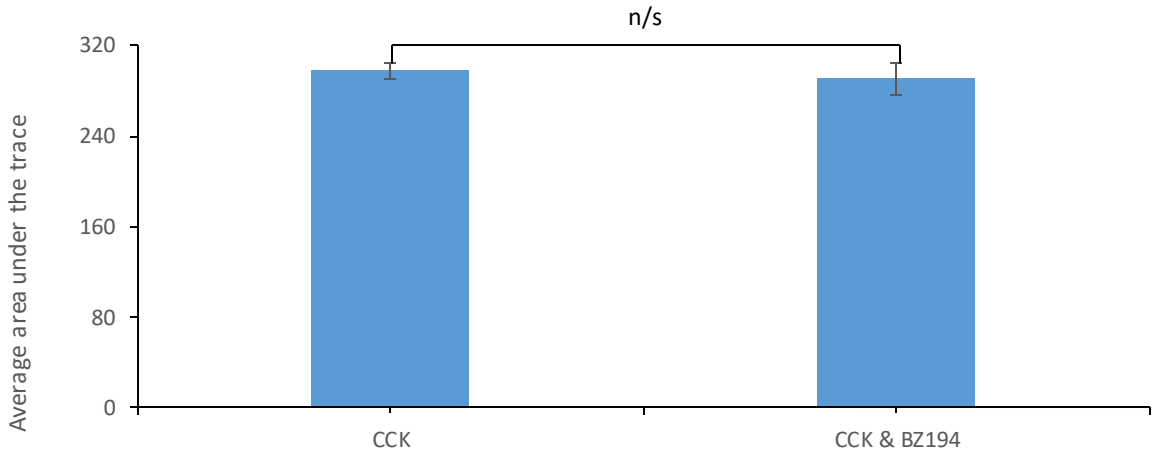

Fig. 7.2.1 The effect of BZ194 on CCK induced calcium oscillations in pancreatic acinar cells

(A) Representative trace of the effect of 1 mM BZ194 on the CCK response in pancreatic acinar cells. **(B)** Bar Chart showing the average area under the trace for the cells sampled; either in the presence or absence BZ194. Together this data shows that BZ194 CCK between 100 s and 400 s and CCK & BZ194 between 400 s and 700s (Data represents mean ± SEM, n = 11; n/s, not significant).

BZ194 (*Fig. 7.2.1B*). While a slight reduction in response was observed after the addition of BZ194, it was deemed not significant by use of a Student's *t*-test, p = 0.63.

While BZ194 showed no ability to block the CCK-induced Ca^{2+} response when applied acutely it may affect the activity of the bile acid TLC-S, which also contains an NAADP element (Gerasimenko, Flowerdew, et al. 2006). Therefore, it was decided to test its ability to reduce necrosis in a biliary model of pancreatitis. As preincubation was required in T cells to produce the best effects with BZ194, PAC were treated for 15min with 100 µM BZ194 and then exposed to 200 µM TLC-S for 1 hour.

Compared to the untreated control cells, those exposed to TLC-S alone or TLC-S and BZ194 both showed an increase in the number of necrotic cells counted. These increases were deemed significant by ANOVA comparison, p = 0.0025 and p = 0.0028 respectively. Interestingly cells treated with 100 µM BZ194 alone for 75 min also showed an increase in necrosis above that observed in the control, however this increase was not deemed to be significant (p = 0.1913). Importantly there was no significant difference in the amount of necrosis between cells exposed to TLC-S either in the presence or absence of BZ194, p = 0.9998.

7.3 Discussion

Our understanding of secondary messenger Ca^{2+} signalling has been greatly aided by pharmacological agents that inhibit specific individual elements of signalling pathways, allowing their roles to be discerned. One such agent is the NAADP specific antagonist Ned-19, discovered based on its similarity to the 3D electrostatic structure of NAADP (Naylor et al. 2009). Due to its autofluorescence Ned-19 is known to stain lysosomes in murine

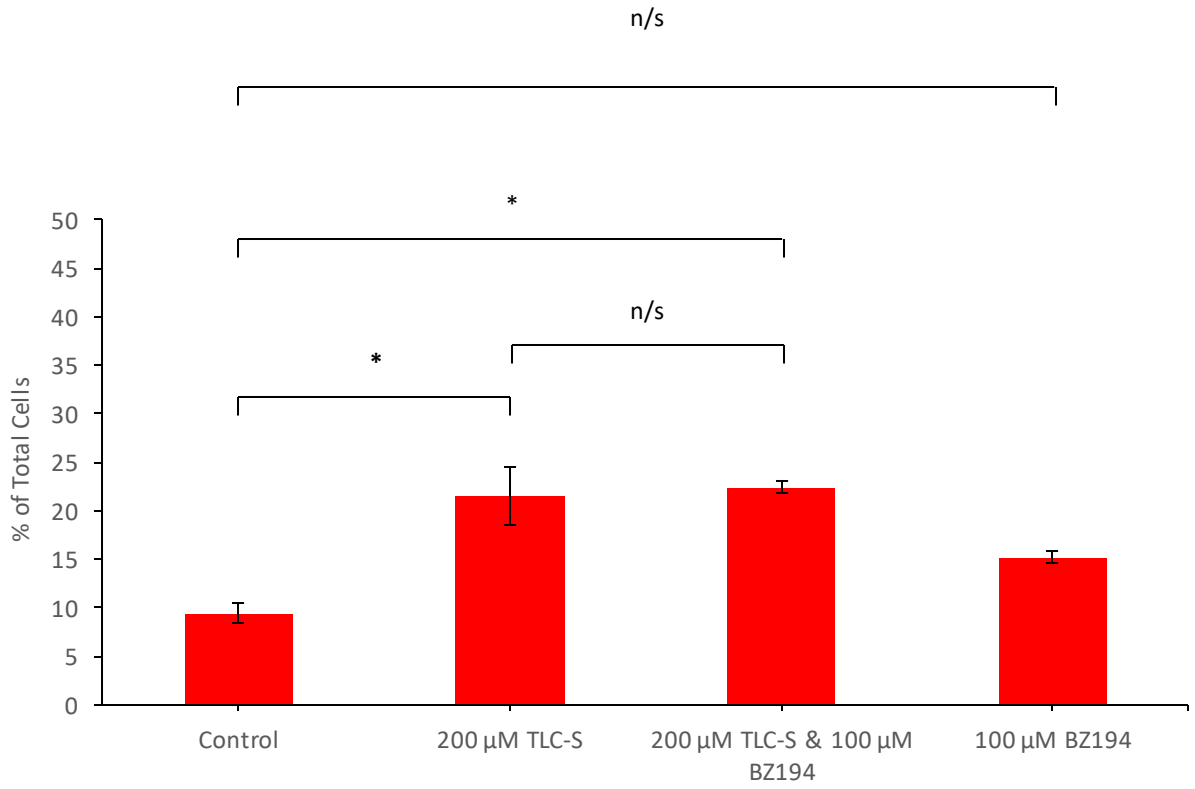

Fig. 7.2.2 Effect of BZ194 on TLC-S-induced cell death in acinar cells

The results of cell death assays performed on pancreatic acinar cells preincubated for 15 min with or without 100 µM BZ194 and subsequently treated with 200 µM TLC-S for 1 hour where applicable. Data represents the number of necrotic cells as a percentage of the total number of cells counted for that specific treatment (Data represents mean ± SEM, n = 3168 cells; *, $P \leq 0.05$; n/s, not significant).

pancreatic beta cells (Naylor et al. 2009) and colocalize with TPC1 staining on acrosomes in murine sperm (Arndt et al. 2014). It has also been used to study the gating of TPC2 channels in lipid bilayers by patch clamping (Pitt et al. 2014), displaying the ability to induce channel opening at low concentrations and inhibit opening at higher concentrations. Ned-19's ability to inhibit NAADP-induced Ca^{2+} release via RyR is unknown as no data on the matter has been published. With Ned-19 localising to organelles that do not contain RyR in their membranes and only a 67.8% inhibition of NAADP-induced Ca^{2+} release in PAC (Gerasimenko et al. 2015) (where NAADP has also been shown to mobilise Ca^{2+} via RyR (Gerasimenko et al. 2003; Gerasimenko, Sherwood, et al. 2006)) it is possible that NAADP-induced Ca^{2+} release via RyRs is insensitive to Ned-19. This possibility is supported by the crystal structure of *At*TPC1, which showed a binding site on the channel for Ned-19 (Guo et al. 2016; Kintzer and Stroud 2016). Which agrees with the finding that Ned-19 is a non-competitive antagonist (Naylor et al. 2009) of NAADP, and so may act by directly inhibiting TPC channels rather than NAADP's action on them. An alternative theory would be that as NAADP acts via binding proteins (Lin-Moshier et al. 2012; Walseth et al. 2012), it is possible that Ned-19 only affects the binding protein/proteins that are responsible for NAADP activity via TPC channels.

With 32.2% of NAADP-induced Ca^{2+} release in PAC being insensitive to Ned-19 it is important that there is a larger range of pharmacological agents capable of disrupting NAADP signalling to investigate this phenomenon. As such BZ194 might have proved an invaluable tool to investigate this and NAADP-induced Ca^{2+} release via RyR in these cells, however the experimental data shows a lack of effect in them. Unlike Ned-19, which showed the ability to cause a complete cessation of oscillations when applied acutely (Gerasimenko et al. 2015), BZ194 showed no effect on CCK-induced Ca^{2+} oscillations (*Fig. 2.2.1*). Previous

reports using BZ194 in Ca^{2+} imaging experiments either used preincubation of the compound or coapplication of it with NAADP rather than an acute application on top of a response (Dammermann et al. 2009; Nebel et al. 2013). These types of application were not tested in PAC as only its effect compared to that of Ned-19 were of interest. Preincubation of PAC with BZ194 before application of CCK might reduce or inhibit any Ca^{2+} oscillations; but would mean the compound would be of little use to treat acute pancreatitis, where it would need to have an acute effect.

Indeed, even with a 15 min preincubation BZ194 had no significant effect on the level of TLC-S-induced necrosis observed (*Fig. 2.2.2*). A longer incubation may yield a protective effect against TLC-S experimentally, e.g. a 48 h preincubation was used to suppress antigen-induced T cell proliferation (though half the concentration of the compound was applied (Dammermann et al. 2009)). However, as previously mentioned this would not be therapeutically useful as any treatment for acute pancreatitis would have to be applied to patients already experiencing an incident of the disease. Additionally, due to the steady deterioration of the preparation of PAC used, any extension of experiment time would increase the basal level of necrosis seen, which could reduce any protective effects of a longer preincubation of BZ194.

In the cell death experiments BZ194 also appeared to have a toxic effect; however, the increase in necrosis in the cells treated with BZ194 alone for 75 min compared to the untreated control was not deemed significant. Previous experiments injecting rats with concentrations of BZ194 up to 1mM for 7 days of 0.5 mM for 14 days showed no evidence of the compound being toxic (Cordiglieri et al. 2010). Preincubation with BZ194 was able to reduce the proliferation of stimulated T cells (Dammermann et al. 2009), though this effect

was attributed to it preventing their activation rather than any toxic effect (which was not tested for).

Together this work shows that BZ194 has no effect on physiological or pathological NAADP related Ca^{2+} signalling in PAC when applied acutely or after a short incubation respectively, and therefore would have little therapeutic use for acute pancreatitis. Its effect as a research tool however cannot be discounted, as further work into its effect after a longer preincubation period would be required.

CHAPTER 8:
CONCLUDING REMARKS

Chapter 8: Concluding remarks

8.1 Summary

The main aim of this study was to provide further insight into the role that NAADP-induced Ca^{2+} release plays in both pathological and physiological signalling in PAC. Of the three known intracellular secondary Ca^{2+} signalling molecules NAADP is the most recently identified (Lee and Aarhus 1995) and therefore the least well characterised. However, it has been shown to mobilise Ca^{2+} in mammalian and non-mammalian cells (Galione et al. 2000; Navazio et al. 2000), and has been shown to have a role in a diverse range of cellular processes (Barceló-Torns et al. 2011; Coxon et al. 2012; Arndt et al. 2014).

PAC were the first mammalian cell type that NAADP was shown to have Ca^{2+} mobilising activity (Cancela et al. 1999), which also linked the secondary messenger to physiological signalling by the secretory hormone CCK. Since this initial report, NAADP has been shown to mobilise Ca^{2+} in these cells from both acidic and ER stores (Gerasimenko, Sherwood, et al. 2006) as well as the nucleus (Gerasimenko et al. 2003); indicating a role for the messenger beyond just secretion of digestive enzymes. NAADP-induced Ca^{2+} release has also been shown to play a role in pathological Ca^{2+} signalling in PAC, with inhibition of this process reducing the amount of Ca^{2+} mobilized in response to the bile acid TLC-S (Gerasimenko, Flowerdew, et al. 2006).

Since these initial discoveries in PAC, two significant discoveries in the field of NAADP signalling have been made. The first was the *in silico* identification of the membrane permeable NAADP-specific antagonist Ned-19 (Naylor et al. 2009). This compound has greatly increased the ease in which the role of NAADP can be highlighted in physiological processes by blocking its activity (Esposito et al. 2011; Aley et al. 2013; Favia et al. 2016). Since the discovery of Ned-19 a second membrane permeable NAADP-specific antagonist

has been identified called BZ194 (Dammermann et al. 2009), however its effectiveness compared to Ned-19 has been questioned (Ali et al. 2016).

The second key discovery was that members of the TPC family of proteins can form NAADP-sensitive ion channels (E. Brailoiu et al. 2009; Calcraft et al. 2009; Zong et al. 2009). While both TRP-ML1 and RyR channels had previously been suggested as fulfilling a similar role (Hohenegger et al. 2002; Zhang et al. 2009), both types of channel suitability had been questioned (Copello et al. 2001; Pryor et al. 2006). A similar challenge was issued against TPC's candidacy (Wang et al. 2012; Cang et al. 2013), which instead suggested that these channels are NAADP insensitive and are instead $PI(3,5)P_2$ gated Na^+ channels regulated by mTOR. These finding have since been reconciled with TPC channels being NAADP sensitive cation channels that are also regulated by a range of factors including $PI(3,5)P_2$, cytoplasmic Mg^{2+}, their phosphorylation state, luminal pH and $[Ca^{2+}]_l$ (Pitt et al. 2010; Jha et al. 2014). Importantly it was shown that the 'TPC1/2$^{-/-}$ double knockout mice' used in the conflicting studies still expressed approximately 90% of the protein's sequence and therefore were not true TPC nulls (Ruas et al. 2015). Creation of a true TPC1/2$^{-/-}$ double knockout mouse model was used to confirm the channels' sensitivity to NAADP, which has generally been accepted since (Pereira et al. 2011; Davis et al. 2015; Sakurai et al. 2015; Nguyen et al. 2017).

As such, it was intended to use these recent developments in the field of NAAPD signalling to further characterise the role that this messenger plays in PAC. This was done by first characterising the mechanism by which it mobilized Ca^{2+} from intracellular stores in this cell type; which was shown to involve the activity of both TPC and RyR channels, with a variable dependence of the different isoforms of both types of channel. Next the key role it plays in both initiating and sustaining intracellular Ca^{2+} responses to the physiological secretagogue

CCK was demonstrate by inhibiting such responses with Ned-19. The importance of NAADP-sensitive Ca^{2+} release in pathological signalling induced by the bile acids TLC-S then highlighted, again using Ned-19. The NAADP-antagonist was able to significantly inhibit both increases in $[Ca^{2+}]_c$ and necrosis induced by TLC-S; suggesting a potential therapeutic role for the compound against AP, a condition that currently does not have a specific treatment (Johnson 2005). Unlike Ned-19, the alternative NAADP-antagonist BZ194 showed no ability to inhibit either the intracellular response to CCK or TLC-S induced necrosis. Use of Ned-19 alone was not enough to significantly reduce the amount of necrosis observed in response to another bile acid, cholate. Neither was use of the CRAC channel blocker GSK-7975A; which had previously shown to have a protective effect against several models of AP, including one induced by TLC-S (Gerasimenko et al. 2013; Wen et al. 2015). However, a combination of both Ned-19 and GSK-7975A was able to cause a significant reduction in cholate-induced necrosis, suggesting a multi-targeted therapeutic approach inhibiting several elements of the cells 'Ca^{2+} signalling toolkit' (Berridge et al. 2000) may be the best solution for the treatment of AP.

8.2 NAADP-induced calcium release from organelle stores in pancreatic acinar cells requires the involvement of both TPC and RyR channels

Since its initial discovery as a distinct intracellular secondary Ca^{2+} messenger in its own right (Lee and Aarhus 1995), NAADP has been shown to mobilise Ca^{2+} from a unique source. This was first identified when the messenger was found to mobilize some Ca^{2+} independently of the activity of Tg (Genazzani and Galione 1996). However NAADP-induced release was diminished in the presence of Tg; and similarly by inhibitors of IP_3 and cADPR induced released, while inhibitors of both completely abolished NAADP responses (Churchill and

Galione 2001). This led to the creation of the 'trigger hypothesis', where NAADP acts on a distinct Tg insensitive Ca^{2+} store to mobilize a small amount of 'trigger Ca^{2+}' which then acts via CICR on IP_3R and RyR in the ER to mobilize more Ca^{2+} from the Tg sensitive ER store, which both amplifies the overall response to NAADP and creates the Ca^{2+} oscillations consistently observed in response to the secondary messenger. This hypothesis, created using results from sea urchin eggs, was strengthened by similar findings in mammalian cells (Cancela et al. 1999) and the discovery that in sea urchin eggs NAADP mobilizes calcium from reserve granules (Churchill et al. 2002), a type of acidic organelle related to lysosomes in mammalian cells.

Since these early discoveries there has been the desire to identify the 'NAADP receptor'; hoped by many in the field to be a single Ca^{2+} channel (or family of channels) directly gated by NAADP, located on lysosomal membranes. This assumption (that NAADP only acts directly on lysosomal Ca^{2+} stores) was the key reason many rule out the possibility of RyR playing a direct role in NAADP-induced Ca^{2+} release, despite evidence supporting this (Hohenegger et al. 2002; Gerasimenko et al. 2003; Dammermann and Guse 2005; Dammermann et al. 2009; Wolf et al. 2015). Meaning that the possibility for NAADP to act directly on both lysosomal (via an unidentified Ca^{2+} channel) and ER stores (via RyR) was not considered as a possibility. However, with the discovery of TPC channels as NAADP sensitive ion channels (E. Brailoiu et al. 2009; Calcraft et al. 2009; Zong et al. 2009) the possibility of this has been strengthened as NAADP has been shown to act on these channels via a separate binding protein rather than directly (Lin-Moshier et al. 2012; Walseth et al. 2012). This creates the possibility of there being multiple such NAADP binding proteins, which may be expressed in a cell type dependent manner. Such a possibility would certainly support the fact the NAADP-dependent activation of RyR has so far only been observed in

PAC (Gerasimenko et al. 2003) and T-cells (Dammermann and Guse 2005; Dammermann et al. 2009; Wolf et al. 2015), as well as membrane preparations from myocytes (Mojžišová et al. 2001; Hohenegger et al. 2002).

Unlike most other cell types, in addition to their traditional sites of action PAC show the ability for IP_3 and cADPR-induced Ca^{2+} release to occur from acidic stores (Gerasimenko, Sherwood, et al. 2006). Due to their secretory function these cells contain a large number of acidic secretory granules, which (due to other acid organelle Ca^{2+} stores being ruled out by pharmacological disruption) is the likely source of unique activity. While IP_3R and RyR are not normally found on acidic organelles it is probable that the high rate of ER turnover required to produce and sustain such a large number of secretory vesicles is the cause of their non-traditional location in this cell type. As well as providing unique sensitivity to secondary messengers these zymogen granules also create an acidic Ca^{2+} store much larger than that found in others cells, increasing the importance of release from such stores. In addition to these findings NAADP was shown to be able to mobilize Ca^{2+} directly from the ER after depletion of acidic Ca^{2+} stores (Gerasimenko, Sherwood, et al. 2006). Based on experimental data produced using the related nuclear envelope (Gerasimenko et al. 2003), this release from the ER is believed to occur via RyR.

The results presented in Chapter 3 expand on these previous reports using PAC to show that NAADP-induced Ca^{2+} release requires the involvement of both TPC and RyR channels (Gerasimenko et al. 2015). Based on the weight of evidence supporting TPC channels' sensitivity to NAADP (E. Brailoiu et al. 2009; Calcraft et al. 2009; Zong et al. 2009; Pitt et al. 2010; Jha et al. 2014; Ruas et al. 2015) it is believed that in PAC they are also directly activated by NAADP. Inhibition of both TPC isoforms activity was not found to completely abolish NAADP-induced Ca^{2+} release, suggesting a component of NAADP's activity is TPC

independent. While no direct evidence was found to confirm that this TPC-independent component was the result of NAADP acting directly on RyR, based on their requirement for NAADP-induced Ca^{2+} and previous findings in PAC (Gerasimenko et al. 2003; Gerasimenko, Sherwood, et al. 2006) it can be assumed that this is probably the case.

The dependence on the different RyR isoforms was found to be different for NAADP and cADPR, which is known to act directly on these channels (Lee 2001). It is possible that the variable dependence observed is the result of each messenger acting directly on only one or two of the 3 RyR isoforms and then indirectly on the others by CICR. Like NAADP-induced Ca^{2+} release, cADPR-induced release is known to require cADPR binding proteins (Walseth et al. 1993; Noguchi et al. 1997; Zhang et al. 2017). These binding proteins could provide the different isoform involvement observed, as they could provide the specificity by only interacting with specific RyR isoforms.

8.3 The activity of NAADP is essential for the physiological response to CCK in pancreatic acinar cells

When NAADP was first shown to play a role in intracellular Ca^{2+} release in mammalian cells using PAC it was found to be required for the initiation of responses to the secretagogue CCK (Cancela et al. 1999). The results in presented in Chapter 4 also show that the secondary messenger is required to sustain the response to CCK, as the acute application of Ned-19 on top of such responses terminated them. It is probable that as NAADP is likely to act directly on both TPC and RyR in PAC that Ned-19 inhibits both types of channel in these cells. However, this inhibition must occur in a similar isoform specific manner as NAADP-induced release, as Ned-19 had no significant effect on cADPR induced Ca^{2+} release in permeabilized PAC. Therefore, the inhibition of NAADP-induced release is enough to terminate responses

to CCK despite PAC producing both cADPR and NAADP when stimulated by the hormone (Yamasaki et al. 2005).

The 100 µM concentration of Ned-19 used was unable to provide a complete inhibition against 100 nM NAADP in permeabilized PAC but did prove a complete inhibition of CCK responses. This suggests that the amount of NAADP produced by PAC upon stimulation with 5 pM CCK is lower than the 100 nM concentration used in the permeabilized cell experiments, and that the Ned-19 insensitive component of the NAADP response observed in them not physiologically relevant.

Unlike Ned-19, the alternative NAADP antagonist BZ194 showed no effect on CCK-induced Ca^{2+} oscillations in PAC. This correlates with the findings of Ali et al.; who found the similar results against the proliferation of naïve CD4 and CD8 T cells by anti-CD3/CD28 stimulation (Ali et al. 2016), with Ned-19 suppressing proliferation and BZ194 having no effect. While BZ194 has been shown to antagonise NAADP responses in several studies (Dammermann et al. 2009; Cordiglieri et al. 2010; Nebel et al. 2013; Nebel et al. 2015), it has been utilized a lot less as a research tool than Ned-19 due to its lack of commercial availability. Because of this it is hard to draw definitive conclusions on its effectiveness compared to Ned-19; though with its proven antagonistic effect (Naylor et al. 2009; Esposito et al. 2011; Pereira et al. 2011; Favia et al. 2016; Kelu et al. 2017), lack of toxic effect (Coxon et al. 2012; Favia et al. 2016) and ready availability; it is likely that Ned-19 will remain the NAADP antagonist of choice for most researchers.

Despite permeabilized PAC isolated from $TPCN2^{-/-}$ mice showing a significantly reduced response to NAADP, intact cells from these knockout animals showed no loss of sensitivity to CCK. While the size of the response was not calculated to see if it was diminished compared to that in wild type PAC, it does suggest that the activity of the remaining

NAADP-sensitive ion channels in TPCN2$^{-/-}$ cells is enough to produce a response to the secretagogue. The knockout cells also showed the same sensitivity to Ned-19 as wild type PAC, with the compound completely inhibiting responses to CCK. This means even with their reduced sensitivity to NAADP, the secondary messenger is still integral to CCK effect on the knockout cells. As the different isoforms of TPC and RyR were found to contribute to the NAADP response in PAC to different extents, it could be of interest to do the same for CCK, and see if the isoform requirements for physiological signalling differs from direct application of secondary messengers.

8.4 Inhibition of NAADP-induced calcium release by Ned-19 is a potential therapeutic solution to acute pancreatitis

Gallstones are the most common cause of AP, contributing to just under 30% of all incidences of the disease in western countries (Joergensen et al. 2010). It is believed that these condensates of bile components create a physical blockage in the common bile duct (Lammert et al. 2016), which results in the reflux of bile into the pancreas, where components of the bile such as bile acids have a toxic effect resulting in an incident of AP (Arendt et al. 1999).

To recreate an experimental model of this biliary form of AP the bile acid TLC-S is often used as a 'model bile acid' (Perides et al. 2010; Muili, Jin, et al. 2013; Orabi et al. 2013; Wen et al. 2015; Huang et al. 2017). This bile acid has been found to instigate increases in the $[Ca^{2+}]_c$ of PAC which can reach cytotoxic levels and result in uncontrolled necrosis typical of AP (Voronina et al. 2002). Such increases in Ca^{2+} are the result of TLC-S inducing the release of Ca^{2+} from organelle stores (Gerasimenko, Flowerdew, et al. 2006) and is dependent on the activity of CD38 (Orabi et al. 2013).

As TLC-S-induced Ca^{2+} release had previously been found to be reduced in the presence of a high autoinhibitory concentration of NAADP (Gerasimenko, Flowerdew, et al. 2006), it was predicted that Ned-19 would have a similar effect. The results in Chapter 5 confirm that Ned-19 is not just capable of reducing the amount of Ca^{2+} mobilized in response to TLC-S, but also has a protective effect against the necrosis induced by this bile acid. While Ned-19 was found to be capable of significantly reducing the amount of necrosis observed in response to TLC-S, it was never able to reduce it to the level of the control. Because of this, it was used in combination with either caffeine or GSK-7975A, which have also both been shown to significantly inhibit TLC-S-induced necrosis (Wen et al. 2015; Huang et al. 2017). Unlike GSK-7975A, caffeine showed an additive protective effect when used in combination with Ned-19, reducing the amount of necrosis observed to a level identical to the control.

The alternative NAADP antagonist BZ194 was found to exhibit no effect against TLC-S-induced necrosis, as this matched the finding against CCK-induced Ca^{2+} release it strengthens the argument that this compound has no effect in PAC. Similarly, $TPCN2^{-/-}$ showed no reduction in sensitivity to the necrotic effects of TLC-S or the protective effect of Ned-19 against it. This suggests that, like for the response to CCK, PAC contain enough NAADP sensitive Ca^{2+} channels to compensated for the loss of TPC2 in the knockout cells; and that any reduction in Ca^{2+} response to TLC-S compared to wild types ones is insignificant, as it has no effect on the bile acid's necrotic effects.

In chapter 6 the primary bile acid cholate was shown to induce Ca^{2+} responses in PAC, which ultimately resulted in the death and loss of membrane integrity of the cell. When used alone either Ned-19 or GSK-7975A was found reduce the amount of necrosis observed in response to cholate, though neither's effect was deemed significant. Unlike when used against TLC-S, a combination of the two compounds had an additive protective effect and reduced the

amount of necrosis significantly. This suggests that different bile acids have different toxicities, and so the protective effect of a compound seen against one bile acid might not be sufficient to significantly inhibit the effect of another. Therefore, under true pathological conditions (where PAC will be exposed to a mixture of bile acids) an optimised treatment, targeting multiple elements of the cells 'Ca^{2+} signalling toolkit' (Berridge et al. 2000) may be required to treat AP.

TLC-S's effect in PAC has been shown to be CD38 dependent (Orabi et al. 2013 p.38), presumably the bile acid stimulates the activity of this enzyme resulting in the production of the secondary messengers NAADP and cADPR. The mechanism by which it does this is unknown; as is if it has a similar effect on PLC to induce the production of IP_3. Potentially it could occur extracellularly via the stimulation of the same plasma membrane receptors used for physiological signalling, or directly by the uptake of bile acids by their transporters, which PAC are known to express (Kim et al. 2002). Identifying which process TLC-S utilises, and if other bile acids share this, could provide several alternative targets for pharmacological inhibition of AP than the ion channels that this report focused on.

Due to its membrane permeability (Naylor et al. 2009), proven lack of toxicity *in vivo* (Favia et al. 2016) and the results presented in this report, Ned-19 offers a potential treatment for AP. Confirmation of this requires further study of its effect against other models of the diseases and progression from cellular models to *in vivo* ones.

BIBLIOGRAPHY

Aarhus, R. et al. 1995. ADP-ribosyl Cyclase and CD38 Catalyze the Synthesis of a Calcium-mobilizing Metabolite from NADP+. *Journal of Biological Chemistry* 270(51), pp. 30327–30333. doi: 10.1074/jbc.270.51.30327.

Aarhus, R. et al. 1996. Activation and Inactivation of Ca Release by NAADP. *Journal of Biological Chemistry* 271(15), pp. 8513–8516. doi: 10.1074/jbc.271.15.8513.

Adebanjo, O.A. et al. 1999. A new function for CD38/ADP-ribosyl cyclase in nuclear Ca2+ homeostasis. *Nature Cell Biology* 1(7), pp. 409–414. doi: 10.1038/15640.

Ahrén, B. 2000. Autonomic regulation of islet hormone secretion--implications for health and disease. *Diabetologia* 43(4), pp. 393–410. doi: 10.1007/s001250051322.

Aley, P.K. et al. 2010. Nicotinic acid adenine dinucleotide phosphate regulates skeletal muscle differentiation via action at two-pore channels. *Proceedings of the National Academy of Sciences of the United States of America* 107(46), pp. 19927–19932. doi: 10.1073/pnas.1007381107.

Aley, P.K. et al. 2013. Nicotinic Acid Adenine Dinucleotide Phosphate (NAADP) Is a Second Messenger in Muscarinic Receptor-induced Contraction of Guinea Pig Trachea. *Journal of Biological Chemistry* 288(16), pp. 10986–10993. doi: 10.1074/jbc.M113.458620.

Ali, R.A. et al. 2014. Activity of nicotinic acid substituted nicotinic acid adenine dinucleotide phosphate (NAADP) analogs in a human cell line: difference in specificity between human and sea urchin NAADP receptors. *Cell calcium* 55(2), pp. 93–103. doi: 10.1016/j.ceca.2013.12.004.

Ali, R.A. et al. 2016. Nicotinic Acid Adenine Dinucleotide Phosphate Plays a Critical Role in Naive and Effector Murine T Cells but Not Natural Regulatory T Cells. *Journal of Biological Chemistry* 291(9), pp. 4503–4522. doi: 10.1074/jbc.M115.681833.

Aliye, N. et al. 2015. Engineering color variants of green fluorescent protein (GFP) for thermostability, pH-sensitivity, and improved folding kinetics. *Applied Microbiology and Biotechnology* 99(3), pp. 1205–1216. doi: 10.1007/s00253-014-5975-1.

Alvarez, C. et al. 1997. The pancreatic duct epithelium in vitro: bile acid injury and the effect of epidermal growth factor. *Surgery* 122(2), pp. 476-483; discussion 483-484.

Amador, F.J. et al. 2013. Ryanodine receptor calcium release channels: lessons from structure-function studies. *The FEBS journal* 280(21), pp. 5456–5470. doi: 10.1111/febs.12194.

Ambily, A. et al. 2014. The role of plasma membrane STIM1 and Ca(2+)entry in platelet aggregation. STIM1 binds to novel proteins in human platelets. *Cellular Signalling* 26(3), pp. 502–511. doi: 10.1016/j.cellsig.2013.11.025.

Amundadottir, L.T. 2016. Pancreatic Cancer Genetics. *International Journal of Biological Sciences* 12(3), pp. 314–325. doi: 10.7150/ijbs.15001.

Andralojc, K.M. et al. 2009. Ghrelin-producing epsilon cells in the developing and adult human pancreas. *Diabetologia* 52(3), pp. 486–493. doi: 10.1007/s00125-008-1238-y.

Apte, M.V. et al. 2012. Pancreatic stellate cells: a starring role in normal and diseased pancreas. *Frontiers in Physiology* 3. Available at: http://www.ncbi.nlm.nih.gov/pmc/articles/PMC3428781/ [Accessed: 25 April 2017].

Arendt, T. et al. 1999. Biliary pancreatic reflux-induced acute pancreatitis--myth or possibility? *European Journal of Gastroenterology & Hepatology* 11(3), pp. 329–335.

Armstrong, C.P. et al. 1985. Effects of bile, infection and pressure on pancreatic duct integrity. *The British Journal of Surgery* 72(10), pp. 792–795.

Armstrong, C.P. and Taylor, T.V. 1986. Pancreatic-duct reflux and acute gallstone pancreatitis. *Annals of Surgery* 204(1), pp. 59–64.

Arndt, L. et al. 2014. NAADP and the two-pore channel protein 1 participate in the acrosome reaction in mammalian spermatozoa. *Molecular Biology of the Cell* 25(6), pp. 948–964. doi: 10.1091/mbc.E13-09-0523.

Arredouani, A. et al. 2015. Nicotinic Acid Adenine Dinucleotide Phosphate (NAADP) and Endolysosomal Two-pore Channels Modulate Membrane Excitability and Stimulus-Secretion Coupling in Mouse Pancreatic β Cells. *The Journal of Biological Chemistry* 290(35), pp. 21376–21392. doi: 10.1074/jbc.M115.671248.

Ashby, M.C. et al. 2002. Localized Ca2+ uncaging reveals polarized distribution of Ca2+-sensitive Ca2+ release sites. *The Journal of Cell Biology* 158(2), pp. 283–292. doi: 10.1083/jcb.200112025.

Ay, A.-S. et al. 2013. Orai3 Constitutes a Native Store-Operated Calcium Entry That Regulates Non Small Cell Lung Adenocarcinoma Cell Proliferation. *PLoS ONE* 8(9). Available at: http://www.ncbi.nlm.nih.gov/pmc/articles/PMC3772818/ [Accessed: 24 April 2017].

Bai, N. et al. 2005. Emerging role of cyclic ADP-ribose (cADPR) in smooth muscle. *Pharmacology & therapeutics* 105(2), pp. 189–207. doi: 10.1016/j.pharmthera.2004.10.005.

Banks, P.A. et al. 2010. The Management of Acute and Chronic Pancreatitis. *Gastroenterology & Hepatology* 6(2 Suppl 5), pp. 1–16.

Barceló-Torns, M. et al. 2011. NAADP mediates ATP-induced Ca2+ signals in astrocytes. *FEBS Letters* 585(14), pp. 2300–2306. doi: 10.1016/j.febslet.2011.05.062.

Bardeesy, N. and DePinho, R.A. 2002. Pancreatic cancer biology and genetics. *Nature Reviews Cancer* 2(12), pp. 897–909. doi: 10.1038/nrc949.

Barreto, S.G. 2016. How does cigarette smoking cause acute pancreatitis? *Pancreatology: official journal of the International Association of Pancreatology (IAP) ... [et al.]* 16(2), pp. 157–163. doi: 10.1016/j.pan.2015.09.002.

Baumgartner, H.K. et al. 2009. Calcium elevation in mitochondria is the main Ca2+ requirement for mitochondrial permeability transition pore (mPTP) opening. *The Journal of Biological Chemistry* 284(31), pp. 20796–20803. doi: 10.1074/jbc.M109.025353.

Beard, N.A. et al. 2004. Calsequestrin and the calcium release channel of skeletal and cardiac muscle. *Progress in Biophysics and Molecular Biology* 85(1), pp. 33–69. doi: 10.1016/j.pbiomolbio.2003.07.001.

Beck, A. et al. 2006. Nicotinic acid adenine dinucleotide phosphate and cyclic ADP-ribose regulate TRPM2 channels in T lymphocytes. *FASEB journal: official publication of the Federation of American Societies for Experimental Biology* 20(7), pp. 962–964. doi: 10.1096/fj.05-5538fje.

Beil, M. et al. 2002. Caspase 8-mediated cleavage of plectin precedes F-actin breakdown in acinar cells during pancreatitis. *American journal of physiology. Gastrointestinal and liver physiology* 282(3), pp. G450-460. doi: 10.1152/ajpgi.00042.2001.

Berg, I. et al. 2000. Nicotinic Acid Adenine Dinucleotide Phosphate (Naadp+) Is an Essential Regulator of T-Lymphocyte Ca2+-Signaling. *The Journal of Cell Biology* 150(3), pp. 581–588. doi: 10.1083/jcb.150.3.581.

Berg, T.O. et al. 1994. Use of glycyl-L-phenylalanine 2-naphthylamide, a lysosome-disrupting cathepsin C substrate, to distinguish between lysosomes and prelysosomal endocytic vacuoles. *The Biochemical journal* 300 (Pt 1), pp. 229–236.

Berridge, M.J. et al. 1983. Changes in the levels of inositol phosphates after agonist-dependent hydrolysis of membrane phosphoinositides. *The Biochemical Journal* 212(2), pp. 473–482.

Berridge, M.J. et al. 2000. The versatility and universality of calcium signalling. *Nature Reviews Molecular Cell Biology* 1(1), pp. 11–21. doi: 10.1038/35036035.

Berridge, M.J. et al. 2003. Calcium signalling: dynamics, homeostasis and remodelling. *Nature Reviews Molecular Cell Biology* 4(7), pp. 517–529. doi: 10.1038/nrm1155.

Bers, D.M. 2004. Macromolecular complexes regulating cardiac ryanodine receptor function. *Journal of Molecular and Cellular Cardiology* 37(2), pp. 417–429. doi: 10.1016/j.yjmcc.2004.05.026.

Bertuzzi, F. et al. 1999. Mechanisms of coordination of Ca2+ signals in pancreatic islet cells. *Diabetes* 48(10), pp. 1971–1978.

Bhatia, M. et al. 1998. Induction of apoptosis in pancreatic acinar cells reduces the severity of acute pancreatitis. *Biochemical and Biophysical Research Communications* 246(2), pp. 476–483. doi: 10.1006/bbrc.1998.8519.

Bhatia, M. 2004. Apoptosis of pancreatic acinar cells in acute pancreatitis: is it good or bad? *Journal of Cellular and Molecular Medicine* 8(3), pp. 402–409.

Biden, T.J. et al. 1984. Inositol 1,4,5-trisphosphate mobilizes intracellular Ca2+ from permeabilized insulin-secreting cells. *Biochemical Journal* 223(2), pp. 467–473. doi: 10.1042/bj2230467.

Billington, R.A. et al. 2004. Triazine dyes are agonists of the NAADP receptor. *British Journal of Pharmacology* 142(8), pp. 1241–1246. doi: 10.1038/sj.bjp.0705886.

Billington, R.A. et al. 2006. A transport mechanism for NAADP in a rat basophilic cell line. *FASEB journal: official publication of the Federation of American Societies for Experimental Biology* 20(3), pp. 521–523. doi: 10.1096/fj.05-5058fje.

Blacher, E. et al. 2015. Inhibition of glioma progression by a newly discovered CD38 inhibitor. *International Journal of Cancer* 136(6), pp. 1422–1433. doi: 10.1002/ijc.29095.

Blanchard, J. and Sawers, S.J.A. 1983. Relationship Between Urine Flow Rate and Renal Clearance of Caffeine in Man. *The Journal of Clinical Pharmacology* 23(4), pp. 134–138. doi: 10.1002/j.1552-4604.1983.tb02716.x.

Blatter, L.A. and Wier, W.G. 1990. Intracellular diffusion, binding, and compartmentalization of the fluorescent calcium indicators indo-1 and fura-2. *Biophysical Journal* 58(6), pp. 1491–1499. doi: 10.1016/S0006-3495(90)82494-2.

Bleasdale, J.E. et al. 1990. Selective inhibition of receptor-coupled phospholipase C-dependent processes in human platelets and polymorphonuclear neutrophils. *Journal of Pharmacology and Experimental Therapeutics* 255(2), pp. 756–768.

Boccaccio, A. et al. 2014. The phosphoinositide PI(3,5)P2 mediates activation of mammalian but not plant TPC proteins: functional expression of endolysosomal channels in yeast and plant cells. *Cellular and Molecular Life Sciences* 71(21), pp. 4275–4283. doi: 10.1007/s00018-014-1623-2.

Bockaert, J. and Pin, J.P. 1999. Molecular tinkering of G protein-coupled receptors: an evolutionary success. *The EMBO Journal* 18(7), pp. 1723–1729. doi: 10.1093/emboj/18.7.1723.

Booth, D.M. et al. 2011. Reactive oxygen species induced by bile acid induce apoptosis and protect against necrosis in pancreatic acinar cells. *Gastroenterology* 140(7), pp. 2116–2125. doi: 10.1053/j.gastro.2011.02.054.

Brailoiu, E. et al. 2005. Nicotinic Acid Adenine Dinucleotide Phosphate Potentiates Neurite Outgrowth. *Journal of Biological Chemistry* 280(7), pp. 5646–5650. doi: 10.1074/jbc.M408746200.

Brailoiu, E. et al. 2006. Messenger-specific Role for Nicotinic Acid Adenine Dinucleotide Phosphate in Neuronal Differentiation. *Journal of Biological Chemistry* 281(23), pp. 15923–15928. doi: 10.1074/jbc.M602249200.

Brailoiu, E. et al. 2009. Essential requirement for two-pore channel 1 in NAADP-mediated calcium signaling. *The Journal of Cell Biology* 186(2), pp. 201–209. doi: 10.1083/jcb.200904073.

Brailoiu, E. et al. 2010. An Ancestral Deuterostome Family of Two-pore Channels Mediates Nicotinic Acid Adenine Dinucleotide Phosphate-dependent Calcium Release from Acidic Organelles. *Journal of Biological Chemistry* 285(5), pp. 2897–2901. doi: 10.1074/jbc.C109.081943.

Brailoiu, G.C. et al. 2009. NAADP-mediated channel 'chatter' in neurons of the rat medulla oblongata. *Biochemical Journal* 419(1), pp. 91–99. doi: 10.1042/BJ20081138.

Brandman, O. et al. 2007. STIM2 Is a Feedback Regulator that Stabilizes Basal Cytosolic and Endoplasmic Reticulum Ca2+ Levels. *Cell* 131(7), pp. 1327–1339. doi: 10.1016/j.cell.2007.11.039.

Brillantes, A.-M.B. et al. 1994. Stabilization of calcium release channel (ryanodine receptor) function by FK506-binding protein. *Cell* 77(4), pp. 513–523. doi: 10.1016/0092-8674(94)90214-3.

Brini, M. and Carafoli, E. 2011. The Plasma Membrane Ca2+ ATPase and the Plasma Membrane Sodium Calcium Exchanger Cooperate in the Regulation of Cell Calcium. *Cold Spring Harbor Perspectives in Biology* 3(2). Available at: http://www.ncbi.nlm.nih.gov/pmc/articles/PMC3039526/ [Accessed: 23 April 2017].

Brock, C. et al. 2013. Pathophysiology of chronic pancreatitis. *World Journal of Gastroenterology : WJG* 19(42), pp. 7231–7240. doi: 10.3748/wjg.v19.i42.7231.

Bruzzone, S. et al. 2003. Cyclic ADP-ribose is a second messenger in the lipopolysaccharide-stimulated proliferation of human peripheral blood mononuclear cells. *The Biochemical journal* 375(Pt 2), pp. 395–403. doi: 10.1042/BJ20030556.

Burgess, G.M., McKinney, J.S., et al. 1984. Inositol 1,4,5-trisphosphate may be a signal for f-Met-Leu-Phe-induced intracellular Ca mobilisation in human leucocytes (HL-60 cells). *FEBS Letters* 176(1), pp. 193–196. doi: 10.1016/0014-5793(84)80939-4.

Burgess, G.M., Godfrey, P.P., et al. 1984. The second messenger linking receptor activation to internal Ca release in liver. *Nature* 309(5963), pp. 63–66. doi: 10.1038/309063a0.

Button, D. and Eidsath, A. 1996. Aequorin targeted to the endoplasmic reticulum reveals heterogeneity in luminal Ca++ concentration and reports agonist- or IP3-induced release of Ca++. *Molecular Biology of the Cell* 7(3), pp. 419–434.

Cahalan, M.D. 2009. STIMulating store-operated Ca2+ entry. *Nature cell biology* 11(6), pp. 669–677. doi: 10.1038/ncb0609-669.

Calcraft, P.J. et al. 2009. NAADP mobilizes calcium from acidic organelles through two-pore channels. *Nature* 459(7246), pp. 596–600. doi: 10.1038/nature08030.

Camiña, J.P. et al. 2003. Regulation of ghrelin secretion and action. *Endocrine* 22(1), pp. 5–12. doi: 10.1385/ENDO:22:1:5.

Cancela, J.M. et al. 1998. Intracellular glucose switches between cyclic ADP-ribose and inositol trisphosphate triggering of cytosolic Ca2+ spiking. *Current Biology* 8(15), pp. 865–868. doi: 10.1016/S0960-9822(07)00347-8.

Cancela, J.M. et al. 1999. Coordination of agonist-induced Ca2+-signalling patterns by NAADP in pancreatic acinar cells. *Nature* 398(6722), pp. 74–76. doi: 10.1038/18032.

Cancela, J.M. 2001. Specific Ca2+ signaling evoked by cholecystokinin and acetylcholine: the roles of NAADP, cADPR, and IP3. *Annual Review of Physiology* 63, pp. 99–117. doi: 10.1146/annurev.physiol.63.1.99.

Cancela, J.M. and Petersen, O.H. 1998. The cyclic ADP ribose antagonist 8-NH2-cADP-ribose blocks cholecystokinin-evoked cytosolic Ca2+ spiking in pancreatic acinar cells. *Pflügers Archiv* 435(5), pp. 746–748. doi: 10.1007/s004240050578.

Cang, C. et al. 2013. mTOR Regulates Lysosomal ATP-Sensitive Two-Pore Na+ Channels to Adapt to Metabolic State. *Cell* 152(4), pp. 778–790. doi: 10.1016/j.cell.2013.01.023.

Capel, R.A. et al. 2015. Two-pore Channels (TPC2s) and Nicotinic Acid Adenine Dinucleotide Phosphate (NAADP) at Lysosomal-Sarcoplasmic Reticular Junctions Contribute to Acute and Chronic β-Adrenoceptor Signaling in the Heart. *The Journal of Biological Chemistry* 290(50), pp. 30087–30098. doi: 10.1074/jbc.M115.684076.

Carafoli, E. 1991. Calcium pump of the plasma membrane. *Physiological reviews* 71(1), pp. 129–153.

Case, R.M. 1978. Synthesis, intracellular transport and discharge of exportable proteins in the pancreatic acinar cell and other cells. *Biological Reviews of the Cambridge Philosophical Society* 53(2), pp. 211–354.

Case, R.M. et al. 2007. Evolution of calcium homeostasis: from birth of the first cell to an omnipresent signalling system. *Cell calcium* 42(4–5), pp. 345–350. doi: 10.1016/j.ceca.2007.05.001.

Casey, J.R. et al. 2010. Sensors and regulators of intracellular pH. *Nature Reviews Molecular Cell Biology* 11(1), pp. 50–61. doi: 10.1038/nrm2820.

Castaing, D. 2008. Surgical anatomy of the biliary tract. *HPB : The Official Journal of the International Hepato Pancreato Biliary Association* 10(2), pp. 72–76. doi: 10.1080/13651820801992518.

Catterall, W.A. 1995. Structure and Function of Voltage-Gated Ion Channels. *Annual Review of Biochemistry* 64(1), pp. 493–531. doi: 10.1146/annurev.bi.64.070195.002425.

Ceni, C. et al. 2003. Evidence for an intracellular ADP-ribosyl cyclase/NAD+-glycohydrolase in brain from CD38-deficient mice. *The Journal of biological chemistry* 278(42), pp. 40670–40678. doi: 10.1074/jbc.M301196200.

Chavis, P. et al. 1996. Functional coupling between ryanodine receptors and L-type calcium channels in neurons. *Nature* 382(6593), pp. 719–722. doi: 10.1038/382719a0.

Chen, B. et al. 2016. Bile acids induce activation of alveolar epithelial cells and lung fibroblasts through farnesoid X receptor-dependent and independent pathways. *Respirology (Carlton, Vic.)* 21(6), pp. 1075–1080. doi: 10.1111/resp.12815.

Chen, X.-Z. et al. 2016. Association of helicobacter pylori infection and chronic atrophic gastritis with risk of colonic, pancreatic and gastric cancer: A ten-year follow-up of the ESTHER cohort study. *Oncotarget* 7(13), pp. 17182–17193. doi: 10.18632/oncotarget.7946.

Cheng, X. et al. 2010. Mucolipins: Intracellular TRPML1-3 Channels. *FEBS letters* 584(10), pp. 2013–2021. doi: 10.1016/j.febslet.2009.12.056.

Chew, C.S. 1986. Cholecystokinin, carbachol, gastrin, histamine, and forskolin increase [Ca2+]i in gastric glands. *American Journal of Physiology - Gastrointestinal and Liver Physiology* 250(6), pp. G814–G823.

Chiang, J.Y.L. 2009. Bile acids: regulation of synthesis. *Journal of Lipid Research* 50(10), pp. 1955–1966. doi: 10.1194/jlr.R900010-JLR200.

Chiang, J.Y.L. 2013. Bile Acid Metabolism and Signaling. *Comprehensive Physiology* 3(3), pp. 1191–1212. doi: 10.1002/cphy.c120023.

Chini, E.N. et al. 1995. Nicotinate Adenine Dinucleotide Phosphate (NAADP) Triggers a Specific Calcium Release System in Sea Urchin Eggs. *Journal of Biological Chemistry* 270(7), pp. 3216–3223.

Chini, E.N. et al. 2002. CD38 is the major enzyme responsible for synthesis of nicotinic acid–adenine dinucleotide phosphate in mammalian tissues. *Biochemical Journal* 362(1), pp. 125–130. doi: 10.1042/bj3620125.

Chiou, C.Y. and Malagodi, M.H. 1975. Studies on the mechanism of action of a new Ca-2+ antagonist, 8-(N,N-diethylamino)octyl 3,4,5-trimethoxybenzoate hydrochloride in smooth and skeletal muscles. *British Journal of Pharmacology* 53(2), pp. 279–285.

Christopoulos, A. and Kenakin, T. 2002. G Protein-Coupled Receptor Allosterism and Complexing. *Pharmacological Reviews* 54(2), pp. 323–374.

Churamani, D. et al. 2012. Domain assembly of NAADP-gated two-pore channels. *Biochemical Journal* 441(Pt 1), pp. 317–323. doi: 10.1042/BJ20111617.

Churchill, G.C. et al. 2002. NAADP Mobilizes Ca2+ from Reserve Granules, Lysosome-Related Organelles, in Sea Urchin Eggs. *Cell* 111(5), pp. 703–708. doi: 10.1016/S0092-8674(02)01082-6.

Churchill, G.C. et al. 2003. Sperm Deliver a New Second Messenger. *Current Biology* 13(2), pp. 125–128. doi: 10.1016/S0960-9822(03)00002-2.

Churchill, G.C. and Galione, A. 2001. NAADP induces Ca2+ oscillations via a two-pool mechanism by priming IP3- and cADPR-sensitive Ca2+ stores. *The EMBO Journal* 20(11), pp. 2666–2671. doi: 10.1093/emboj/20.11.2666.

Clapham, D.E. 2007. Calcium Signaling. *Cell* 131(6), pp. 1047–1058. doi: 10.1016/j.cell.2007.11.028.

Clapper, D.L. et al. 1987. Pyridine nucleotide metabolites stimulate calcium release from sea urchin egg microsomes desensitized to inositol trisphosphate. *Journal of Biological Chemistry* 262(20), pp. 9561–9568.

Clapper, D.L. and Lee, H.C. 1985. Inositol trisphosphate induces calcium release from nonmitochondrial stores i sea urchin egg homogenates. *Journal of Biological Chemistry* 260(26), pp. 13947–13954.

Collins, T.P. et al. 2011. NAADP influences excitation-contraction coupling by releasing calcium from lysosomes in atrial myocytes. *Cell calcium* 50(5), pp. 449–458. doi: 10.1016/j.ceca.2011.07.007.

Contreras-Ferrat, A.E. et al. 2010. An inositol 1,4,5-triphosphate (IP3)-IP3 receptor pathway is required for insulin-stimulated glucose transporter 4 translocation and glucose uptake in cardiomyocytes. *Endocrinology* 151(10), pp. 4665–4677. doi: 10.1210/en.2010-0116.

Copello, J.A. et al. 2001. Lack of effect of cADP-ribose and NAADP on the activity of skeletal muscle and heart ryanodine receptors. *Cell Calcium* 30(4), pp. 269–284. doi: 10.1054/ceca.2001.0235.

Cordiglieri, C. et al. 2010. Nicotinic acid adenine dinucleotide phosphate-mediated calcium signalling in effector T cells regulates autoimmunity of the central nervous system. *Brain* 133(7), pp. 1930–1943. doi: 10.1093/brain/awq135.

Cosker, F. et al. 2010. The ecto-enzyme CD38 is a nicotinic acid adenine dinucleotide phosphate (NAADP) synthase that couples receptor activation to Ca2+ mobilization from lysosomes in pancreatic acinar cells. *The Journal of biological chemistry* 285(49), pp. 38251–38259. doi: 10.1074/jbc.M110.125864.

Coxon, C.H. et al. 2012. NAADP regulates human platelet function. *Biochemical Journal* 441(1), pp. 435–442. doi: 10.1042/BJ20111175.

Criddle, D.N. et al. 2004. Ethanol toxicity in pancreatic acinar cells: Mediation by nonoxidative fatty acid metabolites. *Proceedings of the National Academy of Sciences of the United States of America* 101(29), pp. 10738–10743. doi: 10.1073/pnas.0403431101.

Criddle, D.N., Murphy, J., et al. 2006. Fatty Acid Ethyl Esters Cause Pancreatic Calcium Toxicity via Inositol Trisphosphate Receptors and Loss of ATP Synthesis. *Gastroenterology* 130(3), pp. 781–793. doi: 10.1053/j.gastro.2005.12.031.

Criddle, D.N., Sutton, R., et al. 2006. Role of Ca2+ in pancreatic cell death induced by alcohol metabolites. *Journal of Gastroenterology and Hepatology* 21 Suppl 3, pp. S14-17. doi: 10.1111/j.1440-1746.2006.04577.x.

Criddle, D.N. et al. 2007. Calcium signalling and pancreatic cell death: apoptosis or necrosis? *Cell Death & Differentiation* 14(7), pp. 1285–1294. doi: 10.1038/sj.cdd.4402150.

Criddle, D.N. et al. 2009. Cholecystokinin-58 and cholecystokinin-8 exhibit similar actions on calcium signaling, zymogen secretion, and cell fate in murine pancreatic acinar cells. *American Journal of Physiology - Gastrointestinal and Liver Physiology* 297(6), pp. G1085–G1092. doi: 10.1152/ajpgi.00119.2009.

Cui, J. et al. 2002. CaT1 contributes to the stores-operated calcium current in Jurkat T-lymphocytes. *The Journal of Biological Chemistry* 277(49), pp. 47175–47183. doi: 10.1074/jbc.M205870200.

Dammermann, W. et al. 2009. NAADP-mediated Ca2+ signaling via type 1 ryanodine receptor in T cells revealed by a synthetic NAADP antagonist. *Proceedings of the National Academy of Sciences* 106(26), pp. 10678–10683. doi: 10.1073/pnas.0809997106.

Dammermann, W. and Guse, A.H. 2005. Functional Ryanodine Receptor Expression Is Required for NAADP-mediated Local Ca2+ Signaling in T-lymphocytes. *Journal of Biological Chemistry* 280(22), pp. 21394–21399. doi: 10.1074/jbc.M413085200.

Dargie, P.J. et al. 1990. Comparison of Ca2+ mobilizing activities of cyclic ADP-ribose and inositol trisphosphate. *Cell regulation* 1(3), pp. 279–290.

Davis, L.C. et al. 2012. NAADP Activates Two-Pore Channels on T Cell Cytolytic Granules to Stimulate Exocytosis and Killing. *Current Biology* 22(24), pp. 2331–2337. doi: 10.1016/j.cub.2012.10.035.

Davis, L.C. et al. 2015. Preferential Coupling of the NAADP Pathway to Exocytosis in T-Cells. *Messenger* 4(1), pp. 53–66. doi: 10.1166/msr.2015.1040.

Dawson, P.A. et al. 2009. Bile acid transporters. *Journal of Lipid Research* 50(12), pp. 2340–2357. doi: 10.1194/jlr.R900012-JLR200.

De Flora, A. et al. 1997. The CD38/cyclic ADP-ribose system: A topological paradox. *The International Journal of Biochemistry & Cell Biology* 29(10), pp. 1149–1166. doi: 10.1016/S1357-2725(97)00062-9.

Deaglio, S. et al. 2008. CD38 at the junction between prognostic marker and therapeutic target. *Trends in Molecular Medicine* 14(5), pp. 210–218. doi: 10.1016/j.molmed.2008.02.005.

DeHaven, W.I. et al. 2009. TRPC channels function independently of STIM1 and Orai1. *The Journal of Physiology* 587(Pt 10), pp. 2275–2298. doi: 10.1113/jphysiol.2009.170431.

Delfert, D.M. et al. 1986. myo-Inositol 1,4,5-trisphosphate mobilizes Ca2+ from isolated adipocyte endoplasmic reticulum but not from plasma membranes. *Biochemical Journal* 236(1), pp. 37–44.

Derler, I. et al. 2013. The action of selective CRAC channel blockers is affected by the Orai pore geometry. *Cell Calcium* 53(2), pp. 139–151. doi: 10.1016/j.ceca.2012.11.005.

Di Paolo, G. and De Camilli, P. 2006. Phosphoinositides in cell regulation and membrane dynamics. *Nature* 443(7112), pp. 651–657. doi: 10.1038/nature05185.

Dickey, D.M. et al. 1998. Thio-NADP is not an antagonist of NAADP. *Cell Biochemistry and Biophysics* 28(1), pp. 63–73. doi: 10.1007/BF02738310.

Dipolo, R. and Beaugé, L. 2006. Sodium/Calcium Exchanger: Influence of Metabolic Regulation on Ion Carrier Interactions. *Physiological Reviews* 86(1), pp. 155–203. doi: 10.1152/physrev.00018.2005.

Djerada, Z. et al. 2013. Extracellular NAADP affords cardioprotection against ischemia and reperfusion injury and involves the P2Y11-like receptor. *Biochemical and Biophysical Research Communications* 434(3), pp. 428–433. doi: 10.1016/j.bbrc.2013.03.089.

Dolenšek, J. et al. 2015. Structural similarities and differences between the human and the mouse pancreas. *Islets* 7(1). Available at: http://www.ncbi.nlm.nih.gov/pmc/articles/PMC4589993/ [Accessed: 25 April 2017].

Dong, X. et al. 2010. PI(3,5)P2 controls membrane trafficking by direct activation of mucolipin Ca2+ release channels in the endolysosome. *Nature Communications* 1, p. 38. doi: 10.1038/ncomms1037.

Dong, X.-P. et al. 2008. The type IV mucolipidosis-associated protein TRPML1 is an endolysosomal iron release channel. *Nature* 455(7215), pp. 992–996. doi: 10.1038/nature07311.

Duane, W.C. and Javitt, N.B. 1999. 27-hydroxycholesterol: production rates in normal human subjects. *Journal of Lipid Research* 40(7), pp. 1194–1199.

Dulhunty, A.F. et al. 2017. Core skeletal muscle ryanodine receptor calcium release complex. *Clinical and Experimental Pharmacology & Physiology* 44(1), pp. 3–12. doi: 10.1111/1440-1681.12676.

Durbec, J.P. et al. 1981. Risks of chronic pancreatitis, hepatocirrhosis and pancreas cancer. Role of alcohol consumption, results of 3 retrospective studies (cases-controls). *Materia Medica Polona. Polish Journal of Medicine and Pharmacy* 13(1), pp. 10–14.

Elayat, A.A. et al. 1995. An immunocytochemical and morphometric study of the rat pancreatic islets. *Journal of Anatomy* 186(Pt 3), pp. 629–637.

Endo, M. 2009. Calcium-Induced Calcium Release in Skeletal Muscle. *Physiological Reviews* 89(4), pp. 1153–1176. doi: 10.1152/physrev.00040.2008.

Esposito, B. et al. 2011. NAADP links histamine H1 receptors to secretion of von Willebrand factor in human endothelial cells. *Blood* 117(18), pp. 4968–4977. doi: 10.1182/blood-2010-02-266338.

Ewald, N. and Hardt, P.D. 2013. Diagnosis and treatment of diabetes mellitus in chronic pancreatitis. *World Journal of Gastroenterology : WJG* 19(42), pp. 7276–7281. doi: 10.3748/wjg.v19.i42.7276.

Fagniez, P.-L. and Rotman, N. 2001. *Acute pancreatitis*. Zuckschwerdt. Available at: https://www.ncbi.nlm.nih.gov/books/NBK6932/ [Accessed: 25 April 2017].

Falany, C.N. et al. 1994. Glycine and taurine conjugation of bile acids by a single enzyme. Molecular cloning and expression of human liver bile acid CoA:amino acid N-acyltransferase. *The Journal of Biological Chemistry* 269(30), pp. 19375–19379.

Farina, A. et al. 2009. Proteomic analysis of human bile and potential applications for cancer diagnosis. *Expert Review of Proteomics* 6(3), pp. 285–301. doi: 10.1586/epr.09.12.

Favia, A. et al. 2016. NAADP-Dependent Ca2+ Signaling Controls Melanoma Progression, Metastatic Dissemination and Neoangiogenesis. *Scientific Reports* 6, p. 18925. doi: 10.1038/srep18925.

Feoktistova, M. and Leverkus, M. 2015. Programmed necrosis and necroptosis signalling. *FEBS Journal* 282(1), pp. 19–31. doi: 10.1111/febs.13120.

Ferdek, P.E. et al. 2012. A novel role for Bcl-2 in regulation of cellular calcium extrusion. *Current biology: CB* 22(13), pp. 1241–1246. doi: 10.1016/j.cub.2012.05.002.

Ferdek, P.E. et al. 2016. Bile acids induce necrosis in pancreatic stellate cells dependent on calcium entry and sodium-driven bile uptake. *The Journal of Physiology* 594(21), pp. 6147–6164. doi: 10.1113/JP272774.

Ferrero, E. et al. 1999. The human CD38 gene: polymorphism, CpG island, and linkage to the CD157 (BST-1) gene. *Immunogenetics* 49(7–8), pp. 597–604.

Ferris, C.D. et al. 1989. Purified inositol 1,4,5-trisphosphate receptor mediates calcium flux in reconstituted lipid vesicles. *Nature* 342(6245), pp. 87–89. doi: 10.1038/342087a0.

Feske, S. et al. 2005. A severe defect in CRAC Ca2+ channel activation and altered K+ channel gating in T cells from immunodeficient patients. *The Journal of Experimental Medicine* 202(5), pp. 651–662. doi: 10.1084/jem.20050687.

Feske, S. et al. 2006. A mutation in Orai1 causes immune deficiency by abrogating CRAC channel function. *Nature* 441(7090), pp. 179–185. doi: 10.1038/nature04702.

Feske, S. and Prakriya, M. 2013. Conformational dynamics of STIM1 activation. *Nature structural & molecular biology* 20(8), pp. 918–919. doi: 10.1038/nsmb.2647.

Festjens, N. et al. 2006. Necrosis, a well-orchestrated form of cell demise: Signalling cascades, important mediators and concomitant immune response. *Biochimica et Biophysica Acta (BBA) - Bioenergetics* 1757(9–10), pp. 1371–1387. doi: 10.1016/j.bbabio.2006.06.014.

Finch, E.A. et al. 1991. Calcium as a coagonist of inositol 1,4,5-trisphosphate-induced calcium release. *Science* 252(5004), pp. 443–446. doi: 10.1126/science.2017683.

Fishman, M.P. and Melton, D.A. 2002. Pancreatic lineage analysis using a retroviral vector in embryonic mice demonstrates a common progenitor for endocrine and exocrine cells. *The International Journal of Developmental Biology* 46(2), pp. 201–207. doi: 10.1387/ijdb.011552.

Fitzsimmons, T.J. et al. 2000. Multiple isoforms of the ryanodine receptor are expressed in rat pancreatic acinar cells. *Biochemical Journal* 351(Pt 1), pp. 265–271.

Fjällskog, M.-L.H. et al. 2003. Expression of molecular targets for tyrosine kinase receptor antagonists in malignant endocrine pancreatic tumors. *Clinical Cancer Research: An Official Journal of the American Association for Cancer Research* 9(4), pp. 1469–1473.

Franco, L. et al. 1998. The transmembrane glycoprotein CD38 is a catalytically active transporter responsible for generation and influx of the second messenger cyclic ADP-ribose across membranes. *The FASEB Journal* 12(14), pp. 1507–1520.

Frei, B. et al. 1985. Quantitative and mechanistic aspects of the hydroperoxide-induced release of Ca2+ from rat liver mitochondria. *European Journal of Biochemistry* 149(3), pp. 633–639. doi: 10.1111/j.1432-1033.1985.tb08971.x.

Fruen, B.R. et al. 2000. Differential Ca2+ sensitivity of skeletal and cardiac muscle ryanodine receptors in the presence of calmodulin. *American Journal of Physiology - Cell Physiology* 279(3), pp. C724–C733.

Fukushi, Y. et al. 2001. Identification of Cyclic ADP-ribose-dependent Mechanisms in Pancreatic Muscarinic Ca2+ Signaling Using CD38 Knockout Mice. *Journal of Biological Chemistry* 276(1), pp. 649–655. doi: 10.1074/jbc.M004469200.

Funaro, A. et al. 2004. CD157 is an important mediator of neutrophil adhesion and migration. *Blood* 104(13), pp. 4269–4278. doi: 10.1182/blood-2004-06-2129.

Futatsugi, A. et al. 1999. Facilitation of NMDAR-Independent LTP and Spatial Learning in Mutant Mice Lacking Ryanodine Receptor Type 3. *Neuron* 24(3), pp. 701–713. doi: 10.1016/S0896-6273(00)81123-X.

Gafni, J. et al. 1997. Xestospongins: Potent Membrane Permeable Blockers of the Inositol 1,4,5-Trisphosphate Receptor. *Neuron* 19(3), pp. 723–733. doi: 10.1016/S0896-6273(00)80384-0.

Gagliardi, S. et al. 1999. Chemistry and structure activity relationships of bafilomycin A1, a potent and selective inhibitor of the vacuolar H+-ATPase. *Current Medicinal Chemistry* 6(12), pp. 1197–1212.

Galione, A. et al. 1991. Ca(2+)-induced Ca2+ release in sea urchin egg homogenates: modulation by cyclic ADP-ribose. *Science (New York, N.Y.)* 253(5024), pp. 1143–1146.

Galione, A. et al. 2000. NAADP-induced calcium release in sea urchin eggs. *Biology of the Cell* 92(3–4), pp. 197–204. doi: 10.1016/S0248-4900(00)01070-4.

Galione, A. et al. 2010. NAADP as an intracellular messenger regulating lysosomal calcium-release channels. *Biochemical Society Transactions* 38(6), pp. 1424–1431. doi: 10.1042/BST0381424.

Galione, A. 2011. NAADP Receptors. *Cold Spring Harbor Perspectives in Biology* 3(1). Available at: http://www.ncbi.nlm.nih.gov/pmc/articles/PMC3003455/ [Accessed: 23 August 2016].

Galione, A. et al. 2011. Physiological roles of NAADP-mediated Ca2+ signaling. *Science China Life Sciences* 54(8), pp. 725–732. doi: 10.1007/s11427-011-4207-5.

Galione, A. and Churchill, G.C. 2002. Interactions between calcium release pathways: multiple messengers and multiple stores. *Cell Calcium* 32(5), pp. 343–354. doi: 10.1016/S0143416002001902.

Ge, Z.-D. et al. 2003. Cyclic ADP-Ribose Contributes to Contraction and Ca2+ Release by M1 Muscarinic Receptor Activation in Coronary Arterial Smooth Muscle. *Journal of Vascular Research* 40(1), pp. 28–36. doi: 10.1159/000068936.

Gee, K.R. et al. 2000. Chemical and physiological characterization of fluo-4 Ca(2+)-indicator dyes. *Cell Calcium* 27(2), pp. 97–106. doi: 10.1054/ceca.1999.0095.

Genazzani, A.A. et al. 1996. Unique Inactivation Properties of NAADP-sensitive Ca Release. *Journal of Biological Chemistry* 271(20), pp. 11599–11602. doi: 10.1074/jbc.271.20.11599.

Genazzani, A.A. et al. 1997. Pharmacological properties of the Ca2+-release mechanism sensitive to NAADP in the sea urchin egg. *British Journal of Pharmacology* 121(7), pp. 1489–1495. doi: 10.1038/sj.bjp.0701295.

Genazzani, A.A. and Galione, A. 1996. Nicotinic acid-adenine dinucleotide phosphate mobilizes Ca2+ from a thapsigargin-insensitive pool. *Biochemical Journal* 315(3), pp. 721–725. doi: 10.1042/bj3150721.

Gerasimenko, J.V. et al. 2003. NAADP mobilizes Ca2+ from a thapsigargin-sensitive store in the nuclear envelope by activating ryanodine receptors. *The Journal of Cell Biology* 163(2), pp. 271–282. doi: 10.1083/jcb.200306134.

Gerasimenko, J.V., Flowerdew, S.E., et al. 2006. Bile Acids Induce Ca2+ Release from Both the Endoplasmic Reticulum and Acidic Intracellular Calcium Stores through Activation of Inositol Trisphosphate Receptors and Ryanodine Receptors. *Journal of Biological Chemistry* 281(52), pp. 40154–40163. doi: 10.1074/jbc.M606402200.

Gerasimenko, J.V., Sherwood, M., et al. 2006. NAADP, cADPR and IP3 all release Ca2+ from the endoplasmic reticulum and an acidic store in the secretory granule area. *Journal of Cell Science* 119(2), pp. 226–238. doi: 10.1242/jcs.02721.

Gerasimenko, J.V. et al. 2013. Ca2+ release-activated Ca2+ channel blockade as a potential tool in antipancreatitis therapy. *Proceedings of the National Academy of Sciences* 110(32), pp. 13186–13191. doi: 10.1073/pnas.1300910110.

Gerasimenko, J.V. et al. 2015. Both RyRs and TPCs are required for NAADP-induced intracellular Ca2+ release. *Cell Calcium* 58(3), pp. 237–245. doi: 10.1016/j.ceca.2015.05.005.

Gerasimenko, O. and Gerasimenko, J. 2004. New aspects of nuclear calcium signalling. *Journal of Cell Science* 117(15), pp. 3087–3094. doi: 10.1242/jcs.01295.

Gerasimenko, O.V. et al. 1996. Short pulses of acetylcholine stimulation induce cytosolic Ca2+ signals that are excluded from the nuclear region in pancreatic acinar cells. *Pflügers Archiv - European Journal of Physiology* 432(6), pp. 1055–1061. doi: 10.1007/s004240050234.

Geyer, N. et al. 2015. Bile acids activate ryanodine receptors in pancreatic acinar cells via a direct allosteric mechanism. *Cell Calcium* 58(2), pp. 160–170. doi: 10.1016/j.ceca.2015.03.009.

Ghaneh, P. et al. 2007. Biology and management of pancreatic cancer. *Gut* 56(8), pp. 1134–1152. doi: 10.1136/gut.2006.103333.

Ghosh, T.K. et al. 1988. Competitive, reversible, and potent antagonism of inositol 1,4,5-trisphosphate-activated calcium release by heparin. *Journal of Biological Chemistry* 263(23), pp. 11075–11079.

Gittes, G.K. 2009. Developmental biology of the pancreas: a comprehensive review. *Developmental Biology* 326(1), pp. 4–35. doi: 10.1016/j.ydbio.2008.10.024.

Grapin-Botton, A. 2005. Ductal cells of the pancreas. *The International Journal of Biochemistry & Cell Biology* 37(3), pp. 504–510. doi: 10.1016/j.biocel.2004.07.010.

Grynkiewicz, G. et al. 1985. A new generation of Ca2+ indicators with greatly improved fluorescence properties. *Journal of Biological Chemistry* 260(6), pp. 3440–3450.

Guida, L. et al. 2002. Equilibrative and Concentrative Nucleoside Transporters Mediate Influx of Extracellular Cyclic ADP-Ribose into 3T3 Murine Fibroblasts. *Journal of Biological Chemistry* 277(49), pp. 47097–47105. doi: 10.1074/jbc.M207793200.

Gukovskaya, A.S. et al. 2002. Ethanol metabolism and transcription factor activation in pancreatic acinar cells in rats. *Gastroenterology* 122(1), pp. 106–118.

Guo, J. et al. 2016. Structure of Voltage-gated Two-pore Channel TPC1 from Arabidopsis thaliana. *Nature* 531(7593), pp. 196–201. doi: 10.1038/nature16446.

Gwack, Y. et al. 2007. Biochemical and Functional Characterization of Orai Proteins. *Journal of Biological Chemistry* 282(22), pp. 16232–16243. doi: 10.1074/jbc.M609630200.

van Haasteren, G. et al. 1999. Calcium signalling and gene expression. *Journal of Receptor and Signal Transduction Research* 19(1–4), pp. 481–492. doi: 10.3109/10799899909036666.

Haber, P.S. et al. 1993. Fatty acid ethyl esters increase rat pancreatic lysosomal fragility. *The Journal of Laboratory and Clinical Medicine* 121(6), pp. 759–764.

Haber, P.S. et al. 1994. Chronic ethanol consumption increases the fragility of rat pancreatic zymogen granules. *Gut* 35(10), pp. 1474–1478.

Haber, P.S. et al. 1999. Activation of pancreatic stellate cells in human and experimental pancreatic fibrosis. *The American Journal of Pathology* 155(4), pp. 1087–1095. doi: 10.1016/S0002-9440(10)65211-X.

Hadad, N. et al. 1994. Ca2+ binding sites of the ryanodine receptor/Ca2+ release channel of sarcoplasmic reticulum. Low affinity binding site(s) as probed by terbium fluorescence. *Journal of Biological Chemistry* 269(40), pp. 24864–24869.

Han, B. et al. 2001. CCK independently activates intracellular trypsinogen and NF-κB in rat pancreatic acinar cells. *American Journal of Physiology - Cell Physiology* 280(3), pp. C465–C472.

Han, B. and Logsdon, C.D. 2000. CCK stimulates mob-1 expression and NF-κB activation via protein kinase C and intracellular Ca2+. *American Journal of Physiology - Cell Physiology* 278(2), pp. C344–C351.

Haqq, J. et al. 2014. Pancreatic stellate cells and pancreas cancer: current perspectives and future strategies. *European Journal of Cancer (Oxford, England: 1990)* 50(15), pp. 2570–2582. doi: 10.1016/j.ejca.2014.06.021.

Hashimoto, K. et al. 2004. Functional Analysis of a Rice Putative Voltage-Dependent Ca2+ Channel, OsTPC1, Expressed in Yeast Cells Lacking its Homologous Gene CCH1. *Plant and Cell Physiology* 45(4), pp. 496–500. doi: 10.1093/pcp/pch053.

von Heijne, G. 1989. Control of topology and mode of assembly of a polytopic membrane protein by positively charged residues. *Nature* 341(6241), pp. 456–458. doi: 10.1038/341456a0.

Hellmich, M.R. and Strumwasser, F. 1991. Purification and characterization of a molluscan egg-specific NADase, a second-messenger enzyme. *Cell Regulation* 2(3), pp. 193–202.

Hjelm, R.P. et al. 1995. Form and structure of self-assembling particles in monoolein-bile salt mixtures. *The Journal of Physical Chemistry* 99(44), pp. 16395–16406. doi: 10.1021/j100044a030.

Hofmann, A.F. 1999. The Continuing Importance of Bile Acids in Liver and Intestinal Disease. *Archives of Internal Medicine* 159(22), pp. 2647–2658. doi: 10.1001/archinte.159.22.2647.

Hofmann, A.F. 2004. Detoxification of lithocholic acid, a toxic bile acid: relevance to drug hepatotoxicity. *Drug Metabolism Reviews* 36(3–4), pp. 703–722. doi: 10.1081/DMR-200033475.

Hohenegger, M. et al. 2002. Nicotinic acid–adenine dinucleotide phosphate activates the skeletal muscle ryanodine receptor. *Biochemical Journal* 367(2), pp. 423–431. doi: 10.1042/bj20020584.

Hooper, R. et al. 2011. Membrane topology of NAADP-sensitive two-pore channels and their regulation by N-linked glycosylation. *The Journal of Biological Chemistry* 286(11), pp. 9141–9149. doi: 10.1074/jbc.M110.189985.

Hooper, R. et al. 2015. TPC1 Knockout Knocks Out TPC1. *Molecular and Cellular Biology* 35(10), pp. 1882–1883. doi: 10.1128/MCB.00020-15.

Hoque, R. et al. 2012. The Sterile Inflammatory Response in Acute Pancreatitis. *Pancreas* 41(3), pp. 353–357. doi: 10.1097/MPA.0b013e3182321500.

Hou, X. et al. 2012. Crystal structure of the calcium release-activated calcium channel Orai. *Science (New York, N.Y.)* 338(6112), pp. 1308–1313. doi: 10.1126/science.1228757.

Housset, C. et al. 2016. Functions of the Gallbladder. *Comprehensive Physiology* 6(3), pp. 1549–1577. doi: 10.1002/cphy.c150050.

Howard, M. et al. 1993. Formation and hydrolysis of cyclic ADP-ribose catalyzed by lymphocyte antigen CD38. *Science (New York, N.Y.)* 262(5136), pp. 1056–1059.

Huang, G.N. et al. 2006. STIM1 carboxyl-terminus activates native SOC, I(crac) and TRPC1 channels. *Nature Cell Biology* 8(9), pp. 1003–1010. doi: 10.1038/ncb1454.

Huang, W. et al. 2017. Caffeine protects against experimental acute pancreatitis by inhibition of inositol 1,4,5-trisphosphate receptor-mediated Ca2+ release. *Gut* 66(2), pp. 301–313. doi: 10.1136/gutjnl-2015-309363.

Hue Su, K. et al. 2006. Review of experimental animal models of acute pancreatitis. *HPB : The Official Journal of the International Hepato Pancreato Biliary Association* 8(4), pp. 264–286. doi: 10.1080/13651820500467358.

Husain, S.Z. et al. 2005. The ryanodine receptor mediates early zymogen activation in pancreatitis. *Proceedings of the National Academy of Sciences of the United States of America* 102(40), pp. 14386–14391. doi: 10.1073/pnas.0503215102.

Ikehata, F. et al. 1998. Autoantibodies against CD38 (ADP-ribosyl cyclase/cyclic ADP-ribose hydrolase) that impair glucose-induced insulin secretion in noninsulin- dependent diabetes patients. *Journal of Clinical Investigation* 102(2), pp. 395–401.

Ikura, M. 1996. Calcium binding and conformational response in EF-hand proteins. *Trends in Biochemical Sciences* 21(1), pp. 14–17. doi: 10.1016/S0968-0004(06)80021-6.

Ilic, M. and Ilic, I. 2016. Epidemiology of pancreatic cancer. *World Journal of Gastroenterology* 22(44), pp. 9694–9705. doi: 10.3748/wjg.v22.i44.9694.

Imagawa, T. et al. 1987. Purified ryanodine receptor from skeletal muscle sarcoplasmic reticulum is the Ca2+-permeable pore of the calcium release channel. *Journal of Biological Chemistry* 262(34), pp. 16636–16643.

Insull, W. 2006. Clinical utility of bile acid sequestrants in the treatment of dyslipidemia: a scientific review. *Southern Medical Journal* 99(3), pp. 257–273. doi: 10.1097/01.smj.0000208120.73327.db.

Irwin, J.J. and Shoichet, B.K. 2005. ZINC − A Free Database of Commercially Available Compounds for Virtual Screening. *Journal of Chemical Information and Modeling* 45(1), pp. 177–182. doi: 10.1021/ci049714+.

Ishibashi, K. et al. 2000. Molecular Cloning of a Novel Form (Two-Repeat) Protein Related to Voltage-Gated Sodium and Calcium Channels. *Biochemical and Biophysical Research Communications* 270(2), pp. 370–376. doi: 10.1006/bbrc.2000.2435.

Ishiguro, H. et al. 2012. Physiology and pathophysiology of bicarbonate secretion by pancreatic duct epithelium. *Nagoya Journal of Medical Science* 74(1–2), pp. 1–18.

Iwanaga, Y. et al. 2006. Living Donor Islet Transplantation, the Alternative Approach to Overcome the Obstacles Limiting Transplant. *Annals of the New York Academy of Sciences* 1079(1), pp. 335–339. doi: 10.1196/annals.1375.051.

Jackson, D.G. and Bell, J.I. 1990. Isolation of a cDNA encoding the human CD38 (T10) molecule, a cell surface glycoprotein with an unusual discontinuous pattern of expression during lymphocyte differentiation. *The Journal of Immunology* 144(7), pp. 2811–2815.

Jacob, R. 1990. Agonist-stimulated divalent cation entry into single cultured human umbilical vein endothelial cells. *The Journal of Physiology* 421, pp. 55–77.

Jaiswal, J.K. 2001. Calcium - how and why? *Journal of biosciences* 26(3), pp. 357–363.

James, O. and Freedman, M. 1977. Studies of hyperimmune restricted and partially restricted anti-pneumococcal polysaccharide antibodies from allotype-defined pedigreed rabbits—V variable region heavy chain sequence analysis of the cyanogen bromide C1 fragment obtained from an unusual restricted anti-SVIII antibody from A homozygous a1 partially inbred rabbit. *Immunochemistry* 14(1), pp. 15–24. doi: 10.1016/0019-2791(77)90328-7.

Jayaraman, T. et al. 1992. FK506 binding protein associated with the calcium release channel (ryanodine receptor). *Journal of Biological Chemistry* 267(14), pp. 9474–9477.

Jha, A. et al. 2014. Convergent regulation of the lysosomal two-pore channel-2 by Mg2+, NAADP, PI(3,5)P2 and multiple protein kinases. *The EMBO Journal* 33(5), pp. 501–511. doi: 10.1002/embj.201387035.

Jiang, Y.-L. et al. 2013. Nicotinic Acid Adenine Dinucleotide Phosphate (NAADP) Activates Global and Heterogeneous Local Ca2+ Signals from NAADP- and Ryanodine Receptor-gated Ca2+ Stores in Pulmonary Arterial Myocytes. *The Journal of Biological Chemistry* 288(15), pp. 10381–10394. doi: 10.1074/jbc.M112.423053.

Joergensen, M. et al. 2010. Incidence, Etiology and Prognosis of First-Time Acute Pancreatitis in Young Patients: A Population-Based Cohort Study. *Pancreatology* 10(4), pp. 453–461. doi: 10.1159/000260666.

Johnson 2005. UK guidelines for the management of acute pancreatitis. *Gut* 54(suppl 3), pp. iii1-iii9. doi: 10.1136/gut.2004.057026.

Johnson, J.D. and Misler, S. 2002. Nicotinic acid-adenine dinucleotide phosphate-sensitive calcium stores initiate insulin signaling in human beta cells. *Proceedings of the National Academy of Sciences* 99(22), pp. 14566–14571. doi: 10.1073/pnas.222099799.

Jura, N. et al. 2005. Chronic pancreatitis, pancreatic adenocarcinoma and the black box in-between. *Cell Research* 15(1), pp. 72–77. doi: 10.1038/sj.cr.7290269.

Kadota, Y. et al. 2004. Identification of putative voltage-dependent Ca2+-permeable channels involved in cryptogein-induced Ca2+ transients and defense responses in tobacco BY-2 cells. *Biochemical and Biophysical Research Communications* 317(3), pp. 823–830. doi: 10.1016/j.bbrc.2004.03.114.

Kaiser, A.M. et al. 1995. Relationship between severity, necrosis, and apoptosis in five models of experimental acute pancreatitis. *American Journal of Physiology - Cell Physiology* 269(5), pp. C1295–C1304.

Kang, R. et al. 2014. Cell Death and DAMPs in Acute Pancreatitis. *Molecular Medicine* 20(1), pp. 466–477. doi: 10.2119/molmed.2014.00117.

Kelu, J.J. et al. 2017. Ca2+ release via two-pore channel type 2 (TPC2) is required for slow muscle cell myofibrillogenesis and myotomal patterning in intact zebrafish embryos. *Developmental Biology* . Available at: http://www.sciencedirect.com/science/article/pii/S0012160616308211 [Accessed: 17 April 2017].

Kendall, J.M. et al. 1996. Recombinant apoaequorin acting as a pseudo-luciferase reports micromolar changes in the endoplasmic reticulum free Ca2+ of intact cells. *Biochemical Journal* 318(2), pp. 383–387. doi: 10.1042/bj3180383.

Keulemans, Y.C. et al. 1998. Hepatic bile versus gallbladder bile: a comparison of protein and lipid concentration and composition in cholesterol gallstone patients. *Hepatology (Baltimore, Md.)* 28(1), pp. 11–16. doi: 10.1002/hep.510280103.

Khalaf, A. and Babiker, F. 2016. Discrepancy in calcium release from the sarcoplasmic reticulum and intracellular acidic stores for the protection of the heart against ischemia/reperfusion injury. *Journal of Physiology and Biochemistry* 72(3), pp. 495–508. doi: 10.1007/s13105-016-0498-0.

Khoo, K.M. et al. 2000. Localization of the Cyclic ADP-ribose-dependent Calcium Signaling Pathway in Hepatocyte Nucleus. *Journal of Biological Chemistry* 275(32), pp. 24807–24817. doi: 10.1074/jbc.M908231199.

Kim, J.Y. et al. 2002. Transporter-mediated bile acid uptake causes Ca2+-dependent cell death in rat pancreatic acinar cells. *Gastroenterology* 122(7), pp. 1941–1953. doi: 10.1053/gast.2002.33617.

Kim, M.S. et al. 2009. Deletion of TRPC3 in mice reduces Store-Operated Ca2+ influx and the severity of acute pancreatitis. *Gastroenterology* 137(4), pp. 1509–1517. doi: 10.1053/j.gastro.2009.07.042.

Kintzer, A.F. and Stroud, R.M. 2016. Structure, inhibition, and regulatory sites of TPC1 from Arabidopsis thaliana. *Nature* 531(7593), pp. 258–262. doi: 10.1038/nature17194.

Kirichok, Y. et al. 2004. The mitochondrial calcium uniporter is a highly selective ion channel. *Nature* 427(6972), pp. 360–364. doi: 10.1038/nature02246.

Klöppel, G. and Maillet, B. 1993. Pathology of acute and chronic pancreatitis. *Pancreas* 8(6), pp. 659–670.

Kluth, D. et al. 2003. The embryology of gut rotation. *Seminars in Pediatric Surgery* 12(4), pp. 275–279.

Kogot-Levin, A. et al. 2009. Mucolipidosis Type IV: The Effect of Increased Lysosomal pH on the Abnormal Lysosomal Storage. *Pediatric Research* 65(6), pp. 686–690. doi: 10.1203/PDR.0b013e3181a1681a.

Kolodecik, T. et al. 2014. Risk factors for pancreatic cancer: underlying mechanisms and potential targets. *Frontiers in Physiology* 4. Available at: http://www.ncbi.nlm.nih.gov/pmc/articles/PMC3893685/ [Accessed: 26 April 2017].

Korolchuk, V.I. et al. 2011. Lysosomal positioning coordinates cellular nutrient responses. *Nature cell biology* 13(4), pp. 453–460. doi: 10.1038/ncb2204.

Koshiyama, H. et al. 1991. Novel mechanism of intracellular calcium release in pituitary cells. *The Journal of biological chemistry* 266(26), pp. 16985–16988.

Krause, E. et al. 1996. Depletion of Intracellular Calcium Stores Activates a Calcium Conducting Nonselective Cation Current in Mouse Pancreatic Acinar Cells. *Journal of Biological Chemistry* 271(51), pp. 32523–32528. doi: 10.1074/jbc.271.51.32523.

Kristiansen, T.Z. et al. 2007. Proteomics of Human Bile. In: FRCPT, V. T. M. ed. *Proteomics of Human Body Fluids*. Humana Press, pp. 399–414. Available at: http://link.springer.com/chapter/10.1007/978-1-59745-432-2_18 [Accessed: 26 April 2017].

Kroemer, G. et al. 2009. Classification of cell death. *Cell death and differentiation* 16(1), pp. 3–11. doi: 10.1038/cdd.2008.150.

Krüger, B. et al. 2000. The Role of Intracellular Calcium Signaling in Premature Protease Activation and the Onset of Pancreatitis. *The American Journal of Pathology* 157(1), pp. 43–50. doi: 10.1016/S0002-9440(10)64515-4.

Kurusu, T. et al. 2004. Identification of a Putative Voltage-Gated Ca2+-permeable Channel (OsTPC1) Involved in Ca2+ Influx and Regulation of Growth and Development in Rice. *Plant and Cell Physiology* 45(6), pp. 693–702. doi: 10.1093/pcp/pch082.

Kwon, S.-K. et al. 2016. Organelle-Specific Sensors for Monitoring Ca2+ Dynamics in Neurons. *Frontiers in Synaptic Neuroscience* 8. Available at: http://www.ncbi.nlm.nih.gov/pmc/articles/PMC5025517/ [Accessed: 24 April 2017].

Lam, A.K.M. et al. 2013. Hax-1 identified as a two-pore channel (TPC)-binding protein. *FEBS Letters* 587(23), pp. 3782–3786. doi: 10.1016/j.febslet.2013.10.031.

Lam, A.K.M. and Galione, A. 2013. The endoplasmic reticulum and junctional membrane communication during calcium signaling. *Biochimica et Biophysica Acta (BBA) - Molecular Cell Research* 1833(11), pp. 2542–2559. doi: 10.1016/j.bbamcr.2013.06.004.

Lammert, F. et al. 2016. Gallstones. *Nature Reviews Disease Primers* 2, p. 16024. doi: 10.1038/nrdp.2016.24.

Lange, I. et al. 2008. Synergistic regulation of endogenous TRPM2 channels by adenine dinucleotides in primary human neutrophils. *Cell Calcium* 44(6), pp. 604–615. doi: 10.1016/j.ceca.2008.05.001.

Lange, I. et al. 2009. TRPM2 Functions as a Lysosomal Ca2+-Release Channel in β Cells. *Science signaling* 2(71), p. ra23. doi: 10.1126/scisignal.2000278.

Langhorst, M.F. et al. 2004. Ca2+ release via ryanodine receptors and Ca2+ entry: major mechanisms in NAADP-mediated Ca2+ signaling in T-lymphocytes. *Cellular Signalling* 16(11), pp. 1283–1289. doi: 10.1016/j.cellsig.2004.03.013.

Lanner, J.T. et al. 2010. Ryanodine Receptors: Structure, Expression, Molecular Details, and Function in Calcium Release. *Cold Spring Harbor Perspectives in Biology* 2(11). Available at: http://www.ncbi.nlm.nih.gov/pmc/articles/PMC2964179/ [Accessed: 22 April 2017].

Larisch, N. et al. 2016. The function of the two-pore channel TPC1 depends on dimerization of its carboxy-terminal helix. *Cellular and Molecular Life Sciences* 73(13), pp. 2565–2581. doi: 10.1007/s00018-016-2131-3.

Lee, H.C. et al. 1989. Structural determination of a cyclic metabolite of NAD+ with intracellular Ca2+-mobilizing activity. *Journal of Biological Chemistry* 264(3), pp. 1608–1615.

Lee, H.C. et al. 1994. Cyclic ADP ribose activation of the ryanodine receptor is mediated by calmodulin. *Nature* 370(6487), pp. 307–309. doi: 10.1038/370307a0.

Lee, H.C. et al. 1997. Caged nicotinic acid adenine dinucleotide phosphate. Synthesis and use. *The Journal of biological chemistry* 272(7), pp. 4172–4178.

Lee, H.C. 1997. Mechanisms of calcium signaling by cyclic ADP-ribose and NAADP. *Physiological Reviews* 77(4), pp. 1133–1164.

Lee, H.C. 2001. Physiological Functions of Cyclic Adp-Ribose and Naadp as Calcium Messengers. *Annual Review of Pharmacology and Toxicology* 41(1), pp. 317–345. doi: 10.1146/annurev.pharmtox.41.1.317.

Lee, H.C. and Aarhus, R. 1991. ADP-ribosyl cyclase: an enzyme that cyclizes NAD+ into a calcium-mobilizing metabolite. *Cell Regulation* 2(3), pp. 203–209.

Lee, H.C. and Aarhus, R. 1995. A Derivative of NADP Mobilizes Calcium Stores Insensitive to Inositol Trisphosphate and Cyclic ADP-ribose. *Journal of Biological Chemistry* 270(5), pp. 2152–2157. doi: 10.1074/jbc.270.5.2152.

Lee, H.C. and Aarhus, R. 1997. Structural Determinants of Nicotinic Acid Adenine Dinucleotide Phosphate Important for Its Calcium-mobilizing Activity. *Journal of Biological Chemistry* 272(33), pp. 20378–20383. doi: 10.1074/jbc.272.33.20378.

Lee, H.C. and Aarhus, R. 1998. Fluorescent analogs of NAADP with calcium mobilizing activity. *Biochimica et Biophysica Acta (BBA) - General Subjects* 1425(1), pp. 263–271. doi: 10.1016/S0304-4165(98)00079-8.

Lee, J.-H. et al. 2015. Presenilin 1 Maintains Lysosomal Ca2+ Homeostasis via TRPML1 by Regulating vATPase-Mediated Lysosome Acidification. *Cell Reports* 12(9), pp. 1430–1444. doi: 10.1016/j.celrep.2015.07.050.

Lee, M.G. et al. 1997. Polarized expression of Ca2+ channels in pancreatic and salivary gland cells. Correlation with initiation and propagation of [Ca2+]i waves. *The Journal of Biological Chemistry* 272(25), pp. 15765–15770.

Lefebvre, P. et al. 2009. Role of bile acids and bile acid receptors in metabolic regulation. *Physiological Reviews* 89(1), pp. 147–191. doi: 10.1152/physrev.00010.2008.

Leite, M.F. et al. 1999. Expression and subcellular localization of the ryanodine receptor in rat pancreatic acinar cells. *The Biochemical Journal* 337 (Pt 2), pp. 305–309.

Lerch, M.M. et al. 1993. Pancreatic duct obstruction triggers acute necrotizing pancreatitis in the opossum. *Gastroenterology* 104(3), pp. 853–861.

Lerch, M.M. and Gorelick, F.S. 2013. Models of Acute and Chronic Pancreatitis. *Gastroenterology* 144(6), pp. 1180–1193. doi: 10.1053/j.gastro.2012.12.043.

Leung, P.S. and Ip, S.P. 2006. Pancreatic acinar cell: Its role in acute pancreatitis. *The International Journal of Biochemistry & Cell Biology* 38(7), pp. 1024–1030. doi: 10.1016/j.biocel.2005.12.001.

Lewarchik, C.M. et al. 2014. The ryanodine receptor is expressed in human pancreatic acinar cells and contributes to acinar cell injury. *American Journal of Physiology - Gastrointestinal and Liver Physiology* 307(5), pp. G574–G581. doi: 10.1152/ajpgi.00143.2014.

Lewis, M.P. et al. 1998. Pancreatic blood flow and its role in the pathophysiology of pancreatitis. *The Journal of Surgical Research* 75(1), pp. 81–89. doi: 10.1006/jsre.1998.5268.

Li, J. et al. 2014. Calcium signaling of pancreatic acinar cells in the pathogenesis of pancreatitis. *World Journal of Gastroenterology : WJG* 20(43), pp. 16146–16152. doi: 10.3748/wjg.v20.i43.16146.

Liao, Y. et al. 2007. Orai proteins interact with TRPC channels and confer responsiveness to store depletion. *Proceedings of the National Academy of Sciences of the United States of America* 104(11), pp. 4682–4687. doi: 10.1073/pnas.0611692104.

Liddle, R.A. 1997. Cholecystokinin cells. *Annual review of physiology* 59, pp. 221–242. doi: 10.1146/annurev.physiol.59.1.221.

Lin-Moshier, Y. et al. 2012. Photoaffinity Labeling of Nicotinic Acid Adenine Dinucleotide Phosphate (NAADP) Targets in Mammalian Cells♦. *The Journal of Biological Chemistry* 287(4), pp. 2296–2307. doi: 10.1074/jbc.M111.305813.

Lin-Moshier, Y. et al. 2014. The Two-pore channel (TPC) interactome unmasks isoform-specific roles for TPCs in endolysosomal morphology and cell pigmentation. *Proceedings of the National Academy of Sciences of the United States of America* 111(36), pp. 13087–13092. doi: 10.1073/pnas.1407004111.

Liou, J. et al. 2005. STIM Is a Ca2+ Sensor Essential for Ca2+-Store-Depletion-Triggered Ca2+ Influx. *Current Biology* 15(13), pp. 1235–1241. doi: 10.1016/j.cub.2005.05.055.

Lloyd-Evans, E. et al. 2008. Niemann-Pick disease type C1 is a sphingosine storage disease that causes deregulation of lysosomal calcium. *Nature Medicine* 14(11), pp. 1247–1255. doi: 10.1038/nm.1876.

López, E. et al. 2013. FKBP52 is involved in the regulation of SOCE channels in the human platelets and MEG 01 cells. *Biochimica et Biophysica Acta (BBA) - Molecular Cell Research* 1833(3), pp. 652–662. doi: 10.1016/j.bbamcr.2012.11.029.

López, J.J. et al. 2006. Two distinct Ca2+ compartments show differential sensitivity to thrombin, ADP and vasopressin in human platelets. *Cellular Signalling* 18(3), pp. 373–381. doi: 10.1016/j.cellsig.2005.05.006.

López, J.J. et al. 2012. Two-pore channel 2 (TPC2) modulates store-operated Ca2 + entry. *Biochimica et Biophysica Acta (BBA) - Molecular Cell Research* 1823(10), pp. 1976–1983. doi: 10.1016/j.bbamcr.2012.08.002.

Love, J.A. et al. 2007. Autonomic pathways regulating pancreatic exocrine secretion. *Autonomic Neuroscience: Basic & Clinical* 133(1), pp. 19–34. doi: 10.1016/j.autneu.2006.10.001.

Low, J.T. et al. 2010. Pancreatic acinar cell: New insights into the control of secretion. *The International Journal of Biochemistry & Cell Biology* 42(10), pp. 1586–1589. doi: 10.1016/j.biocel.2010.07.006.

Lowenfels, A.B. et al. 1997. Hereditary pancreatitis and the risk of pancreatic cancer. International Hereditary Pancreatitis Study Group. *Journal of the National Cancer Institute* 89(6), pp. 442–446.

Lowenfels, A.B. et al. 2005. The epidemiology and impact of pancreatic diseases in the United States. *Current Gastroenterology Reports* 7(2), pp. 90–95.

Lu, Y. et al. 2013. Two Pore Channel 2 (TPC2) Inhibits Autophagosomal-Lysosomal Fusion by Alkalinizing Lysosomal pH. *The Journal of Biological Chemistry* 288(33), pp. 24247–24263. doi: 10.1074/jbc.M113.484253.

Lugea, A. et al. 2003. Nonoxidative ethanol metabolites alter extracellular matrix protein content in rat pancreas. *Gastroenterology* 125(6), pp. 1845–1859.

Luik, R.M. et al. 2006. The elementary unit of store-operated Ca2+ entry: local activation of CRAC channels by STIM1 at ER-plasma membrane junctions. *The Journal of Cell Biology* 174(6), pp. 815–825. doi: 10.1083/jcb.200604015.

Luik, R.M. et al. 2008. Oligomerization of STIM1 couples ER calcium depletion to CRAC channel activation. *Nature* 454(7203), pp. 538–542. doi: 10.1038/nature07065.

Lukyanenko, V. et al. 2001. Potentiation of Ca(2+) release by cADP-ribose in the heart is mediated by enhanced SR Ca(2+) uptake into the sarcoplasmic reticulum. *Circulation research* 89(7), pp. 614–622.

Lur, G. et al. 2011. InsP3 receptors and Orai channels in pancreatic acinar cells: co-localization and its consequences. *Biochemical Journal* 436(2), pp. 231–239. doi: 10.1042/BJ20110083.

Macgregor, A. et al. 2007. NAADP Controls Cross-talk between Distinct Ca2+ Stores in the Heart. *Journal of Biological Chemistry* 282(20), pp. 15302–15311. doi: 10.1074/jbc.M611167200.

MacMillan, D. et al. 2005. In smooth muscle, FK506-binding protein modulates IP3 receptor-evoked Ca2+ release by mTOR and calcineurin. *Journal of Cell Science* 118(23), pp. 5443–5451. doi: 10.1242/jcs.02657.

Mahaut-Smith, M.P. et al. 2016. Calcium Signalling through Ligand-Gated Ion Channels such as P2X1 Receptors in the Platelet and other Non-Excitable Cells. *Advances in Experimental Medicine and Biology* 898, pp. 305–329. doi: 10.1007/978-3-319-26974-0_13.

Mahmud, A. and Feely, J. 2001. Acute Effect of Caffeine on Arterial Stiffness and Aortic Pressure Waveform. *Hypertension* 38(2), pp. 227–231. doi: 10.1161/01.HYP.38.2.227.

Maisonneuve, P. and Lowenfels, A.B. 2015. Risk factors for pancreatic cancer: a summary review of meta-analytical studies. *International Journal of Epidemiology* 44(1), pp. 186–198. doi: 10.1093/ije/dyu240.

Malavasi, F. et al. 2008. Evolution and Function of the ADP Ribosyl Cyclase/CD38 Gene Family in Physiology and Pathology. *Physiological Reviews* 88(3), pp. 841–886. doi: 10.1152/physrev.00035.2007.

Malhotra, L. et al. 2015. The Pathogenesis, Diagnosis, and Management of Pancreatic Cancer. *Journal of Gastrointestinal & Digestive System* 2015. Available at: https://www.omicsonline.org/peer-reviewed/the-pathogenesis-diagnosis-and-management-of-pancreatic-cancer-47616.html [Accessed: 26 April 2017].

Mareninova, O.A. et al. 2009. Impaired autophagic flux mediates acinar cell vacuole formation and trypsinogen activation in rodent models of acute pancreatitis. *The Journal of Clinical Investigation* 119(11), pp. 3340–3355. doi: 10.1172/JCI38674.

Marks, A.R. 1996. Cellular functions of immunophilins. *Physiological Reviews* 76(3), pp. 631–649.

Masamune, A. and Shimosegawa, T. 2013. Pancreatic stellate cells--multi-functional cells in the pancreas. *Pancreatology: official journal of the International Association of Pancreatology (IAP) ... [et al.]* 13(2), pp. 102–105. doi: 10.1016/j.pan.2012.12.058.

Masgrau, R. et al. 2003. NAADP. *Current Biology* 13(3), pp. 247–251. doi: 10.1016/S0960-9822(03)00041-1.

Mastracci, T.L. and Sussel, L. 2012. The Endocrine Pancreas: insights into development, differentiation and diabetes. *Wiley interdisciplinary reviews. Membrane transport and signaling* 1(5), pp. 609–628. doi: 10.1002/wdev.44.

Matozaki, T. et al. 1990. Two functionally distinct cholecystokinin receptors show different modes of action on Ca2+ mobilization and phospholipid hydrolysis in isolated rat pancreatic acini. Studies using a new cholecystokinin analog, JMV-180. *The Journal of biological chemistry* 265(11), pp. 6247–6254.

Matthews, G. et al. 1989. Second messenger-activated calcium influx in rat peritoneal mast cells. *The Journal of Physiology* 418, pp. 105–130.

Meda, P. et al. 1983. Short and reversible uncoupling evokes little change in the gap junctions of pancreatic acinar cells. *Journal of Ultrastructure Research* 83(1), pp. 69–84.

Meda, P. 1996. Gap junction involvement in secretion: the pancreas experience. *Clinical and Experimental Pharmacology & Physiology* 23(12), pp. 1053–1057.

Mehra, D. et al. 2014. Multiple modes of ryanodine receptor 2 inhibition by flecainide. *Molecular Pharmacology* 86(6), pp. 696–706. doi: 10.1124/mol.114.094623.

Meis, S. et al. 2010. NF546 [4,4'-(carbonylbis(imino-3,1-phenylene-carbonylimino-3,1-(4-methyl-phenylene)-carbonylimino))-bis(1,3-xylene-alpha,alpha'-diphosphonic acid) tetrasodium salt] is a non-nucleotide P2Y11 agonist and stimulates release of interleukin-8 from human monocyte-derived dendritic cells. *The Journal of Pharmacology and Experimental Therapeutics* 332(1), pp. 238–247. doi: 10.1124/jpet.109.157750.

Meissner, G. 1984. Adenine nucleotide stimulation of Ca2+-induced Ca2+ release in sarcoplasmic reticulum. *Journal of Biological Chemistry* 259(4), pp. 2365–2374.

Mészáros, L.G. et al. 1993. Cyclic ADP-ribose as an endogenous regulator of the non-skeletal type ryanodine receptor Ca2+ channel. *Nature* 364(6432), pp. 76–79. doi: 10.1038/364076a0.

Michon, L. et al. 2005. Involvement of gap junctional communication in secretion. *Biochimica et Biophysica Acta (BBA) - Biomembranes* 1719(1–2), pp. 82–101. doi: 10.1016/j.bbamem.2005.11.003.

Miedel, M.T. et al. 2006. Posttranslational cleavage and adaptor protein complex-dependent trafficking of mucolipin-1. *The Journal of Biological Chemistry* 281(18), pp. 12751–12759. doi: 10.1074/jbc.M511104200.

Mignery, G.A. and Südhof, T.C. 1990. The ligand binding site and transduction mechanism in the inositol-1,4,5-triphosphate receptor. *The EMBO Journal* 9(12), pp. 3893–3898.

Milner, R.E. et al. 1992. Calcium binding proteins in the sarcoplasmic/endoplasmic reticulum of muscle and nonmuscle cells. *Molecular and Cellular Biochemistry* 112(1), pp. 1–13. doi: 10.1007/BF00229637.

Minta, A. et al. 1989. Fluorescent indicators for cytosolic calcium based on rhodamine and fluorescein chromophores. *The Journal of Biological Chemistry* 264(14), pp. 8171–8178.

Mitchell, K.J. et al. 2003. Ryanodine Receptor Type I and Nicotinic Acid Adenine Dinucleotide Phosphate Receptors Mediate Ca2+ Release from Insulin-containing Vesicles in Living Pancreatic β-Cells (MIN6). *Journal of Biological Chemistry* 278(13), pp. 11057–11064. doi: 10.1074/jbc.M210257200.

Miyawaki, A. et al. 1997. Fluorescent indicators for Ca2+based on green fluorescent proteins and calmodulin. *Nature* 388(6645), pp. 882–887. doi: 10.1038/42264.

Moccia, F. et al. 2004. NAADP triggers the fertilization potential in starfish oocytes. *Cell Calcium* 36(6), pp. 515–524. doi: 10.1016/j.ceca.2004.05.004.

Mogami, H. et al. 1997. Ca2+ flow via tunnels in polarized cells: recharging of apical Ca2+ stores by focal Ca2+ entry through basal membrane patch. *Cell* 88(1), pp. 49–55.

Mojžišová, A. et al. 2001. Effect of nicotinic acid adenine dinucleotide phosphate on ryanodine calcium release channel in heart. *Pflügers Archiv* 441(5), pp. 674–677. doi: 10.1007/s004240000465.

Moreland, B.H. and Sanyal, K.K. 1985. pH dependence of the autoactivation of trypsinogen in the presence of bile acids. *Biochemical Society Transactions* 13(6), pp. 1147–1148. doi: 10.1042/bst0131147.

Moreschi, I. et al. 2006. Extracellular NAD+ is an agonist of the human P2Y11 purinergic receptor in human granulocytes. *The Journal of Biological Chemistry* 281(42), pp. 31419–31429. doi: 10.1074/jbc.M606625200.

Moreschi, I. et al. 2008. NAADP+ is an agonist of the human P2Y11 purinergic receptor. *Cell Calcium* 43(4), pp. 344–355. doi: 10.1016/j.ceca.2007.06.006.

Morgan, A. and Galione, A. 2014. Preparation and Use of Sea Urchin Egg Homogenates. In: Carroll, D. J. and Stricker, S. A. eds. *Developmental Biology of the Sea Urchin and Other Marine Invertebrates*. Methods in Molecular Biology. Humana Press, pp. 161–173. Available at: http://dx.doi.org/10.1007/978-1-62703-974-1_10 [Accessed: 5 April 2017].

Mori, Y. et al. 2002. Transient receptor potential 1 regulates capacitative Ca(2+) entry and Ca(2+) release from endoplasmic reticulum in B lymphocytes. *The Journal of Experimental Medicine* 195(6), pp. 673–681.

Morise, H. et al. 1974. Intermolecular energy transfer in the bioluminescent system of Aequorea. *Biochemistry* 13(12), pp. 2656–2662. doi: 10.1021/bi00709a028.

Mourey, R.J. et al. 1990. Purification and characterization of the inositol 1,4,5-trisphosphate receptor protein from rat vas deferens. *Biochemical Journal* 272(2), pp. 383–389.

Muallem, S. et al. 1988. Role of Na+/Ca2+ exchange and the plasma membrane Ca2+ pump in hormone-mediated Ca2+ efflux from pancreatic acini. *The Journal of Membrane Biology* 102(2), pp. 153–162. doi: 10.1007/BF01870453.

Muili, K.A., Wang, D., et al. 2013. Bile Acids Induce Pancreatic Acinar Cell Injury and Pancreatitis by Activating Calcineurin. *Journal of Biological Chemistry* 288(1), pp. 570–580. doi: 10.1074/jbc.M112.428896.

Muili, K.A., Jin, S., et al. 2013. Pancreatic acinar cell NF-κB activation due to bile acid exposure is dependent on calcineurin. *Journal of Biological Chemistry* , p. jbc.M113.471425. doi: 10.1074/jbc.M113.471425.

Mukherjee, R. et al. 2008. Mitochondrial injury in pancreatitis. *Cell Calcium* 44(1), pp. 14–23. doi: 10.1016/j.ceca.2007.11.013.

Mukherjee, R. et al. 2016. Mechanism of mitochondrial permeability transition pore induction and damage in the pancreas: inhibition prevents acute pancreatitis by protecting production of ATP. *Gut* 65(8), pp. 1333–1346. doi: 10.1136/gutjnl-2014-308553.

Mullins, F.M. and Lewis, R.S. 2016. The inactivation domain of STIM1 is functionally coupled with the Orai1 pore to enable Ca2+-dependent inactivation. *The Journal of General Physiology* 147(2), pp. 153–164. doi: 10.1085/jgp.201511438.

Murtaugh, L.C. 2014. Pathogenesis of Pancreatic Cancer: Lessons from Animal Models. *Toxicologic pathology* 42(1), pp. 217–228. doi: 10.1177/0192623313508250.

Nair, R.J. et al. 2007. Chronic pancreatitis. *American Family Physician* 76(11), pp. 1679–1688.

Nathanson, M.H. et al. 1994. Localization of the type 3 inositol 1,4,5-trisphosphate receptor in the Ca2+ wave trigger zone of pancreatic acinar cells. *The Journal of Biological Chemistry* 269(7), pp. 4693–4696.

Navazio, L. et al. 2000. Calcium release from the endoplasmic reticulum of higher plants elicited by the NADP metabolite nicotinic acid adenine dinucleotide phosphate. *Proceedings of the National Academy of Sciences* 97(15), pp. 8693–8698. doi: 10.1073/pnas.140217897.

Naylor, E. et al. 2009. Identification of a chemical probe for NAADP by virtual screening. *Nature chemical biology* 5(4), pp. 220–226. doi: 10.1038/nchembio.150.

Nebel, M. et al. 2013. Nicotinic Acid Adenine Dinucleotide Phosphate (NAADP)-mediated Calcium Signaling and Arrhythmias in the Heart Evoked by β-Adrenergic Stimulation. *Journal of Biological Chemistry* 288(22), pp. 16017–16030. doi: 10.1074/jbc.M112.441246.

Nebel, M. et al. 2015. Calcium Signalling Triggered by NAADP in T Cells Determines Cell Shape and Motility During Immune Synapse Formation. *Messenger (Los Angeles, Calif.: Print)* 4(1), pp. 104–111. doi: 10.1166/msr.2015.1045.

Nguyen, O.N.P. et al. 2017. Two-Pore Channel Function Is Crucial for the Migration of Invasive Cancer Cells. *Cancer Research* 77(6), pp. 1427–1438. doi: 10.1158/0008-5472.CAN-16-0852.

Nguyen, T. et al. 1998. Role of Ca2+/K+ ion exchange in intracellular storage and release of Ca2+. *Nature* 395(6705), pp. 908–912. doi: 10.1038/27686.

Nicholls, A. et al. 2004. Variable selection and model validation of 2D and 3D molecular descriptors> *Journal of Computer-Aided Molecular Design* 18(7–9), pp. 451–474. doi: 10.1007/s10822-004-5202-8.

Nicotera, P. et al. 1998. Intracellular ATP, a switch in the decision between apoptosis and necrosis. *Toxicology Letters* 102–103, pp. 139–142.

Noguchi, N. et al. 1997. Cyclic ADP-ribose binds to FK506-binding protein 12.6 to release Ca2+ from islet microsomes. *The Journal of Biological Chemistry* 272(6), pp. 3133–3136.

Nomikos, M. et al. 2012. Starting a new life: sperm PLC-zeta mobilizes the Ca2+ signal that induces egg activation and embryo development: an essential phospholipase C with implications for male infertility. *BioEssays: News and Reviews in Molecular, Cellular and Developmental Biology* 34(2), pp. 126–134. doi: 10.1002/bies.201100127.

Odinokova, I. et al. 2009. Mechanisms regulating cytochrome c release in pancreatic mitochondria. *Gut* 58(3), pp. 431–442. doi: 10.1136/gut.2007.147207.

Ogunbayo, O.A. et al. 2011. Cyclic Adenosine Diphosphate Ribose Activates Ryanodine Receptors, whereas NAADP Activates Two-pore Domain Channels. *The Journal of Biological Chemistry* 286(11), pp. 9136–9140. doi: 10.1074/jbc.M110.202002.

Ogunbayo, O.A. et al. 2015. Organelle-specific Subunit Interactions of the Vertebrate Two-pore Channel Family. *The Journal of Biological Chemistry* 290(2), pp. 1086–1095. doi: 10.1074/jbc.M114.610493.

Okorokov, L.A. et al. 2001. Ca2+ and H+ homeostasis in fission yeast: a role of Ca2+/H+ exchange and distinct V-H+-ATPases of the secretory pathway organelles. *FEBS Letters* 505(2), pp. 321–324. doi: 10.1016/S0014-5793(01)02852-6.

Omary, M.B. et al. 2007. The pancreatic stellate cell: a star on the rise in pancreatic diseases. *Journal of Clinical Investigation* 117(1), pp. 50–59. doi: 10.1172/JCI30082.

O'Morchoe, C.C. 1997. Lymphatic system of the pancreas. *Microscopy Research and Technique* 37(5–6), pp. 456–477. doi: 10.1002/(SICI)1097-0029(19970601)37:5/6<456::AID-JEMT9>3.0.CO;2-B.

Ong, S.L. et al. 2009. Total pancreatectomy with islet autotransplantation: an overview. *HPB : The Official Journal of the International Hepato Pancreato Biliary Association* 11(8), pp. 613–621. doi: 10.1111/j.1477-2574.2009.00113.x.

Orabi, A.I. et al. 2010. Dantrolene mitigates caerulein-induced pancreatitis in vivo in mice. *American Journal of Physiology - Gastrointestinal and Liver Physiology* 299(1), pp. G196–G204. doi: 10.1152/ajpgi.00498.2009.

Orabi, A.I. et al. 2013. Cluster of Differentiation 38 (CD38) Mediates Bile Acid-induced Acinar Cell Injury and Pancreatitis through Cyclic ADP-ribose and Intracellular Calcium Release. *Journal of Biological Chemistry* 288(38), pp. 27128–27137. doi: 10.1074/jbc.M113.494534.

Orciani, M. et al. 2008. CD38 is constitutively expressed in the nucleus of human hematopoietic cells. *Journal of Cellular Biochemistry* 105(3), pp. 905–912. doi: 10.1002/jcb.21887.

Ortolan, E. et al. 2002. CD157, the Janus of CD38 but with a unique personality. *Cell biochemistry and function* 20(4), pp. 309–322. doi: 10.1002/cbf.978.

Pandol, S.J. et al. 2007. Acute pancreatitis: bench to the bedside. *Gastroenterology* 132(3), pp. 1127–1151. doi: 10.1053/j.gastro.2007.01.055.

Pandol, S.J. 2010. *Digestive Enzymes*. Morgan & Claypool Life Sciences. Available at: https://www.ncbi.nlm.nih.gov/books/NBK54127/ [Accessed: 25 April 2017].

Paredes, R.M. et al. 2008. Chemical calcium indicators. *Methods* 46(3), pp. 143–151. doi: 10.1016/j.ymeth.2008.09.025.

Parekh, A.B. and Putney, J.W. 2005. Store-Operated Calcium Channels. *Physiological Reviews* 85(2), pp. 757–810. doi: 10.1152/physrev.00057.2003.

Park, D. et al. 1993. Activation of phospholipase C isozymes by G protein beta gamma subunits. *The Journal of Biological Chemistry* 268(7), pp. 4573–4576.

Park, M.K. et al. 2001. Local uncaging of caged Ca2+ reveals distribution of Ca2+-activated Cl− channels in pancreatic acinar cells. *Proceedings of the National Academy of Sciences* 98(19), pp. 10948–10953. doi: 10.1073/pnas.181353798.

Parker, I. and Ivorra, I. 1991. Caffeine inhibits inositol trisphosphate-mediated liberation of intracellular calcium in Xenopus oocytes. *The Journal of Physiology* 433(1), pp. 229–240. doi: 10.1113/jphysiol.1991.sp018423.

Parker, N.J. et al. 1996. Molecular cloning of a novel human gene (D11S4896E) at chromosomal region 11p15.5. *Genomics* 37(2), pp. 253–256. doi: 10.1006/geno.1996.0553.

Parkesh, R. et al. 2008. Cell-permeant NAADP: A novel chemical tool enabling the study of Ca2+ signalling in intact cells. *Cell Calcium* 43(6), pp. 531–538. doi: 10.1016/j.ceca.2007.08.006.

Patel, S. et al. 2000. Widespread Distribution of Binding Sites for the Novel Ca2+-mobilizing Messenger, Nicotinic Acid Adenine Dinucleotide Phosphate, in the Brain. *Journal of Biological Chemistry* 275(47), pp. 36495–36497. doi: 10.1074/jbc.C000458200.

Patel, S. and Docampo, R. 2010. Acidic calcium stores open for business: expanding the potential for intracellular Ca2+ signaling. *Trends in cell biology* 20(5), pp. 277–286. doi: 10.1016/j.tcb.2010.02.003.

Payandeh, J. et al. 2011. THE CRYSTAL STRUCTURE OF A VOLTAGE-GATED SODIUM CHANNEL. *Nature* 475(7356), pp. 353–358. doi: 10.1038/nature10238.

Peiter, E. et al. 2005. The vacuolar Ca2+-activated channel TPC1 regulates germination and stomatal movement. *Nature* 434(7031), pp. 404–408. doi: 10.1038/nature03381.

Pelletier, G. 1977. Identification of Four Cell Types in the Human Endocrine Pancreas By Immunoelectron Microscopy. *Diabetes* 26(8), pp. 749–756. doi: 10.2337/diab.26.8.749.

Penna, A. et al. 2008. The CRAC channel consists of a tetramer formed by Stim-induced dimerization of Orai dimers. *Nature* 456(7218), pp. 116–120. doi: 10.1038/nature07338.

Penner, R. et al. 1988. Regulation of calcium influx by second messengers in rat mast cells. *Nature* 334(6182), pp. 499–504. doi: 10.1038/334499a0.

Pereira, G.J.S. et al. 2011. Nicotinic Acid Adenine Dinucleotide Phosphate (NAADP) Regulates Autophagy in Cultured Astrocytes. *The Journal of Biological Chemistry* 286(32), pp. 27875–27881. doi: 10.1074/jbc.C110.216580.

Pereira, G.J.S. et al. 2014. NAADP-sensitive two-pore channels are present and functional in gastric smooth muscle cells. *Cell Calcium* 56(2), pp. 51–58. doi: 10.1016/j.ceca.2014.04.005.

Pereira, G.J.S. et al. 2016. Glutamate induces autophagy via the two-pore channels in neural cells. *Oncotarget* 8(8), pp. 12730–12740. doi: 10.18632/oncotarget.14404.

Perez-Terzic, C.M. et al. 1995. Ca2+ release triggered by nicotinate adenine dinucleotide phosphate in intact sea urchin eggs. *Biochemical Journal* 312(Pt 3), pp. 955–959.

Periasamy, M. and Kalyanasundaram, A. 2007. SERCA pump isoforms: their role in calcium transport and disease. *Muscle & nerve* 35(4), pp. 430–442. doi: 10.1002/mus.20745.

Perides, G. et al. 2010. Biliary Acute Pancreatitis in Mice is Mediated by the G-Protein−Coupled Cell Surface Bile Acid Receptor Gpbar1. *Gastroenterology* 138(2), pp. 715–725. doi: 10.1053/j.gastro.2009.10.052.

Petersen, O.H. et al. 2011. Pathobiology of acute pancreatitis: focus on intracellular calcium and calmodulin. *F1000 Medicine Reports* 3. Available at: http://www.ncbi.nlm.nih.gov/pmc/articles/PMC3155209/ [Accessed: 25 April 2017].

Petersen, O.H. and Sutton, R. 2006. Ca2+ signalling and pancreatitis: effects of alcohol, bile and coffee. *Trends in Pharmacological Sciences* 27(2), pp. 113–120. doi: 10.1016/j.tips.2005.12.006.

Petersen, O.H. and Tepikin, A.V. 2008. Polarized calcium signaling in exocrine gland cells. *Annual Review of Physiology* 70, pp. 273–299. doi: 10.1146/annurev.physiol.70.113006.100618.

Petersen, O.H. and Ueda, N. 1976. Pancreatic acinar cells: the role of calcium in stimulus-secretion coupling. *The Journal of Physiology* 254(3), pp. 583–606. doi: 10.1113/jphysiol.1976.sp011248.

Philipp, S. et al. 2003. TRPC3 mediates T-cell receptor-dependent calcium entry in human T-lymphocytes. *The Journal of Biological Chemistry* 278(29), pp. 26629–26638. doi: 10.1074/jbc.M304044200.

Pictet, R.L. et al. 1972. An ultrastructural analysis of the developing embryonic pancreas. *Developmental Biology* 29(4), pp. 436–467.

Pitt, S.J. et al. 2010. TPC2 Is a Novel NAADP-sensitive Ca2+ Release Channel, Operating as a Dual Sensor of Luminal pH and Ca2+. *Journal of Biological Chemistry* 285(45), pp. 35039–35046. doi: 10.1074/jbc.M110.156927.

Pitt, S.J. et al. 2014. Reconstituted Human TPC1 Is a Proton-Permeable Ion Channel and Is Activated by NAADP or Ca2+. *Sci. Signal.* 7(326), pp. ra46-ra46. doi: 10.1126/scisignal.2004854.

Ploegh, H.L. 2007. A lipid-based model for the creation of an escape hatch from the endoplasmic reticulum. *Nature* 448(7152), pp. 435–438. doi: 10.1038/nature06004.

Ponnappa, B.C. et al. 1981. Characterization of an ATP-dependent Ca2+ uptake system in mouse pancreatic microsomes. *American Journal of Physiology - Gastrointestinal and Liver Physiology* 240(2), pp. G122–G129.

Prakriya, M. and Lewis, R.S. 2015. Store-Operated Calcium Channels. *Physiological Reviews* 95(4), pp. 1383–1436. doi: 10.1152/physrev.00020.2014.

Prasher, D.C. et al. 1992. Primary structure of the Aequorea victoria green-fluorescent protein. *Gene* 111(2), pp. 229–233. doi: 10.1016/0378-1119(92)90691-H.

Prince, W.T. et al. 1972. Role of Calcium and Adenosine-3′:5′-Cyclic Monophosphate in Controlling Fly Salivary Gland Secretion. *Proceedings of the National Academy of Sciences* 69(3), pp. 553–557.

Prins, D. and Michalak, M. 2011. Organellar Calcium Buffers. *Cold Spring Harbor Perspectives in Biology* 3(3). Available at: http://www.ncbi.nlm.nih.gov/pmc/articles/PMC3039927/ [Accessed: 23 April 2017].

Pryor, P.R. et al. 2006. Mucolipin-1 Is a Lysosomal Membrane Protein Required for Intracellular Lactosylceramide Traffic. *Traffic* 7(10), pp. 1388–1398. doi: 10.1111/j.1600-0854.2006.00475.x.

Puri, S. and Hebrok, M. 2010. Cellular plasticity within the pancreas--lessons learned from development. *Developmental Cell* 18(3), pp. 342–356. doi: 10.1016/j.devcel.2010.02.005.

Putney, J.W. 1986. A model for receptor-regulated calcium entry. *Cell Calcium* 7(1), pp. 1–12.

Rahman, T. et al. 2014. Two-pore channels provide insight into the evolution of voltage-gated Ca2+ and Na+ channels. *Science signaling* 7(352), p. ra109. doi: 10.1126/scisignal.2005450.

Raimondi, S. et al. 2010. Pancreatic cancer in chronic pancreatitis; aetiology, incidence, and early detection. *Best Practice & Research Clinical Gastroenterology* 24(3), pp. 349–358. doi: 10.1016/j.bpg.2010.02.007.

Rao, M.S. et al. 1988. Almost total conversion of pancreas to liver in the adult rat: A reliable model to study transdifferentiation. *Biochemical and Biophysical Research Communications* 156(1), pp. 131–136. doi: 10.1016/S0006-291X(88)80814-3.

Rapuri, P.B. et al. 2001. Caffeine intake increases the rate of bone loss in elderly women and interacts with vitamin D receptor genotypes. *The American Journal of Clinical Nutrition* 74(5), pp. 694–700.

Raraty, M. et al. 2000. Calcium-dependent enzyme activation and vacuole formation in the apical granular region of pancreatic acinar cells. *Proceedings of the National Academy of Sciences* 97(24), pp. 13126–13131. doi: 10.1073/pnas.97.24.13126.

Redinger, R.N. 2003. The coming of age of our understanding of the enterohepatic circulation of bile salts. *American Journal of Surgery* 185(2), pp. 168–172.

Rhee, S.G. 2001. Regulation of phosphoinositide-specific phospholipase C. *Annual review of biochemistry* 70, pp. 281–312. doi: 10.1146/annurev.biochem.70.1.281.

Rice, L.V. et al. 2013. Characterization of selective Calcium-Release Activated Calcium channel blockers in mast cells and T-cells from human, rat, mouse and guinea-pig preparations. *European Journal of Pharmacology* 704(1–3), pp. 49–57. doi: 10.1016/j.ejphar.2013.02.022.

Ridlon, J.M. et al. 2014. Bile Acids and the Gut Microbiome. *Current opinion in gastroenterology* 30(3), pp. 332–338. doi: 10.1097/MOG.0000000000000057.

Rietdorf, K. et al. 2011. Two-pore Channels Form Homo- and Heterodimers♦. *The Journal of Biological Chemistry* 286(43), pp. 37058–37062. doi: 10.1074/jbc.C111.289835.

Rinderknecht, H. 1986. Activation of pancreatic zymogens. Normal activation, premature intrapancreatic activation, protective mechanisms against inappropriate activation. *Digestive Diseases and Sciences* 31(3), pp. 314–321.

Rindler, M.J. 2001. Isolation of Zymogen Granules from Rat Pancreas. In: *Current Protocols in Cell Biology*. John Wiley & Sons, Inc. Available at: http://onlinelibrary.wiley.com/doi/10.1002/0471143030.cb0318s29/abstract [Accessed: 25 April 2017].

Ringer, S. 1883. A further Contribution regarding the influence of the different Constituents of the Blood on the Contraction of the Heart. *The Journal of Physiology* 4(1), pp. 29–42.

Roberts-Thomson, S.J. et al. 2010. ORAI-mediated calcium entry: mechanism and roles, diseases and pharmacology. *Pharmacology & Therapeutics* 127(2), pp. 121–130. doi: 10.1016/j.pharmthera.2010.04.016.

Robinson, B.K. et al. 2016. Quantitative analysis of 3D extracellular matrix remodelling by pancreatic stellate cells. *Biology Open* 5(6), pp. 875–882. doi: 10.1242/bio.017632.

Ronco, V. et al. 2015. A novel Ca2+-mediated cross-talk between endoplasmic reticulum and acidic organelles: Implications for NAADP-dependent Ca2+ signalling. *Cell Calcium* 57(2), pp. 89–100. doi: 10.1016/j.ceca.2015.01.001.

Rooman, I. and Real, F.X. 2012. Pancreatic ductal adenocarcinoma and acinar cells: a matter of differentiation and development? *Gut* 61(3), pp. 449–458. doi: 10.1136/gut.2010.235804.

Roos, J. et al. 2005. STIM1, an essential and conserved component of store-operated Ca2+ channel function. *The Journal of Cell Biology* 169(3), pp. 435–445. doi: 10.1083/jcb.200502019.

Rosen, D. et al. 2009. Analogues of the Nicotinic Acid Adenine Dinucleotide Phosphate (NAADP) Antagonist Ned-19 Indicate Two Binding Sites on the NAADP Receptor. *Journal of Biological Chemistry* 284(50), pp. 34930–34934. doi: 10.1074/jbc.M109.016519.

Rosen, D. et al. 2012. Synthesis and use of cell-permeant cyclic ADP-ribose. *Biochemical and Biophysical Research Communications* 418(2), pp. 353–358. doi: 10.1016/j.bbrc.2012.01.025.

Rosendahl, J. et al. 2007. Hereditary chronic pancreatitis. *Orphanet Journal of Rare Diseases* 2, p. 1. doi: 10.1186/1750-1172-2-1.

Rothberg, B.S. et al. 2013. Orai Channel Pore Properties and Gating by STIM: Implications from the Orai Crystal Structure. *Sci. Signal.* 6(267), pp. pe9-pe9. doi: 10.1126/scisignal.2003971.

Ruas, M. et al. 2010. Purified TPC Isoforms Form NAADP Receptors with Distinct Roles for Ca2+ Signaling and Endolysosomal Trafficking. *Current Biology* 20(8–6), pp. 703–709. doi: 10.1016/j.cub.2010.02.049.

Ruas, M. et al. 2014. TPC1 Has Two Variant Isoforms, and Their Removal Has Different Effects on Endo-Lysosomal Functions Compared to Loss of TPC2. *Molecular and Cellular Biology* 34(21), pp. 3981–3992. doi: 10.1128/MCB.00113-14.

Ruas, M. et al. 2015. Expression of Ca2+-permeable two-pore channels rescues NAADP signalling in TPC-deficient cells. *The EMBO Journal* 34(13), pp. 1743–1758. doi: 10.15252/embj.201490009.

Rush, T.S. et al. 2005. A Shape-Based 3-D Scaffold Hopping Method and Its Application to a Bacterial Protein−Protein Interaction. *Journal of Medicinal Chemistry* 48(5), pp. 1489–1495. doi: 10.1021/jm040163o.

Russell DW 2003. The Enzymes, Regulation, and Genetics of Bile Acid Synthesis. *Annual Review of Biochemistry* 72(1), pp. 137–174. doi: 10.1146/annurev.biochem.72.121801.161712.

Rutter, W.J. 1980. The development of the endocrine and exocrine pancreas. *Monographs in Pathology* 21, pp. 30–38.

Rybalchenko, V. et al. 2012. Membrane potential regulates NAADP dependence of the pH and Ca2+ sensitive organellar two-pore channel TPC1. *Journal of Biological Chemistry* , p. jbc.M112.359612. doi: 10.1074/jbc.M112.359612.

Sacks, R.S. et al. 2008. Thrombin-mediated increases in cytosolic [Ca2+] involve different mechanisms in human pulmonary artery smooth muscle and endothelial cells. *American Journal of Physiology - Lung Cellular and Molecular Physiology* 295(6), pp. L1048–L1055. doi: 10.1152/ajplung.90259.2008.

Sakurai, Y. et al. 2015. Two-pore channels control Ebola virus host cell entry and are drug targets for disease treatment. *Science* 347(6225), pp. 995–998. doi: 10.1126/science.1258758.

Salido, G.M. et al. 2009. TRPC channels and store-operated Ca2+ entry. *Biochimica et Biophysica Acta (BBA) - Molecular Cell Research* 1793(2), pp. 223–230. doi: 10.1016/j.bbamcr.2008.11.001.

Sancak, Y. et al. 2010. Ragulator-Rag complex targets mTORC1 to the lysosomal surface and is necessary for its activation by amino acids. *Cell* 141(2), pp. 290–303. doi: 10.1016/j.cell.2010.02.024.

Sánchez-Tusie, A.A. et al. 2014. Characterization of NAADP-mediated calcium signaling in human spermatozoa. *Biochemical and Biophysical Research Communications* 443(2), pp. 531–536. doi: 10.1016/j.bbrc.2013.12.011.

Santulli, G. and Marks, A.R. 2015. Essential Roles of Intracellular Calcium Release Channels in Muscle, Brain, Metabolism, and Aging. *Current Molecular Pharmacology* 8(2), pp. 206–222.

Sarkisov, D.V. and Wang, S.S.-H. 2008. Order-Dependent Coincidence Detection in Cerebellar Purkinje Neurons at the Inositol Trisphosphate Receptor. *Journal of Neuroscience* 28(1), pp. 133–142. doi: 10.1523/JNEUROSCI.1729-07.2008.

Sarles, H. 1992. Chronic pancreatitis and diabetes. *Bailliere's Clinical Endocrinology and Metabolism* 6(4), pp. 745–775.

Schäfer, B.W. and Heizmann, C.W. 1996. The S100 family of EF-hand calcium-binding proteins: functions and pathology. *Trends in Biochemical Sciences* 21(4), pp. 134–140. doi: 10.1016/S0968-0004(96)80167-8.

Schafmayer, C. et al. 2006. Predictors of gallstone composition in 1025 symptomatic gallstones from Northern Germany. *BMC Gastroenterology* 6, p. 36. doi: 10.1186/1471-230X-6-36.

Schanne, F.A. et al. 1979. Calcium dependence of toxic cell death: a final common pathway. *Science* 206(4419), pp. 700–702. doi: 10.1126/science.386513.

Schnefel, S. et al. 1988. Acetylcholine and cholecystokinin receptors functionally couple by different G-proteins to phospholipase C in pancreatic acinar cells. *FEBS Letters* 230(1–2), pp. 125–130. doi: 10.1016/0014-5793(88)80655-0.

Schomer, B. and Epel, D. 1998. Redox Changes during Fertilization and Maturation of Marine Invertebrate Eggs. *Developmental Biology* 203(1), pp. 1–11. doi: 10.1006/dbio.1998.9044.

Schoutteten, L. et al. 1999. Development of Intracellular Calcium Measurement by Time-resolved Photon-counting Fluorescence. *Photochemistry and Photobiology* 70(5), pp. 701–709. doi: 10.1111/j.1751-1097.1999.tb08273.x.

Schrlau, M.G. et al. 2008. Carbon nanopipettes characterize calcium release pathways in breast cancer cells. *Nanotechnology* 19(32), p. 325102. doi: 10.1088/0957-4484/19/32/325102.

Sharp, T.V. et al. 2002. K15 protein of Kaposi's sarcoma-associated herpesvirus is latently expressed and binds to HAX-1, a protein with antiapoptotic function. *Journal of Virology* 76(2), pp. 802–816.

Shen, C.N. et al. 2003. Transdifferentiation of pancreas to liver. *Mechanisms of Development* 120(1), pp. 107–116.

Sherwood, M.W. et al. 2007. Activation of trypsinogen in large endocytic vacuoles of pancreatic acinar cells. *Proceedings of the National Academy of Sciences* 104(13), pp. 5674–5679. doi: 10.1073/pnas.0700951104.

Shimomura, O. et al. 1962. Extraction, purification and properties of aequorin, a bioluminescent protein from the luminous hydromedusan, Aequorea. *Journal of Cellular and Comparative Physiology* 59, pp. 223–239.

Shimomura, O. et al. 1990. Recombinant aequorin and recombinant semi-synthetic aequorins. Cellular Ca2+ ion indicators. *Biochemical Journal* 270(2), pp. 309–312. doi: 10.1042/bj2700309.

Shimomura, O. 1995. Cause of spectral variation in the luminescence of semisynthetic aequorins. *Biochemical Journal* 306(2), pp. 537–543. doi: 10.1042/bj3060537.

Sieberer, B.J. et al. 2009. A nuclear-targeted cameleon demonstrates intranuclear Ca2+ spiking in Medicago truncatula root hairs in response to rhizobial nodulation factors. *Plant Physiology* 151(3), pp. 1197–1206. doi: 10.1104/pp.109.142851.

da Silva, C.P. et al. 1998. Ectocellular CD38-catalyzed synthesis and intracellular Ca2+-signalling activity of cyclic ADP-ribose in T-lymphocytes are not functionally related. *FEBS Letters* 439(3), pp. 291–296. doi: 10.1016/S0014-5793(98)01396-9.

Sjödin, L. and Gylfe, E. 2000. Caffeine inhibits a low affinity but not a high affinity mechanism for cholecystokinin-evoked Ca2+ signalling and amylase release from guinea pig pancreatic acini. *Naunyn-Schmiedeberg's Archives of Pharmacology* 361(2), pp. 113–119. doi: 10.1007/s002109900177.

Skipworth, J.R.A. et al. 2010. Managing acute and chronic pancreatitis. *The Practitioner* 254(1733), pp. 23–27, 2.

Smith, R.J. et al. 1990. Receptor-coupled signal transduction in human polymorphonuclear neutrophils: effects of a novel inhibitor of phospholipase C-dependent processes on cell responsiveness. *Journal of Pharmacology and Experimental Therapeutics* 253(2), pp. 688–697.

Soares, S. et al. 2007. NAADP as a second messenger: neither CD38 nor base-exchange reaction are necessary for in vivo generation of NAADP in myometrial cells. *American Journal of Physiology - Cell Physiology* 292(1), pp. C227–C239. doi: 10.1152/ajpcell.00638.2005.

Soboloff, J. et al. 2006. STIM2 Is an Inhibitor of STIM1-Mediated Store-Operated Ca2+ Entry. *Current Biology* 16(14), pp. 1465–1470. doi: 10.1016/j.cub.2006.05.051.

Soboloff, J. et al. 2012. STIM proteins: dynamic calcium signal transducers. *Nature reviews. Molecular cell biology* 13(9), pp. 549–565. doi: 10.1038/nrm3414.

Söllner, T.H. 2003. Regulated exocytosis and SNARE function (Review). *Molecular Membrane Biology* 20(3), pp. 209–220. doi: 10.1080/0968768031000104953.

Soyombo, A.A. et al. 2006. TRP-ML1 Regulates Lysosomal pH and Acidic Lysosomal Lipid Hydrolytic Activity. *Journal of Biological Chemistry* 281(11), pp. 7294–7301. doi: 10.1074/jbc.M508211200.

Spassova, M.A. et al. 2006. STIM1 has a plasma membrane role in the activation of store-operated Ca2+ channels. *Proceedings of the National Academy of Sciences of the United States of America* 103(11), pp. 4040–4045. doi: 10.1073/pnas.0510050103.

Staels, B. and Fonseca, V.A. 2009. Bile Acids and Metabolic Regulation. *Diabetes Care* 32(Suppl 2), pp. S237–S245. doi: 10.2337/dc09-S355.

Starkus, J.G. et al. 2010. The calcium-permeable non-selective cation channel TRPM2 is modulated by cellular acidification. *The Journal of Physiology* 588(8), pp. 1227–1240. doi: 10.1113/jphysiol.2010.187476.

States, D.J. et al. 1992. Similarities in amino acid sequences of Aplysia ADP-ribosyl cyclase and human lymphocyte antigen CD38. *Trends in Biochemical Sciences* 17(12), p. 495. doi: 10.1016/0968-0004(92)90337-9.

Steen, M. et al. 2007. NAADP Mobilizes Calcium from the Endoplasmic Reticular Ca2+ Store in T-lymphocytes. *Journal of Biological Chemistry* 282(26), pp. 18864–18871. doi: 10.1074/jbc.M610925200.

Steer, M.L. et al. 1995. Chronic Pancreatitis. *New England Journal of Medicine* 332(22), pp. 1482–1490. doi: 10.1056/NEJM199506013322206.

Steinberg, W. and Tenner, S. 1994. Acute pancreatitis. *The New England Journal of Medicine* 330(17), pp. 1198–1210. doi: 10.1056/NEJM199404283301706.

Stieger, B. 2010. Role of the bile salt export pump, BSEP, in acquired forms of cholestasis. *Drug Metabolism Reviews* 42(3), pp. 437–445. doi: 10.3109/03602530903492004.

Stojilkovic, S.S. 2005. Ca2+-regulated exocytosis and SNARE function. *Trends in endocrinology and metabolism: TEM* 16(3), pp. 81–83. doi: 10.1016/j.tem.2005.02.002.

St-Pierre, M.V. et al. 2001. Transport of bile acids in hepatic and non-hepatic tissues. *The Journal of Experimental Biology* 204(Pt 10), pp. 1673–1686.

Straub, S.V. et al. 2000. Calcium wave propagation in pancreatic acinar cells: functional interaction of inositol 1,4,5-trisphosphate receptors, ryanodine receptors, and mitochondria. *The Journal of General Physiology* 116(4), pp. 547–560.

Streb, H. et al. 1983. Release of Ca2+ from a nonmitochondrial intracellular store in pancreatic acinar cells by inositol-1,4,5-trisphosphate. *Nature* 306(5938), pp. 67–9.

Stryke, D. et al. 2003. BayGenomics: a resource of insertional mutations in mouse embryonic stem cells. *Nucleic acids research* 31(1), pp. 278–281.

Su, K.H. et al. 2006. Review of experimental animal models of acute pancreatitis. *HPB* 8(4), pp. 264–286. doi: 10.1080/13651820500467358.

Sun, M. et al. 2000. Mucolipidosis type IV is caused by mutations in a gene encoding a novel transient receptor potential channel. *Human Molecular Genetics* 9(17), pp. 2471–2478. doi: 10.1093/hmg/9.17.2471.

Sutton, R. et al. 2003. Signal transduction, calcium and acute pancreatitis. *Pancreatology: official journal of the International Association of Pancreatology (IAP) ... [et al.]* 3(6), pp. 497–505. doi: 10.1159/000075581.

Sutton, R. et al. 2008. Pancreatitis and calcium signalling: report of an international workshop. *Pancreas* 36(4), pp. e1-14. doi: 10.1097/MPA.0b013e3181675010.

Swaroop, V.S. et al. 2004. Severe acute pancreatitis. *JAMA* 291(23), pp. 2865–2868. doi: 10.1001/jama.291.23.2865.

Takahashi, A. et al. 1999. Measurement of Intracellular Calcium. *Physiological Reviews* 79(4), pp. 1089–1125.

Takasawa, S. et al. 1993. Cyclic ADP-ribose in insulin secretion from pancreatic beta cells. *Science (New York, N.Y.)* 259(5093), pp. 370–373.

Takemura, H. et al. 1989. Activation of calcium entry by the tumor promoter thapsigargin in parotid acinar cells. Evidence that an intracellular calcium pool and not an inositol phosphate regulates calcium fluxes at the plasma membrane. *The Journal of Biological Chemistry* 264(21), pp. 12266–12271.

Tang, L. et al. 2014. Structural basis for Ca2+ selectivity of a voltage-gated calcium channel. *Nature* 505(7481), pp. 56–61. doi: 10.1038/nature12775.

Tang, W.-X. et al. 2002. Role of FKBP12.6 in cADPR-induced activation of reconstituted ryanodine receptors from arterial smooth muscle. *American journal of physiology. Heart and circulatory physiology* 282(4), pp. H1304-1310. doi: 10.1152/ajpheart.00843.2001.

Tao, R. et al. 2011. Cyclic ADP ribose is a novel regulator of intracellular Ca2+ oscillations in human bone marrow mesenchymal stem cells. *Journal of cellular and molecular medicine* 15(12), pp. 2684–2696. doi: 10.1111/j.1582-4934.2011.01263.x.

Tarasov, A.I. et al. 2012. Regulation of ATP production by mitochondrial Ca2+. *Cell Calcium* 52(1), pp. 28–35. doi: 10.1016/j.ceca.2012.03.003.

Taylor, C.W. et al. 1999. Expression of inositol trisphosphate receptors. *Cell Calcium* 26(6), pp. 237–251. doi: 10.1054/ceca.1999.0090.

Taylor, C.W. et al. 2004. IP3 receptors: the search for structure. *Trends in Biochemical Sciences* 29(4), pp. 210–219. doi: 10.1016/j.tibs.2004.02.010.

Taylor, C.W. and Broad, L.M. 1998. Pharmacological analysis of intracellular Ca2+ signalling: problems and pitfalls. *Trends in Pharmacological Sciences* 19(9), pp. 370–375. doi: 10.1016/S0165-6147(98)01243-7.

Taylor, C.W. and Tovey, S.C. 2010. IP3 Receptors: Toward Understanding Their Activation. *Cold Spring Harbor Perspectives in Biology* 2(12), p. a004010. doi: 10.1101/cshperspect.a004010.

Teague, A. et al. 2015. Advanced pancreatic adenocarcinoma: a review of current treatment strategies and developing therapies. *Therapeutic Advances in Medical Oncology* 7(2), pp. 68–84. doi: 10.1177/1758834014564775.

Thastrup, O. et al. 1990. Thapsigargin, a tumor promoter, discharges intracellular Ca2+ stores by specific inhibition of the endoplasmic reticulum Ca2(+)-ATPase. *Proceedings of the National Academy of Sciences* 87(7), pp. 2466–2470.

Thorn, P. et al. 1993. Local and global cytosolic Ca2+ oscillations in exocrine cells evoked by agonists and inositol trisphosphate. *Cell* 74(4), pp. 661–668. doi: 10.1016/0092-8674(93)90513-P.

Timerman, A.P. et al. 1993. The calcium release channel of sarcoplasmic reticulum is modulated by FK-506-binding protein. Dissociation and reconstitution of FKBP-12 to the calcium release channel of skeletal muscle sarcoplasmic reticulum. *Journal of Biological Chemistry* 268(31), pp. 22992–22999.

Timerman, A.P. et al. 1996. Selective Binding of FKBP12.6 by the Cardiac Ryanodine Receptor. *Journal of Biological Chemistry* 271(34), pp. 20385–20391. doi: 10.1074/jbc.271.34.20385.

Tinel, H. et al. 1999. Active mitochondria surrounding the pancreatic acinar granule region prevent spreading of inositol trisphosphate-evoked local cytosolic Ca(2+) signals. *The EMBO journal* 18(18), pp. 4999–5008. doi: 10.1093/emboj/18.18.4999.

Tirlapur, U.K. and König, K. 2002. Cell biology: Targeted transfection by femtosecond laser. *Nature* 418(6895), pp. 290–291. doi: 10.1038/418290a.

Trotman, B.W. 1991. Pigment gallstone disease. *Gastroenterology Clinics of North America* 20(1), pp. 111–126.

Tsuchitani, M. et al. 2016. A comparison of the anatomical structure of the pancreas in experimental animals. *Journal of Toxicologic Pathology* 29(3), pp. 147–154. doi: 10.1293/tox.2016-0016.

Tsujimoto, Y. 1997. Apoptosis and necrosis: intracellular ATP level as a determinant for cell death modes. *Cell Death and Differentiation* 4(6), pp. 429–434. doi: 10.1038/sj.cdd.4400262.

Tsukamoto, H. et al. 1988. Potentiation of ethanol-induced pancreatic injury by dietary fat. Induction of chronic pancreatitis by alcohol in rats. *The American Journal of Pathology* 131(2), pp. 246–257.

Tu, H. et al. 2006. Presenilins form ER Ca2+ leak channels, a function disrupted by familial Alzheimer's disease-linked mutations. *Cell* 126(5), pp. 981–993. doi: 10.1016/j.cell.2006.06.059.

Uhl, W. et al. 2002. IAP Guidelines for the Surgical Management of Acute Pancreatitis. *Pancreatology: official journal of the International Association of Pancreatology (IAP) ... [et al.]* 2(6), pp. 565–573. doi: 71269.

Ullmann, H. et al. 2005. Synthesis and Structure−Activity Relationships of Suramin-Derived P2Y11 Receptor Antagonists with Nanomolar Potency. *Journal of Medicinal Chemistry* 48(22), pp. 7040–7048. doi: 10.1021/jm050301p.

Vaeth, M. et al. 2017. ORAI2 modulates store-operated calcium entry and T cell-mediated immunity. *Nature Communications* 8, p. 14714. doi: 10.1038/ncomms14714.

Venturi, E. et al. 2012. From Eggs to Hearts: What Is the Link between Cyclic ADP-Ribose and Ryanodine Receptors? *Cardiovascular Therapeutics* 30(2), pp. 109–116. doi: 10.1111/j.1755-5922.2010.00236.x.

Verkhratsky, A. 2005. Physiology and pathophysiology of the calcium store in the endoplasmic reticulum of neurons. *Physiological reviews* 85(1), pp. 201–279. doi: 10.1152/physrev.00004.2004.

Vonlaufen, A. et al. 2008. Molecular mechanisms of pancreatitis: current opinion. *Journal of Gastroenterology and Hepatology* 23(9), pp. 1339–1348. doi: 10.1111/j.1440-1746.2008.05520.x.

Voronina, S. et al. 2002. Bile acids induce calcium signals in mouse pancreatic acinar cells: implications for bile-induced pancreatic pathology. *The Journal of Physiology* 540(1), pp. 49–55. doi: 10.1113/jphysiol.2002.017525.

Voronina, S.G. et al. 2004. Effects of Secretagogues and Bile Acids on Mitochondrial Membrane Potential of Pancreatic Acinar Cells COMPARISON OF DIFFERENT MODES OF EVALUATING ΔΨm. *Journal of Biological Chemistry* 279(26), pp. 27327–27338. doi: 10.1074/jbc.M311698200.

Voronina, S.G. et al. 2005. Bile acids induce a cationic current, depolarizing pancreatic acinar cells and increasing the intracellular Na+ concentration. *The Journal of Biological Chemistry* 280(3), pp. 1764–1770. doi: 10.1074/jbc.M410230200.

Voronina, S.G. et al. 2010. Dynamic Changes in Cytosolic and Mitochondrial ATP Levels in Pancreatic Acinar Cells. *Gastroenterology* 138(5), p. 1976–1987.e5. doi: 10.1053/j.gastro.2010.01.037.

Wagner, L.E. et al. 2014. Characterization of ryanodine receptor type 1 single channel activity using 'on-nucleus' patch clamp. *Cell Calcium* 56(2), pp. 96–107. doi: 10.1016/j.ceca.2014.05.004.

Wagner, M. et al. 1998. Malignant transformation of duct-like cells originating from acini in transforming growth factor transgenic mice. *Gastroenterology* 115(5), pp. 1254–1262.

Wakui, M. et al. 1990. Receptor-activated cytoplasmic Ca2+ spiking mediated by inositol trisphosphate is due to Ca2+-induced Ca2+ release. *Cell* 63(5), pp. 1025–1032. doi: 10.1016/0092-8674(90)90505-9.

Waller-Evans, H. and Lloyd-Evans, E. 2015. Regulation of TRPML1 function. *Biochemical Society Transactions* 43(3), pp. 442–446. doi: 10.1042/BST20140311.

Walseth, T.F. et al. 1993. Identification of cyclic ADP-ribose-binding proteins by photoaffinity labeling. *The Journal of biological chemistry* 268(35), pp. 26686–26691.

Walseth, T.F. et al. 2012. Photoaffinity Labeling of High Affinity Nicotinic Acid Adenine Dinucleotide Phosphate (NAADP)-Binding Proteins in Sea Urchin Egg♦. *The Journal of Biological Chemistry* 287(4), pp. 2308–2315. doi: 10.1074/jbc.M111.306563.

Walseth, T.F. and Lee, H.C. 1993. Synthesis and characterization of antagonists of cyclic-ADP-ribose-induced Ca2+ release. *Biochimica et Biophysica Acta (BBA) - Molecular Cell Research* 1178(3), pp. 235–242. doi: 10.1016/0167-4889(93)90199-Y.

Wang, G. et al. 2016. Necroptosis: a potential, promising target and switch in acute pancreatitis. *Apoptosis: An International Journal on Programmed Cell Death* 21(2), pp. 121–129. doi: 10.1007/s10495-015-1192-3.

Wang, G.-J. et al. 2009. Acute pancreatitis: Etiology and common pathogenesis. *World Journal of Gastroenterology : WJG* 15(12), pp. 1427–1430. doi: 10.3748/wjg.15.1427.

Wang, M. et al. 2006. Localized Ca2+ uncaging induces Ca2+ release through IP3R in smooth muscle. *Acta pharmacologica Sinica* 27(7), pp. 939–944. doi: 10.1111/j.1745-7254.2006.00389.x.

Wang, X. et al. 2012. TPC Proteins Are Phosphoinositide- Activated Sodium-Selective Ion Channels in Endosomes and Lysosomes. *Cell* 151(2), pp. 372–383. doi: 10.1016/j.cell.2012.08.036.

Wen, L. et al. 2015. Inhibitors of ORAI1 Prevent Cytosolic Calcium-Associated Injury of Human Pancreatic Acinar Cells and Acute Pancreatitis in 3 Mouse Models. *Gastroenterology* 149(2), p. 481–492.e7. doi: 10.1053/j.gastro.2015.04.015.

Werner, J. et al. 2002. Alcoholic pancreatitis in rats: injury from nonoxidative metabolites of ethanol. *American Journal of Physiology. Gastrointestinal and Liver Physiology* 283(1), pp. G65-73. doi: 10.1152/ajpgi.00419.2001.

Wharton, G.K. 1932. The blood supply of the pancreas, with special reference to that of the islands of Langerhans. *The Anatomical Record* 53(1), pp. 55–81. doi: 10.1002/ar.1090530108.

Whitaker, M. 2010. Genetically-encoded probes for measurement of intracellular calcium. *Methods in cell biology* 99, pp. 153–182. doi: 10.1016/B978-0-12-374841-6.00006-2.

Williams, G.S.B. et al. 2013. Mitochondrial calcium uptake. *Proceedings of the National Academy of Sciences* , p. 201300410. doi: 10.1073/pnas.1300410110.

Williams, J.A. 1980. Regulation of pancreatic acinar cell function by intracellular calcium. *The American journal of physiology* 238(4), pp. G269-279.

Williams, J.A. 2001. Intracellular signaling mechanisms activated by cholecystokinin-regulating synthesis and secretion of digestive enzymes in pancreatic acinar cells. *Annual Review of Physiology* 63, pp. 77–97. doi: 10.1146/annurev.physiol.63.1.77.

Williams, J.A. 2010. Regulation of Acinar Cell Function in The Pancreas. *Current opinion in gastroenterology* 26(5), pp. 478–483. doi: 10.1097/MOG.0b013e32833d11c6.

Wilson, J.S. and Apte, M.V. 2003. Role of alcohol metabolism in alcoholic pancreatitis. *Pancreas* 27(4), pp. 311–315.

Wink, M. 1993. The Plant Vacuole: A Multifunctional Compartment. *Journal of Experimental Botany* 44, pp. 231–246.

Winston, A.P. et al. 2005. Neuropsychiatric effects of caffeine. *Advances in Psychiatric Treatment* 11(6), pp. 432–439. doi: 10.1192/apt.11.6.432.

Wolf, I.M.A. et al. 2015. Frontrunners of T cell activation: Initial, localized Ca2+ signals mediated by NAADP and the type 1 ryanodine receptor. *Sci. Signal.* 8(398), pp. ra102-ra102. doi: 10.1126/scisignal.aab0863.

Xiao, R.P. et al. 1997. The immunophilin FK506-binding protein modulates Ca2+ release channel closure in rat heart. *The Journal of Physiology* 500(2), pp. 343–354. doi: 10.1113/jphysiol.1997.sp022025.

Xu, H. et al. 2007. Activating mutation in a mucolipin transient receptor potential channel leads to melanocyte loss in varitint–waddler mice. *Proceedings of the National Academy of Sciences of the United States of America* 104(46), pp. 18321–18326. doi: 10.1073/pnas.0709096104.

Yadav, D. and Lowenfels, A.B. 2013. The Epidemiology of Pancreatitis and Pancreatic Cancer. *Gastroenterology* 144(6), pp. 1252–1261. doi: 10.1053/j.gastro.2013.01.068.

Yamada, M. et al. 1997. Ultrastructural localization of CD38 immunoreactivity in rat brain. *Brain Research* 756(1–2), pp. 52–60. doi: 10.1016/S0006-8993(97)00117-0.

Yamaguchi, S. et al. 2011. Transient Receptor Potential Mucolipin 1 (TRPML1) and Two-pore Channels Are Functionally Independent Organellar Ion Channels. *Journal of Biological Chemistry* 286(26), pp. 22934–22942. doi: 10.1074/jbc.M110.210930.

Yamamoto-Katayama, S. et al. 2002. Crystallographic studies on human BST-1/CD157 with ADP-ribosyl cyclase and NAD glycohydrolase activities. *Journal of molecular biology* 316(3), pp. 711–723. doi: 10.1006/jmbi.2001.5386.

Yamasaki, M. et al. 2004. Organelle Selection Determines Agonist-specific Ca2+ Signals in Pancreatic Acinar and β Cells. *Journal of Biological Chemistry* 279(8), pp. 7234–7240. doi: 10.1074/jbc.M311088200.

Yamasaki, M. et al. 2005. Role of NAADP and cADPR in the Induction and Maintenance of Agonist-Evoked Ca2+ Spiking in Mouse Pancreatic Acinar Cells. *Current Biology* 15(9), pp. 874–878. doi: 10.1016/j.cub.2005.04.033.

Yang, K. et al. 2007. K+-induced ion-exchanges trigger trypsin activation in pancreas acinar zymogen granules. *Archives of Biochemistry and Biophysics* 459(2), pp. 256–263. doi: 10.1016/j.abb.2006.12.002.

Yang, Z. et al. 2015. The Golgi apparatus is a functionally distinct Ca2+ store regulated by the PKA and Epac branches of the β1-adrenergic signaling pathway. *Sci. Signal.* 8(398), pp. ra101-ra101. doi: 10.1126/scisignal.aaa7677.

Yoshikawa, F. et al. 1999. Cooperative Formation of the Ligand-binding Site of the Inositol 1,4,5-Trisphosphate Receptor by Two Separable Domains. *Journal of Biological Chemistry* 274(1), pp. 328–334. doi: 10.1074/jbc.274.1.328.

Young, G.S. et al. 2006. Decreased cADPR and increased NAD+ in the Cd38-/- mouse. *Biochemical and biophysical research communications* 346(1), pp. 188–192. doi: 10.1016/j.bbrc.2006.05.100.

Yuan, J.P. et al. 2007. STIM1 heteromultimerizes TRPC channels to determine their function as store-operated channels. *Nature Cell Biology* 9(6), pp. 636–645. doi: 10.1038/ncb1590.

Yue, L. et al. 2001. CaT1 manifests the pore properties of the calcium-release-activated calcium channel. *Nature* 410(6829), pp. 705–709. doi: 10.1038/35070596.

Yule, D.I. et al. 1997. Evidence that zymogen granules are not a physiologically relevant calcium pool. Defining the distribution of inositol 1,4,5-trisphosphate receptors in pancreatic acinar cells. *The Journal of Biological Chemistry* 272(14), pp. 9093–9098.

Zator, Z. and Whitcomb, D.C. 2017. Insights into the genetic risk factors for the development of pancreatic disease. *Therapeutic Advances in Gastroenterology* 10(3), pp. 323–336. doi: 10.1177/1756283X16684687.

Zhang, F. et al. 2009. TRP-ML1 functions as a lysosomal NAADP-sensitive Ca2+ release channel in coronary arterial myocytes. *Journal of Cellular and Molecular Medicine* 13(9b), pp. 3174–3185. doi: 10.1111/j.1582-4934.2008.00486.x.

Zhang, F. et al. 2011. Reconstitution of lysosomal NAADP-TRP-ML1 signaling pathway and its function in TRP-ML1−/− cells. *American Journal of Physiology - Cell Physiology* 301(2), pp. C421–C430. doi: 10.1152/ajpcell.00393.2010.

Zhang, F. and Li, P.-L. 2007. Reconstitution and Characterization of a Nicotinic Acid Adenine Dinucleotide Phosphate (NAADP)-sensitive Ca2+ Release Channel from Liver Lysosomes of Rats. *Journal of Biological Chemistry* 282(35), pp. 25259–25269. doi: 10.1074/jbc.M701614200.

Zhang, K. et al. 2017. Identifying Glyceraldehyde 3-Phosphate Dehydrogenase as a Cyclic Adenosine Diphosphoribose Binding Protein by Photoaffinity Protein–Ligand Labeling Approach. *Journal of the American Chemical Society* 139(1), pp. 156–170. doi: 10.1021/jacs.6b08088.

Zhang, S.L. et al. 2005. STIM1 is a Ca2+ sensor that activates CRAC channels and migrates from the Ca2+ store to the plasma membrane. *Nature* 437(7060), pp. 902–905. doi: 10.1038/nature04147.

Zhang, Z.-H. et al. 2013. Two Pore Channel 2 Differentially Modulates Neural Differentiation of Mouse Embryonic Stem Cells. *PLoS ONE* 8(6). Available at: http://www.ncbi.nlm.nih.gov/pmc/articles/PMC3680454/ [Accessed: 25 August 2016].

Zhao, F. et al. 2001. Dantrolene Inhibition of Ryanodine Receptor Ca2+Release Channels MOLECULAR MECHANISM AND ISOFORM SELECTIVITY. *Journal of Biological Chemistry* 276(17), pp. 13810–13816. doi: 10.1074/jbc.M006104200.

Zhao, Y. et al. 2012. Roles of cADPR and NAADP in pancreatic cells. *Acta Biochimica et Biophysica Sinica* 44(9), pp. 719–729. doi: 10.1093/abbs/gms044.

Zhao, Y.J. et al. 2015. Determinants of the membrane orientation of a calcium signaling enzyme CD38. *Biochimica et Biophysica Acta (BBA) - Molecular Cell Research* 1853(9), pp. 2095–2103. doi: 10.1016/j.bbamcr.2014.10.028.

Zhou, Y. et al. 2010. STIM1 gates the store-operated calcium channel ORAI1 in vitro. *Nature Structural & Molecular Biology* 17(1), pp. 112–116. doi: 10.1038/nsmb.1724.

Zhou, Y. et al. 2013. Initial activation of STIM1, the regulator of store-operated calcium entry. *Nature structural & molecular biology* 20(8), pp. 973–981. doi: 10.1038/nsmb.2625.

Zhu, M.X. et al. 2010. Calcium signaling via two-pore channels: local or global, that is the question. *American Journal of Physiology - Cell Physiology* 298(3), pp. C430–C441. doi: 10.1152/ajpcell.00475.2009.

Zimniak, P. et al. 1991. Taurine-conjugated bile acids act as calcium ionophores. *Biochemistry* 30(35), pp. 8598–8604. doi: 10.1021/bi00099a015.

Zong, X. et al. 2009. The two-pore channel TPCN2 mediates NAADP-dependent Ca2+-release from lysosomal stores. *Pflugers Archiv* 458(5), pp. 891–899. doi: 10.1007/s00424-009-0690-y.